UNIVERSITY OF LONDON THESIS

Degree PhD Year 2007 Name of Author SWANN, George Edward Alexander

Diatom oxygen isotopes and biogenic silica concentrations: an examination of their potential for reconstructing palaeoenvironmental change

Thesis submitted for the degree of
Doctor of Philosophy in the
University of London

by

George Edward Alexander Swann

Department of Geography
University College London

September 2007

ProQuest LLC
789 East Eisenhower Parkway
P.O. Box 1346
Ann Arbor, MI 48106-1346

I George Swann confirm that the work presented in this thesis is my own. Where information has been derived from other sources, I confirm that this has been indicated in the thesis

September 2007

Abstract

Diatoms represent between 25% and 45% of all marine primary productivity. As yet, however, the potential of using diatom isotopes, in particular oxygen ($\delta^{18}O_{diatom}$), in palaeoceanographic reconstructions has yet to be fully assessed. Work here within this thesis demonstrates a method for extracting pure, mono or near mono species specific, diatom samples from marine sediments. Over two time intervals, the potential of using $\delta^{18}O_{diatom}$ in palaeoceanographic reconstructions is then shown at ODP site 882 in the North West Pacific Ocean over the onset of major Northern Hemisphere Glaciation (2.73 Ma) and over the last 200 kyr BP. During both periods, major changes in the halocline/stratification of the water column, relating to significant freshwater input to the region, are reconstructed. These results indicate a significant role for the region in initiating glacier growth across the North American continent and in causing changes in atmospheric pCO_2. Strong evidence exists, however, that both an inter- and intra-species vital/species effect of up to 3.51‰ may be present in $\delta^{18}O_{diatom}$. As such, this may limit future applications of $\delta^{18}O_{diatom}$ to samples which are dominated by only one taxa.

Section two of the thesis investigates the potential for wet-alkaline measurements of BSi to provide insights into the global silicon cycle. A sequential Si/Al technique, which directly accounts for levels of clay/aluminosilicate digestion, is demonstrated to produce lower and more accurate measurement of BSi in samples for which a rapid non-BSi digestion phase occurs. However, comparisons between wet-alkaline BSi measurements and diatom biovolume measurements, which more accurately reflect the true amount of BSi within a sample, show a poor relationship between the two variables. This is particularly true in samples where diatom dissolution is high. Consequently, diatom biovolume measurements may be better suited for making quantitative palaeoenvironmental reconstructions.

This thesis/doorstop/microscope stand (delete as appropriate) is dedicated to Polly Collier for her unfailing support, beer for its medicinal properties and to the diatoms: without whom this PhD would not have happened.

Acknowledgments

A multitude of people have provided invaluable help and assistance with this thesis. As such, I apologise to all those who feel they should have been mentioned here but are not. This is either a genuine error for which I'm truly sorry, or it's not. Should you ever wonder which category you fall into, please don't ask. Just assume it's the first one.

At UCL considerable thanks are owed to Jon for confusing me with all his ideas on diatom isotopes, Dave for the monkey impressions, David for the endless cups of tea, Adam for living with me for a year, Alex for being my source of palaeoceanographic information, Ian, Tula and Janet for all their invaluable and creative lab support, Anson for all the alcohol and coffee that was consumed both in London and in Mallorca and Jonathan for reading through my upgrade report. Additional thanks are also owed to a range of past and present PhD students and members of the ECRC including Matt, Gen, Jo, Patrick and anyone else who has ever had to sit through one of my lunchtime talks.

Many thanks also to Jonaotaro Onodera and Kozo Takahashi for their discussions on the diatoms in the North Pacific Ocean, John Barron and Cathy Stickley for solving any taxonomy dilemmas, Patrick Rioual for all things related to Lake Baikal, Rick Murray and Christa Ziegler for looking after me in Boston, Emma Tomlinson for the ICP-AES support at RHUL and finally Gerald Haug for discussions on the palaeoceanographic record at ODP Site 882. A special thank you is also owed to Hilary, who introduced me to the delights of the fluorination line at NIGL and who did all the "fun" bits of the PhD.

Particular thanks are finally owed to my PhD supervisors Mark and Melanie. Mark for convincing me to do a PhD in the first place and for all his support over the past few years. Melanie, for keeping me on the straight and narrow when it came to the isotopes.

This thesis was funded by a NERC PhD studentship (NER/S/A/2004/12193) and a CASE studentship at NIGL (IP/812/0504) with additional support provided by a UCL Geography Teaching Assistantship, a UCL Graduate School award, a NERC ICP-AES facility grant (OSS/314/0906R) and the CONTINENT project. Samples from ODP Site 882 were made available by the Ocean Drilling Program.

Contents

List of figures

List of tables

PhD rationale and structure

To date, the majority of marine isotope records derived from biological organisms have originated from sites rich in biogenic carbonates such as foraminifera and ostracods. While this work has provided key insights into past climatic changes over both long, glacial-interglacial, and short, millennial timescales, a major limitation of current palaeoceanographic research is the absence of biogenic carbonates in high latitude regions such as the Southern Ocean, which are believed to be both sensitive to and potential drivers of global climate change (e.g., Shackleton, 2000; Brzezinski *et al.*, 2002).

Traditionally, palaeoenvironmental research in these high latitude and other carbonate free regions has focused on using a range of other proxies including minerogenic proxies and the analysis of non-carbonate microfossils such as diatoms. Recent years, however, have witnessed considerable advancements in the development of techniques for extracting isotope records from non-carbonate biological organisms (e.g., Lücke *et al.*, 2005; Brzezinski *et al.*, 2006). In particular, isotope measurements of diatoms are widely believed to contain significant potential for enabling isotope based palaeoenvironmental reconstructions to be conducted at carbonate depleted locations. To date, four isotopes have been analysed in diatoms and used for both palaeolimnological and palaeoceanographic research: $\delta^{18}O$, $\delta^{30}Si$, $\delta^{13}C$ and $\delta^{15}N$ (see reviews in Leng and Barker, 2006, De La Rocha, 2006). Within marine systems, it is likely that records of $\delta^{18}O_{diatom}$ hold the greatest potential for use in palaeoenvironmental reconstructions due to its ability to complement and extend existing planktonic foraminifera $\delta^{18}O$ studies that have been carried out at lower latitudes. However, in contrast to lacustrine systems where records of $\delta^{18}O_{diatom}$ are increasingly being used in palaeoenvironmental reconstructions, measurements of $\delta^{18}O_{diatom}$ have yet to be widely applied in marine systems or compared to more established techniques such as planktonic foraminifera or other geochemical/proxy data. Due to this, uncertainty remains as to the true palaeoceanographic potential of $\delta^{18}O_{diatom}$. For example, it remains unknown if $\delta^{18}O_{diatom}$ can be used to complement records of $\delta^{18}O_{foram}$ to provide seasonal/depth constraints on palaeoceanographic reconstructions in instances where diatoms and foraminifera co-exists within the sediment, or whether $\delta^{18}O_{diatom}$ can be used as a direct replacement for planktonic foraminifera at sites where carbonates are not preserved.

Related to this, is the increasing demand for measurement of $\delta^{30}Si_{diatom}$ in palaeoenvironmental reconstruction. Similar to $\delta^{18}O_{diatom}$, measurements of $\delta^{30}Si_{diatom}$, recording rates of nutrient utilisation, should enable a more detailed insight with respect to understanding the global silicon cycle and the possible role of the biological pump in modulating atmospheric variations of pCO_2 (Brzezinski *et al.*, 2002). However, due to the problems in analysing and extracting sufficient clean diatom material for isotope analysis, it is likely that it will be rarely feasible for both $\delta^{18}O_{diatom}$ and $\delta^{30}Si_{diatom}$ to be analysed on the same sample. Consequently, it can be expected that

demand will continue for measurements of sedimentary Biogenic Silica (BSi) concentrations, which provide complementary information to $\delta^{30}Si_{diatom}$ by documenting changes in surface water siliceous productivity.

While $\delta^{18}O_{diatom}$ and BSi concentrations are both very different techniques, they are closely linked by both being primarily derived or based on the fossilised remains of diatom frustule within the sediment record. In addition, as summarised above and within the thesis, both techniques contain significant potential in enabling a more in depth analysis as to the responses and role of carbonate free regions, e.g., high latitude regions, during both regional and global climatic events. Due to this, and given the increasing demand for palaeoenvironmental information from carbonate free systems, it is necessary to establish the validity of both $\delta^{18}O_{diatom}$ and BSi concentrations measurements and the potential problems associated with each that may lead to biases in any palaeoenvironmental reconstructions. For example, as detailed within the literature reviews contained in this thesis, significant uncertainty surrounds the analytical and sample preparation techniques for both $\delta^{18}O_{diatom}$ and BSi concentrations. In addition, both proxies are also potentially affected by issues of dissolution and changes to the diatom frustules during and after burial within the sediment record. Within this thesis, the relative impact of these and other issues which may affect records of $\delta^{18}O_{diatom}$ and BSi concentrations are assessed through a combination of methodological and palaeoenvironmental techniques in order to assess the relative accuracy and potential of both proxies and to determine what future improvements are required in order to increase the reliability of $\delta^{18}O_{diatom}$ and BSi derived reconstructions.

The work in this PhD thesis is presented in a two part hybrid format: Part 1 focusing on $\delta^{18}O_{diatom}$ and Part 2 on sedimentary Biogenic Silica (BSi) concentrations. Chapters within each section are written in the style of a series of journal articles, each of which in turn addresses the main themes and aims being addressed by this thesis, as outlined in the following chapters. Details on individual sites and their environmental setting are presented where relevant within individual chapters rather than in a separate section. In Part 1, Chapter 1 reviews the literature and background behind the use of $\delta^{18}O_{diatom}$ in palaeoceanographic reconstructions as well as summarising existing uncertainties including the $\delta^{18}O_{diatom}$-temperature coefficient, the role of silica maturation and the possibility for vital effects to influence records of $\delta^{18}O_{diatom}$. Subsequent chapters aim to address some of these uncertainties from a palaeoceanographic perspective at ODP Site 882 in the North West Pacific Ocean where other, more established, proxy data in addition to modern day oceanographic information can be drawn upon to assess the potential as well as the difficulties in analysing and understanding measurements of $\delta^{18}O_{diatom}$. A key feature of ODP Site 882 is the presence of both diatoms and planktonic foraminifera in the sediment record, permitting a direct comparison of the isotope records of these two organisms.

Chapters 2 and 3 examine the potential for isotope vital/species effects to exist in $\delta^{18}O_{diatom}$. By analysing fossil diatom material from ODP Site 882 in the North West Pacific Ocean, Chapter 2 documents the development of a technique, based on Morley (2004), to extract pure, near single species specific, diatoms for isotope analysis from marine sediment cores. From the extracted samples large isotope offsets in $\delta^{18}O_{diatom}$ are detected between two size fractions (75-150 μm and >150 μm) across the onset of major Northern Hemisphere Glaciation (NHG) (2.83-2.73 Ma). In Chapter 3 similar, but more variable, $\delta^{18}O_{diatom}$ offsets are observed between other diatom size fractions (38-75 μm and >100 μm) over the last 200 kyr. Although in the absence of contemporary water column and laboratory culture experiments the precise mechanisms behind these offsets can not be conclusively established, the results provide strong evidence for a possible vital/species effects in $\delta^{18}O_{diatom}$. These results have significant implications for the use of $\delta^{18}O_{diatom}$ in palaeoenvironmental reconstructions and indicates that samples need to be as species and size specific as possible. Such issues form the basis of sample selection for the palaeoceanographic reconstructions carried out in subsequent chapters.

In Chapters 4 and 5, the ODP Site 882 $\delta^{18}O_{diatom}$ datasets from Chapters 2 and 3, together with additional $\delta^{18}O_{diatom}$ and other proxy data, are used to reconstruct palaeoceanographic changes in the North West Pacific Ocean. Following consideration of the isotope offsets documented in Chapter 2 and 3, the chapters examine the potential for using $\delta^{18}O_{diatom}$ in palaeoceanographic reconstructions, both as a stand-alone proxy and alongside complementary records such as $\delta^{18}O_{foram}$, U^{k}_{37}, opal accumulation rates and magnetic susceptibility. Particular attention is given towards considering issues which may affect the reliability of the $\delta^{18}O_{diatom}$ record such as secondary isotope exchange (Schmidt et al., 1997; 2001, Brandriss et al., 1998) and the possible impact of dissolution. Chapter 4 focuses on the possible development of a halocline stratification system in the North West Pacific Ocean over the onset of major NHG when large ice-sheets expanded across the Northern Hemisphere. By combing records of $\delta^{18}O_{diatom}$ with planktonic $\delta^{18}O_{foram}$, a seasonally specific record of autumn/early winter ($\delta^{18}O_{diatom}$) and spring ($\delta^{18}O_{foram}$) palaeoceanographic conditions are reconstructed to indicate significant water column changes and freshwater inputs to the region. Chapter 5 examines the stability of the stratified water column at ODP Site 882 between MIS 1 and MIS 7 (0-200 kyr BP) and the role of changes in the water column in controlling atmospheric variations in pCO_2 concentrations both within glacials and over glacial-interglacial cycles. Despite the current uncertainties over the role of diatom dissolution, vital effects and silica maturation in diatoms, these two reconstructions combine to highlight the clear potential that exists in using $\delta^{18}O_{diatom}$ both as a stand alone proxy and as a complement to more conventional palaeoceanographic records such as $\delta^{18}O_{foram}$. In particular, the ability in Chapter 4 to combine measurements of $\delta^{18}O_{diatom}$ and $\delta^{18}O_{foram}$ to obtain a seasonally resolved record of changes in palaeoceanographic conditions is

significant and worthy of attempting to repeat in future studies.

In Part 2, the background and relevance of BSi measurements in palaeoenvironmental reconstructions is examined within the context of investigating the global silicon cycle. A summary of the potential problems with BSi measurements is outlined with an emphasis on the issues of sample methodology and the impact of dissolution. These issues form the basis of the research presented in Chapter 6-8 and are similar in theme to many of the issues discussed in Chapter 2-5 concerning dissolution and silica maturation in $\delta^{18}O_{diatom}$. Chapter 6 outlines existing techniques for measuring BSi concentrations as well as the limitations associated with each method. A sequential Si/Al extraction technique is then introduced, which is argued to provide a more accurate and direct accountability for the dissolution of aluminosilicates. By applying both the sequential Si/Al and conventional wet-alkaline digestion techniques to a range of marine and lacustrine sediment samples from around the globe, it is shown that the Si/Al technique significantly lowers measured BSi concentrations for samples which undergo a significant non-BSi digestion phase during the first two hours of sediment digestion.

The validity of the sequential Si/Al technique is subsequently investigated in Chapter 7 by analysing two sediment cores covering the late glacial/Holocene interval in Lake Baikal, Russia. By comparing BSi measurements to diatom biovolume concentrations, which should provide a more accurate indicator of the true amount of BSi within a sample, it is shown that neither the Si/Al method nor the conventional Si only method are suitable for deriving detailed quantitative palaeoenvironmental information on diatom productivity. Chapter 8 subsequently investigates this issue in greater detail by examining the glacial sediment record from Lake Baikal, which is characterised by extremely high levels of diatom dissolution. Similar to Chapter 7, results in Chapter 8 indicate a very poor relationship between BSi concentrations and measurements of diatom biovolumes. Through comparisons with existing profiles available from the lake, it is suggested that the high level of diatom dissolution removes significant quantities of biogenic derived silica from the sediment record. This, prevents measurements of BSi from being able to accurately detect changes in diatom concentrations, changes which can instead only be observed through time consuming microscopy work. This indicates that non-isotope attempts to investigate the silicon cycle and changes in diatom productivity should be based around the use of diatom biovolume concentrations rather than any geochemical based measurement.

The thesis concludes with Chapter 9, which summarises the findings of the thesis and their relevance within the context of existing research. Within this, future research directions concerning the use of $\delta^{18}O_{diatom}$ and sedimentary concentrations of BSi in palaeoenvironmental reconstructions are discussed. Copies of individual papers based on all these chapters which have been published or submitted for publication are included in the Appendix.

Part 1: Diatom oxygen isotopes

Chapter 1: Isotopes

1.1. Stable isotopes

Stable isotopes of a single element are atoms whose nuclei contain the same number of protons, but different numbers of neutrons. Although virtually identical, variations in the atomic mass cause minor chemical and physical differences between individual isotopes of a single element. These isotopic variations, through biological, chemical and/or physical processes, result in isotopic fractionations which create distinct isotope signatures within individual compounds. As such, the isotopic ratio of any biogenic or minerogenic sample provides information as to the environmental conditions and/or processes in which the sample either lived or was precipitated.

Isotope measurements are recorded as δ, the difference between the analysed sample and a laboratory working standard, and are reported in parts per mille (‰):

$$\delta_{Sample}(\text{in } ‰) = \frac{R_{Sample} - R_{Standard}}{R_{Standard}} \cdot 1000 \qquad \text{(Eq. 1)}$$

where R_{Sample} is the isotope ratio of the compound being analysed and $R_{Standard}$ is the isotope ratio of the working/laboratory standard. Working standards are in turn calibrated with respect to internationally accepted standards, such as those issued by the International Atomic Energy Agency (IAEA) or the National Institute of Standards and Technology (NIST) to enable inter-laboratory comparison of isotope data. Oxygen and carbon isotope standards for carbonates and organic matter are measured relative to V-PDB (Vienna – PeeDee Belemnite). However, oxygen isotopes from waters and silicates are quoted relative to V-SMOW (Vienna – Standard Mean Oceanic Water).

Detailed theoretical and background information on stable isotopes and their application in palaeoenvironmental geochemistry are contained within Urey (1947), O'Neil (1986), Criss (1999) and Hoefs (2004). Below, the processes relating to equilibrium and kinetic isotope exchanges, the most significant forms of isotope fractionation, are briefly summarised in Sections 1.1.1 and 1.1.2. In Section 1.1.3, the application of stable isotopes to palaeoceanographic research is summarised.

1.1.1. Equilibrium isotope exchange

Equilibrium isotope exchanges are isotope changes or a "redistribution" of isotopes between two or more compounds in which no overall net reaction occurs. During such exchanges, heavier isotopes preferentially fractionate into compounds with a higher oxidation state. For example, during phase state changes between water vapour and liquid the gas becomes enriched in ^{16}O and ^{1}H while the liquid increases in ^{18}O and ^{2}H. Within equilibrium isotope exchange, an

equilibrium constant K exists. K is primarily temperature dependent with any pressure dependency usually below analytical detection limits (Clayton *et al.*, 1975). As a broad generalisation, the higher the temperature, the less equilibrium isotope fractionation between two compounds.

1.1.2. Kinetic effects/isotope exchanges

Kinetic effects represent a unidirectional, but typically incomplete, fractionation in which an overall net reaction takes place, such as may occur during evaporation, diffusion, dissociation or some form of biological process in which the product of the reaction becomes physically separated from the reactant (Hoef, 2004). The magnitude of any fractionation is dependent upon reaction rates (determined by the reactive pathways and the energy involved in separating and forming new bonds), isotope abundances in the reactant, environmental conditions and the impact of any vital or life effect. Since bonds between lighter isotopes in the reactant are broken and reacted more easily, the newly formed compound will be preferentially enriched in lighter isotopes while the reactant will become enriched in heavier isotopes.

For both equilibrium and kinetic exchanges, the fractionation of isotopes between two bodies can be defined by the fractionation factor α or the separation factor ε:

$$\alpha_{P-R} = \frac{R_P}{R_R} \qquad \text{(Eq. 2)}$$

where R_P and R_R are the ratio of isotopes in the product and reactant respectively and:

$$\varepsilon_{P\text{-}R} = (\alpha_{P\text{-}R} - 1) \bullet 1000 \qquad \text{(Eq. 3)}$$

1.1.3. Palaeoceanographic application of stable isotopes

The use of stable isotopes to reconstruct palaeoceanographic changes was first proposed by Urey (1947, 1948) who linked $\delta^{18}O$ variations in marine calcite to changes in temperature. This, together with subsequent work on planktonic and benthic foraminifera, resulted in a more detailed understanding as to the occurrence and mechanisms of glacial-interglacial cycles (e.g., McCrea 1950; Urey *et al.*, 1951; Emiliani 1955, 1971; Shackleton, 1967, 1974) as well as the development of a series of palaeotemperature equations (O'Neil *et al.*, 1969; Shackleton 1974; Hays and Grossman 1991). Today, marine $\delta^{18}O$ records from biogenic and inorganic carbonates permit, amongst others, the reconstruction of changes in deep water formation, surface and bottom water temperature, salinity, global ice volume and water column stratification (e.g., Mulitza *et al.*, 1997; Barrera and Johnson 1999; Niebler *et al.*, 1999; Ravelo and Andreasen

1999; Zachos *et al.*, 2001; Simstich *et al.*, 2003; Rohling *et al.*, 2004). In particular, oxygne isotope records of foraminifera ($\delta^{18}O_{foram}$) have provided detailed insights into palaeoclimatic changes over both long, glacial-interglacial and geological, timescales (e.g., Zachos *et al.*, 2001) and over shorter, millennial, timescales such as those studies focusing on Heinrich and Dansgaard-Oeschger events (e.g., Skinner *et al.*, 2003). Similarly, the analysis of other isotopes in marine carbonates, including $\delta^{11}B$, $\delta^{13}C$ and $\delta^{15}N$, has allowed the reconstruction of a series of other parameters including surface water pCO_2, ocean circulation, nutrient utilisation and palaeoproductivity (e.g., Duplessy *et al.*, 1988; Kroon and Ganssen, 1989; Pearson and Palmer, 1999, 2000). Within lacustrine environments, stable isotopes from carbonates have also resulted in a similarly large range of variables being inferred from both biogenic and non-biogenic material (see Leng and Marshall, 2004; Leng *et al.*, 2005a and references within).

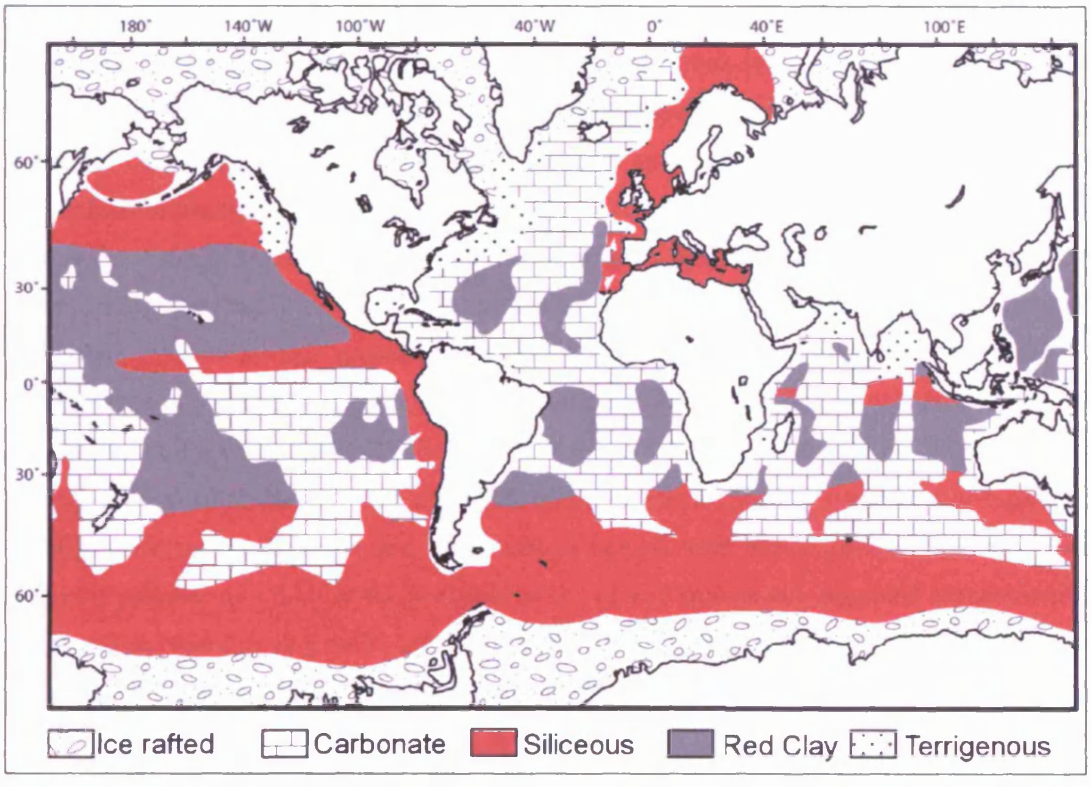

Figure 1: Global distribution of different marine sediment types. Redrawn from Open University, (1989).

While sources of carbonate, both biogenic and non-biogenic, represent one of the most common and valuable archives of stable isotope data for palaeoceanographic reconstructions, a major limitation of their use is the absence of carbonates and in particular biogenic carbonates from many siliceous dominated regions (Fig. 1). This is most notable in high latitude regions such as the North Pacific Ocean and the Southern Ocean which are increasing viewed to be both sensitive to and potential drivers of global climatic change (e.g., Shackleton, 2000; Brzezinski *et al.*, 2002). Despite the absence of carbonates, siliceous records from these regions have long

provided considerable palaeoceanographic data (e.g., Bianchi and Gersonde, 2004; Kohfeld *et al.*, 2005). In particular diatom microfossils, unicellular siliceous eukaryotic algae, have been heavily used; both in transfer function to reconstruct Sea Surface Temperatures (SST) and sea-ice extent (e.g., Crosta *et al.*, 2004; Gersonde *et al.*, 2005) and through measurement of sedimentary Biogenic Silica (BSi) concentrations to reconstruct changes in palaeoproductivity (e.g., Romero *et al.*, 2003; Kienast *et al.*, 2006). However, although these records have resulted in many significant palaeoceanographic reconstructions, it remains desirable to also generate biogenic records of $\delta^{18}O$ from these non-carbonate marine sites.

Firstly, isotope records of $\delta^{18}O$ in high latitude non-carbonate regions would complement and extend existing $\delta^{18}O$ studies derived from foraminifera and other carbonates at low/mid latitudes. This would create a global network of isotope records which could provide a more detailed insight as to past global and regional palaeoceanographic events. Secondly, the incorporation of palaeoenvironmental information is different for both isotope and non-isotope samples. As discussed in more detail below, the $\delta^{18}O$ signal of a biogenic or inorganic sample is generally a direct function of both local and global changes in temperature, mineralisation/calcification processes, habitat, global ice volume and other regional/local processes. In contrast the palaeoclimatic record inferred from biological assemblages within the sediment is additionally influenced by processes such as inter- and intra-species competition, migration, dissolution and taxonomic evolution. Furthermore, any reconstruction from fossil assemblages may also be dependent on the mathematical uncertainties associated with the use of transfer functions (e.g., Birks, 1998; Telford *et al.*, 2004; Telford and Birks, 2005). While it is not possible to state that any one approach, isotope, geochemical or otherwise is superior, the notably different mechanisms and uncertainties behind both isotope and non-isotope records makes it possible to minimise the potential errors of any palaeoenvironmental reconstruction, if both are used together in a multi-proxy study. As such, it is necessary to investigate and develop potential archives of $\delta^{18}O$ which may be suitable for providing further insights into the nature of past climatic and oceanographic changes in carbonate free regions.

Certain types of biogenic silica, in particular diatoms, often flourish in high latitude regions and at other locations where carbonates are either rare or not present within the sediment record. Recent years have also witnessed considerable advancements in the techniques associated with analysing stable isotopes in diatoms ($\delta^{18}O$, $\delta^{30}Si$, $\delta^{13}C$ and $\delta^{15}N$) (e.g., De La Rocha, 2002; Robinson *et al.*, 2004; Lücke *et* al., 2005). As such, diatoms are widely considered to have significant potential for bridging the current absence of a biological archive of $\delta^{18}O$ in non-carbonate lacustrine and marine systems (see reviews in Leng and Barker 2006, De La Rocha, 2006). The sections below review existing work on the development and usage of $\delta^{18}O_{diatom}$ in palaeoceanography. Existing work has shown the unsuitability in analysing other common

marine siliceous organisms such as radiolarians and siliceous sponges for $\delta^{18}O$ with no systematic equilibrium or thermodynamic isotope fractionation occurring between these organisms and the surrounding water (Mopper and Garlick, 1971; Matheney and Knauth, 1989). As such, these organisms are not considered further.

1.2. Oxygen isotopes in diatoms

Oxygen has three stable isotopes: ^{16}O (99.7630%), ^{17}O (0.0375%), ^{18}O (0.1995%) (Garlick, 1969). All silicates, including diatoms, are composed of silica tetrahedrons. Following the uptake and fractionation of oxygen, covalent -Si-O-Si bonds are formed in the diatom frustule through the condensation of two Si-OH groups to form $(SiO_2)_n$:

$$\text{-Si-OH + -Si-OH} \rightarrow \text{-Si-O-Si + } H_2O \qquad \text{(Eq. 4)}$$

Within the centre of the diatom frustule the -Si-O-Si bonds form an isotopically homogeneous dense layer of silica, the $\delta^{18}O$ of which is assumed to reflect the $\delta^{18}O$ of the water in which the oxygen was fractionated (Julliet, 1980a,b) (Fig. 2). Around this, a series of weak -Si-O bond exist.

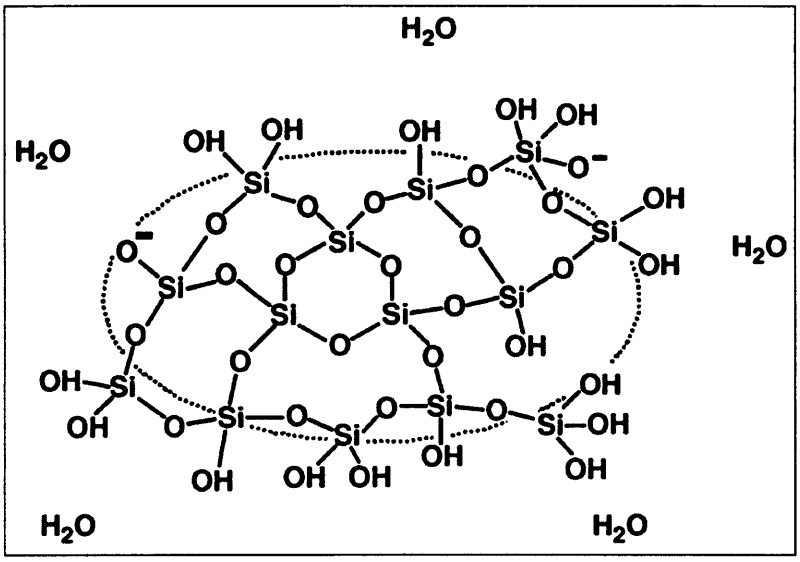

Figure 2: Schematic structure of diatom silica showing the isotopically homogeneous inner -Si-O-Si and the outer -Si-O layer which forms a -Si-OH hydroxyl bond (modified from Perry (1989)).

This weakly bonded, less dense, outer layer of the frustule represents a notable problem for analysing $\delta^{18}O_{diatom}$ with water able to freely attach to form a -Si-OH bond of cubic silica, cristobalite, held together by a hydrated silica gel (Hurd *et al.*, 1979) (Fig. 2). With the porosity of diatoms relatively high (Lewin, 1961), any water used during sample preparation or

atmospheric moisture within the laboratory can easily diffuse into and out of the -Si-OH layer of the diatom causing isotopic exchange during dehydroxylation and hydroxylation. Consequently, between 7% and 30% of all the oxygen in a diatom frustule may originate during the laboratory preparation of a sample for isotope analysis (Knauth, 1973; Labeyrie, 1979; Labeyrie and Juillet, 1982; Leng *et al.*, 2001). Given the importance of accounting for the -Si-OH layer, Section 1.3 below reviews existing methodologies for measuring $\delta^{18}O_{diatom}$. Section 1.4 subsequently reviews the palaeoceanographic processes which control $\delta^{18}O$ changes in the inner -Si-O-Si layer, which is believed to contain a preserved fossil surface water signal.

1.3. Methodologies

Several techniques have been developed for extracting pure and clean diatoms from sediment samples (Table 1). A key pre-requisite of any isotope analysis is the necessity of ensuring samples are free from all sources of non-diatom contamination. Existing work has demonstrated $\delta^{18}O_{diatom}$ to be highly sensitive to the level of non-diatom material within the sample, particularly when sample purity falls below 90% (Morley *et al.*, 2004). Obtaining pure diatom material is physically, though not technically, difficult with diatoms intermixed with similar sized clay and/or silt particles, necessitating the need for a series of chemical and physical preparation stages (Shemesh *et al.*, 1995; Morley *et al.*, 2004; Rings *et al.*, 2004; Tyler *et al.*, 2007). Provided samples are "clean", issues of contamination should be negligible and can be further corrected for through mass balance corrections (Morley *et al.*, 2005; Lamb *et al.*, 2007)

Table 1: Techniques for preparing and extracting pure diatoms samples for isotope analysis

Study
Juillet-Leclerc, (1986)
Morley *et al.* (2004)
Rings *et al.* (2004)
Tyler *et al.* (2007)

As detailed above, for palaeoenvironmental signals to be extracted from $\delta^{18}O_{diatom}$ it is essential to remove or account for the -Si-OH outer hydrous layer which is subject to isotope exchanges during sample preparation and storage. Extraction of the -Si-O-Si layer however, which may require the removal of 20-30% of the total amount of oxygen within diatoms (Leng *et al.*, 2001), is technically challenging requiring specialised equipment, hazardous reagents and highly trained users. Initial attempts to remove the oxygen from the hydroxyl layer involved dehydrating samples under vacuum at 800-1000°C (Mopper and Garlick, 1971; Labeyrie, 1974, 1979). Although analytical reproducibility and accuracy improved (Labeyrie, 1974; Mikkelsen *et al.*, 1978; Wang and Yeh, 1985), the $\delta^{18}O_{diatom}$ signal under vacuum dehydration remained contaminated due to partial isotopic exchanges during sample dehydration (Labeyrie, 1979;

Labeyrie and Juillet, 1982). To date, three reliable techniques have have been established which fully account for the -Si-OH layer (Table 2): Controlled Isotope Exchange (CIE) before fluorination using a fluorine based reagent such as ClF_3 or BrF_5 (Labeyrie and Juillet, 1982; Juillet-Leclerc and Labeyrie, 1987), Stepwise Fluorination (SWF) (Haimson and Knauth 1983; Matheney and Knauth 1989) and inductive High-Temperature carbon Reduction (iHTR) (Lücke *et al.*, 2005).

Table 2: Techniques for analysing $\delta^{18}O_{diatom}$

Study	*Method*
Juillet, (1980a)	Vacuum Dehydration
Juillet, (1980b)	Vacuum Dehydration
Labeyrie and Juillet, (1980)	Vacuum Dehydration
Labeyrie and Juillet, (1982)	Controlled Isotope Exchange
Haimson and Knauth, (1983)	Fluorination
Thorliefson and Knauth, (1984)	Fluorination
Matheney and Knauth, (1989)	Fluorination
Lücke *et al.* (2005)	iHTR

Under controlled isotope exchange, water in the outer hydrous layer of the diatom is replaced with water containing a known $\delta^{18}O$ ratio at 200°C for six hours (Labeyrie and Juillet, 1982; Juillet-Leclerc and Labeyrie, 1987). After vacuum heating at 1000°C to remove as much of the water in the -Si-OH layer as possible, samples are reacted with a fluorine regent to release all remaining oxygen within the diatom frustules. Mass-balance corrections are then applied to correct for any of the labelled water not removed under vacuum:

$$\delta^{18}O_{measured} = x\delta^{18}O_{water} + (1 - x)\,\delta^{18}O_{non\text{-}exch} \quad \text{(Eq. 5)}$$

where $\delta^{18}O_{measured}$ is the measured $\delta^{18}O$ of the sample after vacuum heating, $\delta^{18}O_{non\text{-}exch}$ is the $\delta^{18}O$ of the -Si-O-Si layer within the diatom, $\delta^{18}O_{water}$ is the $\delta^{18}O$ of the labelled water and x is the level of oxygen exchangability in the diatom.

SWF techniques involve the use of a fluorine reagent to extract the oxygen from different layers of the diatom in separate stages, thereby avoiding contamination between the oxygen in the -Si-OH and -Si-O-Si layers (Haimson and Knauth, 1983; Thorliefson and Knauth, 1984; Matheney and Knauth, 1989). Using adaptations of the fluorination procedures established by Taylor and Epstein (1962) and Epstein and Taylor (1971), the -Si-OH layer is stripped away leaving behind the inner -Si-O-Si layer which contains the fossil $\delta^{18}O$ signal. Continuous measurements throughout the process indicate an increasing $\delta^{18}O$ signal during this first stage reflecting the gradual removal of the -Si-OH layer from the diatom (Haimson and Knauth, 1983; Leng *et al.*,

1998). A plateau in $\delta^{18}O$ is subsequently reached representing complete removal of the -Si-OH layer with only the isotopically homogeneous -Si-O-Si layer remaining in the frustule (ibid). A second fluorination stage is subsequently used to liberate oxygen from the -Si-O-Si layer, which is converted to CO_2 and analysed using standard mass spectrometry techniques.

While both CIE and SWF techniques have been readily used to measure $\delta^{18}O_{diatom}$, both methods suffer from limitations. Both necessitate the use of highly volatile chemicals such as ClF_3 or BrF_5. The pre-fluorination stage in the SWF methodology will, however, act to remove a proportion of the non-diatom contamination in samples, ensuring more reliable results (Matheney and Knauth, 1989). In addition, the SWF process should remove all oxygen within the -Si-OH layer regardless of diatom size or age, although the point at which the $\delta^{18}O$ plateau is reached during removal of the -Si-OH layer may vary and require calibration for different samples (Leng and Barker, 2006). With CIE, concerns exist as to the extent to which oxygen in the -Si-OH layer fully exchanges with the oxygen in the labelled water. With suggestions that this can vary significantly between different aged samples, the possibility exists that not all of the contaminant oxygen in the hydroxyl layer is fully removed prior to vacuum heating, particularly in living/recently deposited diatoms and in diatoms which contain a large hydroxyl layer (Juillet, 1980a, b; Schmidt *et al.*, 1997; Brandriss *et al.*, 1998). Direct comparisons of both CIE and SWF techniques have previously indicated similar results (Schmidt *et al.*, 1997). However, since greater uncertainty exists overs the CIE method, due to the possibility of incomplete oxygen exchange and due to the measured $\delta^{18}O_{diatom}$ being dependent on the isotopic composition of the labelled water, calibration of the CIE technique against SWF results is generally advised (Schmidt *et al.*, 1997). Within this thesis all diatom samples are analysed for $\delta^{18}O_{diatom}$ using the SWF method.

A major problem of both the CIE and SWF methods is the magnitude of analytical reproducibility, which, can be as poor as ±0.5‰. This implies that if diatom-temperature coefficients are as low as −0.2‰/°C (see Section 1.4.1) (Brandriss *et al.*, 1998; Moschen *et al.*, 2005), changes of up to 2-3°C may be undetectable in the sediment record. Recent developments in $\delta^{18}O_{diatom}$, however, have demonstrated the potential of a iHTR method, which eliminates the need for a fluorine based reagent and which also improves reproducibility to less than 0.15‰ (Lücke *et al.*, 2005). In iHTR, diatoms are mixed with graphite and heated under vacuum at 1,550°C. Following the volatilisation of sample contaminants and the outer hydroxyl layer at 850°C-1,050°C, oxygen from the -Si-O-Si bonds are converted to CO_2 for analysis. As yet, this method has yet to be replicated and fully testing elsewhere. However, given the potential for more precise $\delta^{18}O_{diatom}$ measurements and the non-requirement for the use of fluorine compounds, it is likely that iHTR will increase the number of laboratories analysing $\delta^{18}O_{diatom}$ in the future.

1.4. Marine controls

Four major influences affect the marine $\delta^{18}O$ record (Equation 6; Table 3). The first is the temperature at which opal is precipitated (δ_T) with warmer water leading to lower $\delta^{18}O_{diatom}$. Second is the $\delta^{18}O$ of the water ($\delta^{18}O_{water}$) in which the diatom frustule is formed. This in turn is controlled by both global influences, such as the amount of freshwater stored in ice sheets ($\delta^{18}O_{Global\ Ice\ Volume}$ ($\delta^{18}O_{GIV}$)), and the local influence at a given site of evaporation, freshwater inputs, salinity and changes in water mass or ocean circulation ($\delta^{18}O_{local}$). In addition, vital effects may or may not exist, Section 1.4.4, which could alter $\delta^{18}O_{diatom}$ within and between individual species. Consequently:

$$\Delta\delta^{18}O_{diatom} = \Delta\delta_T + \Delta\delta^{18}O_{water} = \Delta\delta_T + \Delta\delta^{18}O_{GIV} + \Delta\delta^{18}O_{local} \pm \text{vital effects} \quad \text{(Eq. 6)}$$

The actual mechanisms which control changes in each of these variables, e.g., the mechanisms causing glacial-interglacial cycles and the subsequent growth in ice sheets and associated increase in $\delta^{18}O_{water}$, are not discussed within this chapter. Instead, these processes are detailed within individual chapters where relevant to the interpretation of any data. Instead, the sections below summarise the extent to which a change in any of the variables in equation 6 alters $\delta^{18}O_{diatom}$.

Table 3: Environmental influences on $\delta^{18}O$ in marine systems (from Maslin and Swann, 2005)

Environmental Factor	*Increase*	*Decrease*
Temperature	$\delta^{18}O$ decrease	$\delta^{18}O$ increase
Global Ice Volume	$\delta^{18}O$ increase	$\delta^{18}O$ decrease
Salinity*	$\delta^{18}O$ increase	$\delta^{18}O$ decrease
Density*	$\delta^{18}O$ increase	$\delta^{18}O$ decrease
* sea ice formation can increase surface water salinity and density while lowering surface water $\delta^{18}O$ since $\delta^{18}O$ increases in the formation of ice from water (O'Neil 1968). This affect though is minimal and does not influence palaeoenvironmental records.		

1.4.1. Temperature

Initial attempts to calculate a $\delta^{18}O_{diatom}$-temperature coefficient suggested that a similar isotope equilibrium curve existed between diatoms (Labeyrie, 1974) and that previously established for calcite (e.g., Epstein *et al.*, 1953). Subsequent calibrations have demonstrated significantly different gradients between the two curves by approximately a factor of two (Juillet-Leclerc and Labeyrie, 1987; Matheney and Knauth, 1989; Shemesh *et al.*, 1992; Brandriss *et al.*, 1998; Moschen *et al.*, 2005). The results obtained by Labeyrie (1974) may therefore either indicate a failure to adequately remove the -Si-OH layer or a failure to sufficiently clean the analysed diatom frustules of contaminants prior to analysis. The first, still respected, $\delta^{18}O_{diatom}$-

temperature calibration was developed by Juillet-Leclerc and Labeyrie (1987) who analysed SST, $\delta^{18}O_{water}$ and the $\delta^{18}O$ of marine diatoms from surface sediment assemblages around the globe to produce a palaeotemperature calibration between 1.5°C and 24°C of:

$$1000 \ln \alpha = 3.26 \frac{10^6}{T^2} + 0.45 \qquad \text{[In Kelvin]}$$

(Eq. 7)

or

$$T = 17.2 - 2.4(\delta^{18}O_{diatom} - \delta^{18}O_{water} - 40) - 0.2(\delta^{18}O_{diatom} - \delta^{18}O_{water} - 40)^2$$

(Eq. 8)

where α is the fractionation coefficient between diatoms and ambient water and T is temperature. Although supported by data from marine diatoms in Matheney and Knauth (1989), Shemesh *et al.* (1992) suggested the calibration of Juillet-Leclerc and Labeyrie (1987) to be inaccurate in high latitude waters where localised upwelling imparts a significant control on the diatom-water oxygen isotope equilibrium. Support for this originates from the Southern Ocean where core-top $\delta^{18}O_{diatom}$ data suggests a SST of 8.8°C, under the calibration of Juillet-Leclerc and Labeyrie (1987), whereas observed SST in the region peak at below 4°C (Shemesh *et al.*, 1992). Based on core-top samples from the Southern Ocean, Shemesh *et al.* (1992) therefore proposed a high latitude SST calibration of :

$$T = 11.03 - 2.03(\delta^{18}O_{diatom} - \delta^{18}O_{water} - 40)$$

(Eq. 9)

The calibration of Shemesh *et al.* (1992), however, remains controversial (Clayton 1992; Shemesh, 1992). Despite this both the calibrations of Juillet-Leclerc and Labeyrie (1987) and Shemesh *et al.* (1992), in addition to other work by Matheney and Knauth (1989), suggest a relatively high $\delta^{18}O_{diatom}$-temperature coefficient of between −0.3‰/°C and −0.5‰/°C (Fig. 3). In contrast, more recent investigations suggest a lower coefficient of −0.2‰/°C in freshwater diatoms (Brandriss *et al.*, 1998; Moschen *et al.*, 2005) (Fig. 3):

$$T = 171.12 - 4.68 \, (\delta^{18}O_{diatom} - \delta^{18}O_{water})$$

(Eq. 10: Brandriss *et al.* (1998))

$$T = 190.07 - 5.05 \, (\delta^{18}O_{diatom} - \delta^{18}O_{water})$$

(Eq. 11: Moschen *et al.* (2005))

Due to this, considerable uncertainty currently exists with regards to the true $\delta^{18}O_{diatom}$-temperature coefficient (Fig. 3). The marked difference between the higher, −0.3‰/°C to −0.5‰/°C, coefficients from marine systems (Matheney and Knauth 1989; Juillet-Leclerc and

Labeyrie, 1987; Shemesh *et al.*, 1992) compared to the lower values of −0.2‰/°C in lacustrine systems (Brandriss *et al.*, 1998; Moschen *et al.*, 2005) may reflect improvements in the analytical procedures for measuring $\delta^{18}O_{diatom}$. With all marine calibrations conducted over 15 years ago, compared to lacustrine calibrations calculated in the last 10 years, the coefficient of −0.2‰/°C may be more accurate. Alternatively, the different coefficients may indicate a systematic vital effect between lacustrine and marine diatoms. At present, due to the absence of further calibration work on marine diatoms, it remains unknown whether the lower, freshwater based, or higher, marine based, coefficient should be used in palaeoceanographic work.

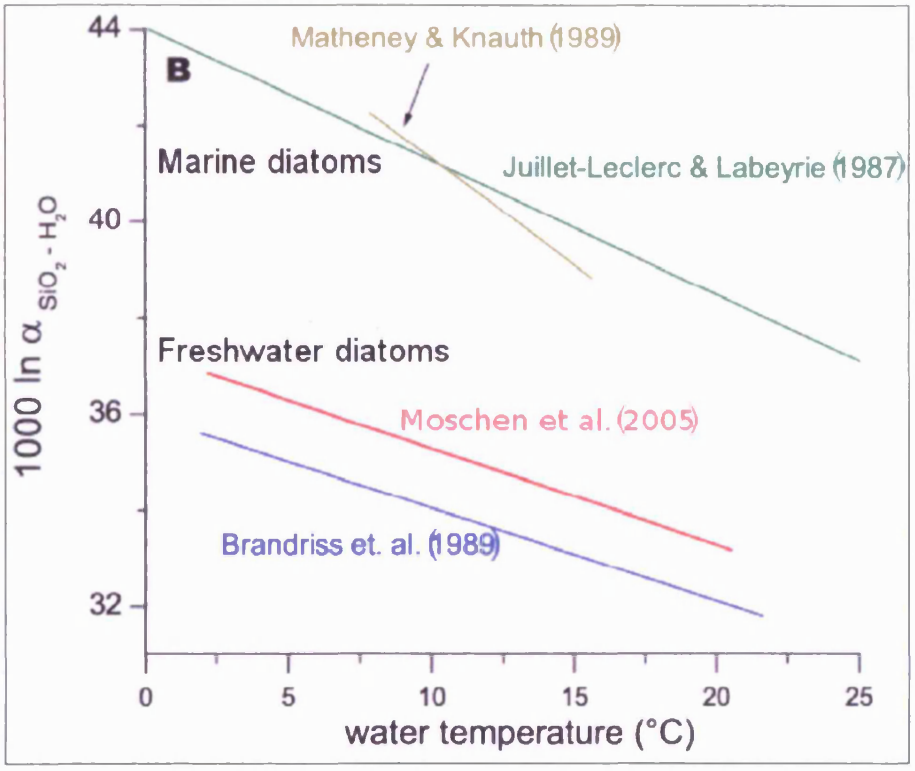

Figure 3: Range of $\delta^{18}O_{diatom}$-temperature calibrations (adapted from Moschen *et al.*, 2005).

Many early palaeoceanographic investigations using records of $\delta^{18}O_{diatom}$ prior to the mid-1980's are now known to have been compromised by the failure to sufficiently account for the -Si-OH layer in diatoms (e.g., Labeyrie 1974; Mikkelsen *et al.*, 1978; Wang and Yeh, 1985). Since then, only a limited number of studies have attempted to use $\delta^{18}O_{diatom}$ in palaeoceanographic reconstructions (Table 4). This compares with the relative widespread use of $\delta^{18}O_{diatom}$ in palaeolimnological reconstructions over the past decade (Table 5). In the first marine study unaffected by issues of -Si-OH contamination, Sancetta *et al.* (1985) related changes in $\delta^{18}O_{diatom}$ within the Bering Sea to shifts in the diatom flora in order to infer changes in SST and Sea Surface Salinity (SSS). Similarly, Juillet-Leclerc and Schrader (1987) reconstructed changes in SST and surface water upwelling in the Gulf of California finding SST variations of 5°C over the last 3,000 years. While in Sancetta *et al.* (1985) the effect of $\delta^{18}O_{GIV}$ on $\delta^{18}O_{diatom}$ was not

considered, in Juillet-Leclerc and Schrader (1987) the contribution of $\delta^{18}O_{GIV}$ was assumed to be negligible due to the minimal changes in global ice volume over this interval (Section 1.4.2).

Table 4: Summary of modern and fossil marine $\delta^{18}O_{diatom}$ studies. Shaded rows indicate publications arising from research carried out during the PhD and presented within this thesis.

Study	*Study Type*	*Location*	*Method*
Labeyrie, (1974)	Calibration	Global	VD
Mikkelsen *et al.* (1978)	Reconstruction	Equatorial Pacific Ocean	VD
Labeyrie, (1979)	PhD Thesis	Southern Ocean	VD
Sancetta *et al.* (1985)	Reconstruction	Bering Sea	CIE
Wang and Yeh, (1985)	Reconstruction	Gulf of California	VD
Labeyrie *et al.* (1986)	Reconstruction	Southern Ocean	CIE
Juillet-Leclerc and Labeyrie, (1987)	Calibration	Global	CIE
Juillet-Leclerc and Schrader, (1987)	Reconstruction	Gulf of California	CIE
Shemesh *et al.* (1992)	Reconstruction	Southern Ocean	CIE
Shemesh *et al.* (1994)	Reconstruction	Southern Ocean	CIE
Shemesh *et al.* (1995)	Reconstruction	Southern Ocean	CIE
Schmidt *et al.* (1997)	Surface water and culture	Global	CIE
Hodell *et al.* (2001)	Reconstruction	Southern Ocean	CIE
Schmidt *et al.* (2001)	Surface water, core tops and culture	Global	CIE
Shemesh *et al.* (2002)	Reconstruction	Southern Ocean	CIE
Haug *et al.* (2005)	Reconstruction	North Pacific Ocean	SWF
Swann *et al.* (2006)	Reconstruction	North Pacific Ocean	SWF
Swann *et al.* (2007)	Vital effects	North Pacific Ocean	SWF

Table 5: Summary of modern and fossil lacustrine $\delta^{18}O_{diatom}$ studies.

Study	*Study Type*	*Location*	*Method*
Binz (1987)	Culture	-	CIE
Brandriss *et al.* (1998)	Culture	-	VD, CIE & SWF
Rietti-Shati *et al.* (1998)	Reconstruction	Mount Kenya, Kenya	CIE
Shemesh and Peteet (1998)	Reconstruction	Connecticut, USA	CIE
Raubitschek *et al.* (1999)	Theoretical	Lake Holzmaar, Germany	-
Rosqvist *et al.* (1999)	Reconstruction	South Georgia, Antarctica	CIE
Barker *et al.* (2001)	Reconstruction	Mount Kenya, Kenya	SWF

Study	*Study Type*	*Location*	*Method*
Leng *et al.* (2001)	Reconstruction	Lake Pinarbasi, Turkey	SWF
Rioual *et al.* (2001)	Reconstruction	Massif Central, France	CIE
Shemesh *et al.* (2001a)	Reconstruction	Northern Sweden	CIE
Shemesh *et al.* (2001b)	Reconstruction	Massif Central, France	CIE
Hu and Shemesh, (2003) (Hu *et al.*, 2003)	Reconstruction	South West, Alaska	CIE
Chondrogianni *et al.* (2004)	Reconstruction	Lake Albano, Central Italy	CIE
Jones *et al.* (2004)	Reconstruction	Lake Chuna, Russia	SWF
Rosqvist *et al.* (2004)	Reconstruction	Northern Sweden	CIE
Street-Perrott *et al.* (2004)	Reconstruction	Mount Kenya, Kenya	SWF
Kalmychkov *et al.* (2005)	Reconstruction	Lake Baikal, Russia	SWF
Lamb *et al.* (2005)	Reconstruction	Lake Tilo, Ethiopia	SWF
Leng *et al.* (2005b)	Reconstruction	Laguna Zacapu, Mexico	SWF
Morley *et al.* (2005)	Reconstruction	Lake Baikal, Russia	SWF
Moschen *et al.* (2005)	Calibration	Lake Holzmaar, Germany	iHTR
Moschen *et al.* (2006)	Calibration	Lake Holzmaar, Germany	iHTR
Polissar *et al.* (2006)	Reconstruction	Venezuelan Andes	CIE
Barker *et al.* (2007)	Reconstruction	Lake Malawi	SWF

1.4.2. Global ice volume

Prior to the growth of large ice sheets, which occurred in Antarctica from 34 Ma (Kennett and Shackleton, 1976; Miller *et al.*, 1991; Zachos *et al.*, 1996, 2001; Lear *et al.*, 2000) and potentially in Greenland from 38 Ma (Eldrett *et al.*, 2007), records of $\delta^{18}O$ in biological organisms are broadly a function of changes in δ_T and $\delta^{18}O_{local}$. Following the transition to and intensification of glacial-interglacial cycles, the relative impact of global ice volume on $\delta^{18}O_{water}$ and consequently $\delta^{18}O_{diatom}$ increases significantly. While the exact contribution of $\delta^{18}O_{GIV}$ on $\delta^{18}O_{diatom}$ will vary according to the magnitude of global ice volume change over each glacial-interglacial cycle, average Quaternary variations in $\delta^{18}O_{water}$ in response to changes in ice volume are on the order of c. 1-2‰ (Lisiecki and Raymo, 2005). Consequently, except for time-slice studies or for periods in which changes in $\delta^{18}O_{GIV}$ are minimal, post-Eocene measurements of $\delta^{18}O_{diatom}$ need to be corrected for $\delta^{18}O_{GIV}$ in order to reconstruct δ_T, $\delta^{18}O_{local}$ or other photic zone changes.

Given the absence of benthic diatoms which live and silicify in ocean bottom waters, $\delta^{18}O_{GIV}$ is best derived from benthic $\delta^{18}O_{foram}$, which is predominantly controlled by changes in $\delta^{18}O_{GIV}$ (Shackleton, 1967). Although uncertainties exist over the impact of deep ocean temperature changes on benthic $\delta^{18}O_{foram}$ over glacial-interglacial cycles (Schrag *et al.*, 1996, 2002; Waelbroeck *et al.*, 2002; Duplessy *et al.*, 2002), stacked records of benthic $\delta^{18}O_{foram}$ largely

eliminate this problem and are suitable for correcting $\delta^{18}O_{diatom}$ for $\delta^{18}O_{GIV}$ (e.g., Waelbroeck *et al.*, 2002; Lisiecki and Raymo, 2005). Alternatively, variations in $\delta^{18}O_{GIV}$ can also be estimated from the $\delta^{18}O$ of sediment pore water (e.g., Schrag *et al.*, 1996; 2002; Burns and Maslin 1999; Adkins and Schrag 2001). The number of studies using this to reconstruct $\delta^{18}O_{GIV}$, however, is limited with studies commonly needing to model issues of water advection and mixing within the sediment (Schrag *et al.*, 1996).

An alternative approach for correcting for $\delta^{18}O_{GIV}$ is demonstrated in Shemesh *et al.* (1992). Using the $\delta^{18}O_{diatom}$-temperature calibration detailed in equation 9, which is significantly different to the palaeotemperature fractionation curve for foraminifera, measurements of $\delta^{18}O_{diatom}$ were combined with a planktonic $\delta^{18}O_{foram}$ record in the Southern Ocean. By assuming that the incorporation of oxygen into both diatoms and foraminifera occurred in the same season and at the same water depth, changes in surface $\delta^{18}O_{water}$ and SST were solved for without the need for measurements of benthic $\delta^{18}O_{foram}$ or $\delta^{18}O_{porewater}$ to correct for $\delta^{18}O_{GIV}$:

$$\Delta T = T_1 - T_2 = 3.85[(\delta^{18}O_{diatom2} - \delta^{18}O_{diatom1}) - (\delta^{18}O_{foram2} - \delta^{18}O_{foram1})] \quad \text{(Eq. 12)}$$

and

$$\Delta\delta^{18}O_{water} = \delta^{18}O_{water1} - \delta^{18}O_{water2} = 0.89[(\delta^{18}O_{diatom2} - \delta^{18}O_{diatom1}) - 1.9(\delta^{18}O_{foram2} - \delta^{18}O_{foram1})] \quad \text{(Eq. 13)}$$

where subscripts 1 and 2 refer to the lower and upper data points of the interval respectively. Using this approach, which is entirely dependent upon the accuracy of the $\delta^{18}O_{diatom}$-temperature calibration in equation 9, Shemesh *et al.* (1992) observed a 2.0°C increase in SST over the glacial-Holocene transition with a concordant 1.2‰ decrease in $\delta^{18}O_{water}$.

1.4.3. Salinity

Changes in salinity are caused by both whole ocean salinity changes, related to changes in global ice volume, and local influences such as evaporation and freshwater input. Consequently, provided a records of SST exists (or changes in SST are minimal) and provided that changes in ocean circulation can be ruled out as influencing $\delta^{18}O_{water}$, the remaining variation in $\delta^{18}O_{diatom}$ can be related to localised changes in SSS after correction for $\Delta\delta^{18}O_{GIV}$. To enable quantitative calculations of SSS, however, an isotope end-member is required to establish the relationship between SSS and $\delta^{18}O_{diatom}$. End-members may alter following changes in evaporation, meltwater input, precipitation and river runoff such that:

$$\Delta\delta^{18}O_{local} = \frac{\delta^{18}O_{ocean} - \delta^{18}O_{freshwater}}{S_{ocean} - S_{freshwater}} \cdot S_{local} + \delta^{18}O_{freshwater}$$

(Eq. 14: Duplessy *et al.* (1991; 1992))

where $\delta^{18}O_{ocean}$ is the $\delta^{18}O$ of the ocean, $\delta^{18}O_{freshwater}$ is the $\delta^{18}O$ of the freshwater entering the system either as precipitation, meltwater or river runoff, S_{ocean} is mean ocean salinity; $S_{freshwater}$ is the salinity of the freshwater and S_{local} is the mean local salinity. Defining the exact SSS-$\delta^{18}O_{diatom}$ relationship at a given site, however, is often complicated by the large range of $\delta^{18}O$ estimates for individual ice sheets, which are commonly the dominant source of freshwater input. For example, $\delta^{18}O$ estimates for the Laurentide ice sheet range from −28‰ to −35‰ (Duplessy *et al.*, 2002). Using a value of −35‰ would results in a relationship of:

$$\Delta S_{local} = 1.12\Delta\delta^{18}O_{local}$$

(Eq. 15).

Mix and Ruddiman (1984) and Maslin *et al.* (1995a), however, have argued that a coastal value of −20‰ is more appropriate for the Laurentide ice sheets to reflect the higher $\delta^{18}O$ of icebergs and melting ice-edge ice sheets such that:

$$\Delta S_{local} = 1.76\Delta\delta^{18}O_{local}$$

(Eq. 16)

Similar debates also exists for other ice-sheets with values for the Eurasian ice sheet at the Last Glacial Maximum ranging from −16‰ to −40‰ (Duplessy *et al.*, 2002) and estimates of Antarctic glacial meltwater ranging from −40‰ to −60‰ (Grootes *et al.*, 1993). In addition, in regions affected by inputs from non-glacier fed rivers, consideration is also required as to the $\delta^{18}O$ of this freshwater, which is likely to be considerably higher than that for glaciers. Consequently, in order to reconstruct SSS at a given site, it is necessary to make assumptions as to the viable range of ice sheet $\delta^{18}O$ values and freshwater end-members which may be present, unless a time-slice approach is being undertaken. In instances where no information exists as to the true or likely end-member values, changes in SSS may be best calculated assuming a range of end-members such that:

$$\Delta S_{local} = \Delta\delta^{18}O_{local} \quad \text{or} \quad \Delta S_{local} = 2\Delta\delta^{18}O_{local}$$

(Eq. 17)

With regards to SSS based reconstructions from $\delta^{18}O_{diatom}$, records from a series of cores across the Southern Ocean have revealed periodic decreases of up to c. 5‰ in $\delta^{18}O_{diatom}$ over the last 430,000 years (Hodell *et al.*, 2001; Shemesh *et al.*, 1994; 1995; 2002). While no quantitative palaeosalinity reconstructions were done, relating such changes to increasing temperatures contradicts other palaeotemperature records from the region based on diatom based transfer functions (ibid). While a proportion of the reconstructed SSS variability is related to change in global ice volume, which was also unaccounted for, decreases in $\delta^{18}O_{diatom}$ were predominantly related to large meltwater influxes from Antarctica (Hodell *et al.*, 2001; Shemesh *et al.*, 1994;

1995; 2002). At present, due to the low resolution nature of the $\delta^{18}O_{diatom}$ record at these sites, the timing, causation and consequently implication of these large meltwater releases from Antarctica remains unknown.

1.4.4. Vital effects

From a biological and isotope perspective, the term vital effect refers to a life process which leads to isotope offsets between or within different species extracted from a core section not affected by turbidites or bioturbation. Within the literature, vital effects have been previously linked to changes in rates of calcification/silicification, pH, nutrient availability, variations in the micro-environment, vertical migration of an organism in the water column and to the incorporation of metabolic fluids. In freshwater ostracods, $\delta^{18}O$ vital effects have been shown to result in isotope deviations from equilibrium of 0.3-2.5‰ (Xia, *et al* 1997; von Grafenstein *et al.*, 1999; Chivas *et al.*, 2002; Holmes and Chivas, 2002). Within marine organisms, vital effects have been most widely studied in foraminifera with variations of up to 6‰ being documented (Duplessy *et al.*, 1970; Wefer and Berger, 1991; Spero and Lea, 1993; 1996; Spero *et al.*, 1997; Bemis *et al.*, 1998). While all the above processes have been widely referred to within the literature as "vital effects", for this thesis the term is better separated into two groups: "vital effect (sensu stricto)" and "vital effect (in equilibrium)" (Fig. 4). In this thesis, a "vital effect (sensu stricto)" is referred to simply as a "vital effect". A "vital effect (in equilibrium)" is referred to as either a "seasonality effect" or a "habitat effect".

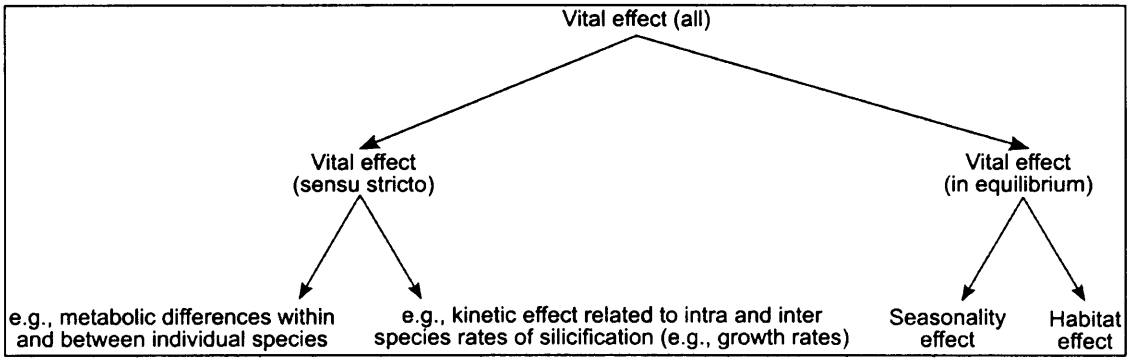

Figure 4: Break-down of vital effects which may affect $\delta^{18}O_{diatom}$.

1.4.4.1. Diatom isotope vital effects

As with other biological organisms, diatoms are assumed to be precipitated in isotope equilibrium as predicted by fractionation thermodynamics. A vital effect (sensu stricto), as defined here and henceforth referred to within this thesis as a "vital effect", refers to instance when biological organisms display kinetic or metabolic isotope fractionation offsets from equilibrium, such as may be induced following changes in diatom growth rates, nutrient availability or silicification. Within larger organisms such as foraminifera and ostracods, the issue of vital effects (in addition to the habitat effects outlined below) are eliminated by picking

individual taxa for isotope analysis which are all at a similar life cycle stage. Diatoms, though, cannot be feasibly picked out to create mono-specific samples due to their significantly smaller size (usually c. 5-75 μm). While in some instances it has proven possible to isolate different sized taxa using gravitational split-flow thin fractionation (SPLITT), which separates different particles and consequently different diatom frustules or taxa of different densities (see Rings *et al.*, 2004), in the majority of cases $\delta^{18}O_{diatom}$ data are derived from samples comprised of multiple species. To date, a limited number of culture (Binz, 1987; Brandriss *et al.*, 1998; Schmidt *et al.*, 2001), sediment trap (Moschen *et al.*, 2005) and down-core studies (Sancetta *et al.*, 1985; Juillet-Leclerc and Labeyrie, 1987; Shemesh *et al.*, 1995) in marine and lacustrine systems have found no conclusive evidence to indicate that vital effects exist in $\delta^{18}O_{diatom}$. While data in Brandriss *et al.* (1998) indicates a 0.6‰ difference between two laboratory cultured diatom taxa and Shemesh *et al.* (1995) found a 0.2‰ offset between two different size fractions of diatoms, offsets of this magnitude are within the range of reproducibility routinely achieved using fluorination based techniques for analysing $\delta^{18}O_{diatom}$. As such, $\delta^{18}O_{diatom}$ vital effects have hitherto been regarded to be either non-existent or within the analytical reproducibility of $\delta^{18}O_{diatom}$ measurements. However, given that samples analysed for $\delta^{18}O_{diatom}$ usually contain multiple taxa and given the importance of consequently ensuring that isotope vital effects are not present in $\delta^{18}O_{diatom}$, further research is needed into this issue. The issue of vital effects in $\delta^{18}O_{diatom}$ is therefore addressed within Chapters 2 and 3 of this thesis.

1.4.4.2. Habitat/seasonality effect

A habitat or seasonality effect is defined to be an offset either within or between individual taxa which occurs despite isotope fractionation occurring in equilibrium with the surrounding water. A habitat effect, as defined here, refers to the different depth habitats in the water column at which a taxa may bloom and consequently the different conditions and $\delta^{18}O_{water}$ encountered at these depths, the signals of which will be incorporated into an organism during calcification/silicification. Within foraminifera, a habitat effect most commonly arises from the different depths which separate taxa live at or from the significant vertical migration which an organism may undertake through the water column at different stages in their life cycle (Sautter and Thunell, 1991). In marine systems, any habitat effect in diatoms is likely be significantly smaller than that occurring in foraminifera due to most diatoms blooming in the photic zone close to the surface. As such, the possibility of a habitat based effect has generally been ignored in previous studies of $\delta^{18}O_{diatom}$, particularly in marine systems where photic zone depth variations in temperature and $\delta^{18}O_{water}$ are generally thought to be small. This may be unwise, however, given that photic zone depths can extend down to c. 100 m at many sites; depths which can display significantly different $\delta^{18}O_{water}$ and environmental conditions relative to those present at the surface (Antonov *et al.*, 2005; Locarnini *et al.*, 2005).

A seasonality effect refers to instance where individual species bloom in different seasons e.g., spring and autumn, at a single location. With each season possibly marked by different environmental conditions and $\delta^{18}O_{water}$ values (e.g., due to changes in temperature and meltwater input), large inter-species offsets in $\delta^{18}O_{diatom}$ may exist between different taxa collected over a year. The issue of inter-species seasonality effects may be particularly prominent in diatoms due to analysed samples usually containing a mixture of taxa, that bloom across different seasons (Raubitschek *et al.*, 1999; Leng *et al.*, 2001). However, even if a single species sample is successfully extracted and analysed for $\delta^{18}O_{diatom}$, an intra-species seasonality effect may still be present if that taxa blooms across different seasons. As such, there is a high potential for $\delta^{18}O_{diatom}$ records to be distorted by bloom-signal dilution/seasonality effects, unless bloom specific samples can be obtained. Ideally, in order to ensure that records of $\delta^{18}O_{diatom}$ are entirely unaffected by both vital effects and seasonality/habitat effects, $\delta^{18}O_{diatom}$ samples need to be comprised of a single taxa which primarily blooms within a single season over which environmental conditions are relatively stable.

1.4.5. Diatom dissolution and diagenesis

Most marine and lacustrine locations are under-saturated with respect to silica. Consequently, rates of diatom dissolution are high. While the number of measurements are low, it is estimated that only 1-10% (mean = 3%) of all living diatoms in the marine system are preserved within the sediment (Tréguer *et al.*, 1995). The extent to which dissolution occurs depends on a range of parameters including, but not restricted to, temperature (Hurd, 1972), sedimentation rate (Ragueneau *et al.*, 2000), alkalinity (Barker, 1992; Ryves *et al.*, 2006), trace metals (van Bennekom *et al.*, 1989, 1991; Dixit *et al.*, 2001; Dixit and van Cappellen, 2002; Koning *et al.*, 2007) organic coating, bacterial and other biological communities (Lewin, 1961; Jacobson and Anderson, 1986 Sullivan *et al.*, 1975; Miller *et al.*, 1990; Cowie and Hedges 1996; Bidle and Azam, 1999; Bidle *et al.*,, 2002, 2003) and the size, morphology, aggregation and silicification of individual frustules (Lewin, 1961; Lawson *et al.*, 1978; Nelson *et al.*, 1995; Ragueneau *et al.*, 2000). At any site, diatom dissolution will continue at the surface-sediment interface and during incorporation/burial into the sedimentary record. The rates at which dissolution occurs in the sediment is generally dependent on temperature and silica concentrations in the pore water of the silica asymptotic concentration zone, which generally lies within the upper 30 cm of the sediment. Below this dissolution is reduced, although diagenesis may continue through either the re-precipitation or diagenetic alterations of the diatom silica (Kastner *et al.*, 1977; Hurd *et al.*, 1981). It would be expected that chemical and biological dissolution of diatom frustules, particularly in alkaline waters, would alter the isotope composition of $\delta^{18}O_{diatom}$. To date, however, no detailed investigation has been undertaken to investigate the impact of dissolution on $\delta^{18}O_{diatom}$. While Mochen *et al.* (2006) observed no isotope alteration in cultured and fossil diatoms placed in waters of pH 9 for 62 days, unless the diatom organic matter coating was first

removed with H_2O_2, it remains wise to only analyse pristine diatoms completely free of dissolution and diagenesis until these results are verified in other studies.

1.4.6. Secondary isotope exchange/silica maturation

A key assumption of analysing $\delta^{18}O$ in diatoms is that no isotope exchange occurs between the inner, -Si-O-Si, layer and the rest of the frustule or surrounding water after the diatom dies (Julliet, 1980a,b). Culture experiments of modern marine and lacustrine diatoms, however, have demonstrated $\delta^{18}O_{diatom}$ fractionation factors of between 2‰ and 10‰ below those observed for fossil diatoms (Section 1.4.1) (Schmidt *et al.*, 1997, 2001; Brandriss *et al.*, 1998; Moschen *et al.*, 2006). Initially these deviations were attributed to partial dissolution of the diatom frustule during sedimentation (Brandriss *et al.*, 1998). Other work, however, has made clear that these isotopic changes are related to silica maturation in the diatom frustule during sedimentation/burial with isotopically light ^{16}O from the -Si-OH layer released and the remaining, heaver, ^{18}O forming isotopically enriched -Si-O-Si linkages (Schmidt *et al.*, 1997; 2001; Moschen *et al.*, 2006):

$$Si\text{-}^{18}OH + H^{16}O\text{-}Si \rightarrow Si\text{-}^{18}O\text{-}Si + H_2{}^{16}O$$

(Eq. 18, from Schmidt *et al.* (2001))

At present, the implication of these isotope exchanges and the extent to which silica maturation affects the use of $\delta^{18}O_{diatom}$ in palaeoenvironmental reconstructions is unknown. On the one hand, deviations from equilibrium of 2‰ to 10‰ arising from silica maturation could blur any environmental signal. However, numerous studies have demonstrated a strong correlation between sediment records of $\delta^{18}O_{diatom}$ and $\delta^{18}O$/proxy records from other sources, which would not be expected were $\delta^{18}O_{diatom}$ predominantly controlled by silica maturation (Leng and Barker, 2006). As such, further laboratory and in-field studies are required to replicate the experiments of Schmidt *et al.* (1997; 2001) and Moschen *et al.* (2006) and the occurrence of secondary isotope exchanges outside the photic zone. However, even if isotope exchanges do occur during silica maturation, as long as such exchanges are systematic and predictable, values of $\delta^{18}O_{diatom}$ should remain usable in palaeoenvironmental reconstructions. For example, since the -Si-OH layer prior to dehydroxylation will reflect either $\delta^{18}O_{bottomwater}$ or $\delta^{18}O_{porewater}$, measurements of $\delta^{18}O_{diatom}$ would reflect, in the worst case scenario, a possible combination of surface/bottom/pore water $\delta^{18}O$ (Schmidt *et al.*, 1997; 2001). The issue of silica maturation is addressed in more detail within the following individual chapters of this thesis alongside the $\delta^{18}O_{diatom}$ data.

1.5. Summary of uncertainties associated with diatom oxygen isotopes

To date, the vast majority of isotope records derived from biological organisms for

palaeoceanographic reconstructions have originated from mid/low latitude carbonate rich sites. However, with diatoms often dominating the sediment record in high latitude and carbonate free regions, measurements of $\delta^{18}O_{diatom}$ opens the possibility for more detailed insights as to the response and role of these localities during past climatic and oceanographic events. Despite this, as highlighted above a number of uncertainties remain over the use of $\delta^{18}O_{diatom}$. These include:

1) the uncertainty over the true $\delta^{18}O_{diatom}$-temperature calibration. While recent work provides compelling evidence for a coefficient of −0.2‰/°C (Brandriss *et al.*, 1998; Moschen *et al.*, 2005), coefficients derived from marine diatoms are higher at −0.3‰/°C to −0.5‰/°C (Juillet-Leclerc and Labeyrie, 1987; Shemesh *et al.*, 1992);
2) the impact of secondary isotope exchange on $\delta^{18}O_{diatom}$;
3) the extent to which isotope vital effects may be present in $\delta^{18}O_{diatom}$;
4) the extent to which habitat and seasonality effects may affect $\delta^{18}O_{diatom}$ reconstructions.

1.6. Aims and objectives

As detailed above, the development and initial application of $\delta^{18}O_{diatom}$ as a palaeoenvironmental proxy originally occurred in marine systems. In recent years, however, $\delta^{18}O_{diatom}$ has been almost solely applied to lacustrine sediment samples (Table 5). As such, excluding papers published as part of this PhD research, only eight papers have presented fossil $\delta^{18}O_{diatom}$ records from marine cores which are not affected by the issue of contaminant oxygen in the -Si-OH layer (Table 4). Of these all but two (Juillet-Leclerc and Schrader, 1987; Sancetta *et al.*, 1985) originate from the Southern Ocean (Labeyrie *et al.*, 1986; Hodell *et al.*, 2001; Shemesh *et al.*, 1992, 1994, 1995, 2002). Consequently, while the difficulties and potential associated with $\delta^{18}O_{diatom}$ are now better understood in freshwater systems, uncertainty remains as to the true potential of $\delta^{18}O_{diatom}$ in palaeoceanographic reconstructions. Furthermore, marine records of $\delta^{18}O_{diatom}$ have yet to be fully tested in relation to other geochemical, stable isotope and other proxy records. As such, it remains unknown whether $\delta^{18}O_{diatom}$ can be considered as a direct replacement for planktonic $\delta^{18}O_{foram}$ in carbonate free regions, or whether the problems and uncertainties with $\delta^{18}O_{diatom}$, highlighted in Section 1.5, significantly hinder its suitability for use in palaeoceanographic reconstructions.

Part 1 of this thesis aims to address these uncertainties from a palaeoceanographic perspective at ODP Site 882 in the North West Pacific Ocean where other, more established, proxy data (in addition to detailed modern day oceanographic information) can be drawn upon to assess the potential of $\delta^{18}O_{diatom}$. Key objectives in Part 1 include:

1) determining whether inter- and intra-species vital effects exist in $\delta^{18}O_{diatom}$ and, if present, the extent to which such effects limit the use of $\delta^{18}O_{diatom}$ in palaeoceanographic

reconstructions (Chapter 2 and 3);

2) evaluating the extent to which records of $\delta^{18}O_{diatom}$ may be affected by seasonality effects (Chapters 2 and 3);

3) assessing the potential for $\delta^{18}O_{diatom}$ to be used as a stand-alone proxy in reconstructing palaeoceanographic changes outside the Southern Ocean at ODP Site 882 in the North West Pacific Ocean (Chapters 4 and 5);

4) assessing the extent to which records of $\delta^{18}O_{diatom}$ complement/differ from conventional palaeoceanographic proxies, such as foraminifera stable isotopes (Chapters 4 and 5).

Chapter 2: Isotope offsets in diatom oxygen isotopes: Part I

2.1. Introduction

Diatom silica represents an important and increasingly viable option for obtaining isotope records from the numerous lacustrine and marine sites devoid of carbonates. Many studies have demonstrated the potential for $\delta^{18}O_{diatom}$ in palaeoenvironmental reconstructions, both as a stand-alone technique and alongside carbonate isotope records (e.g., Shemesh *et al.*, 1992; Leng *et al.*, 2001; Lamb *et al.*, 2005; Morley *et al.*, 2005). Despite recent advances, there remain a number of uncertainties over the use of $\delta^{18}O_{diatom}$ in palaeoenvironmental reconstructions. One is the potential for isotope exchange during burial and early diagenesis, which may act to remove much of the surface water palaeoenvironmental isotope signal (Shemesh *et al.*, 1992; Schmidt *et al.*, 1997, 2001; Moschen *et al.*, 2006). Second is the uncertainty over the true diatom-temperature coefficient with current estimates in marine and lacustrine diatoms ranging from –0.2‰/°C to –0.5‰/°C (Shemesh *et al.*, 1992; Juillet-Leclerc and Labeyrie, 1987; Brandriss *et al.*, 1998; Moschen *et* al., 2005)

Potentially the greatest uncertainty, however, revolves around the possibility for inter- and intra-species vital effects to exist in $\delta^{18}O_{diatom}$. Diatoms are assumed to precipitate in isotope equilibrium. However, many biological organisms including ostracods and foraminifera display significant isotope deviations from isotope equilibrium due to, for example, changes in rates of calcification, speciation and micro-environment (von Grafenstein *et al.*, 1999; Spero *et al.*, 1997; Holmes and Chivas, 2002). As stated in Chapter 1, a range of culture experiments (Binz, 1987; Schmidt *et al.*, 2001) and down-core studies (Sancetta *et al.*, 1985; Juillet-Leclerc and Labeyrie, 1987; Shemesh *et al.*, 1995) have found no evidence of a vital effects in $\delta^{18}O_{diatom}$. In particular, Moschen *et al.* (2005) found no isotope offset between three size fractions of diatoms collected from Lake Holzmaar, Germany. Although a 0.6‰ offset was observed between two laboratory cultured species (Brandriss *et al.*, 1998) and while a 0.2‰ offset was present between two size fraction of diatoms in a stratigraphical core sequence (Shemesh *et al.*, 1995), such offsets are within the range of analytical reproducibility commonly achieved with fluorination based techniques. As such, $\delta^{18}O_{diatom}$ vital effects have until now been assumed to be either non-existent or within the analytical reproducibility of $\delta^{18}O_{diatom}$ measurements. However, this assumption is currently based on a limited data-set, highlighting the need for further investigation. This is important since, in contrast to biogenic carbonates such as ostracods and foraminifera, single species diatom valves cannot be easily picked out to create mono-specific species samples due to their smaller size (diatom frustules commonly range in diameter from 5-75 μm, while foraminifera picked for isotope analysis commonly range from 200-400 μm). While the exact number of taxa within a sample analysed for $\delta^{18}O_{diatom}$ will vary, it is possible that samples may contain upwards of 10-20 different taxa.

Here, following development of a method to extract near single species marine diatom samples for isotope analysis, the issue of $\delta^{18}O_{diatom}$ vital effects is re-examined using down-core material from ODP Site 882 in the North West Pacific Ocean. Comparisons of samples at 25 levels between 2.83 Ma and 2.73 Ma show significant isotope offsets (mean = 1.23‰, max = 3.51‰) between two size fractions (75-150 μm and >150 μm) dominated by only two taxa. Through the use of modern oceanographic and diatom flux data from the region, it is suggested that these offsets may possibly be attributed to the presence of an inter- and/or intra-species vital effects in diatoms.

2.2. Methodology

2.2.1. ODP Site 882

Ocean Drilling Project (ODP) Site 882, situated on the western section of the Detroit Seamounts in the subarctic North West Pacific Ocean (50°22'N, 167°36'E) at a water depth of 3,244 m (Fig. 5) provides the first detailed palaeoclimatic record of the region from the late Miocene onwards (Rea *et al.*, 1995). A major advantage in testing the use of marine records of $\delta^{18}O_{diatom}$ at ODP Site 882 is, as detailed below, the large range of different sized diatom taxa, ranging from c. 10 μm to >200 μm. At ODP Site 882, it is therefore possible to take advantage of this large size variation to extract different size fractions of pure diatom samples, which contain different relative proportions of individual taxa.

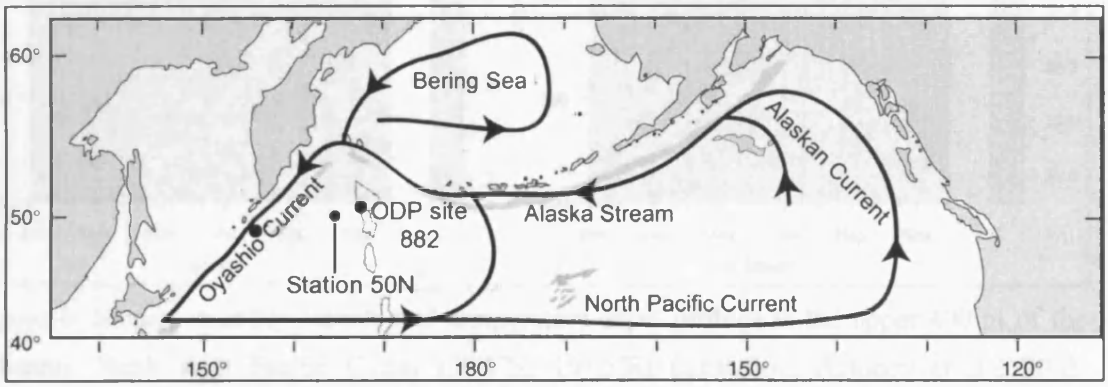

Figure 5: Location of ODP Site 882 (50°22'N, 167°36'E) North West Pacific Ocean together with diatom monitoring station 50N (50.01°N, 165.01°E) and major ocean surface currents in the North Pacific Ocean.

The region around ODP Site 882 in the North West Pacific Ocean is today dominated by the cyclonic Alaskan sub-polar gyre which is bordered to the south by the North Pacific Current (also called the Subarctic Current and West Wind Drift) and to the North by the Alaska Stream (Fig. 5). The North West Pacific Ocean also marks the terminus of the North Pacific Deep Water (NPDW), the final deep ocean section of the global thermohaline circulation, with the upwelling of nutrient rich NPDW to the subsurface forming North Pacific Intermediate Water (NPIW).

Today, the water column in the region is marked by a highly stable surface ocean stratification driven by a deep, 150-200 m, year round halocline which results in a relatively low surface water salinity (SSS) of c. 32.8 psu (Fig. 6). Due to this, nutrient supply to the photic zone is predominantly restricted to diffusion through the stratification boundary (Tabata, 1975; Gargett, 1991). From June to December, the stratification is further enhanced by the presence of a shallower, c. 50 m, thermocline in which Sea Surface Temperatures (SST) of c. 9°C - 10°C (Fig. 6) exist until December. In contrast, waters below the thermocline are closer to 2°C. The oceanographic mechanisms that create and maintain this mesothermal structure and stratification system have been an area of intensive research leading to the suggestion of several different processes that focus on the role of high precipitation/low evaporation in the region together with differential horizontal advection within the water column and minimal inflow of saltier water from the south (Warren, 1983; Gargett, 1991; Emile-Geay et al., 2003). A detailed review of these mechanism is discussed within Ueno and Yasuda (2000).

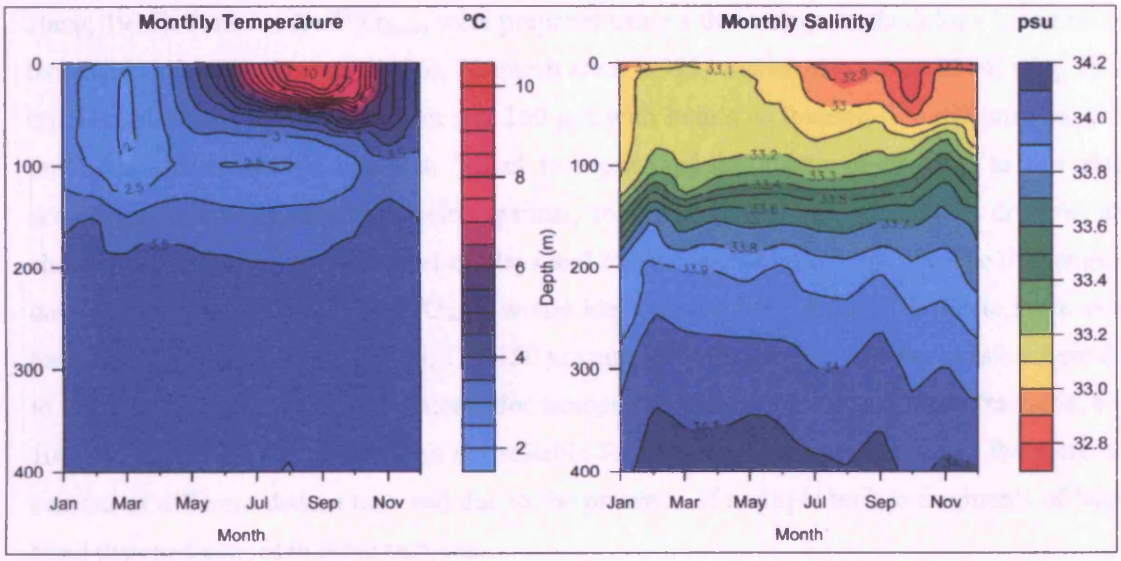

Figure 6: Modern monthly salinity and temperature depth profiles in the upper 400 m of the subarctic North West Pacific Ocean (50.5°N, 167.5°E) (data from Antonov *et al.*, 2005; Locarnini *et al.*, 2005).

Today, the biological community in the North West Pacific Ocean is marked by the year round presence of foraminifera in the water column, particularly during spring and to a smaller extent during the autumn/early winter months (Kuroyanagi *et al.*, 2002; Mohiuddin *et al.*, 2005). During the spring months, however, the photic zone is primarily dominated by a large siliceous bloom containing a number of diatoms species together with a smaller contributions from silicoflagellates (Onodera and Takahashi, 2005). In the summer months, when concentrations of phytoplankton in the surface mixed layer are reduced, dinoflagellates increase in abundance in the water column (Mochizuki *et al.*, 2002). At no point, though, does nutrient limitation prevent

phytoplankton growth (ibid). From late summer to winter a second diatom bloom occurs, but normally at concentrations below that experienced during the spring bloom (Takahashi, 1986; Takahashi *et al.*, 1996; Onodera and Takahashi, 2005; Onodera *et al.*, 2006). In some years, however, the autumn diatom bloom may be of an equal magnitude to that experienced during the spring bloom (Onodera and Takahashi, 2005; Onodera *et al.*, 2006). During this autumn bloom, large numbers of coccolithophores also develop within the photic zone, resulting in the accumulation of alkenones within the sedimentary record (Ohkouchi *et al.*, 1999; Pagani *et al.*, 2002).

2.2.2. Sample extraction

Sediment samples corresponding to the onset of major Northern Hemisphere Glaciation (NHG), 2.84-2.57 Ma (MIS 116 (G12) to MIS 102) were selected from ODP Site 882. High resolution GRAPE density and magnetic susceptibility measurements were orbitally tuned with linear interpolation of sedimentation rates between tie-points to calculate sample ages (Tiedemann and Haug, 1995). Samples for $\delta^{18}O_{diatom}$ were prepared using a three-stage methodology based on the techniques of Juillet-Leclerc (1986), Shemesh *et al.* (1995) and Morley *et al.* (2004) (Fig. 7). In this, samples were sieved at 75 μm and 150 μm with both size fraction (75-150 μm and >150 μm) retained for isotope analysis. Visual inspection of the diatom flora prior to this stage showed these size fractions to be being optimal, both in minimising diatom species diversity and also in ensuring maximum removal of clays and other non-diatom material. While the range of the size fractions analysed for $\delta^{18}O_{diatom}$ would ideally have been reduced to create more sieve bins, e.g., 75-100 μm, 100-125 μm, 125-150 μm and 150-175 μm, this was not possible here due to the need to extract sufficient material for isotope analysis (5 mg). Smaller size fractions, e.g., 10-38 μm and 38-75 μm, were also not suitable for $\delta^{18}O_{diatom}$ analysis here due to the increased number of different diatom taxa and due to the presence of multiple broken fragments of larger sized diatom frustules in these samples.

All size fractions were immersed in 30% H_2O_2 at 80°C for up to a week to remove organic matter attached to the diatom frustule before being centrifuge washed and placed overnight in 5% HCl to remove any carbonates. Following further centrifuge washing, samples were re-sieved at their respective size fractions to remove any remaining contamination and smaller diatoms before being placed in a drying cabinet. Samples younger than 2.70 Ma required the additional use of a Vortex mixer to separate diatoms from the heavier Ice Rafted Debris (IRD), which could then be pipetted off, prior to the final sieving stage. In other studies, diatom samples have been further purified using sodium polytungstate (SPT) at a specific gravity of 2.1 g/ml to remove any non-diatom contamination (see Morley *et al.*, 2004). Due to the large size of the diatom frustules extracted here, an heavy liquid SPT separation stage was not required in this instance. Instead the other cleaning stages, in particular the various sieving stages, were

sufficient to remove all contaminants. This is due to the small size of clays, silts and other forms of non-diatom contamination (<75 μm) relative to the large size of the diatom frustules analysed here for $\delta^{18}O_{diatom}$ (>75 μm).

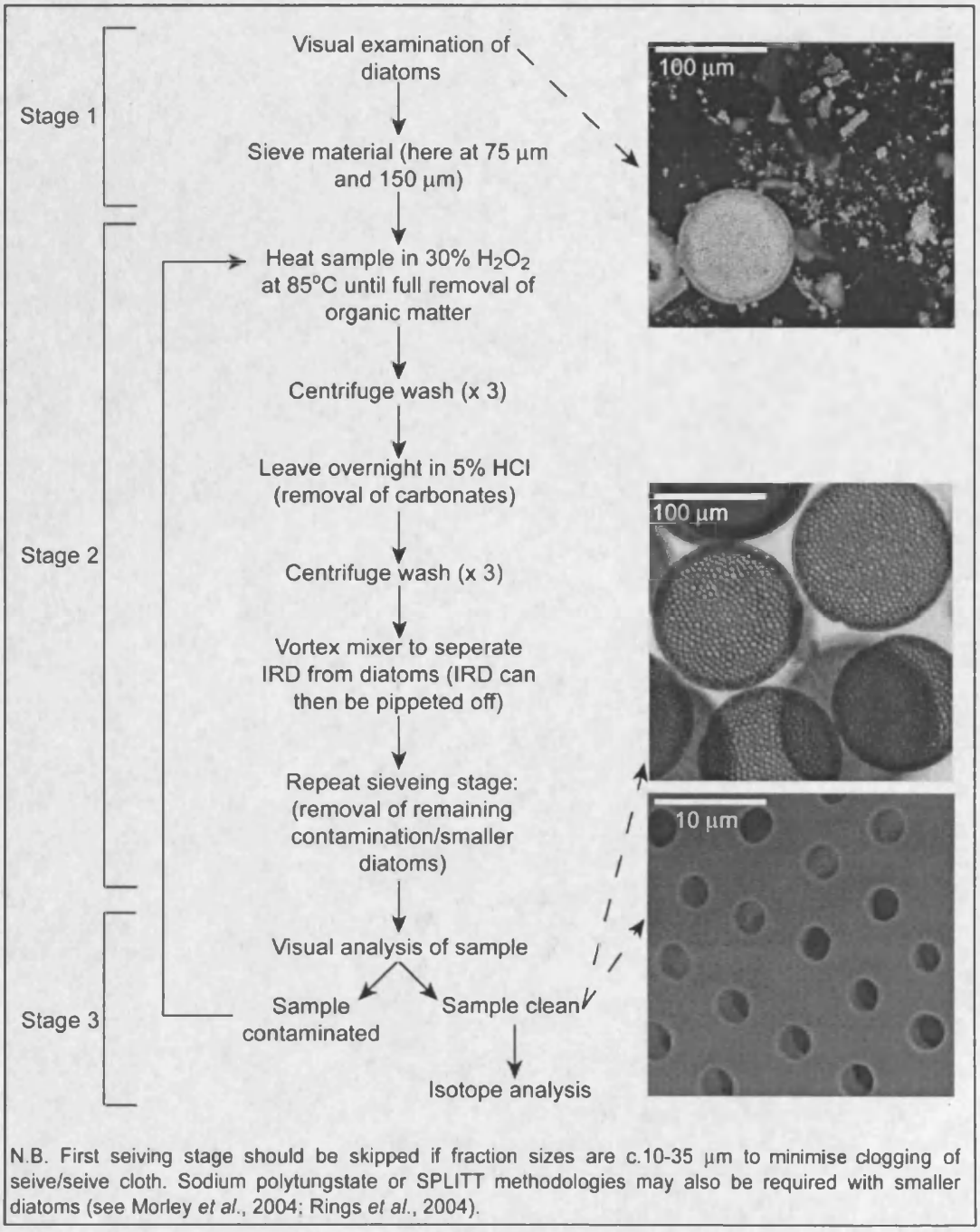

Figure 7: Three stage methodology used to extract pure diatom material for $\delta^{18}O$ analysis based upon the methodologies described in Juillet-Leclerc (1986), Shemesh *et al.* (1995) and Morley *et al.* (2004). Stage one utilises the physical properties of different diatom species to extract a small range of diatom taxa. Stage two chemically removes organic matter attached to the diatom frustule and any carbonates in the sample. Stage three verifies the purity of the diatom sample prior to isotope analysis.

Sub-samples of the final purified material were mounted on a coverslip using a Naphrax® mounting media and visually checked for contamination under a light microscope at x 1000 magnification following the semi-quantitative approach of Morley *et al.* (2004) but using thirty rather than ten randomly selected quadrants on a 100 μm x 100 μm grid graticule. Random quadrants were selected in such a way that the whole coverslip was sampled, including the edge of the coverslip where more contamination may be present. All samples containing more than a few percent of non-diatom material were disregarded for isotope analysis. Further SEM analysis were also undertaken to check for contamination. In addition, a number of samples were also dissolved in a strong 0.5 M KOH solution, which was subsequently analysed by ICP-AES. Concentrations of Al and Ca, which would indicate the presence of clays and aluminosilicates, were then monitored to check for sample purity.

Diatoms were analysed for oxygen isotopes using a SWF method to dissociate the silica and liberate the oxygen. Diatom hydrous layers were stripped during a pre-fluorination outgassing stage in nickel reaction tubes using a BrF_5 reagent at low temperature before full reaction with an excess of reagent at high temperature. Oxygen was converted to CO_2 following the methodology of Clayton and Mayeda (1963) with $\delta^{18}O_{diatom}$ measured on an Optima dual inlet mass spectrometer. $\delta^{18}O_{diatom}$ values were converted to the V-SMOW scale using a within-run laboratory standard (BFC_{mod}) calibrated against NBS28. Diatom species biovolumes for the analysed samples were calculated following the genera specific recommendations of Hillebrand *et al.* (1999). Although measurements of diatom biovolume record the volume rather than the mass or the amount of oxygen within the frustule, the values represent an important tool for identifying the relative contribution of individual taxa to an isotope measurement. All species biovolumes were calculated on the final purified unreacted sample with the assumption that relative hydroxyl layer thicknesses were constant across all diatoms. As such, following Hillebrand *et al.* (1999) the *Coscinodiscus* taxa, which dominate the samples analysed here, were treated as a cylinder:

$$V = \pi.r^2.h \qquad \text{(Eq. 19)}$$

where V is the biovolume, r is the radius and h is the height or thickness of the frustule. Central to the recommendations of Hillebrand *et al.* (1999) is that the individual dimensions used within equation 19 be based on the median, not mean, measurements of at least 25 diatom frustules. All biovolumes calculated here were based on at least 30 observations per taxa, spread across the analysed samples

2.3. Results

2.3.1. Diatom isotope samples

Twenty five levels produced sufficient numbers of diatoms in both the 75-150 μm and >150 μm fraction for oxygen isotope analyses. All diatoms within these analysed samples are pristine and do not appear to have undergone any dissolution or diagenesis (Fig. 8, 9). In addition, levels of non-diatom contamination, as assessed by light microscope and SEM, are minimal in both size fractions (Fig. 8, 9, 10a). Trace element concentrations within the purified samples are also minimal with Al less than 0.5 wt.%, most likely originating from the diatom frustules as opposed to contaminants, and Ca less than 0.1 wt.%. Sample biovolumes for the >150 μm fraction are dominated by *Coscinodiscus marginatus* (Ehrenb.) and *Coscinodiscus radiatus* (Ehrenb.), which are approximately equally distributed throughout with neither contributing more than 65% of any sample biovolume (Fig. 10b). Biovolumes in the 75-150 μm fraction are dominated solely by *C. radiatus* until 2.69 Ma, after which *C. marginatus* becomes dominant (Fig. 10b).

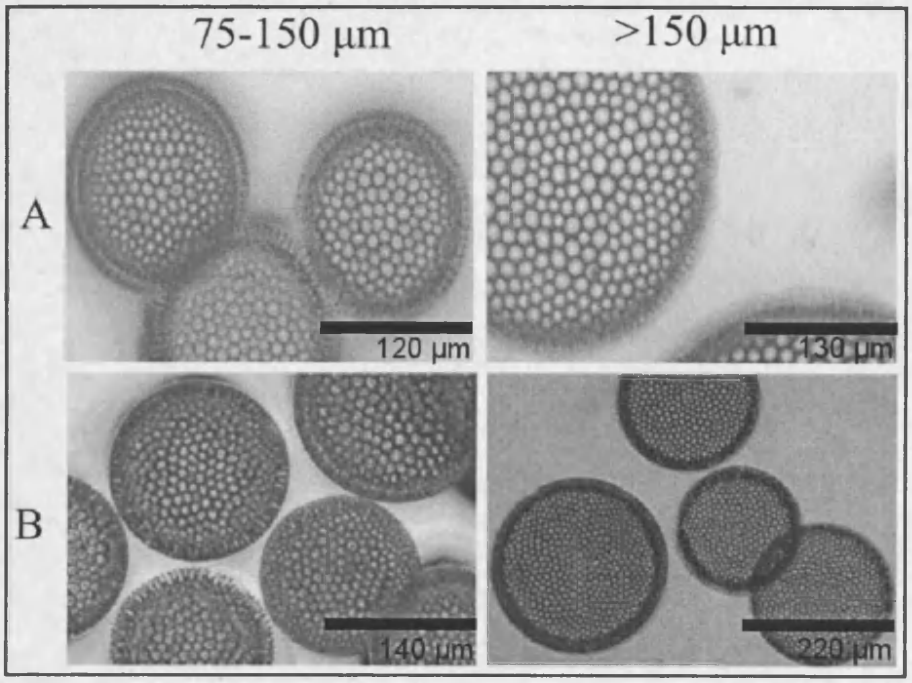

Figure 8: Comparison of the 75-150 μm and >150 μm size fractions at: A) 2.77 Ma (75-150 μm fraction dominated by *C. marginatus*, >150 μm dominated by *C. radiatus*); B) 2.81 Ma (75-150 μm fraction dominated by *C. marginatus* and *C. radiatus*, >150 μm dominated by *C. radiatus*).

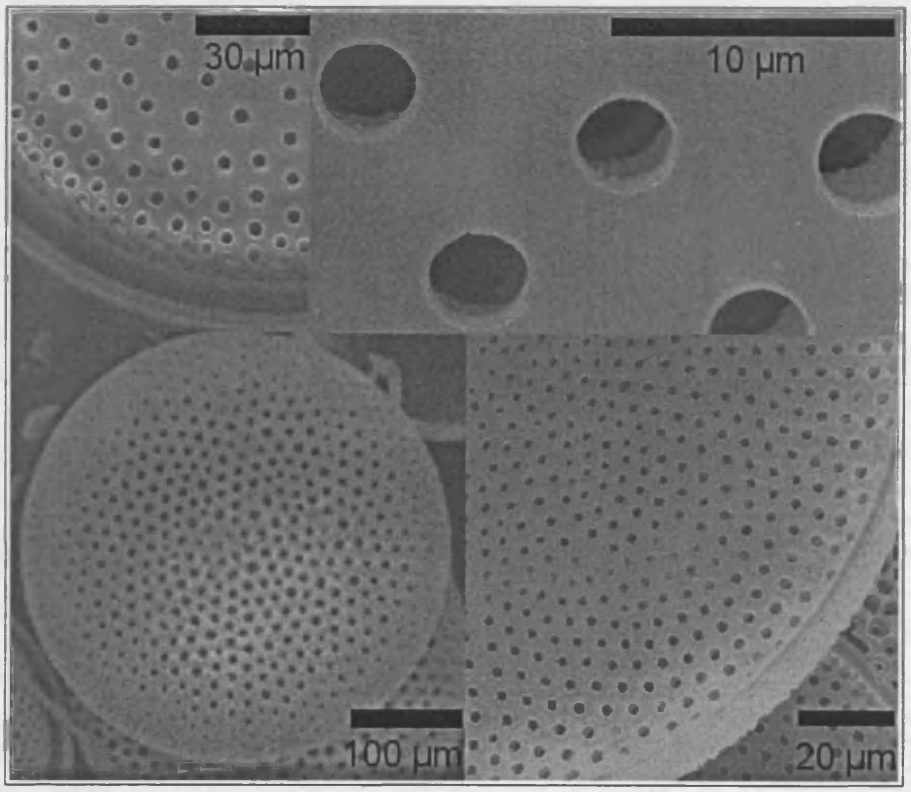

Figure 9: Typical SEM images of extracted diatom material analysed for $\delta^{18}O$ showing the complete removal of adhering clays and other forms of contamination.

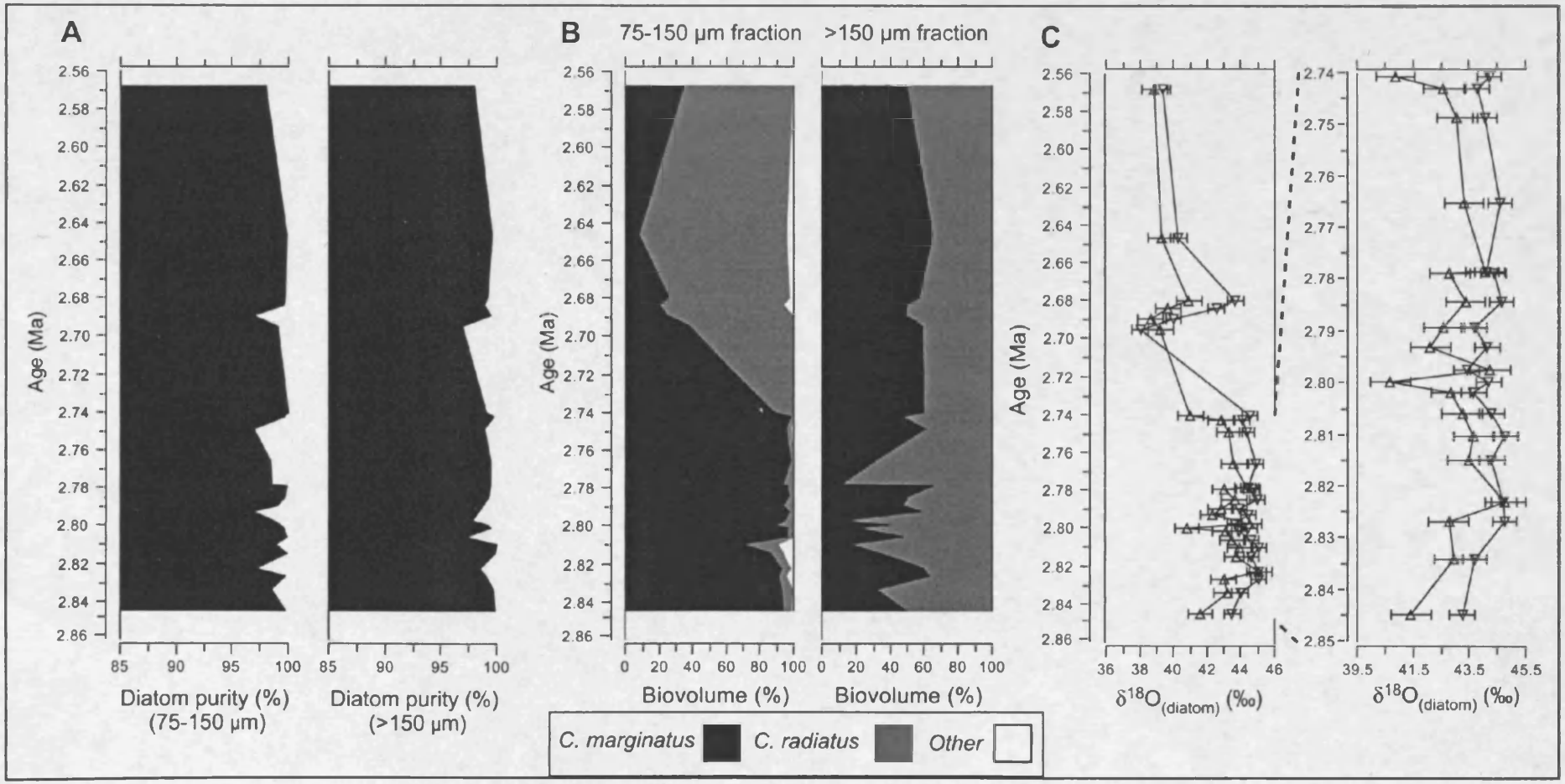

Figure 10: A) Sample purity, percentage of diatom material relative to all other material. B) Relative diatom species biovolumes in purified samples analysed for $\delta^{18}O_{diatom}$. C) Comparison of $\delta^{18}O_{diatom}$ measurements (relative to V-SMOW) from the 75-150 µm fraction (down triangle) and >150 µm fraction (up triangle) between 2.86 Ma and 2.56 Ma. Error bars represent mean, 1σ, analytical reproducibility of 0.44‰ in the 75-150 µm fraction and 0.71‰ in the >150 µm fraction.

Comparisons of the $\delta^{18}O_{diatom}$ data indicates the presence of large isotope offsets between the two size fractions with a mean offset of 1.23‰ and a maximum offset of 3.51‰ (Fig. 10c, 11). Replicate analyses indicate a mean $\delta^{18}O_{diatom}$ analytical error of 0.44‰ in the 75-150 µm fraction, 0.71‰ in the >150 µm fraction and 0.41‰ for BFC_{mod}, the NIGL laboratory diatom standard. Of the 25 analysed levels, 18 contain offsets which are beyond the combined analytical reproducibility (Root Mean Squared Error (RMSE)) for the two size fractions (0.84‰). With the exception of three levels, the smaller 75-150 µm fraction has a higher $\delta^{18}O_{diatom}$ relative to the >150 µm fraction ($p < 0.001$). After the intensification of major Northern Hemisphere Glaciation at 2.73 Ma, when the region undergoes major palaeoenvironmental changes (see Chapter 4 and Haug *et al.* (1999; 2005)), $\delta^{18}O_{diatom}$ values in the 75-150 µm fraction remain statistically higher than the >150 µm fraction, but at a lower confidence interval ($p = 0.08$).

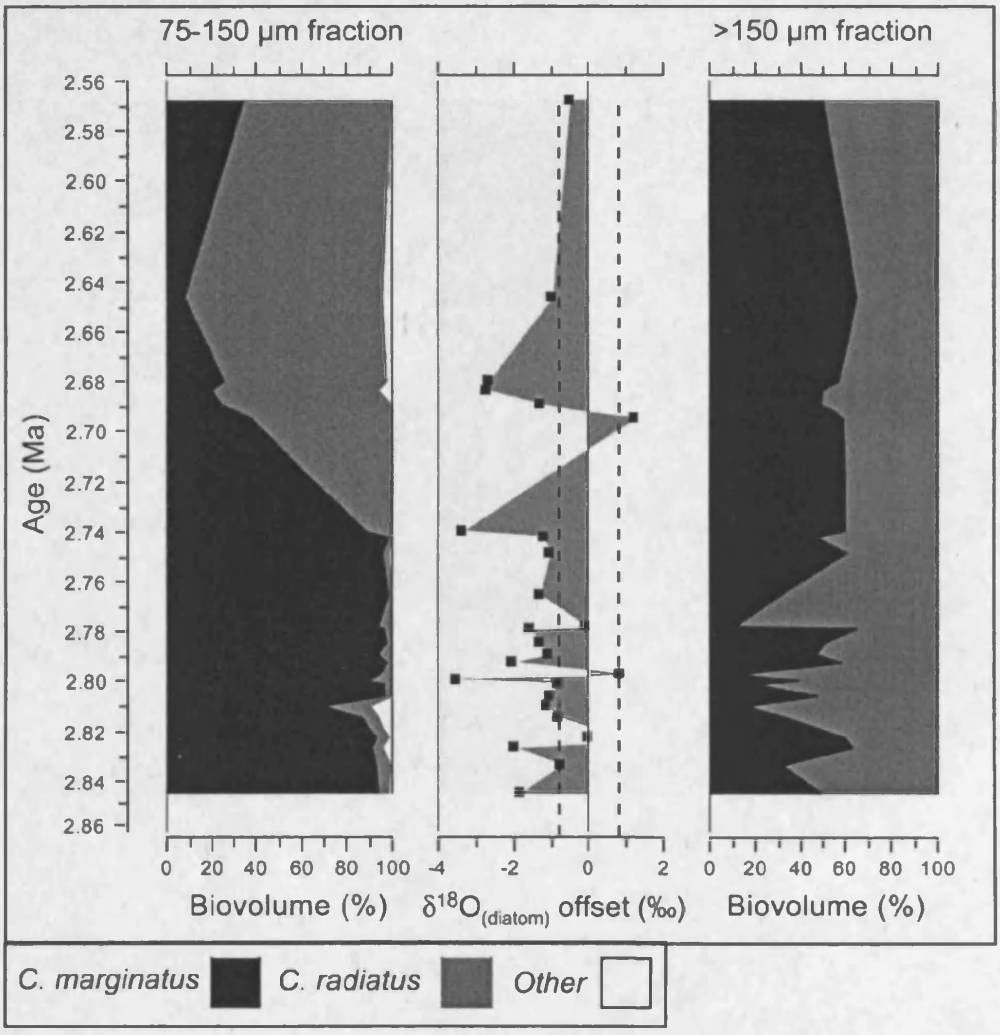

Figure 11) Relative diatom species biovolumes in purified samples analysed for $\delta^{18}O_{diatom}$ alongside the magnitude and direction of the $\delta^{18}O_{diatom}$ offsets between the two size fractions (>150 µm fraction minus 75-150 µm fraction). Dashed lines represent the RMSE of 0.84‰.

2.4. Discussion

2.4.1. Extraction of pure diatoms in marine samples

Measurements of $\delta^{18}O_{diatom}$ are highly sensitive to the degree of sample contamination, particularly when sample purity falls below 90% (Morley *et al.*, 2004). Obtaining pure diatom material for isotope analysis, however, is both time consuming and challenging, particularly when diatoms are intermixed with similar sized clay and silt grains. Several techniques have been suggested in the past to purify and extract pure diatoms from sediment samples (e.g. Shemesh *et al.*, 1995; Morley *et al.*, 2004; Rings *et al.*, 2004; Lamb *et al.*, 2005) but success with one particular technique is no guide to success with material from another site. Here a three-stage methodology is suggested for the purification of marine diatom samples for isotope analysis, similar to that proposed for lacustrine samples by Morley *et al.* (2004) (Fig. 7). The proposed method appears particularly well suited for sites possessing large, >75 μm, marine diatoms and has significant potential in extracting clean samples which also contain only low numbers of individual diatom taxa. In particular, the importance of visual analysis of the sediment prior to the first sieving stage is emphasised as a pre-cursor to selecting sieve fraction sizes in order to ensure low species diversity and in order to minimise any seasonality effect. A balance is needed though between reducing the number of species and ensuring sufficient material is extracted for isotope analysis. Sample purity is also significantly improved in this method by only sieving and collecting large sized diatoms. This results in virtually all contamination, in particular smaller sized clay/detrital contamination, being easily removed during the sieving stages.

2.4.2. Reliability of the isotope record

Analysis of $\delta^{18}O_{diatom}$ for use in palaeoclimatic and palaeoenvironmental reconstructions is a comparatively recent development. As such, consideration is required of all the issues detailed in Chapter 1 which may affect the reliability of the $\delta^{18}O_{diatom}$ signal, namely clay/silt contamination and frustule dissolution/diagenesis. As detailed above and highlighted in Figures 8, 9, 10a, all analysed diatom samples can be considered pristine with minimal non-diatom contamination. In addition, no evidence of diagenesis or dissolution exists either within the sediment or the diatoms analysed for $\delta^{18}O$. Low trace elemental concentrations also indicate the lack of non-diatom contaminants in the analysed samples.

Further evidence to support the purity and lack of contamination within the analysed samples is present within the $\delta^{18}O_{diatom}$ data itself. Firstly, high $\delta^{18}O_{diatom}$ values in all samples makes it unlikely that contamination is an issue since the $\delta^{18}O$ of clays and silts are usually significantly lower than $\delta^{18}O_{diatom}$, although no clay isotope values are available from ODP Site 882 over the analysed interval. Secondly, it would be expected that if contamination was an issue, the relative amount of any contamination, particularly from clays, would be greater in the 75-150 μm

fraction due to the fraction's smaller size. This would then lead to $\delta^{18}O_{diatom}$ values in the 75-150 μm fraction being lower than the >150 μm fraction. In practice, the 75-150 μm fraction displays higher $\delta^{18}O_{diatom}$ values in almost all samples (Fig. 10c, 11). This, combined with high levels of diatom purity (Fig. 10a), reiterates that contamination is not an issue and can not explain the observed offsets.

An important finding in recent years is evidence for secondary isotope exchange in diatoms, caused by silica maturation, which increases sediment values of $\delta^{18}O_{diatom}$ relative to diatoms within the water column (Schmidt *et al.*, 1997, 2001; Brandriss *et al.*, 1998; Moschen *et al.*, 2006). Checking for silica maturation in diatoms is difficult as it does not always visibly alter the diatom frustule and so can not be checked or assessed under a light microscope or SEM. However, it would be expected that any secondary isotope exchange caused by silica maturation would be constant across both size fractions. As such, silica maturation should not lead to the isotope offsets observed here between the two size fractions. The issue of silica maturation is further address in Chapter 4, within the context of the additional data presented in that chapter. By comparing measurements of $\delta^{18}O_{diatom}$ to changes in bottom water $\delta^{18}O$, strong evidence is found to indicate that issues of silica maturation have not had a notable impact on $\delta^{18}O_{diatom}$ at ODP Site 882 over the analysed interval.

2.4.3. Seasonality/temporal effect

C. marginatus and *C. radiatus* are cosmopolitan species found today throughout most of the world's oceans. Both taxa are also present in late Quaternary cores from the North Pacific Ocean (e.g., Sancetta, 1982). Monitoring studies on *C. marginatus* and *C. radiatus* from across the North Pacific Ocean show that these taxa have similar temporal fluxes to one another with peak annual fluxes occurring in the autumn/early winter months (Takahashi, 1986; Takahashi *et al.*, 1996 Onodera *et al.*, 2005). This is reinforced by records of *C. marginatus* and *C. radiatus* at monitoring station 50N in the North West Pacific Ocean, situated close to ODP Site 882 (see Fig. 5), which also show a similar relative flux between *C. marginatus* and *C. radiatus* frustules in the 75-150 μm size range through the course of the year (Table 6; Onodera *et al.*, 2005; *pers comm.* Onodera 2006). No data is available on the temporal flux of >150 μm frustules, due to their almost complete absence from the samples collected at station 50N and due to a lack of other studies investigating the temporal and ecological characteristics of very large frustules for these taxa. However, since all available evidence from the North Pacific Ocean shows peak fluxes of these taxa occurring together during autumn/early winter, it is reasonable to assume that similar patterns also exist for >150 μm sized frustules. Consequently, it is unlikely that the isotope offsets are related to an inter- or intra-species seasonality effect.

Table 6: Relative flux of *C. marginatus* and *C. radiatus* at station 50N (see Fig. 5) from

December 1997 to May 2000 (DJF = December, January, February; MAM = March, April, May; JJA = June, July, August; SON = September October, November). Only minimal numbers of >150 μm diatoms were present in the analysed samples (n=5 for *C. marginatus* and n=0 for *C. radiatus*). Data from Onodera *et al.* (2005) and Onodera *pers. comm.* (2006).

Season	*All sized frustules*		*Frustules 75-150 μm in diameter*	
	C. marginatus (%)	*C. radiatus* (%)	*C. marginatus* (%)	*C. radiatus* (%)
DJF	24.76	26.35	41.32	45.69
MAM	26.02	21.58	27.34	24.79
JJA	16.84	16.11	10.62	3.96
SON	32.38	35.96	20.72	25.56

Given that each sample represents on average a 2000-3000 year interval, it is possible that different conditions within the time interval covered by each sample may have favoured different sized diatoms. For example, diatoms from the 75-150 μm fraction may have predominantly originated from periods of higher salinity/lower temperatures and diatoms in the >150 μm fraction from periods of lower salinity/higher temperatures. However, even if this occurred, it is hard to envisage that environmental conditions could have varied sufficiently at ODP Site 882 in the past to explain the entire magnitude of these offsets. Using a diatom-temperature coefficient of −0.2‰/°C, the mean isotope offset between the two size fractions of 1.23‰ becomes equivalent to a SST change of 6.15°C with the maximum offset of 3.51‰ equivalent to a change of 17.55°C. For a diatom-temperature coefficient of −0.5‰/°C, the offsets are equivalent to SST changes of 2.46°C and 7.02°C respectively. Both sets of values compare with a relatively small mean SST fluctuation of 0.28°C/kyr over the analysed interval (Haug *et al.*, 2005). Similarly, if a record of Sea Surface Salinity (SSS) is calculated (see Chapter 4), mean rates of change in SSS are equivalent to c. 0.10‰/kyr in the analysed samples when using a SSS:$\delta^{18}O$ relationship of 1 and c. 0.20‰/kyr with a SSS:$\delta^{18}O$ relationship of 2. Consequently, it is unlikely that the offsets between the two size fractions are related to different sized diatoms growing in separate intervals of different palaeoenvironmental conditions. This is particularly true from 2.81 Ma to 2.73 Ma when environmental conditions were relatively stable with SST of c. 8°C (Maslin *et al.*, 1995b, 1996; Haug *et al.*, 1999, 2005). Despite this, 11 out of 14 samples from this period display a $\delta^{18}O_{diatom}$ offset greater than the RMSE with a mean offset through this interval of 1.44‰ (Fig. 11).

2.4.4. Evidence of an inter-species effect

Given the existence of only two dominant taxa within the analysed samples, the $\delta^{18}O_{diatom}$ offsets could reflect an inter-species effect between *C. marginatus* and *C. radiatus*. Visual comparisons, however, only provide evidence for a weak, largely unclear, relationship between the $\delta^{18}O_{diatom}$ offsets and differences in diatom species biovolumes between the two fractions (Fig. 11). From

2.86 Ma to 2.74 Ma, when biovolumes in the 75-150 μm fraction contain >90% *C. marginatus*, increases in *C. marginatus/C. radiatus* in the >150 μm fraction are broadly associated with higher/lower $\delta^{18}O_{diatom}$ offsets between the two size fractions (correlation coefficient r = 0.49 for both) (Fig. 11). However from 2.69 Ma onwards, when biovolumes in the >150 μm fraction are constant and biovolumes vary in the 75-150 μm fraction, the relationship reverses with increases in *C. marginatus/C. radiatus* in the 75-150 μm fraction associated with lower/higher $\delta^{18}O_{diatom}$ offsets (r = −0.53 and +0.46 respectively).

2.4.5. Evidence of a size effect

With all but one of the significant offsets marked by higher $\delta^{18}O_{diatom}$ measurements in the smaller 75-150 μm fraction, relative to the >150 μm fraction, it is instead possible that the offsets are related to a size-related species effect. While these offsets may be better described as an isotope vital effect (i.e., non-equilibrium isotope fractionation) the term species effect is used instead since diatom $\delta^{18}O$ equilibrium is unknown. Determining the processes which might cause such a size effect, however, are not straight forward and can only be truly investigated through culturing experiments in addition to diatom monitoring and sediment core top studies. Consequently here it is only possible to speculate as to the causes of the offsets based on the available modern and fossil data. Within foraminifera, size-related vital effects arise from their vertical migration in the water column at different stages in their life cycle (Sautter and Thunell, 1991). This is unlikely to be an issue for diatoms which primarily bloom and take up oxygen into the inner tetrahedrally bonded -Si-O-Si layer within the photic zone. Evidence from the North Pacific Ocean suggests that today all diatoms except *Thalassiosira trifulta* and *Thalassiosira gravida* bloom within the upper 50 m of the water column (Katsuki and Takahashi, 2005). Water column profiles from close to ODP Site 882 show the salinity gradient through the year in the upper 50 m of the water column to be less than 0.2 psu (Antonov *et al.*, 2005) (Fig. 5). As such, any salinity effect on the $\delta^{18}O_{diatom}$ offsets would be minimal and within the analytical reproducibility of the $\delta^{18}O_{diatom}$ measurements. Profiles also show the temperature gradient between the surface and 50 m water depth to be negligible, less than 1°C, through most of the year (Fig. 6) (Locarnini *et al.*, 2005). Consequently, if modern day SST (Fig. 5) and diatom growth patterns at Station 50N (Table 6) are used as an analogue for the past, differences in diatom depth habitats for different sized frustules could only result in a minor offset of c. 0.1‰ if all of the >150 μm frustules are assumed to bloom at the surface and all of the 75-150 μm frustules are assumed to bloom at the limits of the photic zone (50m), when using a diatom-temperature coefficient of either −0.2‰/°C or −0.5‰/°C. Although the temperature gradient increases to 5-6°C between July and September (Locarnini *et al.*, 2002), the blooms of *C. marginatus* and *C. radiatus* over this interval account for only 19.4% and 29.0% of their total annual flux or 13.1% and 6.2% of the 75-150 μm total annual flux respectively (Table 6; Onodera *et al.*, 2005). It is also likely that the majority of frustules will actually bloom nearer

the surface where light penetration is higher and where differences in the temperature gradient are further reduced.

While a proportion of the offsets could be explained if all 75-150 μm diatoms bloomed in spring and all >150 μm diatoms bloomed in autumn, as highlighted above such a combined size effect and seasonality effect appears unlikely given the aforementioned contemporary studies, which show similar temporal fluxes of *C. marginatus* and *C. radiatus* through the year with peak fluxes in autumn/early winter (Table 6; Takahashi, 1986; Takahashi *et al.*, 1996; Onodera *et al.*, 2005). Furthermore 19 out of the 25 analysed samples originate prior to the development of the halocline in the region at 2.73 Ma, when the seasonal SST gradient would have been significantly reduced relative to the 8°C gradient that exists today (Fig. 5) (see Chapter 4 and Haug *et al.* (1999, 2005)). As such for these 19 samples, a size-related seasonality effect is even less likely to be responsible for the observed isotope offsets. While the discussion within the above paragraphs is heavily reliant upon the use of modern day oceanographic and diatom flux data, based on this data it seems unlikely that the offsets between the two size fractions reflect a size-related habitat or seasonality effect.

Schmidt *et al.* (2001) have previously suggested that $\delta^{18}O_{diatom}$ may be partially governed by diatom growth rates with less isotope fractionation occurring in fast-growing diatoms. Today, much of the North West Pacific Ocean is believed to be under Fe limitation with respect to diatom growth (Harrison *et al.*, 1999; Tsuda et al., 2003; Yuan and Zhang, 2006). Consequently, changes in Fe deposition, particularly variations in line with glacial (high Fe aeolian deposition) - interglacial (low Fe aeolian deposition) cycles, and the subsequent impact on diatom growth rates and cell chemistry (see Hutchins and Bruland (1998); Takeda (1998) and reviews in de Baar *et al.* (2005) and Ragueneau *et al.* (2006)) may potentially be initiating the offsets. However, no relationship is apparent between glacial and interglacial intervals, as indicated by a global stacked benthic $\delta^{18}O_{foram}$ record (Lisiecki and Raymo, 2005), and the magnitude of the $\delta^{18}O_{diatom}$ offsets (Fig. 12). Furthermore, there is some doubt as to whether the region was Fe limited in the past (Kienast *et al.*, 2004).

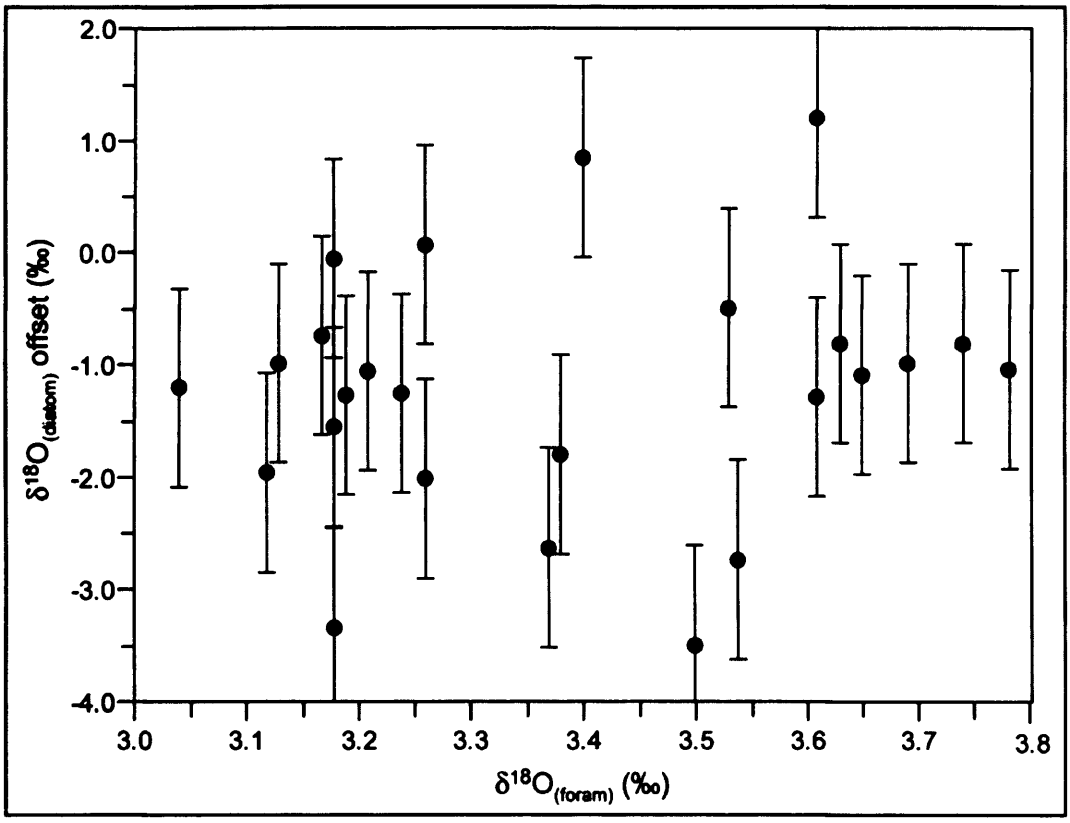

Figure 12: Relationship between a global stacked benthic $\delta^{18}O_{foram}$ record (Lisiecki and Raymo, 2005) and the $\delta^{18}O_{diatom}$ offsets (>150 μm fraction minus 75-150 μm fraction). The absence of any relationship between $\delta^{18}O_{foram}$ and $\delta^{18}O_{diatom}$ suggests that the $\delta^{18}O_{diatom}$ offsets are not related to glacial-interglacial changes in aeolian Fe deposition in the North West Pacific Ocean. Error bars on $\delta^{18}O_{diatom}$ data represents the RMSE of 0.84‰ for the two size fractions.

The availability of nutrients such as N, Si and P may be important in explaining the offsets after c. 2.73 Ma following the development of a halocline stratification system in the region, which significantly limited deep water delivery of nutrients into the photic zone and lowered opal accumulation rates within the sediment (see Chapter 4 and Haug *et al.* (1999; 2005)). For example, the extent to which $\delta^{18}O_{diatom}$ in the 75-150 μm fraction is significantly higher than the >150 μm fraction decreases at this juncture ($p = 0.08$ compared to $p < 0.001$ prior to 2.73 Ma). In addition, the transition from changes in *C. marginatus* being associated with larger to smaller $\delta^{18}O_{diatom}$ offset (Section 2.4.3) also occurs over the same interval. However, N, Si, and P are unlikely to be significant in explaining the offsets prior to 2.73 Ma (a period including 19 of the 25 analysed levels) when a mixed water column was marked by extremely high opal accumulation rates and high nutrient availability (Haug *et al.*, 1999; 2005). It is also unclear whether issues of diatom growth rates and nutrient availability are relevant issues at all for explaining the offsets since any change in diatom growth rates/nutrient availability would presumably be constant across all diatoms, regardless of size, at a given level. However, it is possible that the growth effect identified by Schmidt *et al.* (2001) influences larger diatoms to a

greater extent than smaller diatoms.

Future work

Above, a series of processes were investigated for their potential to explain the large $\delta^{18}O_{diatom}$ offsets observed at ODP Site 882. Given that all but one of the levels are marked by higher values in the 75-150 μm fraction, a size-related species effect may be present. However, based on the available data no one mechanism can be confidently attributed to explain the entire magnitude of the offsets. In Section 2.5.1 the role of silica maturation was discounted as a factor in explaining the isotope offsets. In particular, it was assumed that the magnitude of any silica maturation effect would be constant across both size fractions in a given sediment sample. Theoretically, it is conceivable that the $\delta^{18}O_{diatom}$ offsets reflect a size-related difference in the extent to which silica maturation occurs in diatoms with greater silica maturation occurring in the smaller 75-150 μm fraction. However, at present no evidence exists to indicate that inter- and intra-species variations occur in the magnitude of silica maturation isotope exchange. Consequently, based on current scientific knowledge, issues of silica maturation can not be attributed to explain the $\delta^{18}O_{diatom}$ offsets presented within this chapter.

From the above, there is a clear need for further sediment trap, core top and culture studies on $\delta^{18}O_{diatom}$. Such work on both marine and freshwater diatoms should consider the inter- and intra-species variations in $\delta^{18}O_{diatom}$ that might arise following changes in diatom growth rates, cell chemistry, deep water upwelling, nutrient availability and other physiological and environmental conditions. In addition, given the potential for silica maturation to modify $\delta^{18}O_{diatom}$, experiments are required to both better understand the processes by which silica maturation occurs and the possible extent to which silica maturation may vary between and within individual diatom taxa.

2.5. Conclusions

The presence of large $\delta^{18}O_{diatom}$ offsets between two size fractions at ODP Site 882 represents a notable problem for future applications of $\delta^{18}O_{diatom}$ in palaeoceanographic reconstructions. Both taxa which dominate the two size fractions analysed here bloom together, primarily during the autumn/winter months. With all but one of the isotope offsets marked by higher values in the 75-150 μm fraction, a size-related species effect may be present. Identifying the mechanisms behind such an effect, though, is problematic. Given that the magnitude of the offsets varies throughout, it remains possible that the offsets are also controlled by a combination of other additional processes, such as an inter-species effects. Based on this uncertainty, further studies are required to investigate and understand the $\delta^{18}O$ signal in diatoms with respect to both inter- and intra-species offsets and the extent to which similar isotope offsets may exist outside of *C. marginatus* and *C. radiatus*. To this end, the issue of $\delta^{18}O_{diatom}$ species/vital effects is further

examined in Chapter 3 of this thesis. However, based on this initial study, it appears essential that future samples analysed for $\delta^{18}O_{diatom}$ be as size and species specific as possible in order to minimise or eliminate the isotope offsets observed here.

Chapter 3: Isotope offsets in diatom oxygen isotopes: Part II

3.1. Introduction

Measurements of $\delta^{18}O_{diatom}$ are increasingly being used as a means of obtaining palaeoenvironmental and palaeoclimatic records from sedimentary sequences devoid of carbonates (e.g., Shemesh *et al.*, 1994; Morley *et al.*, 2005). The need for such measurements, for example in high latitude regions, is highlighted by the absence of more traditional materials at these locations for obtaining $\delta^{18}O$ data, e.g., foraminifera in marine systems and ostracods in lacustrine systems (see Figure 1). With high latitude regions particularly sensitive to climate change, so the number of $\delta^{18}O_{diatom}$ measurements is likely to expand as both the procedures and chemicals used for analysing $\delta^{18}O_{diatom}$ become simpler and less hazardous (e.g., Lücke *et al.*, 2005).

An important feature of almost all samples currently analysed for $\delta^{18}O_{diatom}$ is the large number of individual diatom species which may be present within a single sample. Results in Chapter 2 detailed the presence of large $\delta^{18}O_{diatom}$ offsets of up to 3.51‰ (mean offset = 1.23‰) between two size fractions, 75-150 μm and >150 μm, at ODP Site 882 between 2.84 Ma and 2.57 Ma. The existence of large $\delta^{18}O_{diatom}$ offsets up to this magnitude creates significant uncertainty over the validity of many existing $\delta^{18}O_{diatom}$ reconstructions and may limit future measurements of $\delta^{18}O_{diatom}$ to samples dominated by only a single diatom taxa. At present, however, the evidence for a vital/species effect in $\delta^{18}O_{diatom}$ is only based on material from a single site over a single time interval. In addition the precise mechanisms causing the offsets between the two size fractions remains unknown. Whilst evidence in Chapter 2 points towards the existence of at least a size-related species effect in $\delta^{18}O_{diatom}$, there is a need to replicate these results and to investigate the existence of similar offsets over other time-frames. Here, the issue of vital effects in $\delta^{18}O_{diatom}$ is further examined by analysing material from ODP Site 882 (Fig. 5) over the last 200 kyr BP (MIS 7 to MIS 1). Similar to Chapter 2, large isotope offsets are found between different species and size fractions of diatoms (mean offset = 2.02‰), further providing evidence that a vital effect may exist within $\delta^{18}O_{diatom}$.

3.2. Methodology

Sediment samples, as in Chapter 2, were collected from ODP Site 882 in the North West Pacific Ocean covering the last 200 kyr (Fig. 5). Sample ages for this interval were taken from a magnetic susceptibility and GRAPE density derived age model with additional cross correlation between benthic $\delta^{18}O_{foram}$ records from ODP Site 882 and 883 used to verify the stratigraphy (Haug, 1995). Samples for $\delta^{18}O_{diatom}$ were prepared following the three-stage methodology outlined in Chapter 2 with, as detailed below, the additional use of a heavy liquid sodium polytungstate (SPT) stage to remove non-diatom contaminants. Due to the different size range of the diatom frustules present in the sediment, compared to those analysed in Chapter 2,

samples here were sieved at 38 μm, 75 μm and 100 μm with the 38-75 μm and >100 μm size fractions retained for isotope analysis. These size fractions were identified by light microscopy as being the most suited towards minimising species diversity within the final purified samples. The 75-100 μm size fraction range was used in an attempt to collect and prevent fragments of >100 μm diatom frustules from entering the 38-75 μm fraction. While the size range of each extracted size fraction would ideally have been reduced to create more sieve bins, e.g., 38-50 μm, 50-75 μm, 100-125 μm etc, as in Chapter 2 this was not possible due to the necessity of extracting sufficient material for isotope analysis (c. 5 mg). Sieve bins for size fractions smaller than 38 μm were also not suitable for isotope analysis due to the large number of different diatom taxa in this size fraction and due to the presence of multiple fragments of larger sized diatoms. Insufficient numbers of very large diatoms in the sediment also meant that a >150 μm fraction, similar to that analysed in Chapter 2, could not be collected and analysed for $\delta^{18}O_{diatom}$. This can be attributed to the lower diatom accumulation rates at ODP Site 882 over the last 200 kyr, 0.0-1.6g/cm^2 kyr, compared to the 2.84-2.57 Ma interval analysed in Chapter 2, 2.5-4.5g/cm^2 kyr (Haug, 1995).

The use of SPT to remove non-diatom material when preparing samples for diatom isotope analysis has been previously demonstrated by Morley *et al.* (2004) in Lake Baikal over late glacial and Holocene aged samples. An SPT stage was not necessary in Chapter 2 (2.84-2.57 Ma) due to the significantly higher diatom concentrations and lower relative amounts of contamination in those samples. In addition, the extracted size fractions in Chapter 2 were significantly greater than those extracted here in Chapter 3 (75-150 μm and >150 μm compared to 38-75 μm and >100 μm). With most clay and silt contaminants generally ranging in diameter from c. 2 μm to 75 μm, virtually all contamination for the samples analysed in Chapter 2 were removed during the various sieving stages. In contrast here, moderate amounts of contamination remained, particularly in the smaller 38-75 μm fraction, even after sieving. As such, here in Chapter 3 following the treatment of samples with H_2O_2 and HCl to remove organic material and carbonates, all samples, both the 38-75 μm and >100 μm fractions, were further cleaned using SPT at a series of specific gravities from 2.10-2.25 g/ml. For this, similar to the procedure in Morley *et al.* (2004), samples were balanced on top of 6 ml of SPT and centrifuged at 2,500 rpm for 20 minutes. This resulted in denser material, such as silts and clays, sinking to the bottom of the centrifuge tube while diatoms remained suspended on top of or within the solution, from where they could be pipetted off. All samples were centrifuged in SPT three times at three different specific gravities, firstly at a density of c. 2.25 g/ml, secondly at a density of c. 2.20 g/ml and finally at a density of c. 2.10 g/ml with suspended material from each SPT wash used with the next SPT wash and so on. This gradual decrease in SPT density with each wash appeared to be an important factor in improving sample purity, although no quantitative measurements of this improvement were made. The entire SPT procedure was

repeated according to need up to three times (i.e., a total of nine SPT washes). Samples still containing significant visible amounts of non-diatom contaminants after this were disregarded for isotope analysis.

After the final SPT wash, samples were centrifuge washed three time at x1,500 rpm for 5 minutes and then re-sieved at 5 μm using cellulose nitrate membrane filters to remove all traces of the SPT. This is an important stage as trace amounts of SPT can significantly alter measured values of $\delta^{18}O$ (Morley *et al.*, 2004). Sample contamination, diatom biovolumes and analysis of $\delta^{18}O_{diatom}$ was subsequently carried out following the methodology outlined in Chapter 2. Following the recommendations of Hillebrand *et al.* (1999), all *Actinocyclus*, *Coscinodiscus* and *Thalassiosira* taxa present in the extracted samples were treated as cylindrical objects for the purpose of biovolume calculations (Eq. 19).

3.3. Results

Light microscope and SEM work shows the diatoms to be pristine and to have not been affected by dissolution or diagenesis (Fig. 13, 14). Levels of non-diatom contamination in both size fractions were also minimal (Fig. 13, 14, 15a). Diatom biovolumes for the 38-75 μm fraction indicate the $\delta^{18}O_{diatom}$ signal to primarily originate from *Actinocyclus curvatulus* (Janisch in A. Schmidt), *Thalassiosira gravida* (Cleve), *Thalassiosira trifulta* group and multiple fragments of the larger *C. radiatus* (Fig. 15b). The relatively large number of different taxa in this size fraction, compared to samples analysed in Chapter 2, is linked to the smaller size fractions analysed within this chapter (e.g., the 38-75 μm size fraction analysed here compared to 75-150 μm for the smallest size fraction analysed in Chapter 2). Analysis of a 38-75 μm size fraction over the 2.84-2.57 Ma interval covered in Chapter 2, would have resulted in a similar level of diatom flora diversity to that observed here in Chapter 3 for the 38-75 μm fraction.

The high relative biovolume abundance of *C. radiatus* in a few samples of the 38-75 μm fraction is attributable to the presence of multiple *C. radiatus* fragments within some samples. This is most likely due to the multiple centrifuging and sieving stages required to clean sediment samples for diatom isotope analysis. With some samples requiring more centrifuging/sieving than other samples, large (>100 μm) diatom frustules such as *C. radiatus* are in some samples more likely to be broken and fall through to the smaller 38-75 μm size fraction. While in most cases broken fragments were removed by sieving and collecting material with a 75-100 μm size fraction, as indicated in Figure 15b this was not always sufficient to remove all fragments. Despite this, all fragments in the 38-75 μm size fraction show fully preserved surface characteristics and display no visible signs of dissolution or other processes which may alter $\delta^{18}O_{diatom}$.

Samples in the >100 μm fraction are dominated throughout by *C. radiatus* which is constantly above 66%, and typically above 90% relative biovolume abundance. *C. marginatus* increases to c. 20% relative biovolume abundance in the three oldest samples (Fig. 15b). While the >100 μm fraction may potentially contain a large range of different size diatom frutsules, there are few frustules actually above 200 μm in diameter. Measurements across all >100 μm size fraction samples indicate a mean frustule diameter of 144 μm and an upper-quartile diameter of 166 μm.

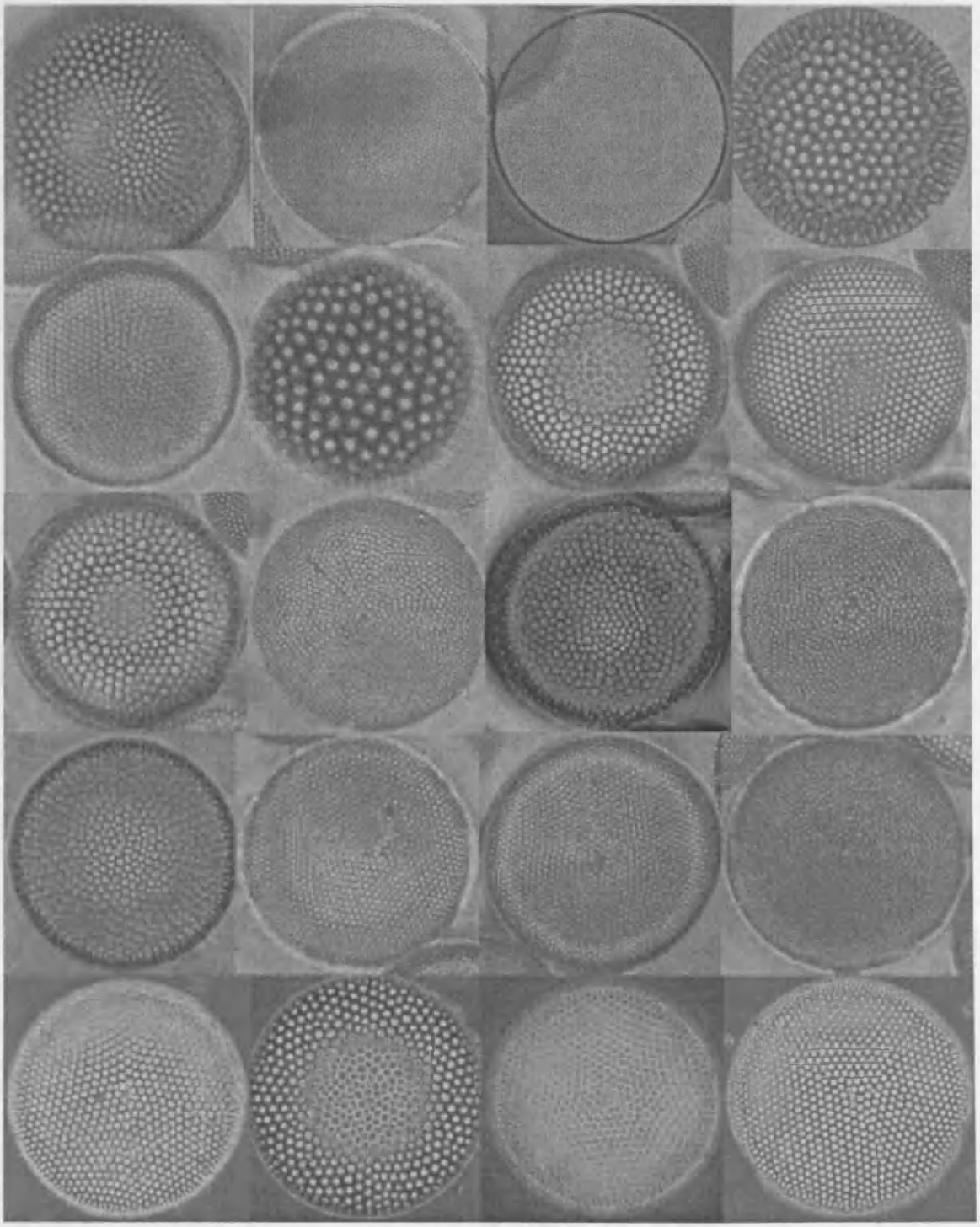

Figure 13: Typical diatom light microscope images at 4.7 kyr BP, 72.4 kyr BP and 115.7 kyr BP. All frustules range in diameter from 75-120 μm expect the frustules in columns 2 and 4 in row 2

which are 40 µm and 45 µm respectively.

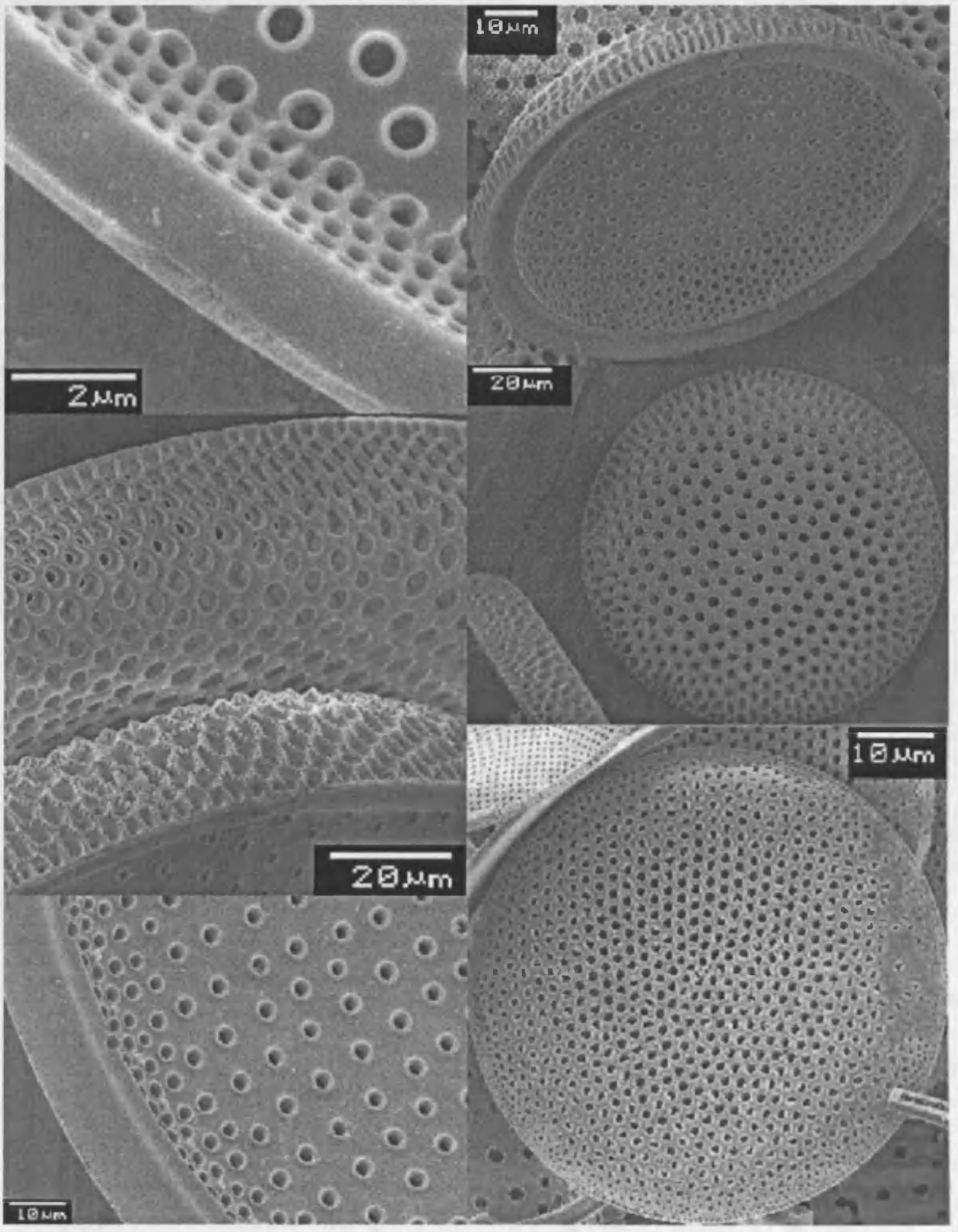

Figure 14: SEM images of diatoms analysed for $\delta^{18}O$ at 4.7 kyr BP, 75.9 kyr BP, 96.8 kyr BP and 115.7 kyr BP.

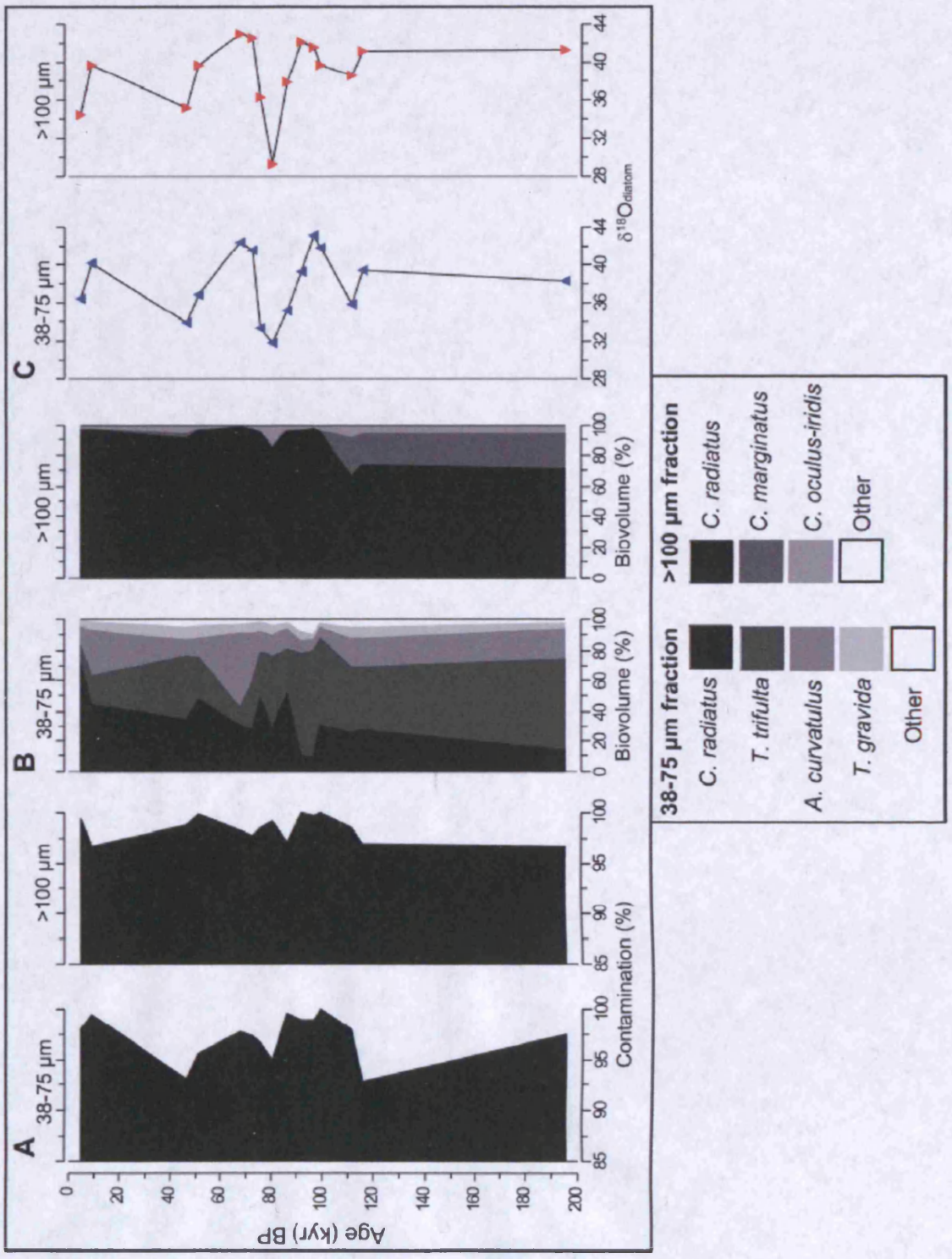

Figure 15: A) Sample purity, percentage of diatom material relative to all other material. B) Relative diatom species biovolumes in purified samples analysed for $\delta^{18}O_{diatom}$. C) Comparison of $\delta^{18}O_{diatom}$ measurements (relative to V-SMOW) between the 38-75 µm fraction (blue up triangle) and the >100 µm fraction (red down triangle) from 200 kyr onwards. Error bars for $\delta^{18}O_{diatom}$ are within the size of the symbols.

$\delta^{18}O_{diatom}$ measurements from both the 38-75 µm and >100 µm fractions show simultaneous variations of up to 13‰ (correlation coefficient r = 0.84) over the analysed interval (Fig. 15c). Direct comparisons, however, show the presence of large and highly variable offsets between the two size fractions with a mean offset of 2.02‰ (offset range = 0.33‰ to 3.07‰) (Fig. 16, Table 7). Replicate analyses indicate an analytical error of 0.49‰ in the 38-75 µm fraction and 0.28‰ in the >100 µm fraction and 0.48‰ for BFC_{mod}, the NIGL diatom standard. Of the 15 analysed levels, only one level (9.1 kyr BP, offset = 0.33‰) contains an offset below the combined analytical reproducibility for the two size fractions (Root Mean Squared Error (RMSE)) of 0.56‰ (Fig. 16, Table 7). In contrast to the results in Chapter 2, the direction of the offsets varies throughout with no one size fraction constantly higher or lower relative to the other. $\delta^{18}O_{diatom}$ is lower in the >100 µm fraction, relative to the 38-75 µm fraction, at 4.7 kyr BP, 80.3 kyr BP, 96.8 kyr BP and 99.3 kyr BP (Fig. 16, Table 7). For all levels in which $\delta^{18}O_{diatom}$ is higher in the >100 µm fraction relative to the 38-75 µm fraction, the mean offset is 2.18‰ (range = 0.63‰ to 3.07‰, n=10). For all levels in which $\delta^{18}O_{diatom}$ is higher in the 38-75 µm fraction, the mean offset is 1.70‰ (range = 0.33‰ to 2.50‰, n = 5).

Table 7: $\delta^{18}O_{diatom}$ data for the 38-75 µm and >100 µm size fractions. Offsets are difference in $\delta^{18}O_{diatom}$ between the two size fractions (>100 µm fraction minus 38-75 µm fraction). Shaded values indicate offsets greater than the RMSE for the two size fractions of 0.56‰.

Age (kyr BP)	*$\delta^{18}O_{diatom}$ (‰)*		*Offset (‰)*
	38-75 µm	*>100 µm*	
4.7	36.55	34.53	−2.02
9.1	40.14	39.82	−0.33
46.6	33.93	35.16	+1.23
51.3	36.86	39.76	+2.90
67.7	42.41	43.04	+0.63
72.4	41.55	42.63	+1.08
75.9	33.33	36.39	+3.07
80.3	31.82	29.32	−2.50
86.1	35.18	37.91	+2.74
92.2	39.34	42.09	+2.76
96.8	43.16	41.56	−1.60
99.3	41.90	39.82	−2.07
111.4	35.91	38.66	+2.75
115.7	39.53	41.20	+1.67
195.4	38.40	41.37	+2.97

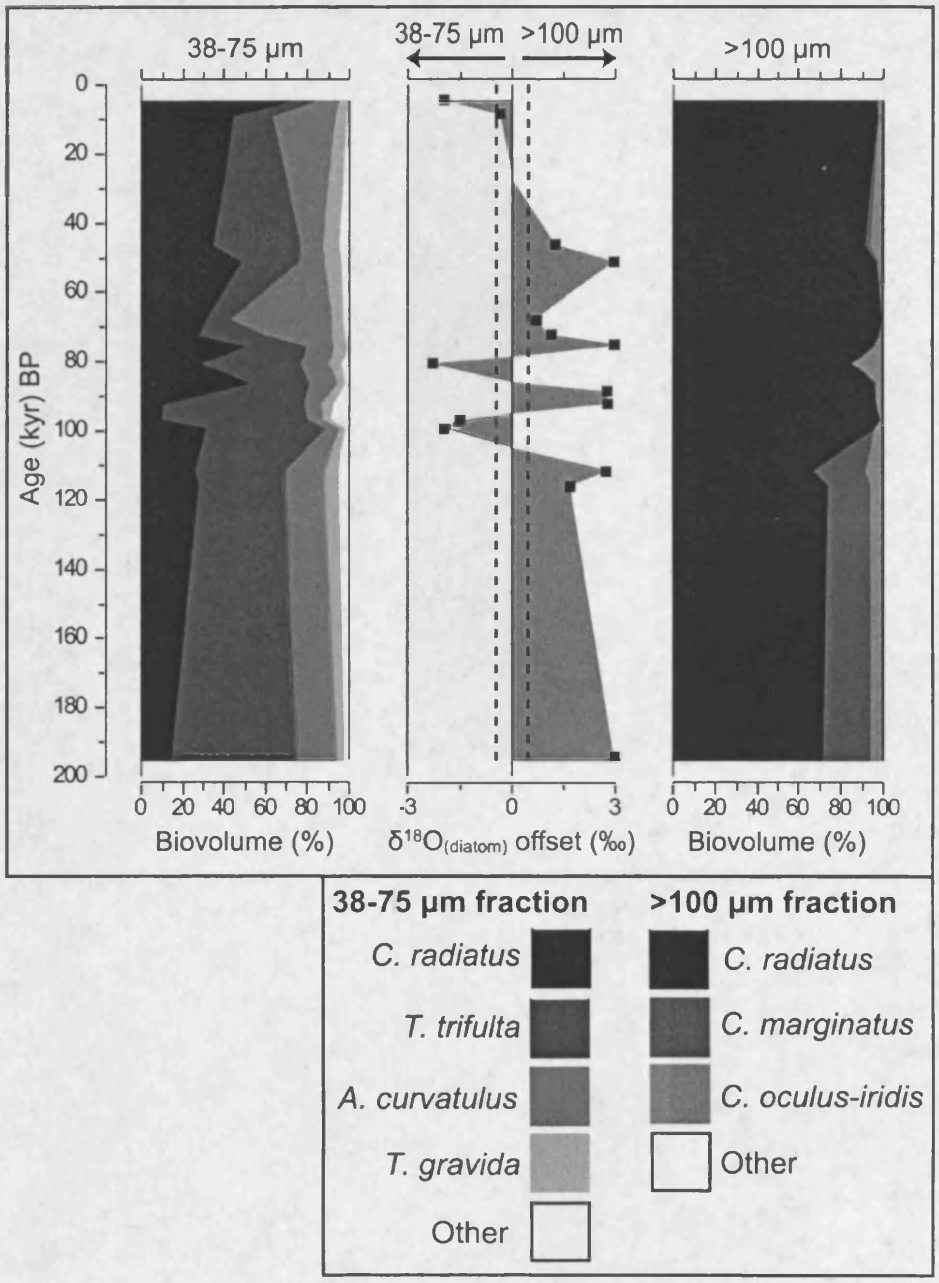

Figure 16: Relative diatom species biovolumes in samples analysed for $\delta^{18}O_{diatom}$ alongside the magnitude and direction of the $\delta^{18}O_{diatom}$ offsets (>100 µm fraction minus 38-75 µm fraction). Dashed lines represent the RMSE of 0.56‰.

3.4. Discussion

Sections 3.4.1 and 3.4.2 below investigate the extent to which non-vital effect processes, such as sample contamination and silica maturation, together with temporal variations in diatom blooms and environmental conditions (seasonality effect), may be contributing to the offsets. With no evidence that these processes are significant, Section 3.4.3 examines whether evidence of a species/vital effect in $\delta^{18}O_{diatom}$ exists within the data.

3.4.1. Reliability of the isotope record

3.4.1.1. Sample contamination

As detailed in Section 3, the samples analysed here show no visual evidence to suggest that the extracted diatoms have been subjected to dissolution or diagenesis (Fig. 13, 14). In addition, visual inspections by light microscopy and SEM show that sample contamination from non-diatom sources is minimal (Fig. 13, 14, 15a). Although sample purity falls to 93% at 46.6 kyr BP and 115.7 kyr BP in the 38-75 μm fraction, these two samples still represent a "clean" sample with purity above the 90% threshold recommended by Morley *et al.* (2005). In addition, if these two levels are removed from the dataset (offsets in these levels are 1.23‰ and 1.67‰ at 46.6 kyr BP and 115.7 kyr BP respectively) the mean $\delta^{18}O_{diatom}$ offset across all remaining samples increases to 2.11‰. As such, these "less clean" samples are not causing the offsets.

Table 8: Levels containing $\delta^{18}O_{diatom}$ offsets less than the RMSE of 0.56‰ when mass balanced corrected for a given theoretical value of $\delta^{18}O_{clay}$.

$\delta^{18}O_{clay}$	*Samples less than combined analytical reproducibility (0.56‰)*
0‰ to +5‰	67.7 kyr BP and 115.7 kyr BP
+6‰ to +9‰,	46.6 kyr BP, 67.7 kyr BP and 115.7 kyr BP
+10‰ to +13‰	9.1 kyr BP, 46.6 kyr BP, 67.7 kyr BP and 115.7 kyr BP
+14‰ to +20‰	9.1 kyr BP, 46.6 kyr BP, 67.7 kyr BP

The possible effect of clay contamination on the measured $\delta^{18}O$ signal can be further examined by mass-balance correcting the isotope composition of each sample (Morley *et al.*, 2005). The measured $\delta^{18}O$ value of all samples can be assumed to be a linear mixture of the $\delta^{18}O$ from diatoms and $\delta^{18}O$ from contaminant clay. By knowing the $\delta^{18}O$ value of the clay contaminants and by using the sample purity data as an estimate of the relative amount of contamination within the sample, the clay contribution to the measured $\delta^{18}O$ signal can be accounted for to provide a contaminant corrected value of $\delta^{18}O_{diatom}$. $\delta^{18}O$ values of clays are usually significantly lower than that for $\delta^{18}O_{diatom}$. No clay $\delta^{18}O$ values, however, were measured at ODP Site 882 over the analysed interval due to the difficulty in obtaining a pure clay sample. However, using a range of $\delta^{18}O_{clay}$ values from 0‰ to +20‰ shows that the $\delta^{18}O_{diatom}$ offsets can not be explained by different amounts of clay contamination between the two size fractions, with at least 11 of the 15 analysed levels always containing isotope offsets greater than the RMSE (Table 8; Fig. 17). This is related to the low/minimal amounts of contamination within most samples and the similar amounts of contamination within both size fractions of a given level (Fig. 15a). For theoretical $\delta^{18}O_{clay}$ values from 0‰ to +5‰, mass balanced corrected $\delta^{18}O_{diatom}$ offsets at 67.7 kyr BP and 115.7 kyr BP are less than the RMSE (Table 8; Fig. 17). For theoretical $\delta^{18}O_{clay}$ values from +6‰ to +9‰, offsets at 46.6 kyr BP, 67.7 kyr BP and 115.7 kyr BP are less than the RMSE. For theoretical $\delta^{18}O_{clay}$ values from +10‰ to +13‰, offsets at 9.1 kyr BP, 46.6 kyr BP,

67.7 kyr BP and 115.7 kyr BP are less than the RMSE. For theoretical $\delta^{18}O_{clay}$ values from 14‰ to +20‰, 9.1 kyr BP, 46.6 kyr BP and 67.7 kyr BP are less than the RMSE.

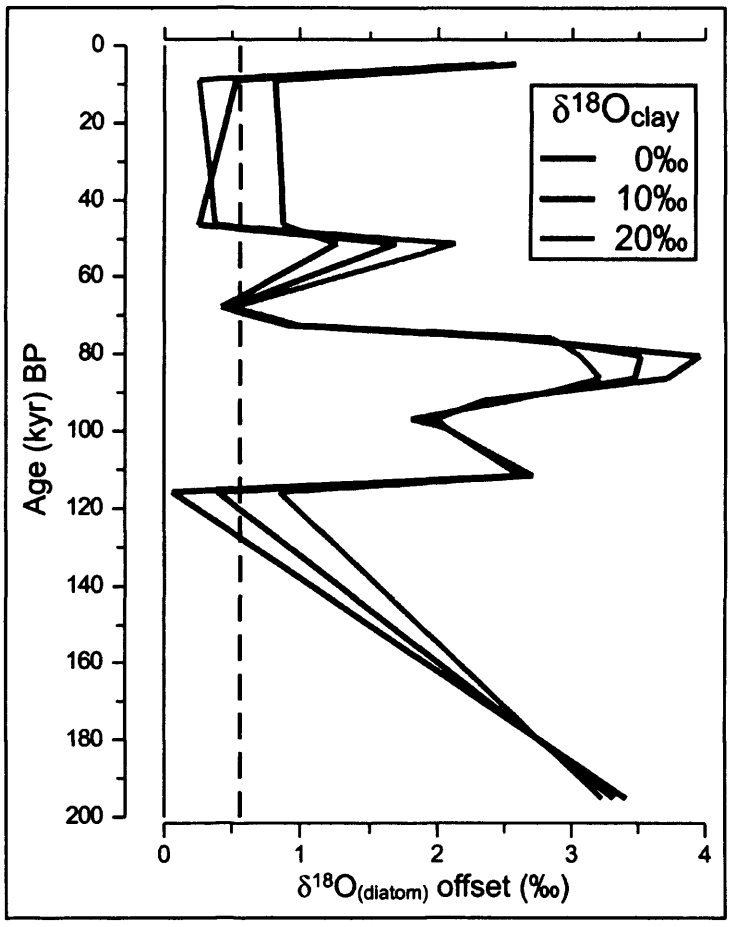

Figure 17: $\delta^{18}O_{diatom}$ offsets (>100 μm fraction minus 38-75 μm fraction) mass balanced corrected for contamination using a range of $\delta^{18}O_{clay}$ values. Magnitude of clay contamination in each sample is based on diatom purity data (Fig. 15a). Dashed lines represent the RMSE of 0.56‰.

3.4.1.2. Silica maturation

A prominent issue affecting fossil records of $\delta^{18}O_{diatom}$ is the possibility of secondary isotope exchanges in diatoms during sedimentation (Schmidt *et al.*, 1997, 2001; Brandriss *et al.*, 1998; Moschen *et al.*, 2006). The process of silica maturation has yet to be fully understood but has previously been related to a 2.5‰ increase between living diatoms and surface-sediment diatoms in Lake Holzmaar, Germany (Moschen *et al.*, 2006) and isotope deviations of up 10‰ in laboratory experiments (Schmidt *et al.*, 1997, 2001; Brandriss *et al.*, 1998). An important feature of silica maturation is that it may not always visibly alter the diatom frustule and so can not be assessed through light microscopy or SEM. If significant silica maturation had occurred in any of the samples analysed here, it would be expected that any isotope alteration would be similar across both size fractions and therefore would not lead to any isotope offsets. However,

no investigation has yet considered whether inter- and/or intra-species variations occur in the magnitude of $\delta^{18}O_{diatom}$ secondary isotope exchange. As such, and as also considered in Chapter 2, it is conceivable that the large $\delta^{18}O_{diatom}$ offsets may reflect inter- and/or intra-species variation in silica maturation. It is notable, though, that the direction of the offsets varies throughout the interval with no one size fraction constantly higher or lower relative to the other (Fig. 16). Given that the species biovolume composition of the two size fractions does not vary markedly during these changes from one size fraction being isotopically enriched in ^{18}O relative to the other, it seems unlikely that silica maturation, particularly inter-species variations in silica maturation, are exerting a dominant control on the $\delta^{18}O_{diatom}$ offsets (Fig. 16). Although the role of silica maturation can not be conclusively ruled out, based on existing studies and the current absence of evidence for inter- and intra-species variations in silica maturation isotope exchange, it is reasonable to assume at this current time that silica maturation does not play a significant role in causing the $\delta^{18}O_{diatom}$ offsets observed here.

3.4.2. Non-species effects

3.4.2.1. Water column variability

As stated in Chapter 2, contemporary evidence from the North Pacific Ocean shows both *C. radiatus*, which dominates the >100 μm fraction (Fig. 16), and *C. marginatus*, which comprises up to 25% of the biovolume in the three oldest samples of the >100 μm fraction, to have similar temporal fluxes throughout the year with peaks fluxes in autumn/early winter (Table 6, Takahashi, 1986; Takahashi *et al.*, 1996; Onodera *et al.*, 2005; Onodera, *pers. comm* 2006). This contrasts with the 38-75 μm fraction which is comprised of multiple species which bloom across different seasons (Fig. 16; Table 9). For example, while the aforementioned autumn/winter *C. radiatus* constitutes on average 33% of the sample biovolume in the 38-75 μm fraction, *A. curvatulus*, contributing on average 18% of the sample biovolume, predominantly blooms during the spring months at Station 50N (Fig. 5; Table 9; Onodera *et al.*, 2005). In addition *T. gravida*, *T. trifulta* and other less common species present in the 38-75 μm fraction bloom in large populations across a number of different seasons (Table 9; Onodera *et al.*, 2005).

With a number of different species contributing to the sample biovolumes in the 38-75 μm fraction, the $\delta^{18}O_{diatom}$ offsets may be partially explained by temporal variations in the flux of individual taxa blooms (i.e., a seasonality effect). SST in the region today are c. 8°C warmer in late summer/autumn than spring (Fig. 6) (Locarnini *et al.*, 2005). As such, when using a diatom-temperature coefficient of −0.2‰/°C, a 1.6‰ offset would exist if all diatoms in the 38-75 μm fraction bloomed in spring and if all diatoms in the >100 μm fraction bloomed in summer/autumn. Under a diatom-temperature coefficient of −0.5‰/°C this would increase to 4.0‰. Such calculations though are crude as taxa can not be solely defined as spring or autumn blooming species. Determining the extent to which temporal variations may be causing the

$\delta^{18}O_{diatom}$ offsets can be better estimated by considering the relative biovolumes of individual diatom species in each analysed sample in relation to the modern day diatom flux and SST data from the region around ODP Site 882. Monthly diatom flux records for all taxa are documented in Onodera *et al.* (2005) from a sediment trap at Station 50N at a depth of 3,260 m (Fig. 5; Table 9). SST from 50.5°N, 167.5°E, also close to ODP Site 882, are included in Locarnini *et al.* (2005) (Fig. 6). Using a diatom-temperature coefficient of −0.2‰/°C, monthly differences in SST and diatom fluxes would result in a maximum offset of 0.08‰ between the two size fractions with a typical, mean, offset of 0.03‰. Under a diatom-temperature coefficient of −0.5‰/°C, predicted offsets would increase to 0.21‰ and 0.07‰ respectively. In both cases these expected offsets are significantly less than the RMSE of 0.56‰.

Table 9: Relative seasonal flux of the dominant taxa in the 38-75 μm fraction at station 50N from December 1997 to May 2000 (DJF = December, January, February; MAM = March, April, May; JJA = June, July, August; SON = September October, November). Flux data for *C. radiatus* is the 75-150 μm flux data from station 50N presented in table 6. Since virtually all *C. radiatus* frustules in the 38-75 μm fraction are broken fragments of larger sized frustules, the 75-150 μm flux data is likely to be more representative of the samples analysed here. Data from Onodera *et al.* (2005) and Onodera *pers. comm.* (2006).

Season	*A. curvatulus (%)*	*C. radiatus (%)*	*T. gravida (%)*	*T. trifulta group (%)*
DJF	17.04	45.69	38.69	18.9
MAM	49.33	24.79	21.19	34.18
JJA	12.4	3.96	6.14	15.2
SON	21.24	25.56	33.98	31.72

Sea Surface Salinity (SSS) in the region today varies by a maximum of 0.36 psu throughout the year (Fig. 6) (Antonov *et al.*, 2005). At present the SSS:$\delta^{18}O_{water}$ and consequently SSS: $\delta^{18}O_{diatom}$ relationship for the surface waters of the North West Pacific Ocean are unknown, preventing its inclusion within the above calculations. However, using published mixing lines for the North East Pacific Ocean and Okhotsk Sea (Schmidt *et al.*, 1999; Yamamoto *et al.*, 2001), the maximum annual SSS variability of 0.36 psu is equivalent to an annual $\delta^{18}O$ variation in the surface waters of 0.13-0.14‰. If the same mixing lines are corrected to account for temporal variations in diatom fluxes, similar to the calculations above, this would lead to a maximum offset of only 0.01‰ between the two size fractions.

A significant assumption of all the above calculations is that modern day diatom, SST and SSS data are representative of conditions over the last 200,000 years. Today the North West Pacific Ocean is marked by a strong seasonal SST gradient of c. 8°C (Locarnini *et al.*, 2005) (Fig. 6), which is driven by the year round halocline and seasonal thermocline (see Section 2.2.1). In the

past this large SST gradient could have been significantly reduced in response to a reduction or removal of the halocline. At present is it unclear whether the strength of the halocline was reduced in the past, see Chapter 4. If it was, expected $\delta^{18}O_{diatom}$ offsets arising from seasonality effects would be lower than those predicted above due to the reduced seasonal SST gradient that would be present in a reduced halocline, more mixed water column (see Chapter 4 and Chapter 5. Any change in SSS in response to variations in the halocline strength would also be approximately constant across all months. As such, possible past changes in the monthly SST and SSS gradients are not capable of explaining the $\delta^{18}O_{diatom}$ offsets.

Further issues not considered within the above calculations included diatom depth habitats together with associated changes in SSS, SST and $\delta^{18}O_{diatom}$ at different water depths. With regards to the issue of diatom depth habitats, diatoms primarily bloom and fix their structurally bonded oxygen isotope ratios in the -Si-O-Si layer within the photic zone. No information exists on the depth of the photic zone at or immediately around ODP Site 882. Estimates from elsewhere in the North Central and North West Pacific Ocean suggest, however, that the photic zone likely extends down to c. 50 m (Komuro *et al.*, 2005; Katsuki and Takahashi, 2005). In addition, studies in the North Central Pacific Ocean indicate that the majority of diatom taxa live in the upper 50 m of the water column (Katsuki *et al.*, 2003; Katsuki and Takahashi, 2005). Measurements of $\delta^{18}O_{water}$ at 49°12'N, 156°2536'E, the closest site to ODP Site 882 for which water column $\delta^{18}O$ measurements exist, indicate minimal variation of 0.22‰ throughout the water column (Schmidt *et al.*, 1999). The total annual salinity range in the upper 50 m of the water column is also low at 0.45 psu (Antonov *et al.*, 2005) while the temperature gradient between the surface water and 50 m is negligible, less than 1°C, through most of the year (Fig. 6) (Locarnini *et al.*, 2005). Although a 5-6°C temperature-depth gradient is present from July to September, the impact of this on the $\delta^{18}O_{diatom}$ offsets is likely to be low given the high relative proportion of frustules which will bloom towards the surface where light penetration is higher and where vertical differences in the temperature gradient are further reduced (Locarnini *et al.*, 2005). Indeed, the overall vertical temperature gradient is smaller than the annual SST variability of 7°C, which was shown above to only explain a minor component of the offsets. While it is not possible to properly model the impact of these depth related issues due to the absence of sediment trap data from the region recording diatom fluxes at different depths, it is likely that the impact of any of these factors on the $\delta^{18}O_{diatom}$ offsets is within the limits of analytical reproducibility.

Evidence does exists that *T. trifulta* and *T. gravida* are primarily present at a water depth of c. 100 m to c. 200 m in the North Central Pacific Ocean (Katsuki *et al.*, 2003; Katsuki and Takahashi, 2005). It is unclear, though, to what extent these results are indicative of diatom habitats at ODP Site 882. At worst, if it is assumed that *T. trifulta* and *T. gravida* both precipitate

their frustules at a water depth of 100-200 m, re-calculation of the above models to take into account modern temperature and salinity values at these depths suggest that a mean $\delta^{18}O_{diatom}$ offset of 0.39‰ could exist between the two size fractions when using a diatom-temperature coefficient of c. −0.2‰/°C. Again these "expected" offsets are within the limits of analytical reproducibility for $\delta^{18}O_{diatom}$. While the expected offsets do increase to 0.81‰ under a diatom-temperature coefficient of c. −0.5‰/°C, this remains less than the observed isotope offsets at all but two levels (Table 7). In addition, these calculated offsets are almost certainly an overestimate since a proportion of the *T. trifulta* and *T. gravida* frustules will live and bloom within the uppermost sections of the water column alongside other taxa, thereby reducing any potential habitat offset.

All of the above calculations in this section contain significant assumptions with regards to diatom depth-habitats, temporal fluxes and past changes in palaeoenvironmental conditions. However, all results suggest that the expected $\delta^{18}O_{diatom}$ offsets between the two size fractions arising from temporal and spatial variations in individual diatom taxa blooms are less than the observed isotope offsets between the two size fractions. Furthermore, all calculations suggest that the measured $\delta^{18}O_{diatom}$ values should, if anything, be lower in the >100 μm fraction relative to the 38-75 μm fraction. This is due to *C. radiatus* and *C. marginatus* in the >100 μm fraction primarily blooming in autumn/early winter when SST are relatively warm, compared to taxa within the 38-75 μm fraction which bloom to a greater extent in spring when SST are cooler. Since the majority of the analysed levels (10 out of 15) are marked by higher values in the >100 μm fraction (Fig. 16), this reiterates that some other processes must be controlling the direction/magnitude and occurrence of the offsets.

3.4.2.2. Influx of extraneous taxa

Other processes which may cause the isotope offsets include the influx of diatoms from other locations with a different $\delta^{18}O_{water}$. In particular *T. gravida*, which contributes between 3% and 8% of the relative biovolume to all samples in the 38-75 μm fraction, is known at some localities to be a coastal taxa. However, frustules of *T. gravida* found at station 50N in the modern ocean are believed to primarily originate from sub-surface, not coastal, waters (Onodera *et al.*,. 2005). In addition, as detailed above and shown below in Section 3.4.3, no relationship exists between the relative amount of *T. gravida* in the analysed samples and the magnitude of the $\delta^{18}O_{diatom}$ offsets. Even if *T. gravida* had originated from coastal waters, it is inconceivable given its low relative abundance (maximum sample biovolume = 8%) that its presence would be sufficient to cause $\delta^{18}O_{diatom}$ offsets as large as those observed here.

3.4.3. Diatom isotope species effects

Above in Sections 4.1.1 and 4.1.2 the possible impact of sample contamination and temporal

variations in the water column have been shown to not be plausible mechanisms in explaining the observed $\delta^{18}O_{diatom}$ offsets. While, depending on the $\delta^{18}O_{clay}$ values used, a small number of the offsets can be explained by possible non-diatom contamination, a significant majority of the analysed levels continue to display large isotope offsets (Fig. 17). $\delta^{18}O_{diatom}$ data in Chapter 2, covering the interval from 2.84-2.57 Ma, provided the first clear evidence that a species effect may exist in $\delta^{18}O_{diatom}$ with large offsets of up to 3.5‰ observed between two size fractions of diatoms (75-150 μm and >150 μm). As stated in Chapter 2, while these offsets may be better described as an isotope vital effect (i.e., non-equilibrium isotope fractionation) the term species effect is used since diatom isotope equilibrium in the core sequence remains unknown. With the isotope offsets between the two size fractions here in Chapter 3 greater than the RMSE in 14 of the 15 analysed levels (Fig. 16, Table 7), the data presented here may provide further evidence of a species/vital effect in $\delta^{18}O_{diatom}$. Although sediment core top studies together with modern laboratory and field culturing experiments are ideally needed to confirm this, in the sections below the $\delta^{18}O_{diatom}$ data is examined for any possible evidence of a systematic species or vital effect which may be initiating or controlling the observed offsets.

3.4.3.1. Inter-species effects

In contrast to the offsets observed in Chapter 2 in which $\delta^{18}O_{diatom}$ values in the smaller 75-150 μm fraction were greater than the >150 μm fraction, in the samples analysed here the direction of the offsets varies throughout (Fig. 16). While a size-related species effect, similar to that found in Chapter 2, may play a part in explaining the $\delta^{18}O_{diatom}$ offsets observed here, other processes/factors must also be occurring. No relationship, though, is apparent between individual diatom species biovolumes and the $\delta^{18}O_{diatom}$ offsets (Fig. 18). In addition, no significant improvement in this relationship can be obtained through any combination of linear or non-linear regression models. This is surprising as an inter-species effect would be a plausible mechanism by which to explain the frequent changes in the direction of the isotope offsets through the analysed interval (Fig. 16). Identifying any inter-species effect, however, may be complicated by the presence of a size effect, similar to that found in Chapter 2, which could be acting to obscure any inter-species signal. In addition, difficulties in generating accurate diatom biovolume measurements may also be preventing detection of any inter-species effect.

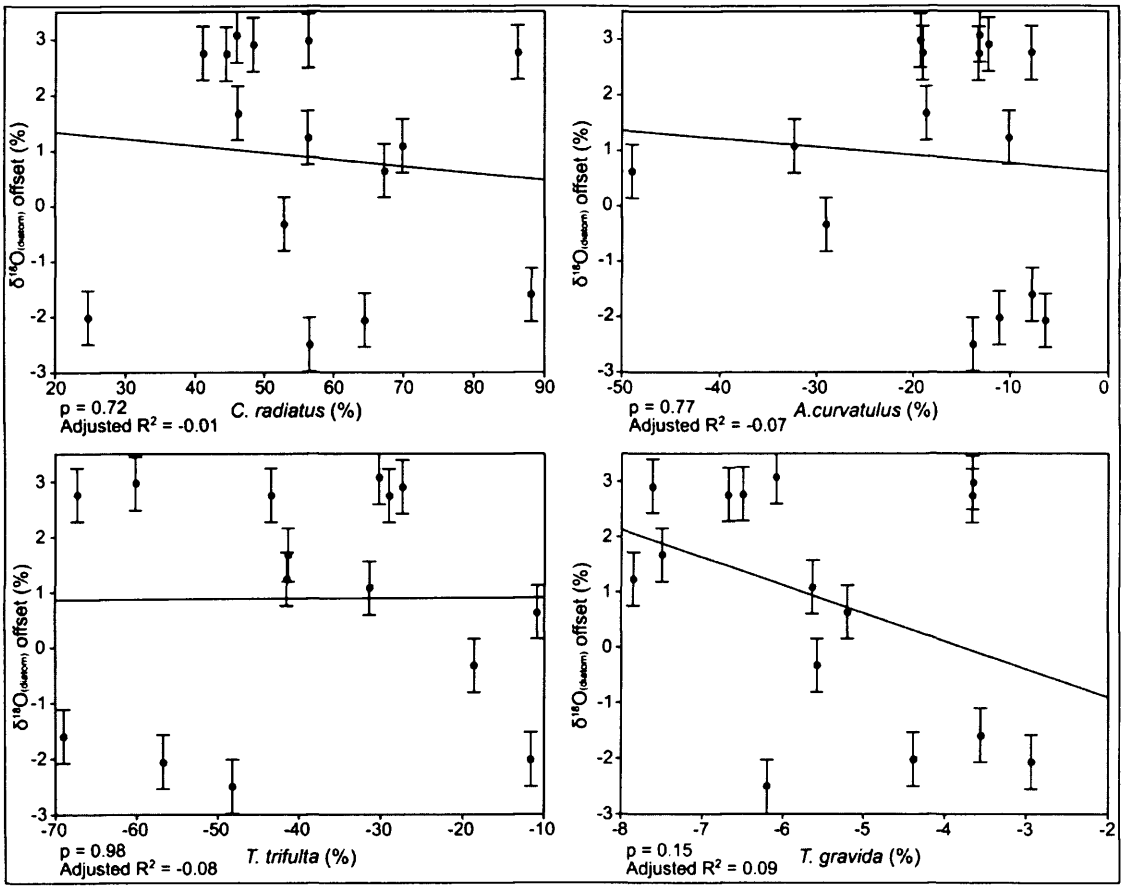

Figure 18: Relationship between differences in diatom species relative biovolumes and $\delta^{18}O_{diatom}$ offsets between the two size fractions (>100 μm fraction minus 38-75 μm fraction) for *C. radiatus*, *T. trifulta*, *A. curvatulus* and *T. gravida* (p = 0.84, 0.98, 0.73 and 0.20 respectively). Error bars on the $\delta^{18}O_{diatom}$ offsets are the RMSE of 0.56‰.

Obtaining accurate diatom biovolume measurements is a prominent issue of discussion (see review in Hillebrand *et al.*, 1999). Within the context of $\delta^{18}O_{diatom}$ measurements, even greater uncertainty surrounds the impact of the pre-fluorination outgassing stage on species biovolumes. All biovolumes measurements, whether calculated under light-microscopy or otherwise, are derived from the purified unreacted sample. The pre-fluorination stage of $\delta^{18}O_{diatom}$ analysis, however, removes the hydroxyl layer of the diatom, which can represent a considerable proportion, up to c. 30-35%, of the total diatom biovolume. Currently, it is assumed that the relative size of the hydroxyl layer is constant between and within individual taxa. However, any variation in this would alter the relative species biovolume measurements of a given sample and potentially lead to the loss of any inter-species effect signal.

During the fluorination process, a fluorination yield is calculated from the amount of oxygen actually converted into CO_2 relative to the amount of gas that would be expected from the equivalent weight of pure diatom SiO_2 initially placed into the fluorination line, assuming no

loss of oxygen in the pre-fluorination stage. With levels of contamination low in the samples analysed here, fluorination yields can be interpreted as being representative of hydroxyl layer thickness and as such biovolume loss during the pre-fluorination stage. Yield values are 64.4% for the 38-75 μm fraction and 69.3% for the >100 μm fraction. While the variability within each size fraction is large at 3.3% and 3.7% (1σ) for the 38-75 μm and >100 μm fractions respectively, this is of a similar magnitude to the 3.0% reproducibility achieved with BFC_{mod}, the NIGL within-run laboratory diatom standard. A paired Wilcoxon signed rank test indicates significant differences between yield values for the two size fractions with larger relative -Si-O-Si layers in the >100 μm fraction ($p < 0.001$). This is marked by a weak relationship between the relative differences in *C. radiatus* and fluorination yield values between the two size fractions (Fig. 19).

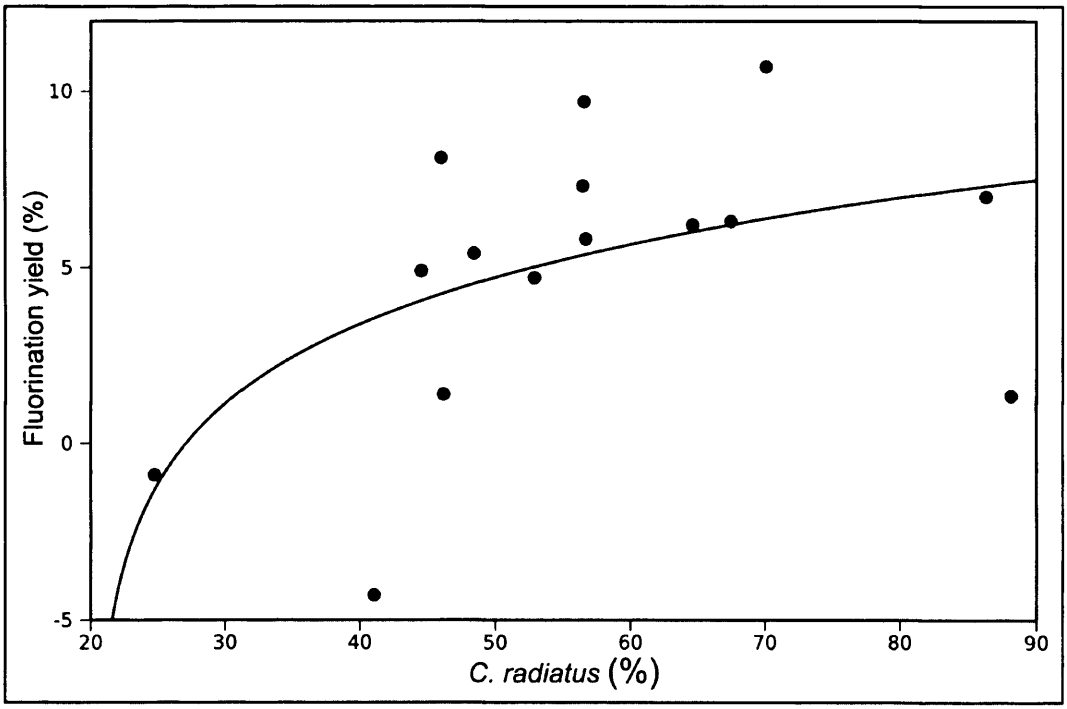

Figure 19: Relationship between the relative difference in *C. radiatus* and fluorination yields between the two size fractions (>100 μm minus 38-75 μm fraction).

While the evidence is not conclusive, the weak relationship between *C. radiatus* and fluorination yields raises the possibility that fluorination yields are species dependent. In Chapter 2, all variations in fluorination yields between the two size fractions were within the limits of analytical reproducibility. To date no other study has investigated the existence of inter- and intra-species variations in diatom fluorination yields. However, consideration of species specific biovolume loss during the pre-fluorination out-gassing stage may be crucial for obtaining the accurate biovolume data needed to further investigate and detect possible inter-species effects in $\delta^{18}O_{diatom}$. Until then, it remains problematic to investigate the issue of inter-species effects in $\delta^{18}O_{diatom}$.

3.4.3.2. Nutrient species effect

One further process which may lead to offsets in $\delta^{18}O_{diatom}$ involves changes in surface water nutrient limitation/availability, both of which can have significant impacts on diatom physiology (see reviews in Martin-Jézéquel *et al.* (2000) and Ragueneau *et al.* (2000, 2006)). Today the region around ODP Site 882 is marked by a strong halocline at c. 150 m which, significantly limits the supply of nutrient to the photic zone (Tabata, 1975; Gargett, 1991). An absence or reduction in the halocline would alter this allowing upwelling of nutrient rich deep water to the surface. To date, relatively few studies have reconstructed palaeoceanographic conditions and the presence/absence of the halocline over the last 200 kyr BP. The halocline has been shown to have first developed at c. 2.73 Ma with suggestions that stratification may have continued uninterrupted from this date (see Chapter 4 and Haug *et al.*, 2005). Indeed, most studies argue for an enhanced halocline during the last glacial, based on foraminifera stable isotopes (Keigwin *et al.*, 1992), diatom assemblage (Sancetta, 1983), biogenic barium (Jaccard *et al.*, 2005) and nitrogen isotope data (Brunelle *et al.*, 2007). Other evidence, however, based on foraminifera stable isotope, assemblage counts and Mg/Ca ratios argues for a more mixed water column during the last glacial with the modern halocline becoming re-established at 11.1-9.3 kyr BP (Sarnthein *et al.*, 2004; 2006). Regardless of whether a halocline did or did not exist in the past, no link is apparent between sample ages and changes in the magnitude/direction of the $\delta^{18}O_{diatom}$ offsets (Fig. 16). For example, glacial aged samples (which may or may not be associated with a reduced halocline) can not be related to larger/smaller offsets or one size fraction having a higher $\delta^{18}O_{diatom}$ relative to the other. Furthermore, the magnitude and direction of the offsets are not related to any changes in stratification state reconstructed in Chapter 5.

Issues of stratification and associated changes in the supply of nitrate, silicate and phosphate to the photic zone, however, may not be the most important variables with regards to changes in diatom physiology. Today large sections of the North Pacific Ocean are Fe limited with respect to diatom growth (Harrison *et al.*, 1999; Tsuda *et al.*, 2003; Yuan and Zhang, 2006). The impact of increased Fe availability on diatoms is well documented with Fe limitation leading to increases in cell Si:N and Si:C ratios and decreases in diatom growth rates (see Hutchins and Bruland (1998); Takeda (1998) and reviews in de Baar *et al.* (2005) and Ragueneau *et al.* (2006)). Despite this, the impact of changes in Fe availability on $\delta^{18}O_{diatom}$ has yet to be investigated. Previous work, however, has suggested that $\delta^{18}O_{diatom}$ may be influenced by changes in diatom growth rates with less isotope fractionation occurring in fast-growing diatoms (Schmidt *et al.*, 2001). While changes in diatom growth rates, in response to increased/decreased Fe deposition, would be expected to be constant across both the 38-75 μm and >100 μm fractions, in Chapter 2 it was questioned whether the diatom isotope growth effect could influence larger frustules to a greater extent than smaller frustules. Fe deposition to the

open North Pacific Ocean primarily occurs via aeolian transportation from the Badain Juran Desert (Duce and Tindale, 1991; Jickells *et al.*, 2005; Yuan and Zhang, 2006). However, similar to results in Chapter 2, no clear link exists between the magnitude or direction of the $\delta^{18}O_{diatom}$ offsets and changes in aeolian/dust deposition to the North Pacific Ocean (Hovan *et al.*, 1991; Kawahata *et al.*, 2000). Likewise, no link exists between the isotope offsets and changes in the accumulation of aeolian deposits at the Chinese Loess Plateau (Sun and An, 2005). As such, it is unlikely that issues of Fe fertilisation and Fe induced changes in diatom growth rates are a dominant factor in explaining the $\delta^{18}O_{diatom}$ offsets.

3.4.4. Explaining the isotope offsets

Above, a number of issues have been examined in an attempt to understand the processes which are leading to the $\delta^{18}O_{diatom}$ offsets between the two size fractions. However, it is not possible to conclusively explain the offsets based on the data currently available. The majority of the $\delta^{18}O_{diatom}$ offsets in Chapter 2 were attributed to a size-related species effect. A major difference between the results in Chapter 2 and the offsets shown here in Chapter 3 are the frequent changes in the direction of the $\delta^{18}O_{diatom}$ offsets over the last 200 kyr (Fig. 16). In addition here, the majority of the analysed levels contain higher $\delta^{18}O_{diatom}$ values in the larger >100 μm fraction relative to the smaller 38-75 μm fraction. In contrast, results in Chapter 2 are marked by higher isotope values in the smaller 75-150 μm fraction relative to the larger >150 μm fraction. As such, if a size-related species effect is operating here, it is likely to be different to the one identified in Chapter 2. The large changes in the direction of the isotope offsets here in Chapter 3, also make it likely that some additional process is operating to control the $\delta^{18}O_{diatom}$ offsets. On the one hand, it is possible that the processes contributing to the $\delta^{18}O_{diatom}$ offsets are different over each of the two time intervals. Alternatively it is plausible that the mechanisms behind the offsets are the same over both intervals, but that the relative importance of each mechanism has changed. Such a scenario, one of multiple processes including a combination of inter- and intra-species effects, the relative importance of which can vary with changes in surface water palaeoenvironmental conditions and nutrient availability, would be particularly well suited for explaining the large changes in the direction and magnitude of the $\delta^{18}O_{diatom}$ offsets over the last 200 kyr BP.

At present it is not possible to conclude further as to what the potential process or processes controlling the isotope offsets may be. As such, it is feasible that the $\delta^{18}O_{diatom}$ offset are controlled by a combination of inter-species, intra-species, size and nutrient-related species effects in addition to possible inter- and intra-species variations in diatom secondary isotope exchange. While it seems likely that a species/vital effect exists in $\delta^{18}O_{diatom}$, further investigation here is hampered by the problems in deriving accurate species biovolume data and by a lack of contemporary information on the systematics of oxygen isotope fractionation and

uptake by diatoms. Furthermore, the operation of multiple processes may be blurring evidence for their existence, particularly if the relative importance of any single process can vary over time. Clearly though, the presence of large $\delta^{18}O_{diatom}$ offsets between different samples has significant implications for the future use of $\delta^{18}O_{diatom}$ in palaeoceanographic reconstructions, requiring that future samples be comprised of only a single taxa over a finite size range. Due to this, all $\delta^{18}O_{diatom}$ samples analysed and used for palaeoceanographic reconstructions in Chapter 4 and 5 will be as mono-species and size specific as possible with samples dominated at most by only two taxa. Although calculations here indicate that seasonality effects have only a minimal impact on $\delta^{18}O_{diatom}$ (Section 3.4.2.1), to eliminate any uncertainty samples containing taxa which predominantly bloom across a number of different seasons will not be analysed or used for reconstructive purposes.

3.5. Conclusions

An urgent need exists for studies on sediment core tops and laboratory culture experiments in order to further investigate the existence of inter- and intra-species effects and other processes which cause isotope offsets in $\delta^{18}O_{diatom}$. Such work is essential if the mechanisms causing the offsets described here and in Chapter 2 are to be constrained. At present, uncertainty over these offsets casts doubt over the validity of any quantitative $\delta^{18}O_{diatom}$ reconstruction in marine sediment cores. However, as long as the isotope shift between samples in a stratigraphical sequence are sufficiently large as to rule out any species effects (maximum offset in Chapters 2 and 3 is 3.51‰), $\delta^{18}O_{diatom}$ remains suitable for providing valuable qualitative information on palaeoenvironmental and palaeoceanographic events. While further work on vital/species effects in $\delta^{18}O_{diatom}$ is primarily needed in marine systems, work should also address the potential for similar effects to occur in lacustrine diatoms. This is important given the increasing use of $\delta^{18}O_{diatom}$ in freshwater systems over the last decade (see Table 4 and review in Leng and Barker (2006)).

Chapter 4: Palaeoceanographic reconstruction of the Northern Hemisphere Glaciation in the North West Pacific Ocean (2.85-2.39 Ma)

4.1. Introduction

The onset of major Northern Hemisphere Glaciation (NHG), marking the large-scale expansion of ice sheets from c. 2.75 Ma, represents a significant climate transition during the prolonged period of global cooling initiated with the late Miocene glaciations of the Northern Hemisphere (Zachos *et al.*, 2001; Kleiven *et al.*, 2002; Ravelo *et al.* 2004; Bartoli *et al.*, 2005). In turn, the onset of major NHG can be viewed as the beginning of a series of significant climatic changes which culminated with the intensification of the Walker circulation at c. 2.0 Ma and the Mid Pleistocene Revolution at c. 0.9 Ma (Ravelo *et al.* 2004). While the occurrence of the NHG is well documented, the precise mechanisms behind its initiation remain uncertain with lower summer isolation at 65°N, related to changes in obliquity from c. 3.2 Ma and precession from c. 2.8 Ma (Haug and Tiedemann, 1998; Li *et al.*, 1998; Maslin *et al.*, 1998), unable alone to force the growth of glaciers across the Northern Hemisphere. Uplift and subsequent tectonic induced chemical weathering of the Tibetan/Himalayan plateau (Ruddiman and Raymo, 1988; Raymo, 1994) and increased volcanic activity in the Kamchatka-Kurile and Aleutian arcs (Prueher and Rea, 2001) have all been proposed, in conjunction with changes in summer isolation, to explain the establishment of cooler conditions.

In addition to climatic cooling, an essential prerequisite for the development and maintenance of glaciers in the Northern Hemisphere is a significant increase in the supply of moisture to the ice sheets. The most viable mechanism to provide this to Eurasia is through the closure of the Panama gateway which began from 4.6 Ma and culminated with a significant increase in SST and decrease in SSS within the Caribbean at 2.95-2.82 Ma (Haug and Tiedemann, 1998; Haug *et al.*, 2001; Lear *et al.*, 2003; Bartoli *et al.*, 2005; Schneider *et al.*, 2006; Steph *et al.*, 2006). This resulted in a strengthening of the Gulf Stream which, through a series of oceanic/atmospheric feedback systems, initiated an increase in the supply of moisture to Eurasia (ibid). However, while these transitions would have been sufficient to result in significant glacial advances across the Eurasian region (ibid), they do not resolve how increased moisture was delivered to the Alaskan and North American ice sheets over the same time interval.

To date, the role of the subarctic Pacific Ocean across the onset of major NHG has been largely ignored, despite the important role of the region today in providing moisture to Northern America (e.g. Koster *et al.*, 1986; Bosilovich, 2002). ODP Site 882 in the North West Pacific Ocean (Fig. 5) provides the first detailed palaeoclimatic record of the region from the late Miocene onwards, enabling key insights into the system both before, during and after beginning of NHG (Rea *et al.*, 1995). Prior to the onset of major NHG in the region at 2.73 Ma, high, c. 70 g cm^{-2} kyr^{-1}, opal concentrations are recorded in the sediment at ODP Site 882 (Haug *et al.*,

1999). The supply of high nutrient concentration necessary for this can only be achieved by significant upwelling of nutrient rich NPDW to the photic zone, suggesting the lack of a stratified system prior to 2.73 Ma (Haug *et al.*, 1999). Such a scenario of high opal concentrations is not feasible in the modern ocean with the halocline restricting the supply of NPDW to the mixed surface layer (Fig. 5). The development of the modern halocline system at ODP Site 882 has therefore previously been related to the intensification of NHG at 2.73 Ma when opal Mass Accumulation Rates (MAR) decreased three-fold (Haug *et al.*, 1999).

However, if the region had become stratified at the onset of NHG, autumn/early winter SST would be expected to increase, despite globally cooler conditions, due to development of both the halocline and thermocline temperature inversion. The presence of both these oceanographic features today leads to unusually warm SST between June/July and December of c. 10°C (Locarnini *et al.*, 2005) (Fig. 6). Without the presence of a halocline driven stratification, the build up and maintenance of a warm pool of surface water would be untenable both today and in the past due to the strong vertical mixing that would occur between the surface and subsurface layers. On this basis, the above suggestion that the modern halocline system in the region developed at c. 2.73 Ma (Haug *et al.*, 1999; Sigman *et al.*, 2004) is disputed by the presence of a 7.5°C cooling signal in $\delta^{18}O_{foram}$ between 2.75 Ma and 2.73 Ma (Maslin *et al.*, 1995b; 1996).

In order to resolve these conflicting lines of evidence over the nature of the palaeoceanographic system in the North West Pacific Ocean and to establish whether or not the modern halocline system developed at the onset of major NHG, a record of autumn changes in SSS and SST are required. One potential source of information for this purpose are records of $\delta^{18}O$ from autumn blooming diatom taxa. Here $\delta^{18}O_{diatom}$ is analysed in pure diatom samples from ODP Site 882, which are dominated by only two species: *C. marginatus* and *C. radiatus*. With both species primarily blooming during autumn/early winter, records of $\delta^{18}O_{diatom}$, in conjunction with U^{k}_{37} data (Haug *et al.*, 2005), provide clear and reliable information as to the palaeoceanographic conditions in the region during the autumn/early winter months. By combining the two records with a benthic $\delta^{18}O_{foram}$ record (Haug, 1995), changes in SSS are calculated from 2.85 Ma to 2.39 Ma to provide definitive evidence of a significant decrease in SSS at 2.73 Ma, which is consistent with the development of a halocline stratification system in the region.

4.2. Methodology

Sediment samples were collected from the North West Pacific Ocean, ODP Site 882 (see Chapter 2 and Figure 6). Sample ages within this chapter are based on a high resolution, astronomical calibrated, GRAPE density and magnetic susceptibility age model with linear interpolation of sedimentation rates used between tie-points (Tiedemann and Haug, 1995). Samples were prepared and analysed for $\delta^{18}O_{diatom}$ using the methodology detailed in Chapter 2

with the 75-150 μm fraction retained for isotope analysis and used for palaeoenvironmental reconstructions. Numbers of large, >150 μm, diatoms are generally restricted to the interval prior to 2.74 Ma and so are not suitable for obtaining palaeoceanographic information over the onset of major NHG at 2.73 Ma. Similarly, size fractions smaller than <75 μm were not considered for isotope analysis due to the multitude of different taxa within this size range which, based on Chapters 2 and 3, may contain vital/species effects. As in Chapter 2, SPT was not required to clean/purify the samples due to the large size of the diatom frustules in the 75-150 μm fraction, relative to the smaller size of clays, silts and other non-diatom contaminants (c. 2 μm to 75 μm). Instead, other cleaning stages, in particularly the individual sieving stages, were sufficient to remove all non-diatom contamination.

4.3. Results

Forty samples in the 75-150 μm fraction were extracted for isotope analysis. Replicate analyses of sample material indicated a mean $\delta^{18}O_{diatom}$ reproducibility of 0.44‰ in the 75-150 μm fraction over this interval. Due to the reduced numbers of diatoms in the sediment and the increased difficulty in purifying diatoms of contaminant material, only a limited number of samples cover the period after 2.63 Ma. Between 2.85 Ma and 2.73 Ma, diatom assemblages were dominated by 60 - 99% relative percent abundance of *C. marginatus* with the remainder principally made up of *C. radiatus* (Fig. 20a). After 2.73 Ma, the relative abundances of *C. radiatus* and *C. marginatus* are reversed except for five samples between 2.69 Ma and 2.57 Ma where the proportion of other species increases to over 40% relative abundance (Fig. 20a). Calculation of diatom species biovolumes, however, shows the influence of these other species to be minimal, constituting on average less than 2.2% of the total volume of silica analysed for $\delta^{18}O_{diatom}$ (Fig. 20b). This highlights the importance of calculating diatom biovolumes rather than percent abundances when analysing $\delta^{18}O_{diatom}$. All analysed samples, with the exception of one sample at 2.42 Ma, were over 96% free of non-diatom material with over half of all samples at least 99% pure (Fig. 9, 20c).

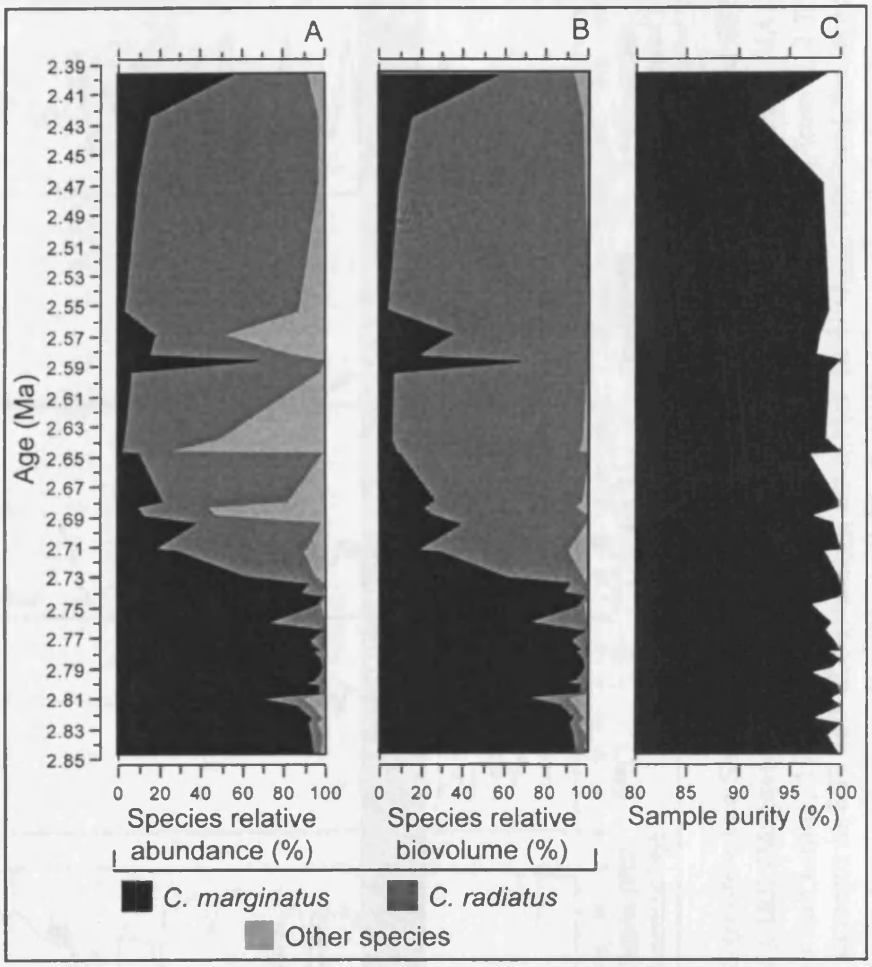

Figure 20: A) Diatom species relative abundance in samples analysed for $\delta^{18}O_{diatom}$ between 2.85 Ma and 2.39 Ma. B) Relative diatom species biovolumes in purified samples analysed for $\delta^{18}O_{diatom}$. C) Sample purity, percentage of diatom material relative to all other material.

$\delta^{18}O_{diatom}$ in the 75-150 μm fraction displays fluctuations between 43.4‰ and 44.8‰ from 2.83 Ma to 2.74 Ma following an initial increase of 1.5‰ between 2.85 Ma and 2.83 Ma (Fig. 21). At 2.73 Ma, $\delta^{18}O_{diatom}$ decreases by 4.6‰ before 2.71 Ma. A rapid 1.7‰ increase in $\delta^{18}O_{diatom}$ is observed over the next c. 2,000 years before values decrease to 38‰ at 2.70 Ma. Sharp oscillations of c. 8‰ characterise the $\delta^{18}O_{diatom}$ record between 2.70 Ma and 2.64 Ma before $\delta^{18}O_{diatom}$ becomes more positive from 37.1‰ to 42.6‰ over the subsequent c. 86,000 years with a short-lived peak in $\delta^{18}O_{diatom}$ at 2.59 Ma. Sample resolution decreases after this interval, due to the difficulties in obtaining sufficient clean diatom material, with $\delta^{18}O_{diatom}$ decreasing by 7.7‰ to 34.9‰ at 2.39 Ma.

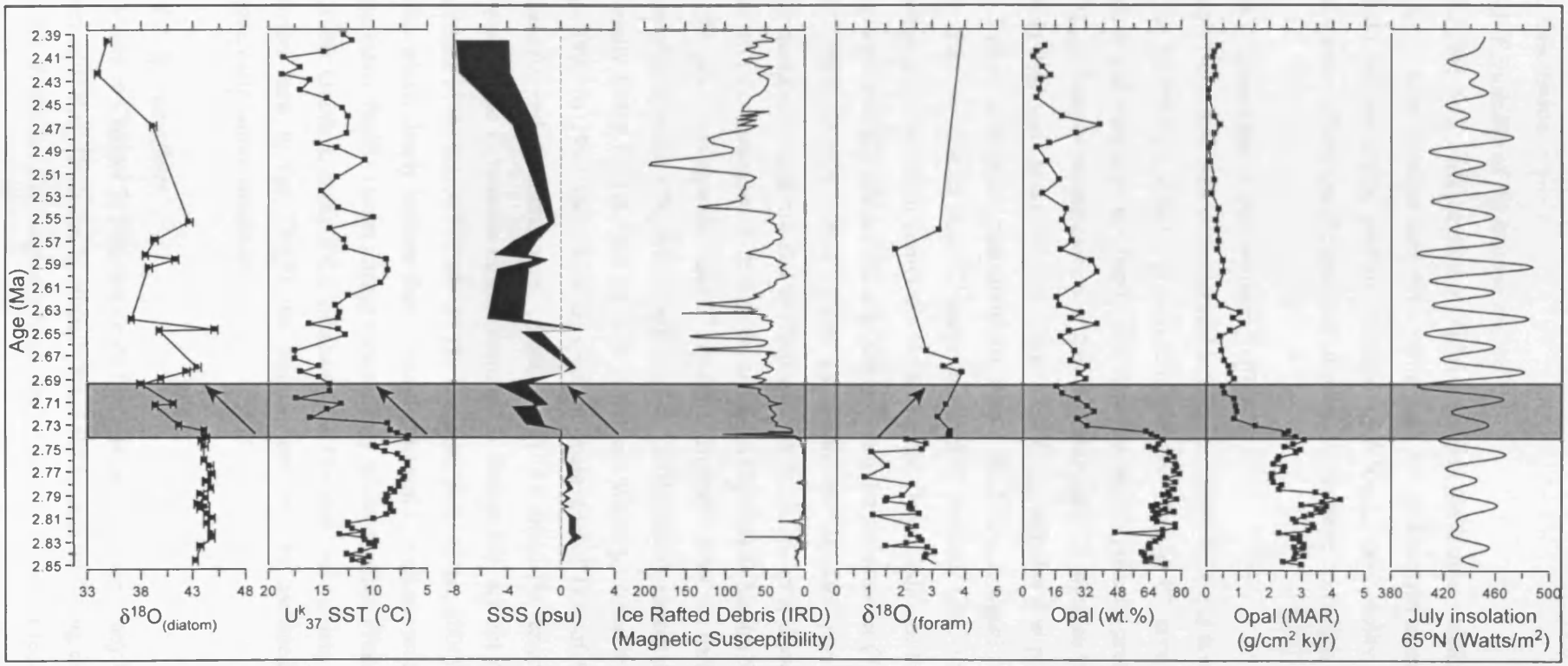

Figure 21: $\delta^{18}O_{diatom}$ (values relative to V-SMOW) with calculated SSS (relative to a SSS of 0 at 2.73 Ma (see Section 4.4.2)), U^{k}_{37} reconstructed SST (Haug *et al.*, 2005), planktonic $\delta^{18}O_{foram}$ (Maslin *et al.*, 1995b; 1996), IRD (Magnetic Susceptibility) (Haug, 1995), opal concentrations and MAR (Haug, 1995; Haug *et al.*, 1999) and July isolation at 65°N (Berger and Loutre, 1991). Warming and freshening of surface waters from c. 2.73 Ma is indicated by decreases in $\delta^{18}O_{diatom}$, SSS and opal MAR and increases in SST and IRD (shaded). Error bars on $\delta^{18}O_{diatom}$ represent the mean analytical reproducibility of 0.44‰. Calculated SSS assumes a $\delta^{18}O_{diatom}$-temperature coefficient of −0.2‰/°C (Brandriss *et al.*, 1998; Moschen *et al.*, 2005). The range of SSS values reflects the uncertainty over the exact SSS:$\delta^{18}O$ relationship (see Section 4.4.2).

4.4. Discussion

4.4.1. Reliability of the isotope record

As in Chapter 2, consideration is required towards the factors which may prevent the use of the $\delta^{18}O_{diatom}$ ratios obtained here from being used for palaeoenvironmental reconstructions. These include sample purity, seasonal dilution of $\delta^{18}O_{diatom}$ (seasonality effects), the influence of vital/species effects and the presence of secondary isotope exchanges.

4.4.1.1. Sample purity and seasonality effects

Sample purity has been demonstrated in Chapter 2 (Fig. 8, 9) and is reiterated here in Figure 20. Of the 40 $\delta^{18}O_{diatom}$ samples presented within this chapter, 25 have a matching >150 μm size fraction and were used in Chapter 2 to demonstrate the possible presence of a species effect in $\delta^{18}O_{diatom}$. Sample contamination within the additional 15 samples presented here for the first time in this thesis is no different to the 25 $\delta^{18}O_{diatom}$ samples first presented in Chapter 2 (Fig. 20). Diatom biovolume measurements shows the $\delta^{18}O_{diatom}$ signal measured here to originate from only two diatom taxa: *C. marginatus* and *C. radiatus* (Fig. 20). As outlined in previous chapters, evidence from across the North Pacific Ocean indicates that peak fluxes of both *C. marginatus* and *C. radiatus* occur together in autumn/early winter (Takahashi, 1986; Takahashi *et al.*, 1996; Onodera, *et al.*, 2005; Takahashi and Onodera, *pers. comm.* 2006) (Table 6). Consequently, as demonstrated in Chapter 2 and 3, isotope related seasonality effects are not an issue with these samples. Although the sediment trap data at Station 50N indicates that fluxes of 75-150 μm *C. marginatus and C. radiatus* frustules peak in early/mid winter rather than autumn/early winter (Table 6; Onodera *et al.*, 2005), this is almost certainly attributable to the unusually strong El Niño and La Niño conditions which persisted over the monitoring interval from 1997 to 1999 and which delayed the main annual flux of these taxa at Station 50N (Takahashi and Onodera, *pers. comm.* 2006). As such, the exact timing of the main *C. marginatus* and *C. radiatus* blooms recorded at Station 50N are not reflective of typical normal conditions in the region (Takahashi and Onodera, *pers. comm.* 2006). However, based on other studies which clearly indicate that *C. marginatus* and *C. radiatus* predominantly bloom together in the North Pacific Ocean during autumn/early winter months, (Takahashi, 1986; Takahashi *et al.*, 1996; Onodera, *et al.*, 2005; Takahashi and Onodera, *pers. comm.* 2006), the $\delta^{18}O_{diatom}$ signal analysed here in the 75-150 μm fraction can still be assumed to be representative of autumn/early winter conditions.

4.4.1.2. Species effects

As shown in Chapter 2, evidence exists that vital/species effect may be present in $\delta^{18}O_{diatom}$. The presence of size effects can be partially ruled out by only analysing diatoms from the 75-150 μm fraction. While the size range would ideally be smaller to further reduce the risk of a size effect

influencing $\delta^{18}O_{diatom}$, such a large size range is necessary in order to extract sufficient numbers of diatoms for isotope analysis. With regards to possible inter-species effects, although the 75-150 μm fraction is marked by a large shift in species biovolume from *C. marginatus* to *C. radiatus* (Fig. 20b), this occurs much later at 2.71 Ma (102.66 meters below sea floor [mbsf]) than the 4.6‰ decreases in $\delta^{18}O_{diatom}$ at 2.73 Ma (102.99 mbsf). In addition, further shifts in $\delta^{18}O_{diatom}$ of 5-10‰ elsewhere in the analysed section after 2.70 Ma do not coincide with large changes in the diatom biovolumes (Fig. 20b, 21). Consequently, while a vital/species effects may be partially influencing some of the $\delta^{18}O_{diatom}$ stratigraphical shift between samples, almost all of the change in $\delta^{18}O_{diatom}$ is likely to be independent of any species/vital effect signal. This is particularly true during the 4.6‰ decrease in $\delta^{18}O_{diatom}$ at 2.73 Ma and the 5-10‰ fluctuations in $\delta^{18}O_{diatom}$ after 2.70 Ma, which are significant greater than the mean 1.23‰ isotope offsets observed in Chapter 2 over approximately the same time interval. In order to avoid any errors, however, no detailed attempt can be made to interpret the minor fluctuation in $\delta^{18}O_{diatom}$ prior to 2.73 Ma when $\delta^{18}O_{diatom}$ varies by only 1.4‰ from 43.4‰ to 44.8‰.

4.4.1.3. Silica maturation/secondary isotope exchanges

As described in previous chapters, a significant issue around the use of $\delta^{18}O_{diatom}$ stems from the occurrence of secondary isotope exchanges during sedimentation and burial within the sediment (Brandriss *et al.* 1998; Schmidt *et al.* 1997, 2001; Moschen *et al.*, 2006). The exact operation of these processes remains uncertain, but appear related to silica maturation in the surface sediments or at the sediment-water interface. As detailed in Chapter 1, during silica maturation isotopically heavier ^{18}O in the outer hydroxyl layer of the diatom forms -Si-O-Si linkages which act to increase the $\delta^{18}O$ composition of the analysed -Si-O-Si layer of the diatom frustule (Schmidt *et al.* 1997; 2001; Moschen *et al.*, 2006). As such, measured $\delta^{18}O_{diatom}$ reflects a weighted linear combination of the pre-silica maturation -Si-O-Si layer ($\delta^{18}O_{\text{-Si-O-Si}}$) and the -Si-O-Si linkages formed during silica maturation after dehydroxylation ($\delta^{18}O_{dehydroxyl}$):

$$\delta^{18}O_{diatom} = \delta^{18}O_{\text{-Si-O-Si}} + \delta^{18}O_{dehydroxyl} \quad \text{(Eq. 20)}$$

In turn, the isotope composition of $\delta^{18}O_{dehydroxyl}$ will be a function of the isotope fractionation, governed by the fractionation factor "*f*", that occurs between the pre-dehydroxylation -Si-OH layer ($\delta^{18}O_{\text{-Si-OH}}$) and the dehydroxyl component of the -Si-O-Si layer:

$$\delta^{18}O_{dehydroxyl} = f[\delta^{18}O_{\text{-Si-OH}}] \quad \text{(Eq. 21)}$$

Since the isotope composition of $\delta^{18}O_{\text{-Si-OH}}$ will reflect the $\delta^{18}O$ of the water it last came into contact with, $\delta^{18}O_{\text{-Si-OH}}$ at the time of silica maturation will reflect either $\delta^{18}O_{bottomwater}$ or $\delta^{18}O_{porewater}$ or a combination of the two. Based on this, several lines of evidence can be found to

indicate that issues of silica maturation are not adversely altering the isotopic composition of the diatoms analysed here.

Firstly, diatoms in the 75-150 μm fraction are dominated by only two taxa. At present, no evidence exists to suggest that inter- and intra-species variations exist in the magnitude of secondary isotope exchange in diatoms, i.e., the fractionation factor "*f*" is constant. Consequently, any silica maturation effect should be consistent across all analysed samples, allowing $\delta^{18}O_{diatom}$ to still be used in quantitative palaeoceanographic reconstructions. Even if "*f*" does vary between different taxa, since the relative biovolume composition of individual species are constant over many of the large changes in $\delta^{18}O_{diatom}$ (Fig. 20, 21), it makes it unlikely that inter-species variations in silica maturation are controlling changes in $\delta^{18}O_{diatom}$.

Secondly, as outlined above, the isotopic composition of $\delta^{18}O_{dehydroxyl}$ is a function of $\delta^{18}O_{-Si-OH}$, which in turn is controlled by changes in $\delta^{18}O_{bottom/porewater}$. Consequently if silica maturation was having a significant impact on $\delta^{18}O_{diatom}$, and if it is assumed that "*f*" is constant or near constant between different taxa and over time, stratigraphical changes in $\delta^{18}O_{diatom}$ should follow changes in $\delta^{18}O_{bottom/porewater}$. However, variations in bottom water $\delta^{18}O$ across the analysed time interval, as recorded by both a local and a stacked benthic foraminifera record (Maslin *et al.*, 1995b; 1996; Shackleton et al., 1995; Lisiecki and Raymo, 2005), are not synchronous with changes in $\delta^{18}O_{diatom}$.

Further evidence to suggest that issues of silica maturation are not significant in controlling $\delta^{18}O_{diatom}$ are found within other data at ODP Site 882. Here, as with other studies (see Leng and Barker, 2006), a strong correlation exists between changes in $\delta^{18}O_{diatom}$ and other more established palaeoceanographic proxies. For example, changes in U^{k}_{37} SST closely match changes in $\delta^{18}O_{diatom}$ (Fig. 21), particularly at 2.73 Ma when $\delta^{18}O_{diatom}$ decreases by 4.6‰ and SST increases by 7°C (Haug *et al.*, 2005). This suggest that a strong surface water palaeoceanographic signal prevails in $\delta^{18}O_{diatom}$ and that this signal, at the very least, significantly overrides any possible silica maturation effect.

Finally, it is important to note that while silica maturation has resulted in isotope deviations of up to 10‰ in laboratory experiments (Schmidt *et al.* 1997; 2001), many of the isotope shifts in $\delta^{18}O_{diatom}$ here at ODP Site 882 (Fig. 21) are greater than the peak, in-field, silica maturation effect of 2.5‰ observed by Moschen *et al.* (2006). Consequently, whilst issues of secondary isotope exchange can not be completely ruled out, given the above lines of evidence together with the extremely well preserved state of the diatom frustules and the lack of any visible signs of diagenesis, the impact of secondary isotope exchange on $\delta^{18}O_{diatom}$ can be assumed to be limited throughout the analysed interval. This, combined with other evidence in Section 4.4.1

that changes in $\delta^{18}O_{diatom}$ are unlikely to be related to vital/species effects, sample contamination or seasonality effects, indicates that variations in $\delta^{18}O_{diatom}$ can be interpreted to reflect changes in surface water palaeoceanographic conditions over the onset of major NHG.

4.4.2. Sea Surface Salinity (SSS) reconstruction

In the modern North Pacific Ocean coccoliths primarily calcify during the autumn months with a peak flux in October/November (Ohkouchi *et al.*, 1999; Pagani *et al.*, 2002; Harada *et al.*, 2006; Seki *et al.*, 2007). Recently published coccolith U^{k}_{37} measurements, from *Emiliana huxleyi*, therefore provide an autumn SST reconstructions at ODP Site 882 between 2.85 and 2.39 Ma (Fig. 21) (Haug *et al.*, 2005). Since $\delta^{18}O_{diatom}$ also reflects autumn/winter conditions in the photic zone, the two records can be combined to calculate changes in SSS. The benthic $\delta^{18}O_{foram}$ record at ODP Site 846 (Shackleton *et al.*, 1995) is utilised to remove the $\delta^{18}O_{GIV}$ component from $\delta^{18}O_{diatom}$, while changes in SST are accounted for using the previously mentioned U^{k}_{37} SST record (Haug *et al.*, 2005). While a benthic $\delta^{18}O_{foram}$ record does exist for ODP Site 882 (Maslin *et al.*, 1995b; 1996), the very low resolution nature of this record is not suitable for comparison with the $\delta^{18}O_{diatom}$ data.

As outlined in Chapter 1, the relationship between SSS and $\delta^{18}O_{water}$ may vary over time in response to changes in the $\delta^{18}O$ composition of the oceanic and freshwater end-members. Defining the exact SSS:$\delta^{18}O$ relationship is complicated by the large range of different estimates for the $\delta^{18}O$ value of individual ice sheets (Duplessy *et al.*, 2002). For example, at the Last Glacial Maximum estimates of $\delta^{18}O$ for the Eurasian and North American ice-sheets range from −16‰ to −40‰ and −28‰ to −34‰ respectively (ibid). To avoid making incorrect assumptions, a range of SSS values are reconstructed here in order to account for the fact that SSS:$\delta^{18}O$ may have varied from 1 to 2 over time. Similar uncertainties also exist over the true marine $\delta^{18}O_{diatom}$-temperature coefficient, with estimates ranging from −0.2‰/°C to −0.5‰/°C (see Chapter 1; Juillet-Leclerc and Labeyrie, 1987; Shemesh *et al.*, 1992; Brandriss *et al.*, 1998; Moschen *et al.*, 2005). To again avoid making any errors, changes in SSS using a $\delta^{18}O_{diatom}$-temperature coefficient of −0.2‰/°C are displayed in Figure 21 and Figure 22 and primarily used throughout the remainder of the discussion. For clarity, since a $\delta^{18}O_{diatom}$-temperature coefficient of −0.5‰/°C can not be ruled out, alternative SSS calculations using this higher coefficient are displayed in Figure 22.

A major assumption of this SSS reconstruction is that the coccoliths (*E. huxleyi*), *C. marginatus* and *C. radiatus* all bloom within the same months. In the modern North Pacific Ocean, blooms of *C. marginatus* and *C. radiatus* can continue into the early winter months (Takahashi, 1986; Takahashi *et al.*, 1996; Onodera, *et al.*, 2005) when SST are lower than during autumn. This introduces an error into the above calculations which can not be fully quantified. However, this

error would act to increase, not decrease, the magnitude of the SSS changes over the analysed interval. As such, the reconstructed changes in SSS in Figure 22 should, if anything, be regarded as a lower-range estimate of the true salinity changes over this time interval.

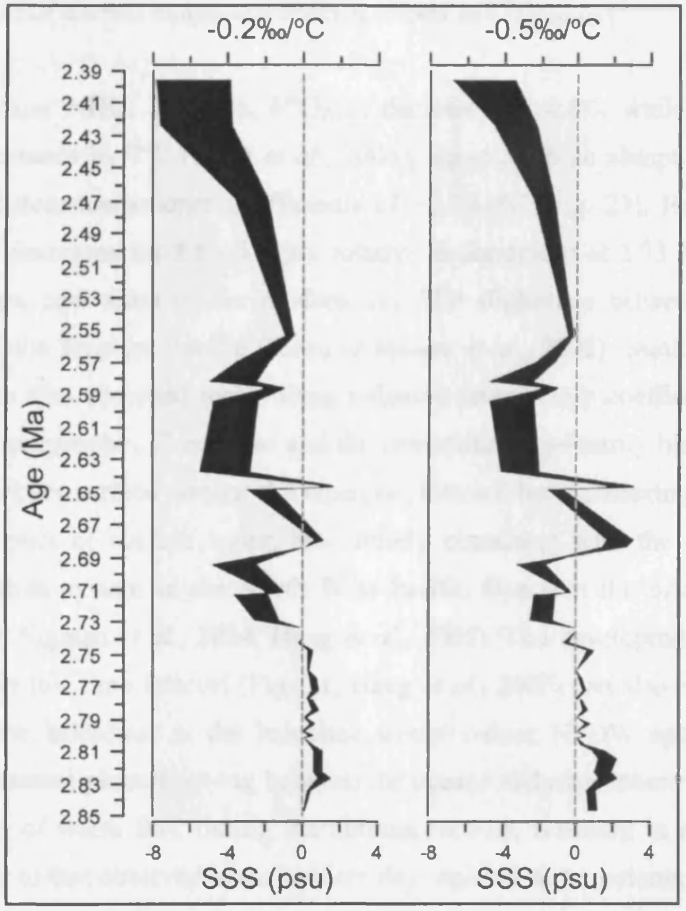

Figure 22: Calculated changes in SSS in the North West Pacific Ocean from 2.85 Ma to 2.39 Ma, relative to a SSS of 0 psu at 2.73 Ma, assuming different $\delta^{18}O_{diatom}$-temperature coefficients. Since the SSS:$\delta^{18}O$ relationship may vary between 1 and 2, a range of SSS values are reconstructed (shaded).

4.4.3. Onset of major NHG at ODP Site 882

$\delta^{18}O_{diatom}$ variations of less than 1.4‰ prior to 2.73 Ma suggest the presence of comparatively uniform autumn/winter condition in the North West Pacific Ocean (Fig. 21). Stable autumn U^{k}_{37} SST reconstructions of below 11°C verify this except from 2.83 Ma to 2.81 Ma when U^{k}_{37} SST indicate a 2°C increase to 13°C (Haug *et al.*, 2005) while no corresponding shift occurs in $\delta^{18}O_{diatom}$ (Fig. 21). During this interval, calculated SSS therefore appear to have increased by 0.5-1 psu (Fig. 21, 22). However, the lack of any change in $\delta^{18}O_{diatom}$ during this period may also reflect an insensitivity of $\delta^{18}O_{diatom}$ to record small-scale changes in SST. This could be related to the relatively high $\delta^{18}O_{diatom}$ reproducibility (up to 0.44‰ in some samples in this study), combined with the possibility for $\delta^{18}O_{diatom}$-temperature coefficients to be as low as −0.2‰/°C

(Brandriss *et al.*, 1998; Moschen *et al.* 2005). Using this coefficient, the 2°C disparity between $\delta^{18}O_{diatom}$ and U^{k}_{37} SST is within our 0.44‰ $\delta^{18}O_{diatom}$ analytical reproducibility. Consequently, minor shifts in SST recorded in $\delta^{18}O_{diatom}$ may be inseparable from the analytical error. Alternatively, as suggested in Section 4.4.1.2, it is possible that the difference between the two records is as a result of a small magnitude species effects in $\delta^{18}O_{diatom}$.

At the onset of major NHG, 2.73 Ma, $\delta^{18}O_{diatom}$ decreases by 4.6‰ while U^{k}_{37} autumn SST simultaneously increases by 7°C (Haug *et al.*, 2005), equating to an abrupt SSS freshening of 1.9 psu under a diatom-temperature coefficients of −0.2‰/°C (Fig. 21). By 2.70 Ma, SSS is calculated to have decreased by 2.5 - 5.1 psu relative to conditions at 2.73 Ma (Fig. 21, 22), a considerable change equivalent to the modern day SSS difference between the North West Pacific Ocean and the Tropical Pacific Ocean (Antonov *et al.*, 2005). Similar high magnitude changes in SSS are also observed when using a diatom-temperature coefficients of −0.5‰/°C (Fig. 22). With *C. marginatus*, *C. radiatus* and the coccoliths all primarily blooming together in the autumn/early winter surface waters, the changes observed here, indicating the development of a low salinity pool of surface water, are entirely consistent with the development of a halocline stratification system in the North West Pacific Ocean at the onset of major NHG (Haug *et al.*, 1999; Sigman *et al.*, 2004; Haug *et al.*, 2005). The development of warm, rather than cold, SST over this time interval (Fig. 21, Haug *et al.*, 2005) can also be attributed to the establishment of the halocline, as the halocline would reduce NPDW upwelling while also reducing the temperature phase/time-lag between the oceans and atmosphere (ibid). This would allow the build up of warm SST during the autumn months, resulting in a marked seasonal thermocline similar to that observed in the modern day regional water column (Fig. 6).

Mechanisms for the initiation and development of the halocline in the region have previously been investigated by Sigman *et al.* (2004). This paper, reiterated here by the reconstruction of a significant SSS decrease after 2.73 Ma and concordant increase in IRD (Fig. 21), makes it clear that freshwater input to the region is a significant factor in causing a stratified system to develop in and around ODP Site 882. Sigman *et al.* (2004) conclude, however, that freshwater inputs alone are unlikely to be the direct instigator for the development of the stratified system. While this suggests the potential operation of some other climatic cooling or solar forcing mechanism/feedback system (ibid), it currently remains unknown as to what this initial trigger may have been. Model evidence raises the possibility that the closure of the Panama Ocean gateway, previously identified to have increased moisture supply to Europe (Haug and Tiedemann, 1998; Haug *et al.*, 2001; Lear *et al.*, 2003; Bartoli *et al.*, 2005; Schneider *et al.*, 2006; Steph *et al.*, 2006), could also have played a significant role by causing a reduction in the Pacific Ocean deep water thermohaline circulation (Motoi *et al.*, 2005). The exact mechanisms by which this reduction could have led to the development of a halocline in the North West

Pacific Ocean is not made clear. One possibility, though, is that an interval of reduced NPDW upwelling could have led to an initial phase of freshwater build-up in the photic zone, which was sufficient to generate an initial stratification system. Once established, the stratified water column in the North West Pacific Ocean would have become self-sustaining through further influxes of meltwater, enhancing and reinforcing the existing salinity gradient between the surface and sub-surface layers (Sigman *et al.*, 2004).

4.4.3.1. Evidence against halocline stratification at 2.73 Ma

Records of $\delta^{18}O_{diatom}$ and U^{k}_{37}, in combination with the opal MAR outlined in Section 4.1, provided strong evidence for the development of a halocline stratified water column in the region from 2.73 Ma (Fig. 21). However, these interpretations at first sight appear inconsistent with a 2.6‰ increase in $\delta^{18}O_{foram}$ over the same interval (Maslin *et al.*, 1995b; 1996), which are indicative of significantly cooler conditions and an unstratified water column (see Section 4.1). However, it is highly unlikely that the two planktonic foraminifera species analysed for $\delta^{18}O$, *Globigerina bulloides* and *Neogloboquadrina pachyderma*, are reflective of autumn/winter surface water conditions (Maslin *et al.*, 1995b; 1996). Sediment trap studies from across the globe indicate that the $\delta^{18}O$ composition of *G. bulloides* and *N. pachyderma* is primarily indicative of spring conditions (Kohfeld *et al.*, 1996; Ganssen and Kroon, 2000; Kuroyanagi *et al.*, 2002; Mohiuddin *et al.*, 2002). In particular, nearby sediment trap data at 50°01'N, 165°02'E shows these species to be most prevalent in spring, although some fluxes do occur during the early winter months (Kuroyanagi *et al.*, 2002). As such, it is highly likely that the records of $\delta^{18}O_{foram}$ in Maslin *et al.* (1995b; 1996) are reflective of spring, not autumn, palaeoceanographic conditions at ODP Site 882. Such a spring cooling trend in $\delta^{18}O_{foram}$ at 2.73 Ma is actually consistent with what would be expected to occur following the development of a halocline system. As described above in Section 4.4.3, the development of a stratified water column would reduce the temperature phase lags between the ocean and atmosphere relative to unstratified state conditions. While this would increase autumn/early winter SST, reduced phase-lags would also lower spring SST, causing an unusually large seasonal SST gradient similar to that found in the modern day water column around ODP Site 882 (Fig. 6). This spring cooling trend would then be further enhanced by the cooler atmospheric conditions that would accompany the onset of major NHG, and by spring increases in the delivery of cold freshwater and melting icebergs to ODP Site 882 (as indicated by the increase in IRD from c. 2.73 Ma in Figure 21). Verification that the cooling trend in $\delta^{18}O_{foram}$ is reflective of and consistent with expected spring conditions could be obtained by measuring $\delta^{18}O_{diatom}$ in spring blooming taxa. Spring blooming diatom taxa are present in the <75 μm size fractions at ODP Site 882. However, these size fractions also contain a number of autumn blooming taxa in addition to numerous fragments of the larger *C. marginatus* and *C. radiatus* frustules analysed here. As such, any isotope record would be heavily influenced by both the species effects, observed in

Chapters 2 and 3, and by a possible seasonality effect.

Further evidence to indicate that the increase in $\delta^{18}O_{foram}$ over the onset of major NHG is not reflective of autumn/early winter surface water conditions is found by examining the depth-habitats of *G. bulloides* and *N. pachyderma*. Records of $\delta^{18}O_{foram}$ are highly susceptible to a species vertical migration and seasonal position in the water column (Hemleben *et al.*, 1989; Kohfeld *et al.*, 1996; Kuroyanagi and Kawahata, 2004). Studies in the North Pacific Ocean indicate that *G. bulloides* and *N. pachyderma* live at a water depth of between 0 m and 300 m with a strong peak between 80 m and 200 m for *N. pachyderma* (Kohfeld *et al.*, 1996; Kuroyanagi and Kawahata, 2004). *N. pachyderma* has also been found at some sites in the North Pacific Ocean to occur entirely below the pycnocline (Kuroyanagi and Kawahata, 2004). Consequently, even if the foraminifera's dominant growth season had switched in the past from spring to autumn, $\delta^{18}O_{foram}$ does not have the potential to reflect conditions within the autumn/early winter thermocline that today lies at c. 50 m (Fig. 6).

4.4.3.2. Onset of NHG palaeoclimatic implications

The growth and establishment of a halocline system in the North West Pacific Ocean has significant implications for our understanding of events at the beginning of NHG. Prior to the onset of major NHG at 2.73 Ma when the region was marked by an open water column, upwelled nutrient rich NPDW would have ventilated carbon sequestered within the deep ocean to the atmosphere (Haug *et al.*, 1999). The development of a halocline driven water column in the region would have significantly restricted any deep water ventilation. As such, the region over the onset of major NHG likely played a significant role in causing globally cooler climatic conditions and further permitting the growth of ice sheets across the Northern Hemisphere. Indeed estimates in Haug *et al.* (1999) suggest that the development of a stratified system in the region could have led to a lowering in atmosphere pCO_2 by as much as 30-40 ppmv.

Evidence here and in Haug *et al.* (2005) for a warm, c. 17-18°C, pool of surface water from the onset of major NHG (Fig. 21), also suggests the region may have acted as a key moisture source to the North American ice sheets. This is reinforced by a climate model simulation testing the significance of the presence/absence of a halocline in the North West Pacific Ocean (Haug *et al.*, 2005). Importantly, measurements of $\delta^{18}O_{diatom}$ indicate that warm SST conditions could have prevailed well into the winter months. Consequentially the delivery of large quantities of moisture to North America could have continued at the time most favourable to glacial advance and snow accumulation. This, may have been further aided by decreasing SST in the eastern tropical Pacific Ocean over the same time interval, which would have acted to reduce temperatures across much of the North American continent (e.g., Huybers and Molnar, 2007).

4.4.3.3. Post 2.73 Ma changes at ODP Site 882

Following the development of the halocline system at 2.73 Ma, large fluctuations in $\delta^{18}O_{diatom}$ and SSS remain apparent in the sedimentary record, particularly from 2.70 Ma onwards. Given the current low resolution nature of the $\delta^{18}O_{diatom}$ record, however, it is unwise to make any palaeoceanographic interpretations at this time at to their meaning. Such large changes in $\delta^{18}O_{diatom}$, however, make it clear that major palaeoceanographic changes must have continued in the region after the initial onset of major NHG at 2.73 Ma. While, for example, the $\delta^{18}O_{diatom}$ and SSS records indicate a possible reversal to pre-halocline conditions at 2.65 Ma (Fig. 21), the lack of concordant changes in U^{k}_{37} and opal MAR fails to support this suggestion. Several attempts have been made during the course of this PhD to improve the temporal resolution of the $\delta^{18}O_{diatom}$ record after c. 2.70 Ma, in order to assess the stability of the halocline and the relationship between $\delta^{18}O_{diatom}$ and U^{k}_{37} over the glacial-interglacial cycles that follow the initial onset of major NHG at 2.73 Ma. However, these attempts have so far failed due to the difficulties in extracting sufficiently clean diatoms for isotope analysis. While at some levels it has proven possible to extract clean material, in almost all cases the amount extracted was too small for isotope analysis.

4.5. Conclusions

Results here provide the first $\delta^{18}O_{diatom}$ record across the onset of major NHG. By analysing season specific diatom samples for $\delta^{18}O$, strong evidence was found to support claims that a halocline system developed in the North West Pacific Ocean from 2.73 Ma. Confirmed by recently published U^{k}_{37} data which indicates a simultaneous c. 7°C increase in SST over the same interval, a plausible mechanism now exists by which adequate supplies of moisture could have been delivered to the growing North American ice sheets (Haug *et al.*, 2005). The onset of stratification further supports claims that the region may have made a significant contribution towards lowering atmospheric CO_2 concentrations by preventing deep water ventilation at the surface (Haug *et al.*, 1999). In contrast to the autumn/early winter $\delta^{18}O_{diatom}$ and U^{k}_{37}, the increase in planktonic $\delta^{18}O_{foram}$ most likely indicates oceanographic changes during spring months. This use of $\delta^{18}O_{diatom}$ alongside $\delta^{18}O_{foram}$ therefore highlights the considerable potential that both proxies contain, when utilised together, in aiding our understanding and interpretation of past climatic events. Consequently, $\delta^{18}O_{diatom}$ should not be considered solely as an alternative measure of $\delta^{18}O$ at sites where foraminifera, and other carbonates, are not present in the sedimentary record.

Chapter 5: Palaeoceanographic reconstruction of changes in North West Pacific Ocean stratification over the last 200 kyr

5.1. Introduction

Records from Antarctica and Greenland ice-cores indicate significant variations in atmospheric concentrations of CO_2 (pCO_2) over glacial-interglacial cycles. During glacials, in which fluctuations of up to 60 ppmv occur, concentrations of atmospheric pCO_2 are 80-100 ppmv lower than in interglacials (Anklin *et al.*, 1997; Petit *et al.*, 1999). In light of the role of CO_2 in determining global climatic conditions, considerable palaeoclimatic research in recent years has been concerned with attempting to understand the processes which lead to these large changes over both long, glacial-interglacial, and shorter, millennial, timescales. Despite this, the mechanisms behind these past changes in pCO_2 have yet to fully identified or explained.

One process which may explain a significant proportion of the above changes in atmospheric pCO_2 is the marine biological pump and associated export of organic matter into the ocean interior (Broecker, 1982 a,b). Changes in the marine biological pump at both high and low latitudes may be significant in modulating atmospheric pCO_2 (e.g., Sigman and Haug (2003); Marchitto *et al.* (2007) and references within). Attention to date, though, has primarily focused on the role of the biological pump, in combination with other oceanographic processes such as changes in ocean circulation and Sea Surface Temperature (SST), in the Antarctic and Subantarctic waters of the Southern Ocean (e.g., Francois *et al.*, 1997; Brzezinski *et al.*, 2002; Matsumoto *et al.*, 2002; Sigman *et al.*, 2004). Within this region, the role of the biological pump has been considered within the modern day framework of high nutrient availability, Fe limitation and significant ventilation of deep water at the surface-atmosphere interface. As such, increased Southern Ocean sequestration of atmospheric pCO_2 during glacials has been proposed through higher aeolian Fe deposition and associated increases in diatom productivity (Martin, 1990; Brzezinski *et al.*, 2002; Matsumoto *et al.*, 2002). Similarly, increased marine storage of carbon and reduced deep water ventilation has also been proposed through a variety of oceanographic processes including extended sea-ice cover, enhanced stratification and/or decreases in deep water upwelling (Francois *et al.*, 1997; Moore *et al.*, 2000; Stephens and Keeling, 2000; Keeling and Stephens, 2001; Keeling and Visbeck, 2001; Sigman *et al.*, 1999; Sigman and Boyle, 2000, 2001 Sigman *et al.*, 2004; Hillenbrand and Cortese, 2006).

However, whilst some models support the suggestion that changes in the Southern Ocean are sufficient to explain all or a significant majority of the observed glacial-interglacial and glacial variability in atmospheric pCO_2 (e.g., Stephens and Keeling, 2000) others suggest that the region can only explain a proportion of the observed pCO_2 variations (Morales Maqueda and Rahmstorf, 2002). This was reiterated in a review of sediment core palaeoceanographic data from across the Southern Ocean (Kohfeld *et al.*, 2005). Consequently, in an attempt to better

understand the mechanisms which may control past fluctuations in atmospheric pCO_2, there is a need to investigate other aspects of the marine system such as the role of the biological pump outside of the Southern Ocean. One of the regions most likely to play an important role within this context is the North Pacific Ocean.

5.1.1. North Pacific Ocean biological pump

Similar to the Southern Ocean much of the North Pacific Ocean is today nutrient limited with respect to Fe (Harrison *et al.*, 1999; Tsuda *et al.*, 2003; Yuan and Zhang, 2006). As described in Chapter 2, the North West Pacific Ocean differs significantly from the Southern Ocean by the presence of a strong, year round, halocline which limits deep water upwelling and gas-exchange at the ocean-atmosphere interface (Tabata, 1975; Gargett, 1991). From a biological perspective, stratification in the region also plays an important role in controlling surface water productivity by limiting the transportation of nutrients from the deep water to the photic zone (ibid). As shown in Chapter 4, and references within, the initial development of the halocline in the region was linked to the onset of major NHG at 2.73 Ma, resulting in increased moisture supply to the North American ice sheets and an overall net decrease in oceanic release of CO_2 into the atmosphere. While considerable research has and continues to be undertaken over this interval, comparatively little is known about changes in the North West Pacific Ocean over recent glacial-interglacial cycles.

Understanding past changes in the halocline and water column stratification in the North West Pacific Ocean may be essential for determining the palaeoclimatic role of the region in modulating atmospheric pCO_2. Today, the stratified water column acts as a net sink of atmospheric CO_2 (Honda *et al.*, 2002; Chierici *et al.*, 2006). The presence of a mixed water column in the past, however, would have altered this by allowing significant upwelling of nutrient and carbon rich deep water to the surface. Depending on the response of the biological pump, this could either have caused a significant increase in the oceanic ventilation of CO_2 to the atmosphere or, if the net increase in biological productivity was sufficiently high, resulted in an increased draw-down of CO_2. Previous transitions in the regional water column from a stratified to unstratified ocean at 2.73 Ma have been estimated to have lowered atmospheric pCO_2 by 30-40 ppmv (Haug *et al.*, 1999). Consequently it is viable that water column changes in the opposite direction could also have resulted in global atmospheric pCO_2 changes of a similar magnitude: sufficient to explain approximately half of the total glacial-interglacial shift in atmospheric pCO_2 (Anklin *et al.*, 1997; Petit *et al.*, 1999).

At present, conflicting evidence exists over the state of the North West Pacific Ocean halocline over the last glacial cycle. The majority of studies, based on isotope, biogenic barium and diatom assemblage data, argue for an enhanced halocline (Sancetta, 1983; Keigwin *et al.*, 1992;

Jaccard *et al.*, 2005; Brunelle *et al.*, 2007). With these studies also indicating minimal changes in biological productivity, the role of the North Pacific Ocean in controlling past atmospheric variations in pCO_2 has been interpreted to be negligible (e.g., Keigwin *et al.*, 1992; Sigman *et al.*, 2004; Jaccard *et al.*, 2005). Palaeoceanographic evidence derived from planktonic $\delta^{18}O_{foram}$, foraminifera assemblage counts and Mg/Ca ratios in cores close to ODP Site 882, however, suggest that a mixed water column may have prevailed during at least part of the last glacial period (Keifer *et al.*, 2001; Sarnthein *et al.*, 2004; 2006). In addition, results from elsewhere in the North Pacific Ocean may also be indicative of a mixed water column with periodic large fluxes of diatoms to the sediment and high levels of surface water palaeoproductivity during the last glacial (e.g., McDonald *et al.*, 1999; Kienast *et al.*, 2004; Katsuki and Takahashi, 2005). Consequently, whilst most evidence points towards the existence of a permanently stratified water column, and a minimal role for the North Pacific Ocean in regulating changes in atmospheric pCO_2 over the last glacial cycle, other evidence raises the possibility that the region may have instead played a key role in altering pCO_2. Much of this uncertainty can be attributed to the absence of planktonic foraminifera in the sediment record at many cored sites in the North Pacific Ocean. Here, in this chapter, it is intended to clarify the palaeoceanographic changes in the North West Pacific Ocean over the last 200 kyr by investigating the stability of the halocline at ODP Site 882 using $\delta^{18}O_{diatom}$. By analysing $\delta^{18}O_{diatom}$, the signal of which is entirely derived from the photic zone, changes in salinity and consequently changes in surface water density can be calculated to provide definitive evidence as to past changes in the stratification of the North West Pacific Ocean.

5.2. Methodology

Sediment samples analysed within this chapter were collected from ODP Site 882 in the North West Pacific Ocean (Fig. 5). Site details are presented in Chapter 2. Details on the age model, diatom extraction and isotope methodology for this interval are covered in Chapter 3. Purified diatom samples were analysed for $\delta^{18}O$ over two size fractions, 38-75 μm and >100 μm.

5.3. Results

Levels of non-diatom contamination, both in the samples presented in Chapter 3 and in the additional samples analysed here, are minimal throughout the interval (Fig. 13, 14, 23). $\delta^{18}O_{diatom}$ results from both the 38-75 μm and >100 μm fractions show large, simultaneous, variations of 10-13‰ over the last 200 kyr BP, indicating significant palaeoceanographic changes in the region (Fig. 23). Replicate analyses indicate a mean analytical error of 0.49‰ in the 38-75 μm fraction, 0.28‰ in the >100 μm fraction and 0.48‰ for BFC_{mod} (the NIGL within-run laboratory diatom standard). Samples in the >100 μm fraction are dominated by *C. radiatus*, which in the North Pacific Ocean predominantly blooms in autumn/early winter (e.g., Takahashi, 1986; Takahashi *et al.*, 1996; Onodera et al., 2005). In contrast, the 38-75 μm fraction contains

multiple species which bloom in different seasons, e.g,. the spring dominated *A. curvatulus* and the autumn/winter *C. radiatus*. Despite the high $\delta^{18}O_{diatom}$ correspondence between the two size fractions, in order to eliminated any seasonality effect in addition to any inter-species and size-related vital/species effects (Chapter 3), palaeoenvironmental interpretations can only be derived from the >100 μm fraction.

In contrast to results from ODP Site 882 over the intensification of major NHG (Chapter 4), no correlation exists between the U^{k}_{37} SST record Haug (1995) and $\delta^{18}O_{diatom}$ values in the >100 μm fraction (Fig. 24). For example, high $\delta^{18}O_{diatom}$ values between 121.6 kyr BP and 92.2 BP correspond with high SST of c. 14°C while high $\delta^{18}O_{diatom}$ values between 72.4 kyr BP and 51.3 kyr BP correspond to a period of low SST of less than 7°C. While for much of the interval changes in opal Mass Accumulation Rates (MAR) are not concurrent with changes in $\delta^{18}O_{diatom}$, notable decreases in $\delta^{18}O_{diatom}$ from 92.2 kyr BP, 67.7 kyr BP and 9.1 kyr BP onwards are synchronous with decreases in opal MAR. While large changes in opal MAR do occur throughout the interval, accumulation rates of 0.0-1.6 g/cm^2 kyr remain significantly below the 2.5-4.5 g/cm^2 kyr which typified the open-water column at ODP Site 882 prior to 2.73 Ma (see Chapter 2 Figure 21:, Haug, 1995; Haug *et al.*, 1999).

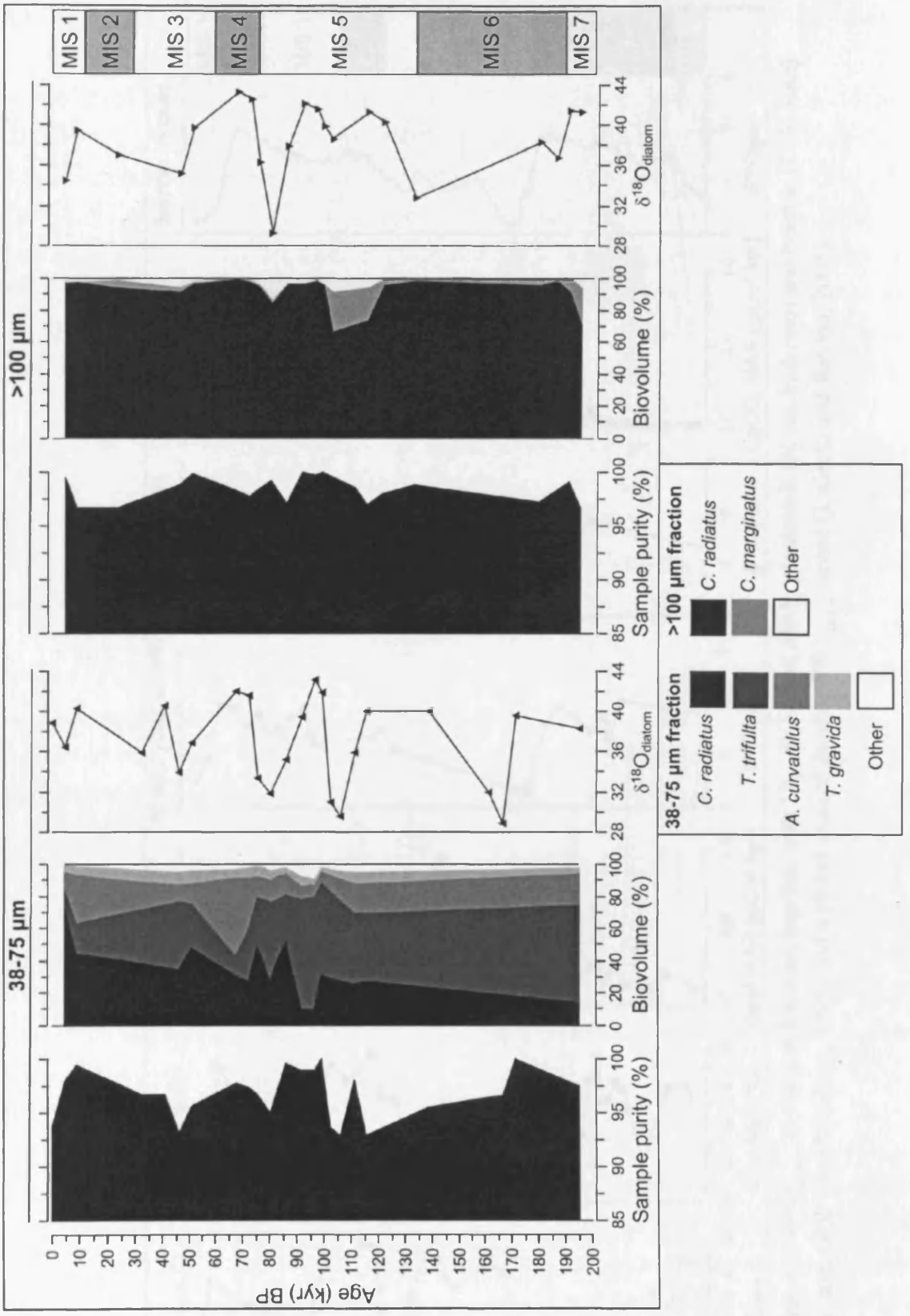

Figure 23: Comparison of the 38-75 µm and >100 µm fractions showing sample purity (percentage of diatom material relative to all other material), the relative diatom species biovolume and $\delta^{18}O_{diatom}$ (relative to V-SMOW). Error bars for $\delta^{18}O_{diatom}$ are within the size of the symbols.

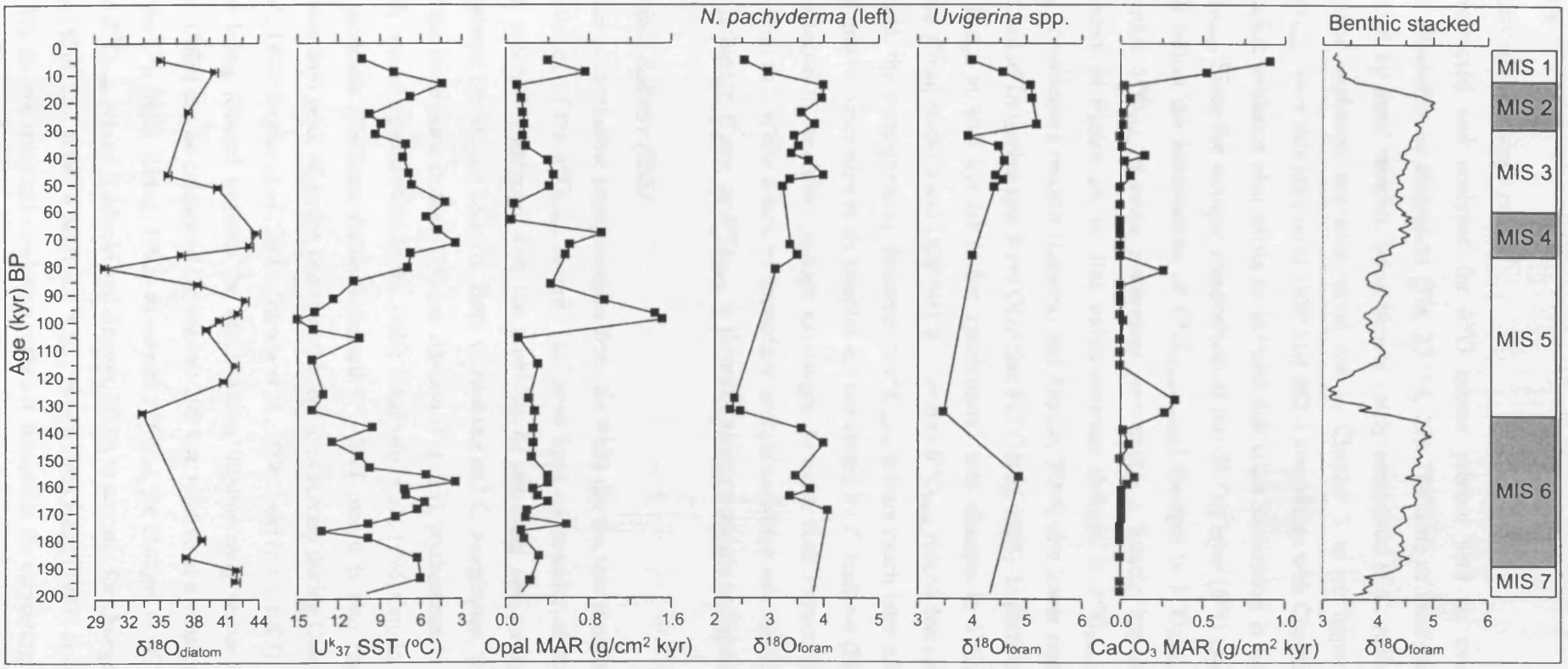

Figure 24: Comparison of $\delta^{18}O_{diatom}$ (>100 µm fraction) together with U^{k}_{37} SST, opal MAR, planktonic (*N. pachyderma*) and benthic (*Uvigerina*) $\delta^{18}O_{foram}$ records from ODP site 882 (Haug, 1995) and a global stacked benthic $\delta^{18}O_{foram}$ record (Lisiecki and Raymo, 2005).

5.4. Discussion

5.4.1. Reliability of the isotope record

All diatoms extracted and analysed for $\delta^{18}O$ appear pristine with no evidence of any contamination, dissolution or diagenesis (Fig. 13, 14, 23). The issue of vital/species effects is largely eliminated by most samples being almost solely comprised of *C. radiatus* (Fig. 23). Secondary isotope exchange has been ruled out in Chapter 3 as an important factor in controlling $\delta^{18}O_{diatom}$ over this interval at ODP Site 882. However, as with Chapter 4, additional palaeoceanographic evidence also exists to indicate that silica maturation is not significantly impacting $\delta^{18}O_{diatom}$. Since the isotopic composition of the -Si-OH layer ($\delta^{18}O_{-Si-OH}$) during silica maturation will reflect the composition of $\delta^{18}O_{bottom/porewater}$, changes in $\delta^{18}O_{diatom}$ would mirror changes in benthic $\delta^{18}O_{foram}$ if silica maturation was having a notable impact on $\delta^{18}O_{diatom}$. However as shown in Figure 24, no link exists between changes in $\delta^{18}O_{diatom}$ and a global stacked benthic foraminifera records (Lisiecki and Raymo, 2005) or a lower resolution benthic foraminifera record of *Uvigerina* spp. from ODP Site 882 (Haug, 1995). In particular, the 12.9‰ decrease in $\delta^{18}O_{diatom}$ at 80.3 kyr BP is not synchronous with changes in $\delta^{18}O_{foram}$. Similarly, whereas both the global stacked and ODP Site 882 benthic $\delta^{18}O_{foram}$ record decrease from MIS 2 into the Holocene, the corresponding decrease in $\delta^{18}O_{diatom}$ occurs much later after 9.1 kyr BP (Fig. 24). Furthermore, since almost all samples are dominated by *C. radiatus* (Fig. 23), even if inter-species variation in secondary isotope exchanges do exist, their impact on the $\delta^{18}O_{diatom}$ record will be minimal. While issues of secondary isotope exchange can not be conclusively ruled out, their influence, if any, on $\delta^{18}O_{diatom}$ is therefore almost certainly negligible.

5.4.2. Sea Surface Salinity (SSS)

Generating palaeoceanographic interpretations from the >100 μm fraction is not ideal given the low resolution nature of the $\delta^{18}O_{diatom}$ record. This arise from the scarcity of large, >100 μm, diatoms in the sediment combined with the problems of obtaining and purifying sufficient quantities of diatoms for isotope analysis. Both *C. radiatus* and *C. marginatus*, which comprise virtually all of the biovolume in the >100 μm fraction (Fig. 23), predominantly bloom during the autumn/early winter months (Takahashi, 1986; Takahashi *et al.*, 1996; Onodera *et al.*, 2005). Similarly, the coccolith (*Emiliana huxleyi*) derived U^{k}_{37} SST record is also representative of autumn conditions with peak alkenone fluxes in the region occurring during October/November (Ohkouchi *et al.*, 1999; Pagani *et al.*, 2002; Harada *et al.*, 2006; Seki *et al.*, 2007). With fluxes of both organisms being focused towards the same season, autumn/early winter change in Sea Surface Salinity (SSS) can be calculated for the last 200 kyr, relative to a value of 0 psu at 195 kyr BP, using the U^{k}_{37} index (Haug, 1995) to correct $\delta^{18}O_{diatom}$ for changes in SST and a global stacked benthic $\delta^{18}O_{foram}$ record (Lisiecki and Raymo, 2005) to account for changes in global ice volume ($\delta^{18}O_{GIV}$) (Fig. 25). While a benthic $\delta^{18}O_{foram}$ record from Haug (1995) also exists at ODP Site 882 (Fig. 24), its low temporal resolution makes it unsuitable for correcting for the $\delta^{18}O_{GIV}$

component of $\delta^{18}O_{diatom}$.

Due to the potential for $\delta^{18}O_{diatom}$-temperature coefficient to range from −0.2‰/°C to −0.5‰/°C, (Juillet-Leclerc and Labeyrie, 1987; Shemesh *et al.*, 1992; Brandriss *et al.*, 1998; Moschen *et al.*, 2005) two estimates of SSS are calculated (Fig. 25). Further assumptions are also required as to the relationship between SSS and $\delta^{18}O$, which can vary from 1 to 2 depending on the $\delta^{18}O$ composition of the oceanic and freshwater end-members (Rohling, 2000). As stated in previous chapters, defining the exact SSS:$\delta^{18}O$ relationship at ODP Site 882 is complicated by the large range of $\delta^{18}O$ estimates for individual ice sheets. For example, values for the Eurasia and North American ice-sheets at the Last Glacial Maximum vary from −16‰ to −40‰ and −28‰ to −34‰ respectively (Duplessy *et al.*, 2002). To avoid making incorrect assumptions regarding the true SSS:$\delta^{18}O$ relationship, a range of SSS values should be calculated to take into account that SSS:$\delta^{18}O$ may have varied from 1 to 2 over time. However, a relationship of 2 produces SSS values of 40-50 psu for most of the last 200 kyr. Such values are unrealistic and would make the region 20-50% saltier than today and saltier than any part of the modern ocean. The aim of this work is to determine whether waters in the photic zone were ever sufficiently dense to generate overturning and remove the halocline stratification. Due to the nature of SSS changes over the last 200 kyr, the SSS curve produced using a SSS:$\delta^{18}O$ ratio 1 is the most conservative. Consequently, it is sufficient to only use a SSS:$\delta^{18}O$ ratio of 1 in any SSS reconstruction since any unstratified intervals indicated by this ratio would only be reiterated by a higher SSS:$\delta^{18}O$ ratio. Using a SSS:$\delta^{18}O$ of 1, reconstructed changes in SSS display long periods of apparent stability over the last 200 kyr BP (Fig. 25). At 186.5 kyr BP, 133.3 kyr BP, 92.2-72.4 kyr BP, 51.3-23.9 kyr BP and 4.7 kyr BP, however, large freshening events of 6-12 psu are apparent when using both a $\delta^{18}O_{diatom}$-temperature coefficient of −0.2‰/°C and a coefficient of −0.5‰/°C (Fig. 25).

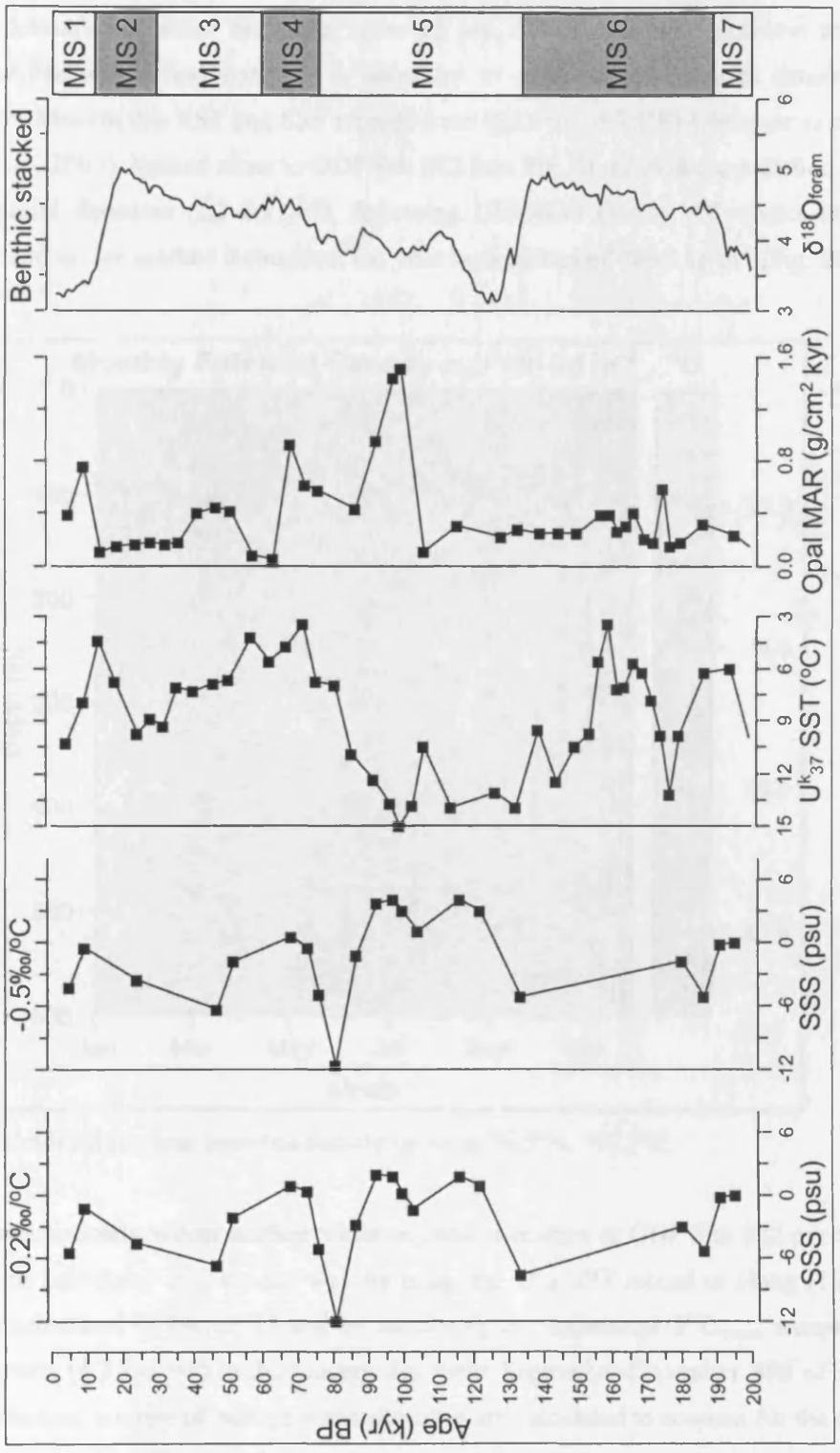

Figure 25: Changes in autumn/early winter SSS relative to a salinity of 0 psu at 195 kyr BP, calculated using a $\delta^{18}O_{diatom}$-temperature coefficient of −0.2‰/°C and −0.5‰/°C and a SSS:$\delta^{18}O$ relationship of 1, together with U^{k}_{37} SST, opal MAR (Haug, 1995) and a stacked global benthic $\delta^{18}O_{foram}$ record (Lisiecki and Raymo, 2005).

5.4.3. Stratification changes in the North Pacific Ocean

In order to determine whether the large, up to 12 psu, SSS fluctuations represent transitions between stratified/unstratified states, it is necessary to calculate the potential density of the water column. Modern day SST and SSS records from (50.5°N, 167.5°E) (Antonov *et al.*, 2005; Locarnini *et al.*, 2005), located close to ODP Site 882 (see Fig. 5), allow the calculation of water column potential densities (σ_θ) for ρ=0, following UNESCO (1983). All waters above the halocline, c. 150 m, are marked throughout the year by densities of <26.8 kg m^{-3} (Fig. 26).

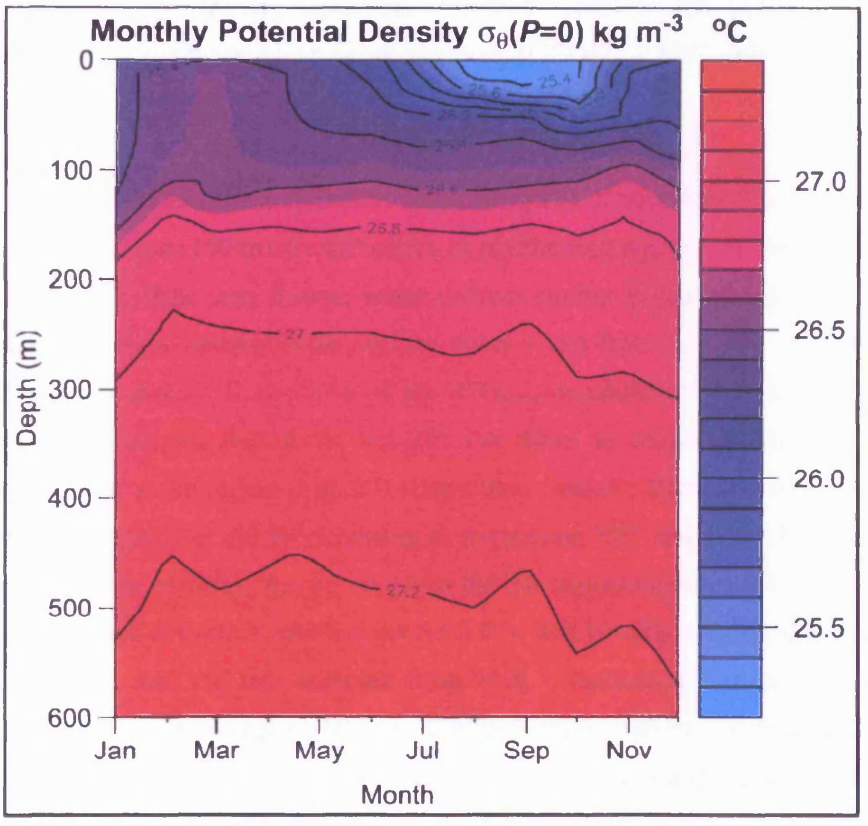

Figure 26: Calculated modern potential density (ρ=0) at 50.5°N, 167.5°E.

Changes in autumn/early winter surface water potential densities at ODP Site 882 over the last 200 kyr can be calculated in a similar way by using the U^k_{37} SST record of Haug (1995), the SSS records calculated in Figure 25 and by anchoring the uppermost $\delta^{18}O_{diatom}$ sample in the >100 µm fraction (4.7 kyr BP) to the modern day mean September-December SSS of 32.8 psu (Fig. 27). As before, a range of surface water densities are calculated to account for the different $\delta^{18}O_{diatom}$-temperature coefficients. In order to assess whether these changes in surface water density are indicative of a stratified or mixed water column, it is also necessary to calculate past changes in the potential density of the halocline boundary (water depth = 150 m) relative to the modern day potential density of 26.8 kg m^{-3} (Fig. 26). For all halocline boundary calculations, the mean modern day September-December temperature (3.46°C) and salinity (33.68 psu) at a water depth of 150 m are assumed to be representative of halocline boundary conditions over

the past 200 kyr BP (Antonov *et al.*, 2005; Locarnini *et al.*, 2005). These assumptions are considered in Section 5.3.1 and are shown to not affect any of the results. Salinity measurements at the halocline boundary are further corrected for changes in global ice volume using the Relative Sea Level (RSL) record of Siddall *et al.* (2003):

$$\Delta S = S_{modern} * \Delta SL/(3900 - \Delta SL) \quad \text{(Eq. 22)}$$

where ΔS is the change in whole ocean salinity relative to today due to variations in global ice volume, S_{modern} is the modern day September-December salinity at 150 m of 33.68 psu (Antonov et al., 2005), 3900 is the mean ocean depth in meters (GEOSEC, 1987) and ΔSL is the change in sea level relative to today.

In the subsequent potential density record (ρ=0) (Fig. 27), higher densities in the surface water relative to the halocline (150 m) are indicative of overturning and the presence of a mixed water column. A stratified, halocline driven, water column similar to the modern day is assumed to exist when the potential density of the surface water is less than the calculated potential density at the halocline boundary. Regardless of the $\delta^{18}O_{diatom}$-temperature coefficient used, evidence exists for up to 4 periods during the last 200 kyr when an unstratified mixed water column would have existed in the region (Fig. 27). Transitions between stratified/unstratified conditions appear linked to periods of either increasing or decreasing SST and, as such, transitions into or out of interglacial/interstadials. However, given the low resolution nature of the $\delta^{18}O_{diatom}$ record, it is difficult to make definitive conclusions from this. It is notable, though, that much of MIS 5, including MIS 5e, and the two samples from MIS 7 indicate a possible unstratified water column during previous interglacials. This contrasts with evidence both here and elsewhere (e.g., Sarnthein *et al.*, 2004) that indicates that a halocline driven stratification system existed from at least the early Holocene onwards.

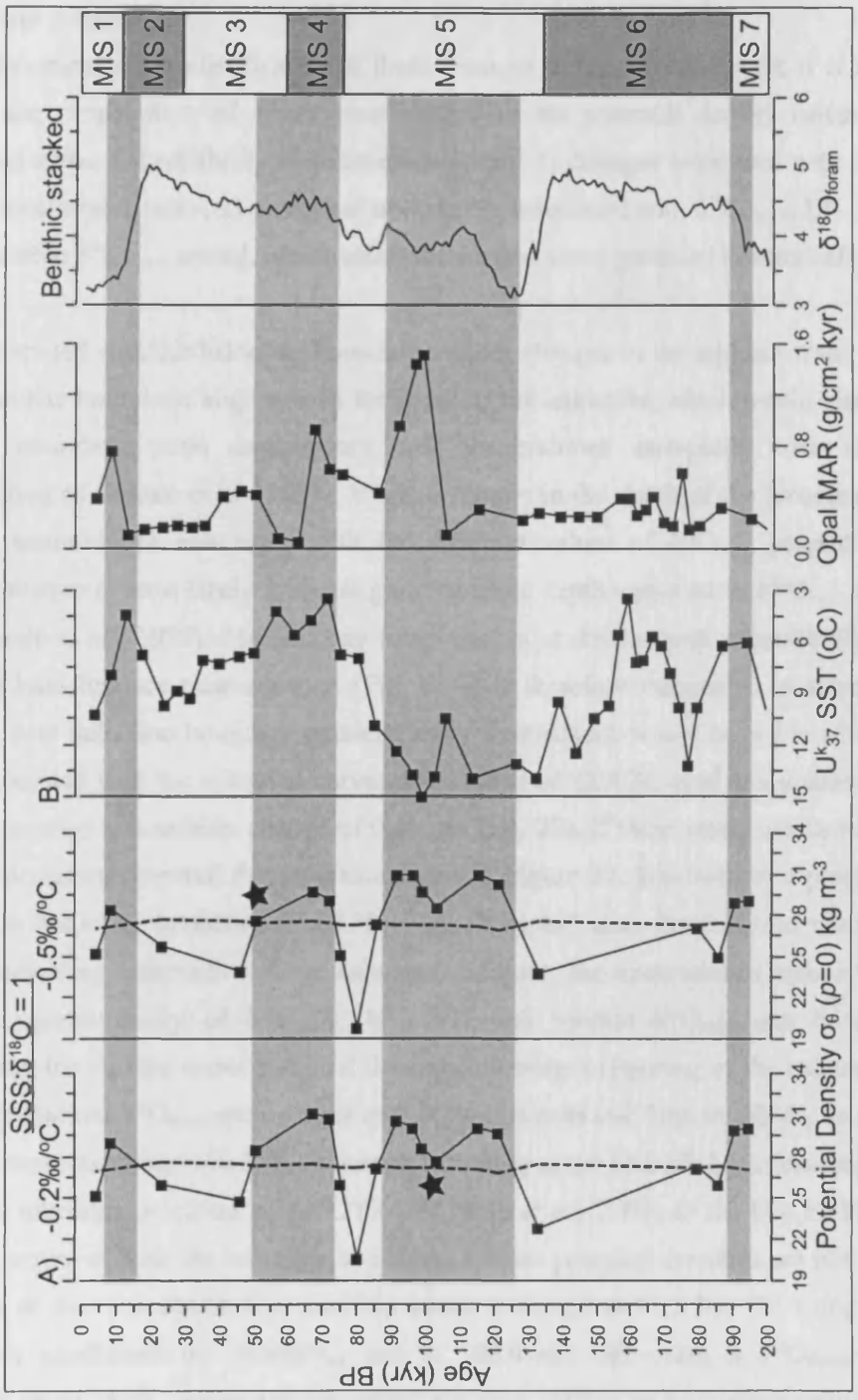

Figure 27: A) Reconstructed potential surface water densities (p=0) at ODP Site 882 for the last 200 kyr using a $\delta^{18}O_{diatom}$-temperature coefficient of −0.2‰/°C and −0.5‰/°C and a SSS:$\delta^{18}O$ ratio of 1 (solid lines). Dashed lines represent changes in the potential density (p=0) at the halocline boundary (150 m). Star symbols indicate unstratified intervals which are within the limits of uncertainty for the potential density calculations (see Section 5.4.3.1 below). B) U^{k}_{37} SST, opal MAR (Haug, 1995) and a global stacked benthic $\delta^{18}O_{foram}$ record (Lisiecki and Raymo, 2005). Shaded intervals indicate an unstratified water column, in which surface water potential densities are greater than the halocline boundary potential densities.

5.4.3.1. Error propagation

In order to examine the significance of these changes in stratification state, it is necessary to calculate the propagation of errors associated with the potential density calculations. Two factors may affect the reliability of these calculations: 1) changes associated with the halocline boundary potential density; 2) analytical uncertainty associated with $\delta^{18}O_{diatom}$, U^{k}_{37} SST and the stacked benthic $\delta^{18}O_{foram}$ record, which effect the surface water potential density calculations.

Errors associated with the halocline boundary include changes in the ambient water temperature at the halocline boundary, migration in the depth of the halocline, which would also change the halocline boundary water temperature, and uncertainties associated with the sea-level reconstruction of Siddall *et al.* (2003). While a change in the depth of the halocline might also introduce uncertainties associated with the different values of $\delta^{18}O_{water}$ present at different depths, this error is most likely minimal give the small depth variation in $\delta^{18}O_{water}$ in the region (c.f. Schmidt *et al.*, 1999). Modern day temperatures at depths both immediately below and above the halocline are near constant (Fig. 6). It is therefore reasonable to assume that any change in past halocline boundary ambient water temperature would have been less than 1°C. Errors associated with the sea-level curve of Siddall *et al.* (2003), used in equation 22, are ±30 m, which equates to a salinity change of 0.26 psu (Eq. 22). If these errors are included into the halocline boundary potential density calculations in Figure 27, this leads to a potential density error in the halocline boundary of ±0.30 to ±0.33 kg m^{-3} over the analysed interval. For all samples indicating unstratified water column conditions, the uncertainties associated with the analytical reproducibility of $\delta^{18}O_{diatom}$, U^{k}_{37} SST and benthic $\delta^{18}O_{foram}$ can be assessed by recalculating the surface water potential density following a lowering of the calculated SSS by the benthic stacked $\delta^{18}O_{foram}$ record error of 0.06‰ (Lisiecki and Raymo, 2005), by the $\delta^{18}O_{diatom}$ analytical reproducibility of 0.28‰, adjusted according to the SSS:$\delta^{18}O_{diatom}$ relationship, and by adding the alkenone precision of 1.6°C (Rosell-Melé *et al.*, 2001) to the U^{k}_{37} SST record. The combined errors of both the halocline and surface water potential densities are not sufficient to affect any of the reconstructed unstratified intervals except at 51.3 kyr BP, using a $\delta^{18}O_{diatom}$-temperature coefficient of −0.5‰/°C, and at 102.6 kyr BP, using a $\delta^{18}O_{diatom}$-temperature coefficient of −0.2‰/°C, when surface waters are calculated to be only marginally heavier than those at the halocline boundary (Fig. 27).

5.4.3.2. Mechanisms for water column transitions

Changes in potential density are a function of temperature and salinity with warmer and fresher (low salinity) waters leading to a decrease in density and a more enhanced stratification. The relative role of temperature over salinity, however, increase at higher temperatures while in cooler waters changes in salinity have a disproportionally greater impact on the density of the

water column. Two lines of evidence suggest that the changes in potential density and the transitions between stratified/unstratified conditions observed here are primarily a function of salinity. Firstly, the last 200 kyr at ODP Site 882 is marked by large, up to 12 psu, variations in salinity (Fig. 25). Secondly, even when SST are constantly high, prolonged intervals of unstratified water column conditions exist (e.g., MIS 5; Fig. 27). Given that increased SST should act to enhance stratification, large changes in SSS and freshwater input to the region, such as those observed in Figure 25, are the only viable mechanism to explain the transitions into and the maintenance of prolonged unstratified intervals. Whist difficult given the low resolution nature of the $\delta^{18}O_{diatom}$ record, especially from 180-130 kyr BP, it is nevertheless important to access possible mechanisms which could be causing these large changes in SSS/freshwater input to the region and, consequently, initiating transitions between stratified/unstratified states.

ODP Site 882 lies beyond both the modern and past southernmost sea-ice extent (Nürnberg and Tiedemann, 2004; Jaccard *et al.*, 2005). Changes in salinity around ODP Site 882 are therefore unlikely to be related to issues of brine rejection and migration of the sea-ice margin. The continental land immediately surrounding ODP Site 882, i.e., the Kamchatka peninsula contains insufficient river runoff or glacial ice sheets to provide large quantities of freshwater to the region (Sarnthein *et al.*, 2004). Furthermore changes in stratification state at ODP Site 882 do not coincide with records of GRAPE density, which can be used as a proxy of Ice Rafted Debris (IRD) (Kotilainen and Shackleton, 1995). Other investigations have also indicated that the amount of IRD at ODP Site 882 is relatively small compared to sites elsewhere in the North Pacific Ocean (Rea and Schrader, 1985; Krissek, 1995; St. John and Krissek, 1999). As such, the freshwater must be originating from elsewhere in the North Pacific region. Following Sarnthein *et al.* (2004), increased freshwater in the North West Pacific Ocean may arise from a variety of processes including: 1) increased precipitation; 2) increased freshwater advection from the low-salinity Aleutian Current; 3) increased freshwater input from the Arctic Sea via the Bering Straights and the Oyashio Current; and 4) increased freshwater from the Sea of Okhotsk.

At present, no proxy record is available at ODP Site 882 to investigate possible relative contributions of freshwater input from different sources. However, it seems unlikely that the up to 12 psu changes in SSS could be caused solely by an increase in precipitation. Given the significant uncertainty surrounding the palaeoceanographic history of both the North West Pacific Ocean and the surrounding marginal seas, particularly with respect to ocean currents (e.g., Keigwin, 1998; Matsumoto *et al.*, 2002), at this time it is not possible to evaluate any further the causes of the large changes in SSS observed at ODP Site 882 (Fig. 25). Similarly difficulties in identifying the origin of freshwater inputs to the North Pacific Ocean during the last glacial are also found in Sancetta (1983), Sancetta *et al.* (1985) and Keigwin *et al.* (1992)

Sarnthein *et al.* (2004). However, as outlined in Chapter 4, it is possible that prolonged periods of stratified/unstratified conditions may reflect the existence of a series of positive feedback cycles rather than continuous intervals of permanently increased/decreased freshwater input to the region. For example, once established a stratified water column in the North West Pacific Ocean would become self-sustaining through further influxes of freshwater, which would reinforce the salinity gradient between the surface and sub-surface layers (c.f. Sigman *et al.*, 2004). Consequently even if freshwater input partially decreased, the existing halocline would be sufficiently strong to maintain a stratified state. A transition from a stratified to unstratified system could then only be initiated by a significant large scale reduction in freshwater input to the region. Such a scenario could have occurred after the onset of MIS 5 following a reduction in global ice sheets and associated freshwater release from them, as indicated by lower benthic $\delta^{18}O_{foram}$ (Fig. 25, 27). From this, SSS could have been able to rise sufficiently to generate an initial phase of overturning. This would have permitted an increase in the upwelling of saltier deep water into the photic zone, further increasing SSS and establishing a permanently mixed water column. A subsequent modest increase in freshwater input, would then be insufficient to revert the system back to a halocline state due to the constant mixing of surface/sub-surface waters. Only a major and rapid freshwater surge to the region would be sufficient to lower SSS below the critical threshold required to establish a temporary halocline, and allow the re-adjustment of the system back to a stratified state.

5.4.4. Biological pump

While evidence exists for periodic switching between stratified/unstratified water column conditions, biogenic productivity at ODP Site 882, as indicated by opal MAR (Haug *et al.*, 1999) and biogenic barium (Jaccard *et al.*, 2005) remained low over the last 200 kyr (Fig. 27). During an unstratified interval unimpeded upwelling of nutrient rich NPDW would be expected to occur, resulting in significant increases in both diatom and other biogenic productivity relative to stratified periods. Although almost all maxima in the opal MAR record occurs within unstratified intervals, e.g., at 99.1-96.7 kyr BP, 67.5 kyr BP 9.1 kyr BP, opal MAR of 0.8-1.5 g/cm^2 kyr remain significantly below the 2.5-4.5 g/cm^2 kyr present in the unstratified ocean prior to 2.73 Ma (Fig. 27) (see Chapter 4, Haug, 1995; Haug *et al.*, 1999). Furthermore, long periods of unstratified conditions over the last 200 kyr are marked by low opal MAR of 0-0.4 g/cm^2 kyr, which are similar to concentrations during stratified intervals (Fig. 27).

As outlined in previous chapters, today much of the North West Pacific Ocean is Fe limited with respect to diatom productivity (Harrison *et al.*, 1999; Tsuda *et al.*, 2003; Yuan and Zhang, 2006). In the open North Pacific Ocean at sites such as ODP Site 882, which are situated away from continental influences, Fe availability is primarily controlled by aeolian deposition (Duce and Tindale, 1991; Jickells *et al.*, 2005), which predominantly originates from the Badain Juran

Desert, China (Yuan and Zhang, 2006). On a generalised scale, rate of Fe deposition at a given site should vary from high to low in line with glacial to interglacial conditions (Kohfeld and Harrison, 2001; Werner *et al.*, 2002). The lack of an increase in opal productivity within a warm and unstratified system, such as from 86.1-121.6 kyr BP, may therefore reflect the continuing presence of Fe limitation under decreased aeolian deposition. Such an explanation can not be used during glacial periods of unstratified conditions when increased Fe deposition, combined with increased deep water nutrient upwelling, should have removed any nutrient limitation to cause a significant increase in biological productivity.

One problem in examining the issue of Fe limitation at ODP Site 882 is the absence of an actual dust/Fe flux record at the site. This is important since records show distinct episodic changes in the rates of Fe deposition superimposed on glacial-interglacial changes in Fe deposition (e.g., Nagashima *et al.*, 2007). Records from Hess Rise (34°54.25′N and 179°42.18′E), the closest open ocean site containing an aeolian dust record, shows distinct glacial changes in dust/Fe accumulation (Kawahata *et al.*, 2000), which are in turn aligned to rates of aeolian accumulation on the Chinese Loess plateau (Sun and An, 2005). Comparisons further indicate synchronous changes between dust/Fe deposition and diatom/opal accumulation at Hess Rise and ODP Site 882 (Fig. 28).

Assuming that records of dust accumulation at Hess Rise are representative of dust/Fe deposition at ODP Site 882, periods of increased diatom productivity during unstratified intervals are marked by increased Fe/dust deposition while periods of low productivity in unstratified intervals are marked by low Fe/dust deposition (Fig. 28). This correlation therefore reiterates the importance of Fe availability for diatom productivity within the region. Based on this requirement by diatoms for both Fe, delivered via aeolian deposition, as well as N and Si, which primarily originates via deep water upwelling/advection, four productivity regimes can be concluded to have existed in the North West Pacific Ocean over the last 200 kyr: 1) stratified, halocline driven, system marked by low Fe deposition, 2) stratified, halocline driven, system marked by high Fe deposition, 3) unstratified mixed water column marked by low Fe deposition; 4) unstratified mixed water column marked by high Fe deposition (Fig. 29). In model 1 Fe, N and Si limitation inhibits diatom blooms. In model 2, increased Fe/dust deposition removes Fe limitation to diatom growth, causing a moderate increase in diatom productivity. This in turn forces an increased demand for N and Si which can not be met due to the presence of the halocline, which prevents upwelling of nutrient rich deep water to the photic zone. In system 3, Fe limitation prevents significant diatom blooms from occurring despite increased N and Si concentrations in the surface water following the transition to unstratified conditions. In model 4 both high Fe deposition and deep water upwelling combined to cause a significant increases in diatom and other biogenic productivity.

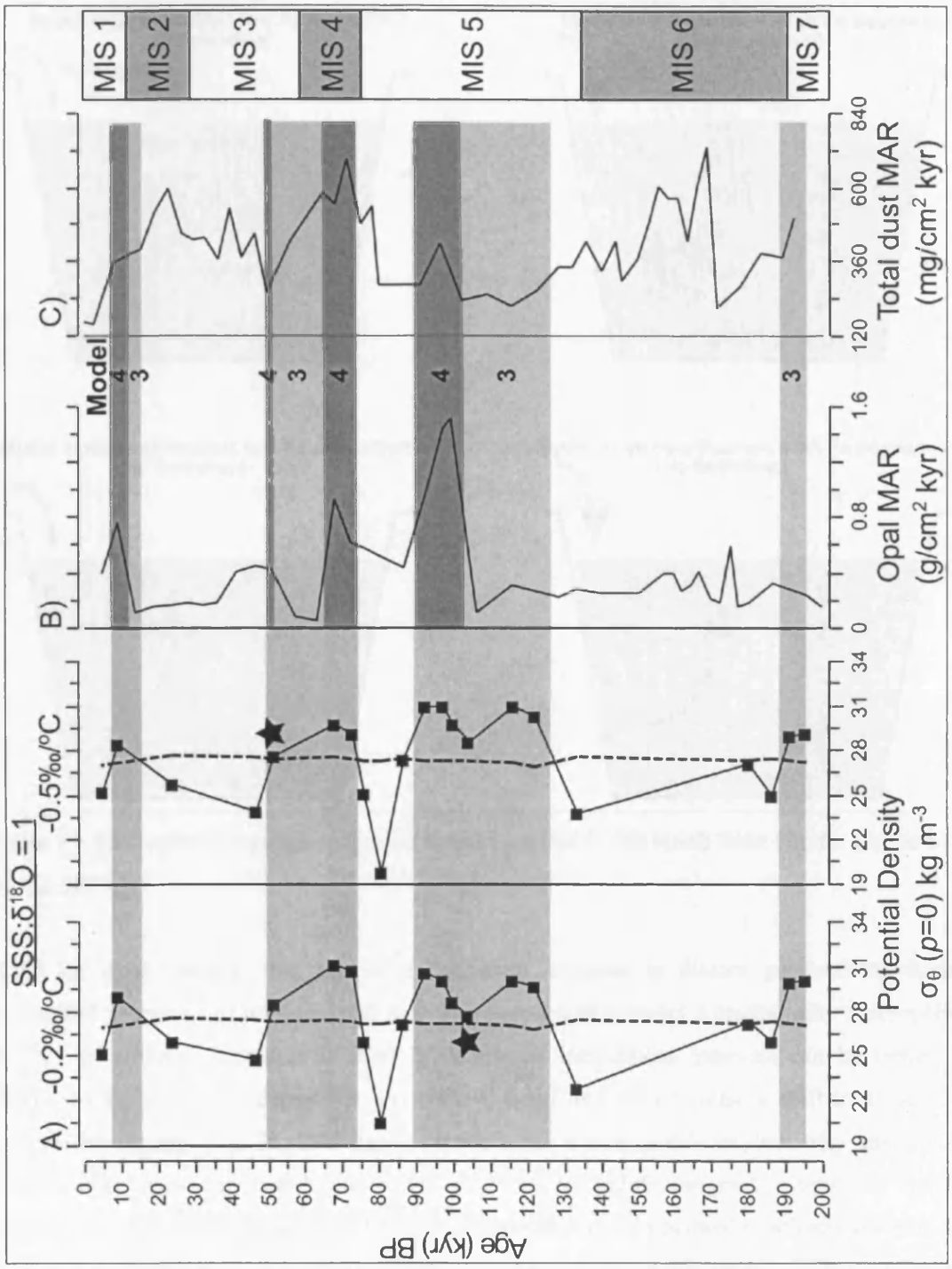

Figure 28: A) Reconstructed surface water potential densities with light grey shaded intervals indicating an unstratified water column and dashed lines representing changes in the halocline boundary potential density. Star symbols indicate unstratified intervals which are within the limits of uncertainty for the potential density calculations. B) Opal MAR from ODP Site 882 (Haug, 1995) with model numbers indicating productivity regime (see text below and Figure 29). C) Dust flux from Hess Rise (Kawahata *et al.*, 2000). Dark grey shading between B and C indicate possible correlations between opal and dust fluxes.

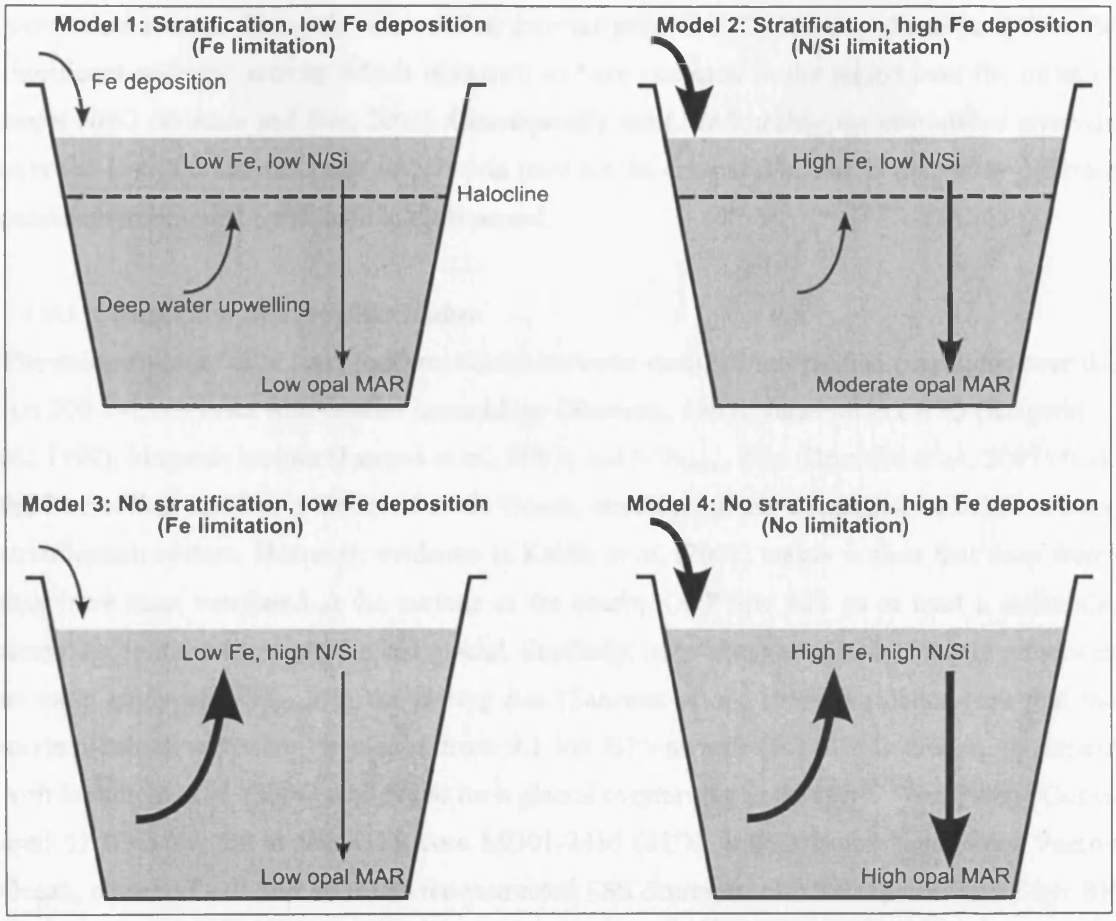

Figure 29: Productivity regimes suggested to have existed in the North West Pacific Ocean over the last 200 kyr.

Based on these models, the lack of a consistent increase in diatom productivity during unstratified intervals can be associated with the operation of a model 3 productivity system (Fig. 28, 29). In contrast, increases in opal MAR during unstratified intervals can be linked to sustained increases in Fe deposition and NPDW upwelling which cause a shift to a model 4 productivity regime (Fig. 28, 29). However, while the above models explain why unstratified intervals were marked by both higher and lower levels of opal/diatom productivity over the last 200 kyr, they do not explain why opal MAR accumulation rates remained relatively low at c. 1.6 g/cm^2 kyr compared to the 2.5-4.5 g/cm^2 kyr recorded prior to stratification at 2.73 Ma (Chapter 4, Haug, 1995; Haug *et al.*, 1999). Relatively low diatom accumulation rates during model 4 productivity regimes within glacials may reflect reduced rates of deep ocean circulation and consequently reduced nutrient concentrations in deep water upwelled to the photic zone (Keigwin, 1998; de Boer *et al.*, 2007). However this can not explain why rates of diatom productivity also remained low during model 4 productivity regimes in interglacial unstratified conditions, such as during MIS 5e when rates of deep ocean circulation would have been similar to or higher than today (ibid). It has recently been shown, however, that significant quantities of

Fe in the ocean can originate from volcanic activity (Duggen *et al.*, 2007). Higher opal accumulation rates during the unstratified interval prior to 2.73 Ma may therefore reflect the significant volcanic activity which is known to have occurred in the region over the onset of major NHG (Prueher and Rea, 2001). Consequently, opal MAR during the unstratified intervals over the last 200 kyr and prior to 2.73 Ma may not be comparable, due to the vastly different palaeoenvironmental conditions in each period.

5.4.4.1. Comparison with previous studies

The reconstruction of at least four transitions between stratified/unstratified conditions over the last 200 kyr contrasts with diatom assemblage (Sancetta, 1983), foraminifera $\delta^{18}O$ (Keigwin *et al.*, 1992), biogenic barium (Jaccard *et al.*, 2005) and $\delta^{15}N_{diatom}$ data (Brunelle *et al.*, 2007) from the North West and North Central Pacific Ocean, which argue for a constant, halocline driven, stratification system. However, evidence in Keifer *et al.* (2001) makes it clear that deep water may have been ventilated at the surface at the nearby ODP Site 883 on at least a millennial timescale periodicity during the last glacial. Similarly, large changes of c. 4-10‰ are present in an early study of $\delta^{18}O_{diatom}$ in the Bering Sea (Sancetta *et al.*, 1985). Evidence here that the modern halocline system developed from 9.1 kyr BP onwards (Fig. 27) is also in agreement with Sarnthein *et al.* (2004) who argue for a glacial overturning in the North West Pacific Ocean until 11.1/9.3 kyr BP at IMAGES core MD01-2416 (51°N, 168°E) in the North West Pacific Ocean, close to ODP Site 882. The reconstructed SSS decreases of 3.0-4.0 psu from 12 kyr BP in Sarnthein *et al.* (2004) is also similar to the 3.6-4.2 psu freshening calculated here between 9.1 kyr BP and 4.7 kyr BP (Fig. 25).

5.4.4.2. Planktonic foraminifera isotope records

Given the above summary of evidence in favour of stratified/unstratified transitions over the last 200 kyr, it is necessary to assess why many studies from the region argue for a permanently stratified system (e.g., Sancetta, 1983; Keigwin *et al.*, 1992; Jaccard *et al.*, 2005; Brunelle *et al.*, 2007). Doing so, however, is not straightforward. At the broadest level, most records only cover the last glacial-interglacial transition onwards and are therefore not suitable for making interpretations as to the state of the halocline during earlier time periods. In addition, while several sites across the North Pacific Ocean contain benthic $\delta^{18}O_{foram}$ records (e.g., Keigwin *et al.*, 1992) only a few sites contain sufficient numbers of foraminifera for planktonic $\delta^{18}O_{foram}$ analyses to be undertaken. Consequently, many sites do not contain a record of surface water palaeoceanographic conditions.

Those sites that do contain planktonic $\delta^{18}O_{foram}$ data indicate a maximum glacial-interglacial change of c. 1‰ (e.g., Zahn *et al.*, 1991; Kiefer *et al.*, 2001; Cook *et al.*, 2005; Gorbarenko *et al.*, 2005; Sarnthein *et al.*, 2006). This compares with the 10-13‰ fluctuations observed in

$\delta^{18}O_{diatom}$ (Fig. 23). Almost all of this 1‰ change in planktonic $\delta^{18}O_{foram}$ can be attributed to changes in $\delta^{18}O_{GIV}$. Due to this, with records of planktonic $\delta^{18}O_{foram}$ suggesting virtually no difference between Holocene and glacial surface water values of $\delta^{18}O_{water}$, except during Dansgaard-Oeschger and Heinrich events (Keifer *et al.*, 2001), it has been concluded that a stratified water column must have existed during the last glacial (Keigwin *et al.*, 1992; Jaccard *et al.*, 2005). In contrast, transitions into/out of an unstratified water column would be expected to result in much larger changes in planktonic $\delta^{18}O_{foram}$ (ibid). These conclusions with regards to records of planktonic $\delta^{18}O_{foram}$, however, assume that all planktonic foraminifera are living above the halocline in the photic zone. As highlighted in Chapter 4, it is possible that the foraminifera in the North Pacific Ocean may instead be living and reflecting conditions below the halocline boundary (Hemleben *et al.*, 1989; Kohfeld *et al.*, 1996; Kuroyanagi and Kawahata, 2004). Indeed such a scenario would result in exactly the c. 1‰ change actually observed within records of planktonic $\delta^{18}O_{foram}$.

Within a palaeoceanographic context, the exact depth habitats of individual foraminifera taxa can not be conclusively established. However, by comparing records of planktonic $\delta^{18}O_{foram}$ to the coccolith based U^{k}_{37} SST record, which is known to reflect surface water conditions (Ohkouchi *et al.*, 1999; Harada *et al.*, 2006), strong evidence can be found to indicate that records of planktonic $\delta^{18}O_{foram}$ are not faithfully reflecting changes in the uppermost sections of the water column. Over the last 70 kyr, the length of the most extended North Pacific Ocean planktonic $\delta^{18}O_{foram}$ record (Kiefer *et al.*, 2001; Gorbarenko *et al.*, 2005), U^{k}_{37} SST were up to 7°C colder than today (Fig. 6, 27). Using a $\delta^{18}O_{foram}$-temperature coefficient of −0.25‰/°C (Kim and O'Neil, 1997), planktonic $\delta^{18}O_{foram}$ would be expected to be 1.75‰ higher (2.75‰ after consideration of $\delta^{18}O_{GIV}$) during the last glacial relative to the Holocene if planktonic $\delta^{18}O_{foram}$ is reflecting surface water conditions. As mentioned above, in practise records of $\delta^{18}O_{foram}$ are only c. 1‰ higher during the last glacial. This points toward planktonic foraminifera in the North Pacific Ocean living and reflecting conditions beneath the halocline boundary.

As with Chapter 4, this highlights the potential problems that may be encountered when attempting to use planktonic $\delta^{18}O_{foram}$ to reconstruct changes in the uppermost sections of the water column. Given, though, that only a few studies have investigated the potential of using $\delta^{18}O_{diatom}$ in palaeoceanographic reconstructions, it remains unwise to suggest that records of $\delta^{18}O_{diatom}$ are better than planktonic $\delta^{18}O_{foram}$. Indeed, far more uncertainties exist over the use of $\delta^{18}O_{diatom}$ than for planktonic $\delta^{18}O_{foram}$ (see Chapter 1). However, since the $\delta^{18}O_{diatom}$ record here is the first comprehensive biogenic $\delta^{18}O$ record from the North Pacific Ocean which can definitely be presumed to reflects true surface water conditions, it suggests that the large $\delta^{18}O_{diatom}$ derived changes in SSS and potential density reflect real oceanographic changes in the region.

5.4.4.3. Other studies

Other evidence arguing for a constantly stratified water column in the past originates from the palaeoproductivity reconstructions in both the open North Pacific Ocean and from the surrounding marginal seas such as the Okhotsk Sea. Evidence of stratification in the Okhotsk Sea, based on low levels of surface water productivity (Narita *et al.*, 2002; Seki *et al.*, 2004) should not, however, be used as an analogue for the open North Pacific Ocean. Changes in palaeoproductivity within the Okhotsk Sea are principally controlled by localised and highly seasonal changes in sea-ice (ibid). This causes a seasonal summer stratification which can not be regarded to reflect conditions at ODP Site 882 as the region lies beyond both the present and past sea-ice margin (Nürnberg and Tiedemann, 2004; Jaccard *et al.*, 2005).

With regards to palaeoproductivity reconstructions from the open North Pacific Ocean, which argue for a permanently stratified water column (e.g., Nakatsuka *et al.*, 1995; Narita *et al.*, 2002; Gorbarenko *et al.*, 2005; Jaccard *et al.*, 2005 Brunelle *et al.*, 2007), major assumptions are made in all these studies with regards to Fe limitation. Such studies assume that: 1) the region was constantly Fe limited in the past; and 2) glacial periods would have been marked by consistently high levels of aeolian Fe deposition. Under these assumptions, glacial stratified intervals would be expected to coincide with low levels of diatom/opal productivity while glacial unstratified intervals would be characterised by sustained levels of higher productivity. With all work indicating that productivity was generally low throughout the last glacial, it has been assumed that a situation similar to a stratified, model 2, system must have prevailed in the past (ibid). However, as outlined in Kienast *et al.* (2004) and in Section 5.4.4, the region was probably not constantly Fe limited in the past. In addition, rates of dust/Fe deposition in the North Pacific Ocean are known to have varied markedly during the last glacial cycle (Fig. 28c, Kawahata et al., 2000; Nagashima *et al.*, 2007). The assumptions in these previous studies that an unstratified system would coincide with higher levels of productivity is therefore incorrect, since a model 3 stratification regime can exist in which deep water upwelling occurs but productivity is kept low due to limited dust/Fe deposition (Fig. 29).

In addition to these theoretically considerations, the isotope records used as indicators of palaeoproductivity and hence stratification state within the above studies are also open to debate; e.g., the $\delta^{13}C_{organic}$ and $\delta^{15}N_{diatom}$ studies of Gorbarenko *et al.* (2005) and Brunelle *et al.* (2007) respectively. Firstly, records of $\delta^{13}C_{organic}$ are subject to numerous influences including both different organic sources, changes in productivity as well as changes in the DIC and the pCO_2 of surface waters. Given that large changes in both productivity, upwelling and surface water pCO_2 could have occurred over the last glacial cycle (see Fig. 30 and Section 5.4.5 below) records of $\delta^{13}C_{organic}$ can not be assumed to faithfully document changes in palaeoproductivity alone and consequently distinguish between stratified or unstratified conditions. Similarly,

within the study of Brunelle *et al.* (2007) records of $\delta^{15}N_{diatom}$ are assumed to predominantly reflect changes in nutrient utilisation. If this is correct, $\delta^{15}N_{diatom}$ would increase in a stratified system, due to reduced N availability caused by lower upwelling of nutrient rich deep water (ibid). Conversely, a mixed water column would be expected to decrease $\delta^{15}N_{diatom}$ in response to increased NPDW upwelling and increased N availability (ibid). However, there are also other viable scenarios that can cause a change in $\delta^{15}N_{diatom}$. For example, a decrease in Fe input to a stratified system (Fig. 29 model 1) would further drive the system towards increased Fe limitation which could lower $\delta^{15}N_{diatom}$. Similarly, if the system switched from a model 1 stratified system to a model 4 unstratified system marked by high Fe deposition (Fig. 29), the additional Fe deposition could have increased diatom productivity to such an extent, that increased diatom demand for N (increasing $\delta^{15}N_{diatom}$) may have overridden the effects of increased deep water upwelling (decreasing $\delta^{15}N_{diatom}$). This may be further complicated by changes in the rates of NPDW upwelling in an unstratified system, which could cause either an increase or decrease in $\delta^{15}N_{diatom}$ without a corresponding change in diatom productivity/nutrient utilisation. Consequently, while records of $\delta^{15}N_{diatom}$ remain a valuable palaeoceanographic tool, the conflicting nutrient utilisation signals, in addition to the other controls on $\delta^{15}N_{diatom}$ (De La Rocha., 2006), introduce significant uncertainty over any interpretation.

Further concerns also exist as to the reliability of the $\delta^{15}N_{diatom}$ data in Brunelle *et al.* (2007). Firstly, analysis of $\delta^{15}N_{diatom}$ is susceptible to significant analytical difficulties due to the low concentrations of N organic matter within diatoms (Leng, *pers. comm.* 2007). Secondly, it has been documented that different analytical techniques for $\delta^{15}N_{diatom}$ create significantly different results (Robinson *et al.*, 2004 (method used in Brunelle *et al.* (2007)); Crosta *et al.*, 2005). Thirdly, diatom samples analysed in Brunelle *et al.* (2007) were cleaned of diatom organic coatings by being placed for one hour in a H_2O_2 solution. Given that samples analysed for $\delta^{18}O_{diatom}$ in this thesis required a 2 week digestion period to fully remove all organic coatings, it is questionable whether the samples in Brunelle *et al.* (2007) contained only pure diatom included organic matter.

5.4.5. Palaeoclimatic implications

The North West Subarctic Pacific Ocean represents one end of the deep water section of the global thermohaline circulation. In a stratified ocean, such as today, NPDW is prevented from reaching the surface. This limits the ventilation of CO_2 from the ocean to the atmosphere and causes the region to act as a net sink of atmospheric CO_2 (Honda *et al.*, 2002; Chierici *et al.*, 2006). In contrast during an unstratified state, it is likely that upwelled NPDW would have reached the surface and released CO_2 into the atmosphere. The transition from unstratified to stratified conditions at the onset of major NHG is estimated to have reduced atmospheric pCO_2 by 30-40 ppmv (Chapter 4, Haug *et al.*, 1999). Consequently, it is plausible that similar changes

between stratified/unstratified states over the last 200 kyr also resulted in changes of a similar magnitude. One factor which may mitigate any carbon release during unstratified intervals, is an increase in photic zone productivity. Transitions both into and out of stratified/unstratified phases in addition to transitions between models 3 and model 4 productivity regimes during unstratified intervals are therefore of potential palaeoclimatic significance (Fig. 29).

From Figure 28, it is clear that both model 3 (unstratified, low Fe deposition, low opal/diatom accumulation) and model 4 (unstratified, high Fe deposition, high opal/diatom accumulation) productivity systems operated at ODP Site 882 over the last 200 kyr. Transitions from a stratified to unstratified model 3 productivity system at ODP Site 882 would, in theory, be expected to increase atmospheric pCO_2 by 30-40 ppmv, due to deep water being ventilated at the surface-atmosphere interface (c.f. Haug *et al.*, 1999). Conversely, transitions from a stratified to unstratified (model 4) system would be expected to lead to a more muted increase in atmospheric pCO_2 due to the higher diatom productivity, which should act to redraw some of the ventilated carbon back into the deep ocean (Fig. 29). Indeed if diatom productivity increased sufficiently during such a transition, it is conceivable that the region may have become a net sink of atmospheric CO_2. A transition from an unstratified model 3 to an unstratified model 4 system would be expected to lead to a decrease in the release of any CO_2, due to the increase in diatom productivity that would accompany any such shift (Fig. 29).

A comparison of actual changes in the potential density at ODP Site 882 to Vostok (Antarctica) records of CO_2 indicates a moderate relationship between the stratification/productivity regime and atmospheric pCO_2 (Fig. 30). The unstratified interval at c. 195-189 kyr BP is associated with a period of higher pCO_2 concentrations of 220-240 ppmv. Following the transition to a stratified phase in which the halocline would have limited any upwelling of deep water, atmospheric pCO_2 decrease, as predicted above, by c. 30 ppmv. No conclusions can be made over the next 40 kyr due to an absence of $\delta^{18}O_{diatom}$ data. However, given the low levels of atmospheric pCO_2 through this interval, it would be interesting to assess whether a stratified water column existed during this period. The development of an unstratified system at c. 127 kyr BP, a period of low diatom productivity, coincides with the onset of the last interglacial (MIS 5e) and a c. 100 ppmv increase in atmospheric pCO_2. Of interest, is the subsequent transition to a model 4 productivity system at 105-90 kyr BP. This interval is marked by increased diatom productivity and a period of reduced atmospheric pCO_2 concentrations, culminating with a marked decrease in pCO_2 from c. 94-90 kyr BP to c. 210 ppmv. However, given that the overall increase in diatom/opal productivity is only moderate, peaking at 1.6 g/cm^2 (Fig 30b), it remains uncertain to what extent the higher productivity in the region could have counteracted the effects of deep water ventilation and re-sequestered carbon back into the deep ocean. This reiterates that while the North West Pacific Ocean may have potentially played

an important role in changing atmospheric pCO_2, the overall contribution is almost certainly less significant than that from other sources, such as the Southern Ocean.

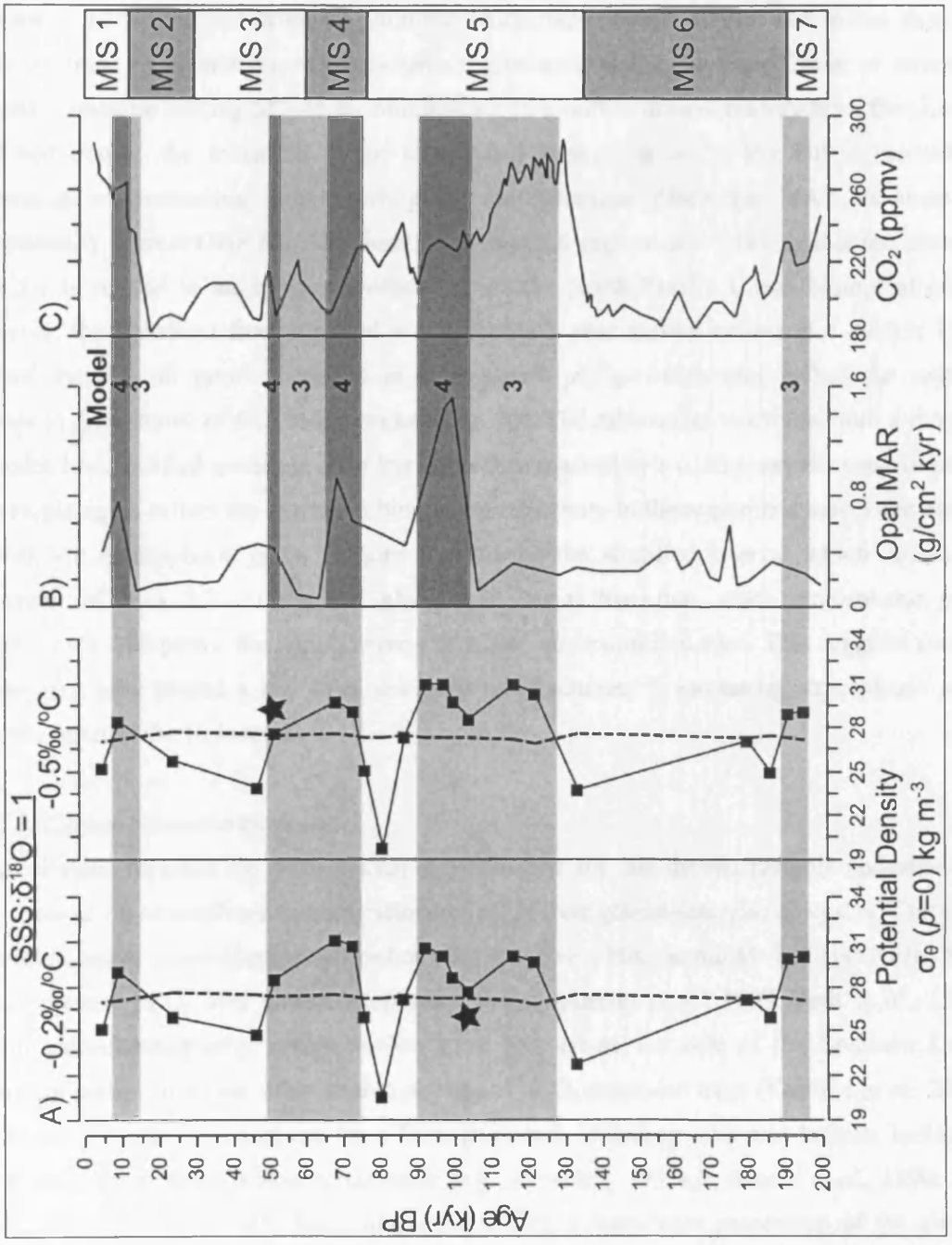

Figure 30: A) Reconstructed surface water densities with light grey shaded intervals indicating an unstratified water column and dashed lines representing changes in the halocline boundary potential density. Star symbols indicate unstratified intervals which are within the limits of uncertainty for the potential density calculations. B) Opal MAR (Haug, 1995) with model numbers indicating productivity regime. C) *p*CO2 records from Vostok (Anklin *et al.*, 1997; Petit *et al.*, 1999). Dark grey shading between B and C indicate periods of high productivity during unstratified events (model 4 productivity regime).

Following the fall in Fe deposition and the shift back to a stratified system at c. 90 kyr BP, opal MAR decrease while atmospheric pCO_2 increase by c. 35 ppmv (Fig. 28, 30). Since this increase in pCO_2 can not originate from the North West Pacific Ocean, due to the stratified water column, an alternative process/source region such as the Southern Ocean or terrestrial biosphere must be leaking CO_2 to the atmosphere. In a further diversion away from the changes predicted above, the transition to an unstratified interval at c. 74 kyr BP is marked by decreasing, not increasing, atmospheric pCO_2 concentrations. Since opal MAR are again not exceptionally high at ODP Site 882 during this model 4 regime, it is unlikely that the decrease in pCO_2 is related to an increased efficiency of the North Pacific Ocean biological pump. However, the transition from a model 4 to a model 3 productivity system at c. 64 kyr BP is marked by a c. 30 ppmv increases in atmospheric pCO_2, which may reflect the reduced biological draw-down of CO_2 in the region (Fig. 30). The subsequent transition from a model 3 to model 4 unstratified system at c. 54 kyr BP is then marked by a c. 30 ppmv decrease in pCO_2. This might again reflect the increased biogenic productivity in the region and associated carbon draw-down. Atmospheric pCO_2 remains low during the stratified interval which covers the remainder of MIS 3/2. At the last glacial-interglacial transition, when atmospheric pCO_2 increase by c. 100 ppmv, the region reverts briefly to an unstratified state. This suggests that the region may have played a key role, alongside other sources, in increasing atmospheric pCO_2 over the onset of the Holocene.

5.4.5.1. Carbon release/drawdown

Palaeoclimatic research has been heavily devoted over the last decade towards understanding past controls on atmospheric concentrations of pCO_2 over glacial-interglacial cycles. Currently, no mechanism or series of mechanisms has been able to explain the full 80-100 ppmv variability in atmospheric pCO_2 over glacial-interglacial cycles (Anklin *et al.*, 1997; Petit *et al.*, 1999). Within palaeoceanography, recent studies have focused on the role of the Southern Ocean biological pump. However, other source regions of pCO_2 must also exist (Kohfeld *et al.*, 2005). While other sources/mechanisms have been proposed, including the mid-latitude biological pump and the terrestrial biosphere/reservoir (e.g., Broecker, 1982a,b; Adams *et al.*, 1990; Bird *et al.*, 1994; Crowley, 1995; Marchitto *et al.*, 2007), a significant proportion of the glacial-interglacial pCO_2 variability remains unexplained.

While by no means conclusive, with evidence here showing apparent correlations between changes in the North West Pacific Ocean stratification state and changes in atmospheric pCO_2 (Fig. 30), a further source of this CO_2 variability may have been found. Given that changes in the stratification state have previously been suggested to lead to changes of 30-40 ppmv (Haug *et al.*, 1999), 25% of the total glacial-interglacial variability, such a proposal does not appear

unrealistic. While this potential CO_2 source may not be as significant as that from the Southern Ocean, it nevertheless potentially represents an important net control on global atmospheric pCO_2 and global climatic conditions. In particular, if it is assumed that the net contribution of the region to the atmosphere during a transition from a stratified to unstratified state is on the order of 30-40 ppmv, then changes in the North Pacific Ocean alone are sufficient to explain many of the smaller, c. 20-30 ppmv, variations in CO_2 which occurred in the past (Anklin *et al.*, 1997; Petit *et al.*, 1999). Furthermore, with the exception of transitions at c. 90 kyr BP and c. 74 kyr BP, all changes between stratified/unstratified intervals and all transitions between model 3 and model 4 productivity systems appear synchronous with predicted changes in atmospheric pCO_2 concentrations. Consequently, whilst it remains unclear as to whether changes in the North Pacific Ocean led or lagged any initial change in atmospheric pCO_2, evidence here opens the possibility that the North West Pacific Ocean may have played a significant role in regulating past global atmospheric concentrations of pCO_2. However, it should be noted that this can not be truly verified in the absence of a surface water pCO_2 record and a higher resolution $\delta^{18}O_{diatom}$/potential density record to better investigate the occurrence, timing and mechanism of stratification changes in the region.

5.4.6. Future work

Future work at ODP Site 882 over the last 200 kyr is required to increase the resolution of the $\delta^{18}O_{diatom}$ record in the >100 μm fraction. As stated above, the higher resolution 38-75 μm fraction can not be used for palaeoceanographic reconstructions due to the multiple diatom taxa and consequently the possible isotope species/vital effects within it. However, the large $\delta^{18}O_{diatom}$ fluctuations in the 38-75 μm fraction may suggest additional stratification changes beyond those indicated here by the >100 μm fraction (Fig. 23). Establishing a higher resolution $\delta^{18}O_{diatom}$ record in the >100 μm fraction would also be important in confirming the precise timing of the stratification changes. This is necessary both in order to understand the mechanisms which control these transitions and in order to establish whether stratification changes led or followed global climatic changes in pCO_2. Additionally, in order to verify the conclusions here as to the possible role of the region in contributing towards past variations in atmosphere pCO_2, a direct record of surface water pCO_2 is required. This information could, for example, be obtained from $\delta^{13}C$ measurements of the intrinsic organic matter within diatoms or alkenones to reconstruct εp (e.g., Popp et al., 1989). Such work could also be complemented by analysing $\delta^{30}Si_{diatom}$ to better understand past changes in nutrient utilisation and nutrient delivery to the photic zone. However, given the low sediment diatom concentrations over the last 200 kyr and the difficulties in extracting sufficiently pure diatom material for isotope analysis, it has not proven possible to measure either $\delta^{13}C_{diatom}$ or $\delta^{30}Si_{diatom}$ within the time-frame of this research. Alkenone based measurements of pCO_2 may also be complicated by the low amounts of organic carbon within the sediment record.

Further work is also required to extend the SSS and potential density record back to MIS 11, a possible analogue to the Holocene (Loutre and Berger 2003). Evidence both within this study and elsewhere (e.g., Sarnthein *et al.*, 2004) indicates that the Holocene was marked by a stratified water column. This compares with results here showing an unstratified water column during MIS 5 and possibly during MIS 7 (Fig. 30). It is therefore necessary to assess whether the Holocene reflects a unique palaeoceanographic period within the Earth's recent history, or whether MIS 11 was also marked by a similar halocline driven stratification. Finally, work is also required to assess the spatial covered of the changes observed here. This is needed to assess whether the reconstructed changes at ODP Site 882 simply reflect a highly localised signal, or a signal indicative of changes across larger sections of the North Pacific Ocean. For example, evidence in McDonald *et al.* (1999) opens the possibility that significant ocean-atmosphere drawdown of CO_2 may have occurred at least in the North East Pacific Ocean during the last glacial period.

5.5. Conclusions

Measurements of $\delta^{18}O_{diatom}$ from the >100 μm fraction at ODP Site 882 indicates significant changes in salinity and surface water palaeoceanographic conditions over the last 200 kyr with fluctuations of up to 13‰. With the >100 μm size fraction dominated by a single taxa, *C. radiatus*, the presence of vital/species effects can be largely ruled out. Potential density calculations indicate up to four intervals over the last 200 kyr when densities in the photic zone would have been sufficient to generate overturning, causing a transition from stratified to unstratified conditions. Furthermore transitions into an unstratified water column, together with transitions between model 3 and model 4 productivity systems, appear synchronous with changes in atmospheric pCO_2. However, whilst evidence points towards the North West Pacific Ocean as having had a, previously unrecognised, significant impact on atmospheric pCO_2, this can not be verified in the absence of an independent record documenting actual changes in surface water pCO_2.

The current, low resolution, nature of the $\delta^{18}O_{diatom}$ record also prevents the development of a precise relationship between the timing of these water column changes and possible changes in global climatic conditions. Whilst a broad relationship over long timescales appears to exist between increased deep water ventilation and higher atmospheric pCO_2 concentrations, it remains to be seen whether similar changes occurred over millennial timescales. Assessing this, however, may be important in further understanding the large, 60 ppmv, variations in pCO_2 which took place during the last glacial period (Anklin *et al.*, 1997; Petit *et al.*, 1999). Future work at this site is therefore required to improve the temporal resolution of the $\delta^{18}O_{diatom}$ record in order to better understand the timing and number of stratification changes in the North West

Pacific Ocean and their possible impact on both global and local climatic events. In addition, an actual record of changes in surface water pCO_2 is needed to verify both the occurrence and magnitude of surface water pCO_2 changes during unstratified intervals.

Part 2: Biogenic silica concentrations

Introduction

An original aim of the thesis was to examine the potential of using $\delta^{30}Si_{diatom}$ as a tool for reconstructing palaeoceanographic changes within the marine silicon cycle (De La Rocha, 2006). However, due to difficulties in setting up a line for $\delta^{30}Si_{diatom}$, no such measurements were obtained during the PhD. Over the next decade, it is likely that the number of $\delta^{30}Si_{diatom}$ measurements will expand considerable as increasing numbers of laboratories develop and set up systems for it's analysis (e.g., Brzezinski *et al.*, 2006). This is believed to be crucial given the key role of the global silicon cycle, and in particular the biogeochemical silicon cycle, in controlling changes in atmospheric pCO_2 (Conley, 2002). Despite this, in any eventuality it remains likely that the number of $\delta^{30}Si_{diatom}$ measurements in a given core section will always remain low. This is due to the complexity of extracting sufficient clean diatom material for isotope analysis and the competing demand for measurements of both $\delta^{18}O_{diatom}$ and $\delta^{30}Si_{diatom}$. At present, with the exception of the facility at the NERC Isotope Geosciences Laboratory, all laboratories are only able to analyse $\delta^{18}O_{diatom}$ or $\delta^{30}Si_{diatom}$. As such, while in some instances the amount of pure diatom material that can be extracted may be sufficient for separate measurements of both $\delta^{18}O_{diatom}$ and $\delta^{30}Si_{diatom}$, in the majority of cases it is likely that the investigator will have to choose whether $\delta^{18}O_{diatom}$ or $\delta^{30}Si_{diatom}$ is analysed. These issues are likely to be further exemplified at sites/samples which are low in diatom concentrations and where a demand also exists for the isotope analysis of the included organic matter with diatoms ($\delta^{13}C_{diatom}$ and $\delta^{15}N_{diatom}$) (see reviews in De La Rocha, 2006).

Within the context of $\delta^{30}Si_{diatom}$, information on the silicon cycle in lacustrine and marine systems can also be obtained through measurements of sedimentary concentrations of Biogenic Silica (BSi). Indeed over the past 20-30 years, investigations into the silicon cycle have been primarily based on measurements of sedimentary BSi. Measurements of BSi, however, are usually reflective of changes in surface water productivity (Conley and Schelske, 2001), whereas measurements of $\delta^{30}Si_{diatom}$ document rates of silicic acid utilisation or input to the photic zone (De La Rocha, 2006). Despite this difference, both records potentially provide an important and complementary insight into changes in the global and regional silicon cycle, rates of diatom/siliceous microfossil productivity and consequently the role and response of the biological pump to palaeoclimatic events (e.g, Brzezinski *et al.*, 2002). It is therefore viable that future investigations into the silicon cycle will involve a hybrid approach comprised of low resolution $\delta^{30}Si_{diatom}$ measurements, for samples where sufficient quantities of diatoms can be extracted for isotope analysis, with higher resolution BSi measurements between $\delta^{30}Si_{diatom}$ data points. One major advantage in analysing BSi over $\delta^{30}Si_{diatom}$ is the relative simplicity, speed and reduced financial costs associated with it. This is particularly true for wet-alkaline digestion BSi

measurements: the most commonly used method for BSi determination. Therefore, even if measurements of $\delta^{30}Si_{diatom}$ become more commonplace and even if it becomes viable to analyse smaller samples sizes, it is likely that the overall number of BSi measurements will remain high. Given this, it is therefore relevant to examine the reliability of BSi measurements used in palaeoenvironmental reconstructions. Three main issues may potentially affect the reliability of BSi measurements:

1) sediment winnowing/focusing, resulting in BSi concentrations not reflecting changes in overlying surface water productivity;
2) inaccurate corrections for levels of non-BSi simultaneously digested alongside sources of BSi in wet-alkaline digestions, resulting in an over-estimation of the true amount of BSi within a sediment sample;
3) high frustule dissolution, which may act to remove BSi from diatoms in the sedimentary record and thereby lead to an underestimation of true BSi concentrations.

The issue of sediment winnowing/focusing has been widely discussed within the literature, particularly within the context of marine systems and the "opal paradox" of the Southern Ocean (e.g., Pondaven *et al.*, 2000). As such, many studies have demonstrated the importance at some localities of normalising BSi fluxes using, for example, ^{230}Th (ibid). Issues of diatom dissolution and non-BSi corrections, however, have yet to be widely considered within the context of palaeoenvironmental reconstructions and/or are currently regarded as being negligible in terms of affecting BSi measurements. Part 2 of the thesis aim to examines these issues in more detail in order to assess their impact on the accuracy of BSi measurements in palaeoenvironmental reconstructions.

Chapter 6 outlines the background of BSi measurements before assessing the potential for more accurate BSi measurements to be derived through a sequential Si/Al extraction procedure which directly considers and accounts for sources of non-BSi leached during the wet-alkaline digestion. In Chapter 7 the sequential Si/Al technique is applied to two sediment cores from Lake Baikal, where wet-alkaline measurements of BSi have been pivotal in elucidating the palaeoenvironmental history of the local region. Finally, in Chapter 8, the issue of diatom dissolution is addressed by analysing a glacial sequence from Lake Baikal, which is characterised by large numbers of highly dissolved diatoms. Within Chapter 8 all BSi and diatom measurements, excluding diatom biovolume measurements, were made during a NERC MSc studentship. All diatom biovolume measurements, interpretations and discussions presented within the chapter, however, were carried out during the PhD and do not appear in any MSc related work or thesis.

Chapter 6: Improving estimates of biogenic silica through Si/Al corrections

6.1. Introduction

Measurements of sediment Biogenic Silica (BSi) concentrations provide a valuable tool for reconstructing past environmental changes and events at both marine and lacustrine sites. With a strong relationship between BSi and primary productivity in the water column, measurements of BSi can often be interpreted as a record of surface water productivity (Nelson *et al.*, 1995; Ragueneau *et al.*, 2000). Measurements of BSi also often represent a more pragmatic approach to obtaining accurate estimates of oceanic and lacustrine palaeoproductivity, due to its order of magnitude higher preservation than that for organic carbon (Berger *et al.*, 1989). As such, analysis of BSi concentrations has enabled an insight into large scale palaeoclimatic and palaeoenvironmental events (e.g., Haug *et al.*, 1999; Cortese *et al.*, 2004), including the role of the biological pump in, for example, modulating oceanic draw-down of pCO_2 (Broecker, 1982a; Harrison, 2000; Ragueneau *et al.*, 2000, 2006; Dugdale *et al.*, 2004; Kemp and Dugdale, 2006).

One problem with analysing sedimentary concentrations of BSi is the absence of a standardised methodology for its determination in aquatic systems. Various techniques exist including X-Ray Diffraction (XRD) (Goldberg, 1958; Calvert, 1966; Eisma and Van der Gaast, 1971), diatom/microfossil point counting (Leinen, 1985; Pudsey, 1992), infrared spectroscopy (Chester and Elderfield, 1968; Fröhlich, 1989), normative calculation of mineral silicates (Leinen, 1977) and wet-alkaline digestion (Hurd, 1972; De Master, 1979, 1981; Eggiman *et al.*, 1980; Mortlock and Fröhlich, 1989; Muller and Schneider, 1993; Lyle and Lyle, 2002). Of these wet-alkaline digestions, in which the sediment sample is dissolved in an alkaline solution and then analysed for Si, are most commonly used due to the methods simplicity and perceived robustness relative to other techniques (De Master, 1981; Conley, 1998; Conley and Schelske, 2001; Sauer *et al.*, 2006).

At present, several variations of wet-alkaline digestion techniques exist (see review in Sauer *et al.*, 2006). Most, however, follow either a timed sequential extraction (De Master 1979; 1981) or a single-step approach (Mortlock and Fröhlich 1989). A feature of all wet-alkaline digestions is the non-BSi simultaneously digested alongside sources of BSi. Either all Si is assumed to originate from sources of BSi with no/negligible non-BSi contributions (single-step digestion) or concentrations of digested non-BSi are corrected for (timed sequential extraction). In a single-step digestion, for sediments in which all BSi originates from diatoms, samples are digested in an alkaline solution for 5 hours with all dissolved Si at this interval assumed to originate and be representative of the total amount of BSi within the sample. In the timed sequential extraction method, measurements of dissolved silicon in the alkaline solution are taken at hourly interval between 2 and 5 hours of sample digestion (De Master 1979, 1981; Conley and Schelske, 2001). A least-squares regression of Si against time is then used to

separate the different BSi and non-BSi components of the digestion (Fig. 31). A significant assumption of the Si/time approach, is that the release of non-BSi is constant throughout the course of digestion (De Master 1979, 1981). Recent work, however, has shown the rate of non-BSi release to be significantly greater during the first two hours of digestion; indicating a parabolic, not linear, kinetic release of non-BSi over time (Schlüter and Rickert, 1998; Kamatani and Oku, 2000; Koning *et al.*, 2002). Consequently, applying a conventional Si/time correction to correct for non-BSi likely results in an over-estimation of the true amount of BSi, particularly in samples low in BSi where the relative contributions from sources of non-BSi may be high.

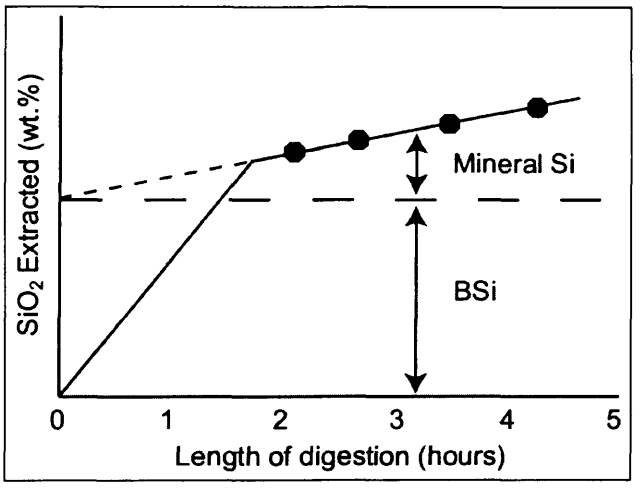

Figure 31: Theoretical dissolution curve (solid line) of Si (or SiO_2) from a sediment sample, containing a mixture of diatoms and clays/aluminosilicates, during the first five hours of digestion. Following c. 1-2 hours, full digestion of BSi is achieved. Short dashed line indicates a least-squares linear regression of the analysed samples to the y-intercept, enabling the separation of BSi from sources of mineral/non-BSi (De Master 1979; 1981). Figure adapted from De Master (1979) and Conley and Schelske (2001).

6.1.1. Si/Al measurements of BSi

A more accurate method for performing non-BSi correction in wet-alkaline digestions may lie in an examination of Al concentrations within the digested solution (Eggimann *et al.*, 1980). In alkaline digestions, strong linear relationships have previously been observed between the release of Si and Al from a range of clays including allophane, kaolinite, illite and montmorillonite (r = 0.988, 0.998, 0.994, 0.997 respectively) (Kamatani and Oku, 2000). Higher-resolution, one second, measurements also indicate that these relationships are established within the first 10 minutes of digestion (Koning *et al.*, 2002). As such, by assuming that concentrations of Al in sources of BSi are negligible, concentrations of digested Al can be directly linked to and used to correct for the digestion of non-BSi into the alkaline solution (Kamatani and Oku, 2000; Koning *et al.*, 2002). Within wet-alkaline BSi measurements, Al

concentrations can be used to correct for non-BSi in two ways. Firstly, in single-step digestions, Si/Al ratios from catchment or clay standard can be applied to digested sample concentrations of Si and Al in order to calculate BSi (e.g., Eggimann *et al.*, 1980; Carter and Colman, 1994; Colman, 1998). Although issues have been raised over whether modern Si/Al ratios are indicative of fossil clay ratios (Eggiman *et al.*, 1980), it is unlikely that palaeoclimate changes and other factors could have altered sediment Si/Al ratios sufficiently to distort these non-BSi corrections (Colman, *pers. comm.* 2005). Alternatively, Si/Al ratios can be used to calculate non-BSi corrections through a double leachate procedure, following an initial four or five hour alkaline digestion (Eggimann *et al.*, 1980; Ragueneau *et al.*, 2005), or through a single sequential extraction (Schlüter and Rickert, 1998; Kamatani and Oku, 2000), which allows the non-BSi Si/Al ratio to be calculated for each sample.

Recent work has focused on the single sequential Si/Al technique due to the method's relative simplicity compared to the double leachate procedure, which requires recovering and drying a sample following an initial alkaline digestion, and due to the method's direct accountability for digested concentrations of non-BSi. As stated above, the release of Si and Al from the sediment into the alkaline solution after complete BSi dissolution can be directly linked to the Si/Al ratio of the leached non-BSi. Within a typical sediment sample in which diatoms are the dominant source of BSi, BSi dissolution would be expected to be complete within 1-2 hours, leading to the appearance of near-constant dissolved Si/Al ratios from c. 3-4 hours onwards (Fig. 32). In the sequential Si/Al method, by establishing the rate at which Si and Al are released following complete BSi digestion, and as such the Si/Al ratio of digested non-BSi, a Si/Al linear regression to the y-intercept can be performed to separate out the non-BSi phase and to calculate the amount of BSi within the sample (Fig. 33) (Kamatani and Oku, 2002).

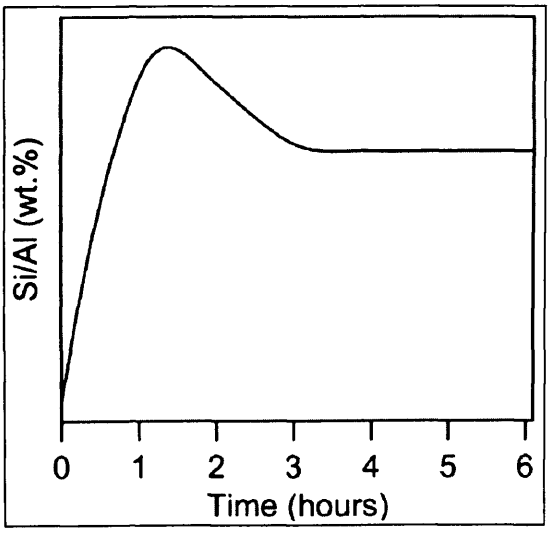

Figure 32: A) Theoretical evolution of dissolved Si/Al ratios in the alkaline solution over time. For samples containing non-diatom forms of BSi, such as radiolarian, constant Si/Al ratios may appear after 6-12 hours of digestion, depending on the strength of the alkaline solution used.

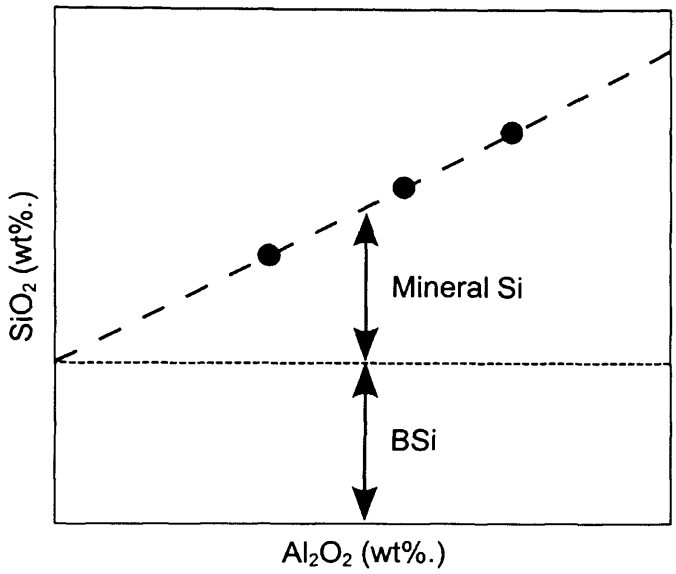

Figure 33: Assuming a linear relationship in the release of Si and Al from non-BSi, BSi concentrations can be calculated using a linear regression to the y-intercept between concentrations of dissolved Si (or SiO_2) and Al (or Al_2O_3) once BSi dissolution is complete.

To date, studies examining the potential of this Si/Al sequential extraction approach have focused on analysing marine surface sediment material with digested Si and Al concentrations measured during the first 1-2 hours of sample digestion (e.g., Kamatani and Oku (2000), Koning *et al.* (2002) and Ragueneau *et al.* (2005)). If concentrations of Al are to be used to correct for non-BSi, however, it is essential to consider the Si/Al relationship only once all BSi is fully digested. In fresh samples, particularly those dominated by diatoms, BSi dissolution is likely to be rapid, c. 20-100 minutes. However, from a palaeoenvironmental perspective the dissolution of BSi into an alkaline solution is dependent upon a variety of factors including age, type of BSi and nature of sample preservation (Lyle and Lyle, 2002). Because of this, it is more desirable for sequential Si/Al corrections to be derived after at least two/three hours or longer periods of digestion. For example in marine samples where sponges spicules and radiolarians are present, full BSi digestion may only occur after 10-11 hours (Conley and Schelske, 2001; Lyle and Lyle, 2002).

Here, within this chapter, wet-alkaline derived BSi concentrations are measured at a range of marine and lacustrine sites using Si/Al ratios to correct samples for simultaneously digested concentrations of non-BSi. Particular attention is made towards samples known to be low in BSi due to the increased relative amount of Si in these samples which may originate from sources of non-BSi. In addition, it is ensured that Si and Al measurements are only taken after complete BSi digestion. By using Inductively Coupled Plasma Emission Spectrometry (ICP-AES), the potential for deriving more accurate non-BSi corrections from Si/Al ratios is evaluated

compared to conventional Si only single-step and Si/time sequential leaches in which only concentrations of digested Si are considered. To complement earlier work which has focused on fresh sediment, older aged material is also examined. In addition, the potential for other elemental concentrations to be used in generating non-BSi corrections is also assessed.

6.2. Samples and methodology

Samples were collated from marine and lacustrine sites which cover the range of BSi concentrations generally analysed for palaeoclimatic purposes (Table 10). Particular emphasis was placed on three samples (C1-C3) previously analysed within the BSi inter-laboratory comparison study of Conley (1998). In addition, pure diatom material from ODP Site 882 was also analysed to determine the elemental composition of pure opal (Table 10).

Table 10: Information and site location details for samples analysed in this study together with alkaline solutions used for sample digestion.

Sample	*Environment*	*Site*	*Sample age*	*Solution*
C1	Lacustrine	Still pond, Chesapeake Bay, Virginia, USA	< 20 years	1% Na_2CO_3
C2	Lacustrine	Lewis Lake, Grand Teton National Park, WY, USA	< 20 years	1% Na_2CO_3
C3	Coastal	R-64, Chesapeake Bay, Virginia, USA	< 20 years	1% Na_2CO_3
EQ1	Marine	East Equatorial Pacific (ODP Site 1256)	Homogenised core samples (c. 2.0 Ma)	1% Na_2CO_3
EQ2	Marine	East Equatorial Pacific (ODP Site 1256)	Homogenised core samples (c. 2.0 Ma)	2-M KOH
LB1	Lacustrine	Lake Baikal, Russia	MIS 3 (50.2 kyr BP)	1% Na_2CO_3
LB2	Lacustrine	Lake Baikal, Russia	MIS 3 (25.2 kyr BP)	1% Na_2CO_3
D	Marine diatoms	North West Pacific (ODP Site 882)	2.8 Ma	0.5-M KOH

Following Conley and Schelske (2001) and De Master (1979, 1981), 30 mg of freeze-dried samples were weighed into flat bottomed acid-washed bottles containing 40 ml of alkaline solution (Table 10), within the acceptable sample-solution ratios for wet-alkaline digestions proposed by Gehlen and van Raaphorst (1993). Samples were immersed in a waterbath heated to 85°C and periodically shaken throughout the digestion period to ensure full exposure of the sediment to the solution. A recent debate has arisen over the need to pre-treat samples with HCl and H_2O_2 prior to digestion in order to removal newly formed aluminosilicates and,

consequently, improve the accuracy of BSi measurements. So far, however, the need for such a pre-treatment stage has only been demonstrated in soil samples (Saccone *et al.*, 2006). Since existing aquatic system BSi techniques both use (Mortlock and Fröhlich, 1989) and do not use (De Master, 1979; 1981, Conley and Schelske, 2001) pre-treatment stages, and since previous studies have demonstrated similar results between the two techniques (Conley, 1998), it further seems unlikely that there is a significant advantage in such a pre-treatment stage for aquatic samples. It has also been established that errors and poor levels of reproducibility in BSi measurements are most often caused by "human error", such as may occur during the weighing out of samples and solutions (Conley and Schelske, 2001). With any pre-treatment necessitating the need for several weighing out stages and the recovery of small, <40 mg, samples without any loss of BSi, it seems wise to avoid any pre-treatment stage whenever possible. As such, no pre-treatment stage is used within this study.

For wet-alkaline BSi measurements, a single alkaline digestion is normally required per sediment sample with c. 1-2 ml of the solution taken at timed intervals. Here this was not possible due to the need for up to 5 ml of solution in order to analyse all the intended trace elements via ICP-AES. Continuing digestion after the removal of 5 ml of solution would have lowered sample-solution ratios below those recommended by Gehlen and van Raaphorst (1993). Consequently, a single alkaline digestion was undertaken for each timed aliquot of a given sediment sample. All digestions were run in duplicate with reaction times varying from 1 to 13 hours, except for sample EQ2 when duplicate data was not available for the 9 and 13 hour digestion aliquots due to ICP-AES analytical difficulties. Following sample digestion, bottles were immediately centrifuged at 1,500 rpm for five minutes with c. 20 ml aliquots subsequently decantered into a further set of vessels, thereby removing any undigested material. All aliquots were immersed in a cold waterbath awaiting analysis to further minimise the risk of leaching from any remaining suspended particles. Whereas some laboratories employ a weak HCl solution to neutralise the alkaline solution following sample digestion (see Conley and Schelske, 2001), here this stage is left out to avoid diluting samples beyond ICP-AES detection limits.

Sample aliquots were assessed for dissolved Al, Ba, Ca, Fe, Mn, P, Si and Ti, using a Jobin Yvon Ultima C ICP-AES in the Analytical Geochemistry Laboratories at Boston University with results corrected for analytical drift and elemental concentrations in procedural blanks. ICP-AES permits faster analysis of samples than is achievable through conventional methods, such as molybdate blue, while enabling a range of other elemental concentrations to be simultaneously analysed and the avoidance of issues of polymerisation. Prior to ICP-AES analysis, aliquots were removed from the waterbath and allowed to warm to room temperature. Synthetic standards used during ICP-AES were constructed and matrix matched using the same alkaline concentrations as for the analysed samples (Table 10). Solutions were spiked with

differing concentrations of single element standards (Si, Al, Ti, Mn, Fe, Ba, and P) designed to cover the range of concentrations expected in the digested samples. Calibration curves were constructed with no less than five standards, and all correlation coefficients exceeded 0.999.

6.3. Results and discussion

6.3.1. Analytical results

ICP-AES analytical reproducibility for all elements were low and are presented in Table 11.

Table 11: ICP-AES analytical reproducibility

Element	*Concentration (ppm)*
Al	0.03
Ba	0.04
Ca	0.09
Fe	0.02
Mn	0.01
P	0.02
Si	0.46
Ti	0.01

6.3.2. Diatom trace element concentrations

Concentrations of Ba, Ca, Fe, Mn, P and Ti within the analysed pure diatom material were negligible (Table 12). This, combined with equally low concentrations from sediment samples, less than 0.1 wt.% for all elements except for Ca which displayed slightly higher concentrations of up to 0.2 wt.%, highlights the unsuitability of these elements for deriving non-BSi corrections. As such these elements are not considered further. In contrast, levels of Al were both negligible within diatoms (Table 12) and high within digested sediment samples (see Appendix), highlighting the potential for Al to be used as a tracer for non-BSi digestion.

Table 12: Trace elements in pure diatoms from ODP Site 882, North West Pacific Ocean (n=5).

Element	*Concentration (wt. %)*
Al	0.34 ± 0.006
Ba	0.02 ± 0.001
Ca	0.08 ± 0.008
Fe	0.12 ± 0.010
Mn	0.01 ± 0.000
P	0.00 ± 0.000
Ti	0.01 ± 0.000

6.3.3. Inter-laboratory samples (C1-C3)

As predicted (Fig. 32), samples C1, C2 and C3 show a rise and peak in dissolved Si/Al ratios during the first 2 hours before falling to a constant ratio from 3-4 hours onwards (Fig. 34a). An essential part of wet-alkaline digestions is the recovery and visual analysis of the remaining sediment to confirm full BSi dissolution. Alternatively, BSi dissolution can be verified through examination of the slope of Si increase over time (Conley and Schelske, 2001). Here, changes in a sample's dissolved Si/Al ratio over time can provide similar information whilst also confirming that a linear relationship exists between the release of Si and Al from sources of non-BSi. Although laboratory experiment have indicated that the release of Si and Al from clays is linear (Kamatani and Oku, 2000; Koning *et al.*, 2002), it is important to verify this as far as possible in each sample due to this linearity being an essential assumption of Si/Al derived non-BSi corrections. Whilst this can only be done at a low resolution from the four hour period onwards, such checking may still identify possible instances of non-linear non-BSi Si/Al release. Consequently here, Si/Al corrections are only derived from the 4 hour period onward.

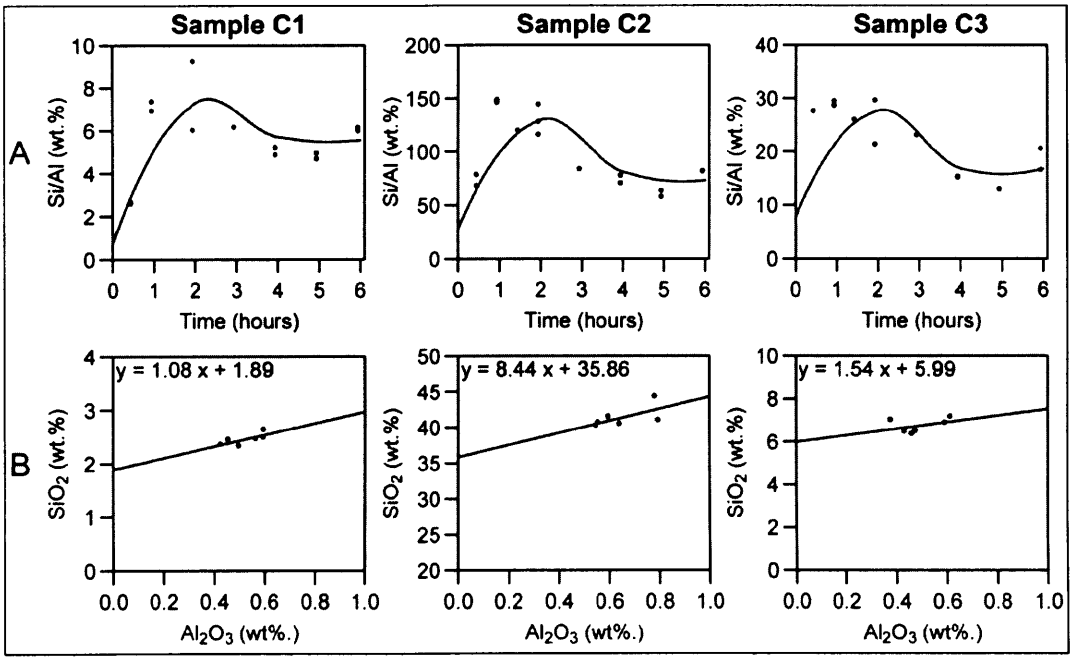

Figure 34: A) Si/Al ratios for samples C1, C2 and C3. B) Sequential SiO_2/Al_2O_3 corrections for concentrations of digested non-BSi.

Use of the sequential Si/Al methodology to measure BSi assumes:

1) a constant linear relationship between the digestion of Si and Al from sources of non-BSi;

2) changes in dissolved concentration of Si and Al after four hours of digestion are entirely related to and representative of non-BSi release throughout the entire digestion procedure. For samples containing other forms of BSi which take longer to digest, such as radiolarians,

the length of this period needs to be adjusted accordingly;

3) all Al digested during the alkaline extraction originates from non-BSi with negligible/no contributions from sources of BSi.

Conventional Si single-step and Si/time measurements for the inter-laboratory lacustrine samples C1-C3 produces BSi values within the range reported by Conley (1998) (Table 13). A Si/Al least-squares linear regression on measurements from 4-6 hours produces significantly lower BSi values compared to those obtained from the Si single-step and Si/time sequential extractions in which only digested Si concentrations are considered (Table 13, Fig. 34b).

Table 13: Previously published BSi measurements from conventional Si only single step and Si/time sequential extractions together with BSi values calculated here.

Sample	*Conley (1998)*+*		*Calculated here++*			
	*Single-step**	*Si/time***	*Single-step**	*Si/time***	*Si/Al method*	*Change (%) ****
C1	2.40 ± 0.41	2.27 ± 0.34	2.57	2.45 ± 0.31	1.89 ± 0.27	24.9
C2	42.4 ± 2.81	44.9 ± 3.10	42.73	41.45 ± 4.21	35.86 ± 3.56	14.8
C3	6.13 ± 0.23	5.39 ± 1.43	7.05	5.99 ± 0.86	5.99 ± 0.83	8.1
			Calculated here++			
LB1	N/A		4.74	4.36 ± 0.93	0.45 ± 0.73	90.1
LB2			1.99	1.71 ± 0.23	0.81 ± 0.38	56.2
			Calculated here++			
EQ2	N/A		8.65	7.85 ± 1.23	2.22 ± 1.77	73.1

+: Reported errors are ± 1 standard deviations about the mean for all analysed samples (see Conley, (1998)).

++: Reported errors are linear regression standard errors for the calculation of the intercept.

*: Amount of Si digested after five hours of digestion with no correction for non-BSi (after Mortlock and Fröhlich, (1989)).

**: Si/time least squares linear regression applied to correct samples for non-BSi (after De Master (1979; 1981)).

***: Change in BSi between the sequential Si/Al approach and the mean value of the Si single-step and Si/time measurements calculated here.

In contrast to existing studies which argue for no significant difference between conventional Si only and sequential Si/Al measurements of BSi (Schlüter and Rickert 1998, Kamatani and Oku 2000), here Si/Al corrections lower BSi concentrations by between 8% and 25% for all three samples. Calculation of the standard error associated with these measurements, however, indicates that all of the sequential Si/Al BSi values are actually within the reported range of Si

only BSi values published in Conley (1998) (Table 13). Consequently for samples C1-C3, there is no statistical difference or benefit in using a sequential Si/Al approach over conventional BSi methods. Below, the sequential Si/Al method is applied to older fossilised material from two other sites: a MIS 3 sequence from Lake Baikal, Russia, in which diatoms are scarce and/or highly dissolved, and samples from the East Equatorial Pacific which are also low in BSi (Table 10).

6.3.4. Lake Baikal (LB1-LB2)

Sample LB1 contains moderate numbers of highly dissolved diatoms (c. 3.03 x 10^7 valves/g dry wt.) while sample LB2 contains virtually no diatoms (c. 0.03 x 10^7 valves/g dry wt.) or other sources of BSi (Swann *et al.*, 2005). In both samples the level of BSi is further minimised by exceptionally high diatom frustule dissolution (Chapter 8). This is reflected by the increase in dissolved Si/Al ratios over time with, unlike other samples, no marked peak in the ratios during the first 2-3 hours of sample digestion (Fig. 35a). Clay mineralogy analyses at the same core site in Lake Baikal (Continent Ridge) indicate that the samples analysed here are dominated by a mixture of illite and smectites (Fagel *et al.*, 2007).

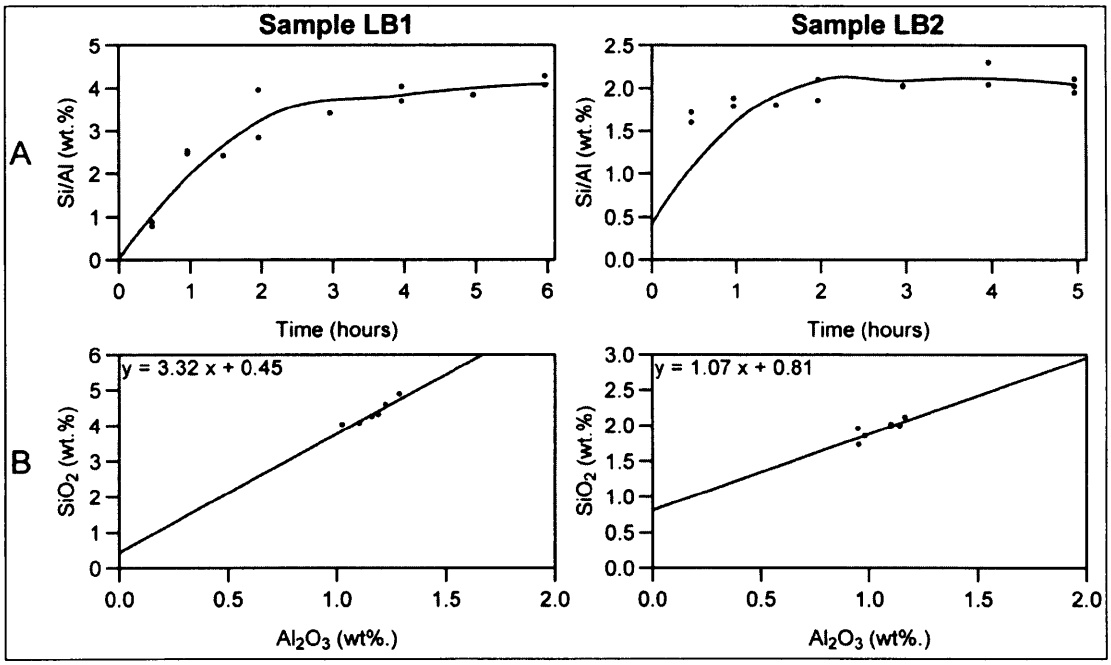

Figure 35: A) Si/Al ratios for samples LB1 and LB2 from Lake Baikal. B) Sequential SiO_2/Al_2O_3 corrections for concentrations of digested non-BSi.

Samples LB1 and LB2 produce BSi concentrations using conventional Si/time corrections of 4.37 wt.% as SiO_2 and 1.71 wt.% as SiO_2 respectively (Table 13). A single-step measurement from the five hour digestion point containing no correction for non-BSi produces similar values of 4.74 wt.% as SiO_2 and 1.99 wt.% as SiO_2 respectively (Table 13). Following application of a

sequential Si/Al correction, final BSi values are markedly lower at 0.45 wt.% as SiO_2, 90% reduction, and 0.81 wt.% as SiO_2, 56% reduction, respectively (Table 13; Fig. 35b). In contrast to samples C1-C3, significant differences remain between the sequential Si/Al and conventional, Si only, BSi values even after consideration of the standard errors associated with the regression coefficients (Table 13).

The marked difference in BSi between the sequential Si/Al and conventional Si only methods for samples LB1 and LB2, compared to samples C1-C3, can be attributed to the relativity high levels of digested Al in both Lake Baikal samples. For example, after four hours of digestion, mean dissolved Al concentrations were 0.61 wt.% in samples LB1 and LB2 compared to 0.30 wt.% for samples C1-C3. Together with low Si/Al ratios for samples LB1 and LB2 throughout the extraction (Fig. 33a), this suggests the presence of a relatively large, easily digested, aluminosilicate pool in which comparatively large amount of non-BSi are released relative to BSi. The presence of a rapid non-BSi digestion phase in the first few hours would further explain why no peak in dissolved Si/Al ratios is detected during the first two hours of sample digestion with the relative release of non-BSi significantly greater than that from BSi (Fig. 35a). Importantly, the non-BSi release during this initial digestion period can not be accounted for with conventional Si only measurements, which either ignore non-BSi digestion (single-step digestion) or assume the rate of non-BSi digestion after 3-4 hours to be representative of the rate throughout the entire digestion period (Si/time method). As detailed by Schlüter and Rickert (1998), Kamatani and Oku (2000) and Koning *et al.* (2002) and as shown in Figure 33a for sample LB2, a parabolic release of non-BSi actually occurs. This results in levels of non-BSi being underestimated with conventional Si only measurements of BSi. Consequently, it is suggested that the lower, sequential Si/Al derived, BSi measurements for samples LB1 and LB2 are more accurate than either the conventional single-step or Si/time BSi values, since the non-linear rate of non-BSi digestion is directly accounted and corrected for within this method.

Since only a limited number of samples were analysed from Lake Baikal, making such an interpretation about a notable aluminosilicate pool which significantly distorts BSi measurements in Lake Baikal requires further investigation. If confirmed, however, the presence of a comparatively large non-BSi release relative to BSi release during the first few hours of sediment digestion is worrying, particularly given that conventional Si only methods are not able to sufficiently correct for this early non-BSi release phase. This is demonstrated by the significant, up to 90%, decrease in BSi achieved when using sequential Si/Al corrections over Si only measurements. Such concerns over the accuracy of conventional Si only measurements should apply not only to Lake Baikal, but also to other sedimentary sites or samples containing easily digestible sources of non-BSi. This is particularly true when the amount of BSi within the sample is low. Chapter 7 will investigate this issue in more detail within the context of existing

palaeoclimatic records from Lake Baikal.

6.3.5. East Equatorial Pacific (EQ1-EQ2)

Sample EQ1 from the East Equatorial Pacific Ocean shows a peak followed by a decrease in dissolved Si/Al ratios to near-constant ratios after c. 4 hours (Fig. 36a). Visual microscope analysis of the recovered material, however, indicates incomplete digestion of BSi at this interval. Digestion of the sample in a stronger 2-M KOH solution over 14 hours (sample EQ2) reveals the complete digestion of BSi from 4 hours onwards when Si/Al ratios stabilise at c. 11 wt.% (Fig. 36b). Calculation of BSi from the greater than four hour interval in sample EQ2 using a Si/time non-BSi correction indicates a value of 7.85 wt.% as SiO_2 with the Si single step method indicating a BSi concentration of 8.65 wt.% as SiO_2 (Table 13). Applying a sequential Si/Al non-BSi correction significantly lowers the final BSi value to 2.22 wt.% as SiO_2 (Fig. 36b, c; Table 13).

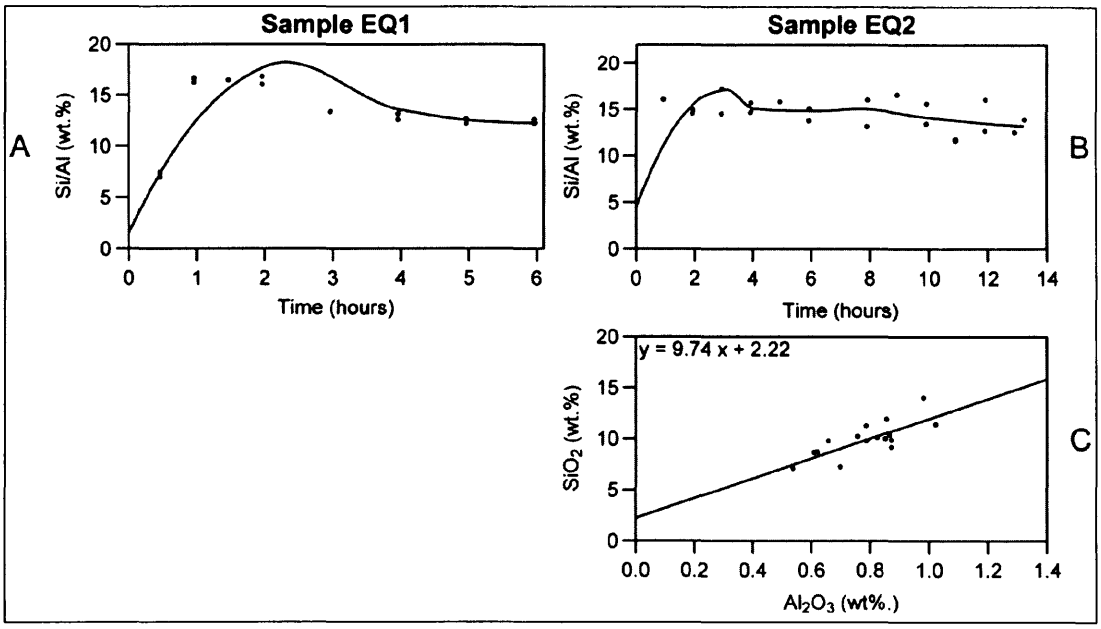

Figure 36: A) Si/Al ratios for sample EQ1, East Equatorial Pacific Ocean. B) Si/Al ratios for sample EQ2. C) Sequential SiO_2/Al_2O_3 correction for concentrations of digested non-BSi in sample EQ2.

Similar to the samples from Lake Baikal, mean digested Al concentrations are high within sample aliquots for EQ2 relative to samples C1-C3 (0.45 wt.% compared to 0.30 wt.%). Consequently as before, it is possible that a relatively rapid phase of non-BSi release is occurring during the first few hours of digestion, which is unaccounted for with conventional Si only measurements. This reiterates the potential of the sequential Si/Al method, which is able to directly account for non-BSi digestion during the alkaline extraction regardless of the rate or changes in rate of clay/aluminosilicate digestion. As stated above, this appears to be particularly

important when aluminosilicate release is rapid during the initial digestion period and/or when BSi concentrations are low, in which case the relative amount of digested non-BSi increases significantly.

The regression gradients of Si/Al or SiO_2/Al_2O_3 for each analysed sample should be reflective of the clay matrix, with Kamatani and Oku (2000) finding gradients of 1.20 ± 0.07, 1.19 ± 0.02, 2.40 ± 0.27, and 2.93 ± 0.09 for allophane, kaolinite, illite and montmorillonite respectively. All samples analysed here produce a regression gradient within this range, i.e., around or less than 3, except for sample C2 (Fig. 34b) and the east Equatorial Pacific Ocean samples (Fig. 36c). For sample C2, removing the aliquot with the highest Si concentration reduces the gradient from 8.44 to 1.48 with only a small change in calculated BSi concentrations. This indicates the general unsuitability of using sample gradients to obtain information on the sample clay matrix, unless large numbers of aliquots are analysed. For the Equatorial Pacific Ocean samples, the regression gradient remains above 9 regardless of which aliquots are included in the regression. It is possible therefore that these samples include authigenic clays that are unique to the eastern Equatorial Pacific Ocean and which can contain unusually high Si/Al ratios (Kastner and Stonecipher, 1978, Kastner, 1981). This should not affect the application of a sequential Si/Al method to these samples, since a linear release of Si and Al should still occur from these clays.

6.3.6. Evaluation of the Si/Al method

Values calculated here for surface sediment samples C1-C3 show no significant difference between sequential Si/Al BSi measurements and conventional Si only single-step or Si/time measurements (Table 13). In contrast the samples from Lake Baikal and the Equatorial Pacific Ocean show markedly lower values when using the sequential Si/Al approach (Table 13). It is not possible to conclusively demonstrate that the sequential Si/Al method provides a more accurate measure of BSi for these samples, which are both low in BSi and appear to have a rapid phase of aluminosilicate digestion associated with them during the first few hours of the alkaline extraction. However, the basis, theory and assumptions behind the sequential Si/Al approach are more valid than those for either a Si only single-step, for which no non-BSi correction is made, or a Si/time approach, which assumes a constant release of non-BSi over time. With non-BSi actually displaying a parabolic release over the first few hours of digestion (Schlüter and Rickert, 1998; Kamatani and Oku, 2000; Koning *et al.*, 2002), both Si single step and measurements incorporating a Si/time correction are liable to overestimate the true amount of BSi, particularly when levels of BSi are low and the relative release from non-BSi is high, as occurs for the Lake Baikal and East Equatorial Pacific samples. Consequently, it is likely that the lowering produced by sequential Si/Al corrections reflects a more reliable adjustment of BSi for sources of non-BSi. While using a sequential Si/Al technique may involve additional costs and laboratory time, this should be minimal in laboratories able to analyse Si and Al

concentrations via ICP-AES.

As stated in the introduction (Section 6.1.1), an alternative approach to the sequential Si/Al method used here is a single-step Si/Al method, in which Si/Al ratios from catchment material or clays standards are used to separate the biogenic and non-biogenic components (e.g., Eggimann *et al.*, 1980; Carter and Colman, 1994; Colman, 1998). This though requires the availability of catchment material or, more problematically, an exact understanding of the sample clay matrix which, at a given site, may vary both spatially and temporally. Alternatively, high-resolution monitoring of digested Si and Al concentrations can be performed at one second intervals (Koning *et al.*, 2002). Levels of BSi are then determined by modelling theoretical BSi and non-BSi dissolution curves. While this results in significant improvements with regards to data quality, whilst also potentially providing a more accurate and detailed insight into the dissolution of non-BSi, the equipment required for this is generally beyond the capabilities of most laboratories (Conley and Schelske, 2001).

Two issues may affect the reliability of the sequential Si/Al corrections. A significant pre-requisite of sequential Si/Al non-BSi corrections is that the relationship between Si and Al released from the clay matrix is constant throughout sample digestion. As stated above, this has been conclusively demonstrated for a range of clay minerals (Kamatani and Oku 2000; Koning *et al.*, 2002). The Si/Al relationship only deviates from this during the first 5-10 minutes of digestion when Si release is greater than Al (Koning *et al.*, 2002). The extent to which this occurs can vary spatially according to the precise clay composition of each sample (ibid). Consequently, part of the non-BSi release during this initial period will remain under-accounted for when using sequential Si/Al corrections. More accurate corrections for non-BSi release during this initial interval may be achieved by quantitatively assessing the exact composition of clay minerals within each individual sample. Such considerations, however, are beyond the scope of this investigation but are deserving of future research. It is likely, though, that any errors from this initial non-linear phase will be minimal compared to the improvements in BSi accuracy achieved when using a sequential Si/Al approach, relative to conventional Si only methods. Furthermore, any errors will also most likely be minimal relative to analytical and sample preparation errors, which are usually the largest source of error for BSi measurements (Conley and Schelske, 2001). Indeed, as shown within Figures 34a, 35a and 36a.b, dissolved Si/Al ratios between sample duplicates can vary widely. This most likely reflect the possible errors in weighing out samples/solutions together with the analytical reproducibility of the ICP-AES. However, samples always plot either on or close to the Si/Al regression line (Fig. 34b, 35b, 36c), indicating that these offsets are not affecting the final BSi value.

Secondly, it is explicitly assumed with the sequential Si/Al method that all digested Al

originates from sources of non-BSi. Within the water column, level of Al in diatoms are minimal with Al/Si ratios of $8.3x10^{-3}$ to $7.0x10^{-5}$ (Lewin, 1961; Martin and Knauer, 1973; Kamatani, 1974; van Bennekom *et al.*, 1989; Schlüter and Rickert, 1998; Beck *et al.*, 2002; Gehlen *et al.*, 2002). However, at the surface-sediment interface further amounts of Al can become incorporated into the diatom frustule (van Bennekom *et al.*, 1988, 1991; Dixit *et al.*, 2001; Dixit and van Cappellen, 2002; van Cappellen *et al.*, 2002; Gehlen *et al.*, 2002; Rickert *et al.*, 2002; Koning *et al.*, 2007). Despite this, the overall amount of digested Al within a sample originating from sources of BSi is likely to be negligible relative to contributions from non-BSi. This is particularly true when sample BSi concentrations are low. Whilst van Bennekom *et al.* (1989) reported fossilised diatom Al concentrations of up to 6 wt.% in sediments from the Zaire/Congo deep-sea fan, a wealth of other data makes its clear that fossilised diatom Al concentrations actually peak at c. 1.0 wt.% with typical concentrations of less than 0.3 wt.% and many concentrations of c. 0.01 wt.% (e.g., Shemesh *et al.*, 1988; Schlüter and Rickert, 1998; Ellwood and Hunter, 1999; 2000; Dixit *et al.*, 2001; Dixit and van Cappellen, 2002; Lin and Chen, 2002; Gehlen *et al.*, 2002; van Cappellen *et al.*, 2002; Kryc *et al.*, 2003; Lal *et al.*,2006). While the available data on diatom Al concentrations is heavily biased towards samples from the Southern Ocean, these values are supported here by mean diatom Al concentration of 0.34 wt.% in fossilised diatoms from ODP Site 882 in the North West Pacific Ocean (Table 12). It should be noted, though, that further work is required towards measuring the Al concentrations of diatoms in lacustrine systems and in other forms of BSi, such as radiolarians, in marine systems.

It is rarely feasible to extract pure diatoms from sites/samples which are low in BSi. As such, within a palaeoenvironmental reconstruction, it would be virtually impossible to extract pure diatom/BSi material for every analysed sample in order to test for Al concentrations. Within the context of this study, it is not possible to obtain pure diatom/BSi material from samples LB1, LB2 and EQ2, which all display significantly lower BSi concentrations when using the sequential Si/Al method relative to the Si only methods. If BSi concentrations, however, are recalculated for these samples incorporating a mass balanced correction for an assumed diatom Al concentration of 0.01 wt.% and 0.3 wt.%, sequential Si/Al BSi values for samples LB1 and LB2 do not alter. Similarly for sample EQ2, an Al concentration of 0.01 wt.% has no impact on the sequential Si/Al BSi concentration while a diatom Al concentration of 0.30 wt.% marginally increases BSi marginally from 2.22 wt.% as SiO_2 to 2.35 wt.% as SiO_2. If diatom Al concentrations are increased to 1.00 wt.%, which based on the published literature should represent an uppermost estimate of possible diatom Al concentrations, sequential Si/Al estimates of BSi increase marginally to 0.48 wt.% as SiO_2, 0.82 wt.% as SiO_2 and 2.72 wt.% as SiO_2 for samples LB1, LB2 and EQ2 respectively. Importantly, all of these adjustments are low and within the errors associated in calculating the regression coefficients for the original

sequential Si/Al BSi concentrations (Table 4). Furthermore, these corrected sequential Si/Al BSi values remain significantly below conventional, Si only, BSi values (Table 34). Similar Al correction can also be calculated for samples C1, C2 and C3, which display no significant difference between the sequential Si/Al and Si only methodologies, most likely due to the low overall amount of Al digested from these samples during the alkaline extraction (Table 13). With these samples, a diatom bound Al concentration of 1.00 wt.% increase BSi by less than 0.20 wt.% SiO_2 for samples C1 and C2. In sample C3, however, an Al correction increases BSi by 6.80 wt.% as SiO_2 due to the high number of diatoms within this sample. This increase remains high at 1.80 wt.% as SiO_2 even when using a diatom Al concentration of 0.30 wt.%. As such, whilst for most of the samples analysed here, the uncertainty and presence of BSi associated Al is not detrimental to the application of a sequential Si/Al methodology for calculating BSi concentrations, caution is need in samples of high BSi unless actual values of diatom or BSi bound Al within these sediments are well constrained.

6.4. Conclusions

The current popularity of wet-alkaline BSi measurements is largely based on the methods perceived robustness and the comparative ease by which samples can be analysed. However, conventional corrections for sources of non-BSi in wet-alkaline digestions are either non-existent, Si single-step, or overtly simplistic, Si/time. Comparisons until now have provided no conclusive evidence for the benefits in using a sequential Si/Al approach over these existing techniques. Results here, however, show that sequential Si/Al measurements can significantly lower estimates of BSi, particularly in samples low in BSi. This is emphasised in the samples from Lake Baikal and the East Equatorial Pacific Ocean where a large non-BSi release appears to be occurring during the first few hours of samples digestion. Following the application of sequential Si/Al non-BSi corrections, measured BSi concentrations at these sites are reduced by 56-90% relative to conventional Si only techniques.

While it is not possible to state with absolute certainty that such a lowering represent an "improvement", it is likely that the sequential Si/Al measurements are more accurate as the method permits a direct accountability for non-BSi leached throughout the course of the alkaline digestion. Undoubtedly, further investigations and assessments of the sequential Si/Al methodology will be called for across a greater range of sites. However, based on these results together with previous studies demonstrating a linear relationship between Si and Al leached from clays throughout all but the first few minutes of sample digestion (Schlüter and Rickert, 1998; Kamatani and Oku, 2000; Koning *et al.*, 2002), it is suggested that sequential Si/Al measurements represent a simple, yet key, improvement in the measurement of aquatic sediment BSi concentrations. Consequently, the use of a sequential Si/Al method for determining BSi is recommended when expected BSi concentrations are low and/or when aluminosilicate digestion

is rapid during the first few hours of sample digestion. This is important in ensuring that the recorded stratigraphical changes in BSi reflect changes in surface water productivity, rather than fluxes in sample clay content. However, caution is required in applying the technique to samples rich in BSi, unless the concentration of Al intrinsically linked and bound to the BSi is known and accounted for.

Chapter 7: Testing Si/Al derived biogenic silica concentrations in Lake Baikal

7.1. Introduction

Chapter 6 demonstrated the potential of a sequential Si/Al method for obtaining more accurate sedimentary BSi concentrations. While suggested to produce lower and more accurate records of BSi, relative to conventional Si/time (De Master, 1979, 1981) and Si single step (Mortlock and Fröhlich, 1989) methods, the sequential Si/Al BSi method has yet to be applied to a long stratigraphical core section. In addition, it is also necessary to evaluate the accuracy of the sequential Si/Al method against samples for which the true amount of BSi is known. Assessment of the sequential Si/Al method can be performed in a number of ways ranging from laboratory experiments using siliceous standards to in-field experiments. One of the most common uses of BSi concentrations, though, is as a proxy for reconstructing palaeoenvironmental and palaeoclimatic changes in marine and lacustrine sediment cores. In addition, based on the results in Chapter 6, it is likely that the palaeoenvironmental community would benefit the most from the sequential Si/Al method due to the high clay content which may be present in aquatic sediment samples. Within this context, the sequential Si/Al method is best "tested" against lacustrine or marine sediment samples where measurements of BSi can be compared to microscope counts of siliceous organisms that document the true absolute amount of BSi within a sample.

In a palaeoclimate context, BSi concentrations have been widely used in Lake Baikal, Russia (Fig. 37), a lake which potentially contains an uninterrupted sedimentary sequence dating back to the Middle Eocene (Hutchinson *et al.* 1992) or Middle/Late Miocene (Williams *et al.* 2001; Sapota *et al.*, 2004). A significant limitation of conducting palaeoclimatic research in Lake Baikal is the very low amounts of carbonates within the sedimentary record due a water column pH of 6.9-7.4. However, diatoms are widely present in the sediment record constituting c. 98% of all BSi within the sediment (Granina *et al.*, 1992). Measurements of BSi in the lake therefore in theory provide a simple and effective way of recording past variations in diatom productivity. Existing studies have previously documented strong first-order linkages between conventional wet-alkaline (Si single step and Si/time) records of BSi and orbital insolation in Lake Baikal with high levels of BSi in interglacials (c. 10-30 wt.% as SiO_2) indicative of high diatom productivity and lower concentrations in glacials (c. 0-5 wt.% as SiO_2) suggestive of low diatom productivity (Granina *et al.* 1993; Colman *et al.* 1995, 1999; Williams *et al.* 1997). Similarly, other work over shorter timescales has shown strong relationships between diatom populations and BSi concentrations in the sediment (Qui *et al.*, 1993; Horiuchi *et al.*, 2000; Edlund and Stoermer, 2000; Khursevich *et al.*, 2001). As such, conventional (Si only) wet-alkaline BSi concentrations have been widely used in Lake Baikal, as a proxy for diatom productivity, to reconstruct palaeoenvironmental and palaeoclimatic changes over both glacial-interglacial (Colman *et al.* 1995, 1999; Williams *et al.* 1997) and shorter, millennial/interglacial timescales

(e.g., Qui *et al.*, 1993; Karabanov *et al.*, 1998; Horiuchi *et al.*, 2000; Prokopenko *et al.*, 2001a,b; Karabanov *et al.*, 2004). In addition, due to the cyclic nature of the BSi record over glacial-interglacial cycles, measurements of BSi have also been crucial in developing age models for sediment cores from Lake Baikal (Prokopenko *et al.*, 2006). BSi concentrations, however, can not be related to the overall level of biological productivity in the lake given that half of the modern day chlorophyll *a* production originates from picoplankton (Popovskaya 2000; Fietz and Nicklisch 2004; Fietz *et al.*, 2007), which are rarely preserved in the sediment record.

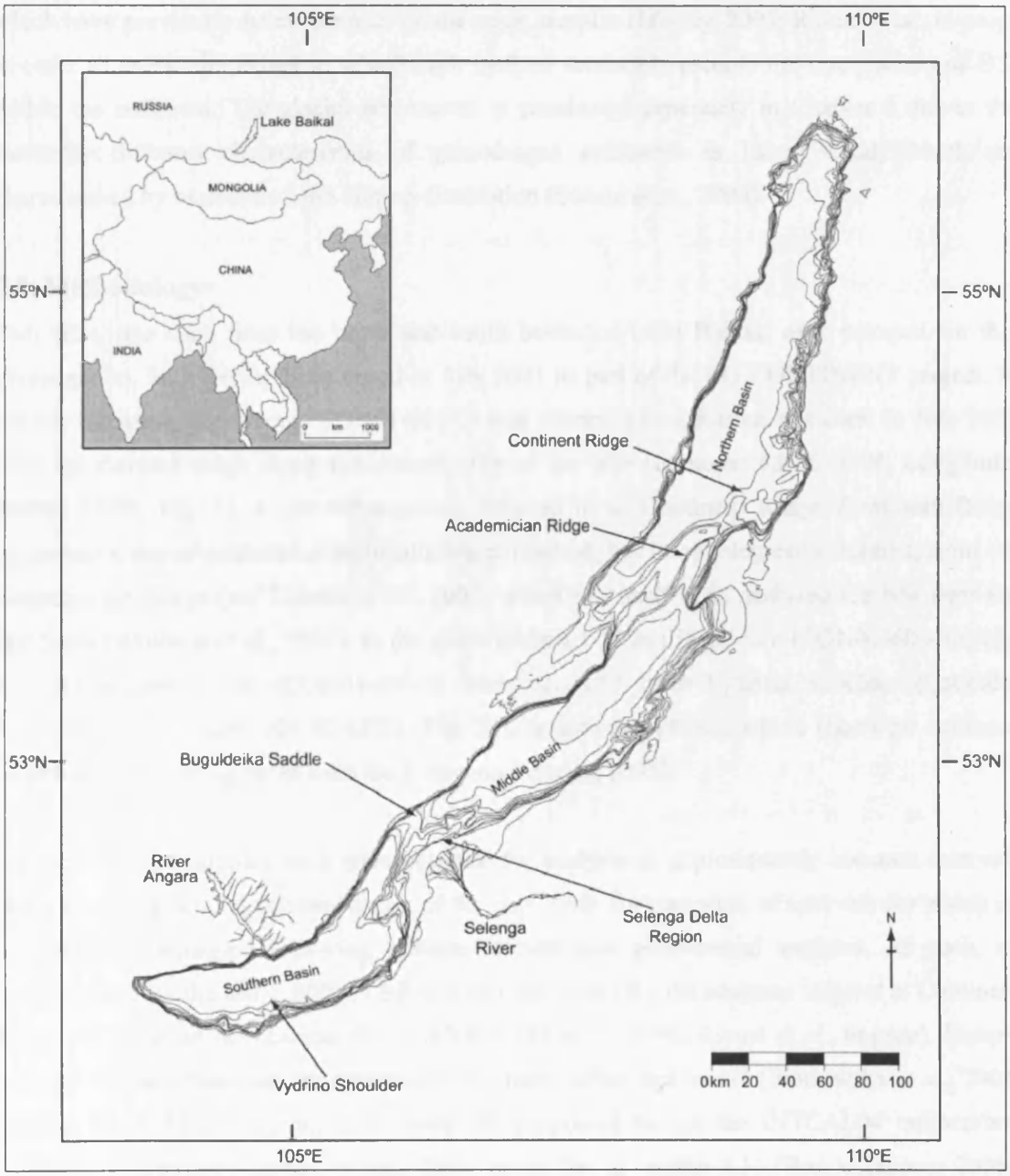

Figure 37: Location of Continent Ridge (north basin) and Vydrino Shoulder (south basin), Lake Baikal (adapted from Swann *et al.*, 2005).

The strong link that exists between diatom populations and the amount of BSi within the Lake Baikal sediment record provides an opportunity to test the accuracy of sequential Si/Al BSi measurements. Here in this chapter, records of BSi are measured at two sites in Lake Baikal on samples covering the late glacial/Holocene interval, a period of variable but high diatom productivity within the lake (Morley, 2005). First, records of sequential Si/Al and Si only (Si/time) BSi concentrations are compared relative to one another to examine the degree of similarity between the two records and to further assess potential differences between the two techniques. Secondly the two datasets are compared to the detailed diatom biovolume records which have previously been recorded on the same samples (Morley, 2005; Rioual *et al.*, in prep) in order to assess the extent to which each method accurately records the true amount of BSi within the sediment. The glacial BSi record is considered separately in Chapter 8 due to the markedly different characteristics of glacial-aged sediments in Lake Baikal, which are characterised by extremely high diatom dissolution (Swann *et al.*, 2005).

7.2. Methodology

Two sites, one each from the north and south basins of Lake Baikal, were selected for this investigation, both having been cored in July 2001 as part of the EU CONTINENT project. In the north basin a 3.9-m core (CON01-603-5) was collected by a Kasten box corer in July 2001 from an elevated ridge along the eastern side of the lake (Latitude: 53°95′46″N, Longitude: 108°91′37″W; Fig. 1), a site subsequently referred to as Continent Ridge. Continent Ridge represents a site of continuous sedimentation connected, but morphologically isolated, from the Academician Ridge (see Charlet *et al.*, 2005) which has itself been analysed for BSi over the last 5 Ma (Williams *et al.*, 1997). In the south basin a 1.73 m trigger core (CON01-605-3a) and a 10.45 m piston core (CON01-605-3) were collected from Vydrino Shoulder (Latitude: 51°58'49"N, Longitude: 104°85'48"E) (Fig. 37), an elevated plateau which shows no evidence of sediment reworking for at least the Holocene (Morley, 2005).

At both sites 64 samples each were selected for analysis at approximately constant intervals along the late-glacial/Holocene section of the core, with the exception of intervals for which no core material remained following previous diatom and geochemical analyses. As such, no samples exist for the last c. 800 yrs BP at either site. Dates for the analysed interval at Continent Ridge are based on radiocarbon dating (Piotrowska *et al.*, 2004; Rioual *et al.*, in prep). Sample ages for Vydrino Shoulder are also based on a radiocarbon age model (Piotrowska *et al.*, 2004; Morley, 2005; Morley *et al.*, 2005) with dates updated to use the INTCAL04 radiocarbon calibration curve (*pers. comm.* Rioual, 2006) using OxCal version 3.10 (Bronk Ramsey, 2005). Details on the correlation and creation of a composite depth for the cores from Vydrino Shoulder are contained in Morley (2005).

All samples selected at both sites have previously been analysed for diatom assemblages (Morley, 2005; Rioual *et al.*, in prep). While these records of diatom populations and diatom valve concentrations can be compared to BSi measurements, such records do not account for the large variations in size that exist between different taxa. For example, two common species in the Holocene section at Continent Ridge, *Aulacoseira baicalensis* (Meyer) Simonsen and *Cyclotella minuta* (Skv.) Antipova, have biovolumes of 6540 μm^3 and 860 μm^3 respectively while the biovolume of *Cyclotella baicalensis* (Meyer) Skv. is 81500 μm^3 (Rioual *et al.*, in prep). Diatom biovolume measurements, calculated from the species assemblage data, provide a more accurate record of the actual amount of BSi within the sediment by taking into account the size variation between different taxa. Sample diatom biovolumes for the analysed section at Continent Ridge are taken from Rioual *et al.* (in prep) in which species biovolumes are calculated following the recommendations of Hillebrand *et al.* (1999). Sample diatom biovolumes for the late-glacial/Holocene section at Vydrino Shoulder are based on the results of Morley (2005) but with individual species biovolume values updated to reflect the recommendations of Hillebrand *et al.* (1999) and to take advantage of the recent late-glacial/Holocene species biovolume data included in Rioual *et al.* (in prep).

One limitation over the sequential Si/Al method is the potential for significant levels of Al, digested during the alkaline extraction, to originate from diatoms and other forms of BSi. As shown in Chapter 6, if left unaccounted for this may result in significant errors unless diatom bound Al concentrations are minimal. While sedimentary diatom Al concentrations are almost always less than 1.0 wt.% (e.g., Shemesh *et al.*, 1988; Schlüter and Rickert, 1998; Ellwood and Hunter, 1999; 2000; Dixit *et al.*, 2001; Dixit and van Cappellen, 2002; Lin and Chen, 2002; Gehlen *et al.*, 2002; van Cappellen *et al.*, 2002; Kryc *et al.*, 2003; Lal *et al.*, 2006), this ideally needs to be assessed at each individual site. Consequently, 22 pure diatom samples from Lake Baikal, previously extracted and cleaned for diatom isotope analysis at Continent Ridge (Mackay *et al.*, in prep), were also dissolved and analysed using the same methodology. No pure diatom material was available for any late glacial or Holocene aged samples. Instead, all analysed pure diatom samples originate from the Kazantsevo, a warm period within Lake Baikal which is broadly synchronous with MIS 5e (Shackleton *et al.*, 2003).

7.2.1. BSi methodology

Samples for BSi were digested and analysed for Si and Al following adaptation of the wet-alkaline methodology outlined in Chapter 6. A major difference between the two chapters is the use here of a single digestion for each sediment sample with 2 ml of the alkaline solution collected at timed intervals for ICP-AES analysis. In Chapter 6 a single digestion was instead performed for each timed aliquot measurement. This was due to the need for c. 5 ml of solution for the ICP-AES in Chapter 6 in order to analyse the eight different elements measured within

that chapter (see Section 6.2). In contrast here, only concentrations of Si and Al were analysed.

Sediment samples were freeze dried with c. 40 mg weighed into flat bottomed acid-washed bottles containing 40 ml of 5% Na_2CO_3, within the sample-solution ratios proposed by Gehlen and van. Raaphorst (1993). The stronger 5% Na_2CO_3 solution used here, compared to 1% Na_2CO_3 in Chapter 6, arises from the high amounts of BSi expected within the Holocene aged samples. Samples were immersed in a waterbath heated to 85°C and periodically shaken throughout the digestion period to ensure full exposure of the sediment to the solution. For each core a series of replicates were analysed to check method reproducibility with a set of blanks run every ten samples. Sample aliquots were collected after 4, 5 and 6 hours of digestion and stored at c. 2°C prior to ICP-AES analysis. As in Chapter 6, aliquots were not neutralised with a weak HCl or other acidic solution in order to avoid diluting samples beyond ICP-AES detection limits. Dissolved concentrations of Si and Al within the sample aliquots were analysed using a Perkin Elmer Optima 3300RL ICP-AES at Royal Holloway, University of London with matrix matching for all standards and calibrations. Prior to analysis, sample aliquot were allowed to warm to room temperature. All results were corrected for analytical drift and elemental concentrations in procedural blanks. BSi was then calculated using both the Si/time (De Master 1979, 1981) and the Si/Al methods (Kamatani and Oku, 2002) (see Chapter 6 for details).

7.3. Results

7.3.1. Analytical accuracy

Analytical precision of the ICP-AES was low at 0.50 ppm for Si and 0.03 ppm for Al. Replicate analyses of sediment samples from Lake Baikal indicated a final mean BSi reproducibility of 0.60 wt.% as SiO_2 (1σ) under the Si/time method and 0.79 wt.% as SiO_2 (1σ) under the sequential Si/Al method. Sediment BSi concentrations for both methods ranged from 0-34 wt.% as SiO_2

7.3.2. Method comparison

BSi results for both the Si/time and sequential Si/Al method at Continent Ridge and Vydrino Shoulder show large changes through the late-glacial/Holocene interval with BSi concentrations peaking at 4.0 kyr BP and at 1.5 kyr BP (Fig. 38). Analysis of the Kazantsevo pure diatoms frustules from Lake Baikal indicates mean Al concentrations in diatoms of 0.09 wt.% (1σ = 0.02). These values lie at the lower range of reported diatom bound Al concentrations (Shemesh *et al.*, 1988; Schlüter and Rickert, 1998; Ellwood and Hunter, 1999; 2000; Dixit *et al.*, 2001; Dixit and van Cappellen, 2002; Lin and Chen, 2002; Gehlen *et al.*, 2002; van Cappellen *et al.*, 2002; Kryc *et al.*, 2003; Lal *et al.*,2006), suggesting that the relative contribution of diatom Al to the total amount of leached Al within the alkaline solution is minimal. One parameter which may potentially play a significant role in alternating the relative amount of Al within diatoms is

changes in the sediment clay composition (Koning *et al.*, 2007). Records from a series of cores across Lake Baikal, however, including Continent Ridge and Vydrino Shoulder, indicate that the sediment clay composition has not varied significantly over recent glacial/interglacial cycles (Fagel *et al.*, 2003, 2007).

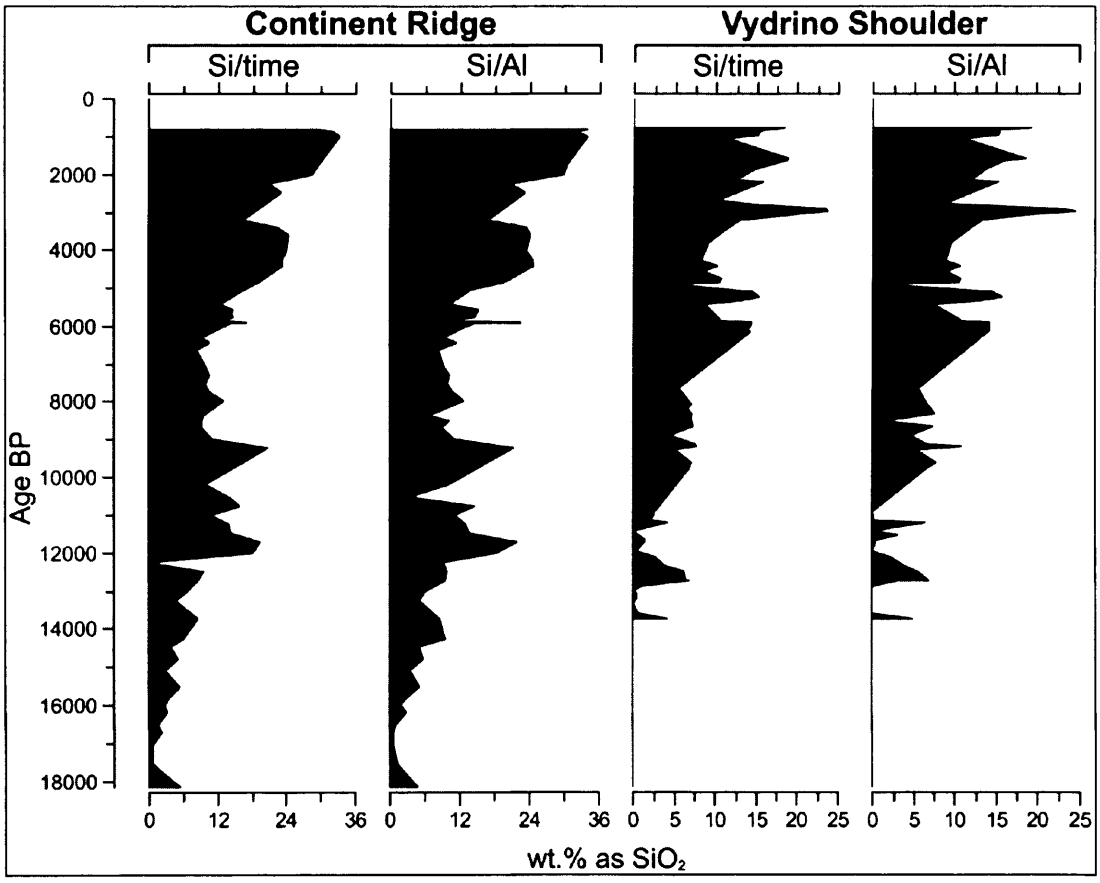

Figure 38: Lake Baikal Si/time and sequential Si/Al late-glacial/Holocene changes in BSi.

Consequently, whilst the pure diatom frustules analysed here originate from the Kazantsevo rather than the Holocene or late glacial, it is reasonable to assume that the diatom bound Al values remain representative of concentrations within all the analysed samples. By assuming this, the contributions of diatoms to dissolved Al concentrations within the sample aliquots can be shown to be minimal with only a negligible impact on sequential Si/Al BSi results. For example, when using the Si and Al sample aliquot data at 0.8 kyr BP at Continent Ridge (Si/Al derived BSi concentration for this sample is 33.7 wt.% as SiO_2, the highest value observed in this chapter), a mass balanced correction for a diatom Al concentration of 0.09 wt.% lowers the final sequential Si/Al BSi value by only 0.15 wt.% as SiO_2. At lower BSi values, the magnitude of this error will be further reduced. As such, here in Lake Baikal, issues of diatom bound Al can be ruled out as a factor in controlling the sequential Si/Al BSi record.

In contrast to results in Chapter 6, here comparisons of the Si/time and sequential Si/Al methods

at both sites indicates a strong 1:1 relationship between the two methods, which is significant at the 99.9% confidence interval (Fig. 39).

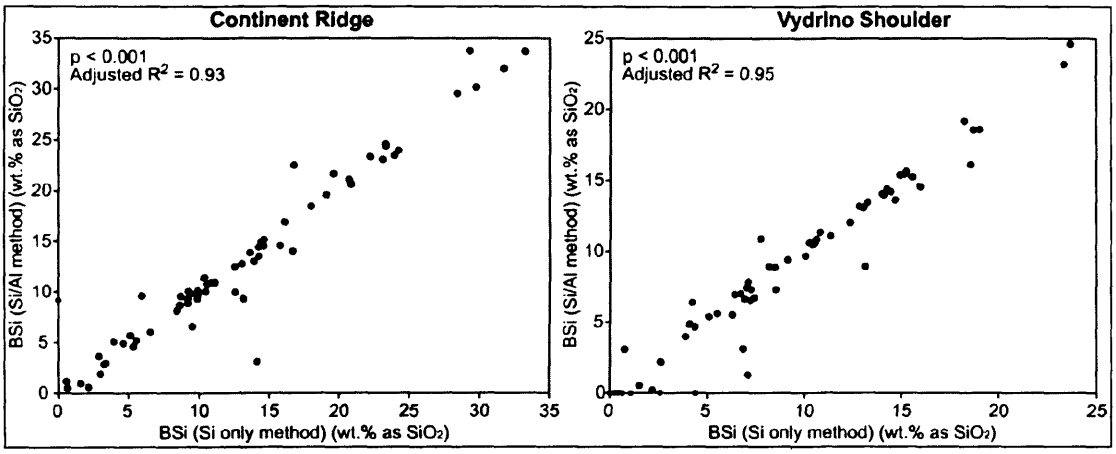

Figure 39: Comparison of the Si/time and sequential Si/Al BSi methods.

7.3.3. Diatom biovolumes

At both sites a statistical relationship exists between increasing diatom biovolumes and increasing BSi concentrations for both methods ($p < 0.001$) (Fig. 40).

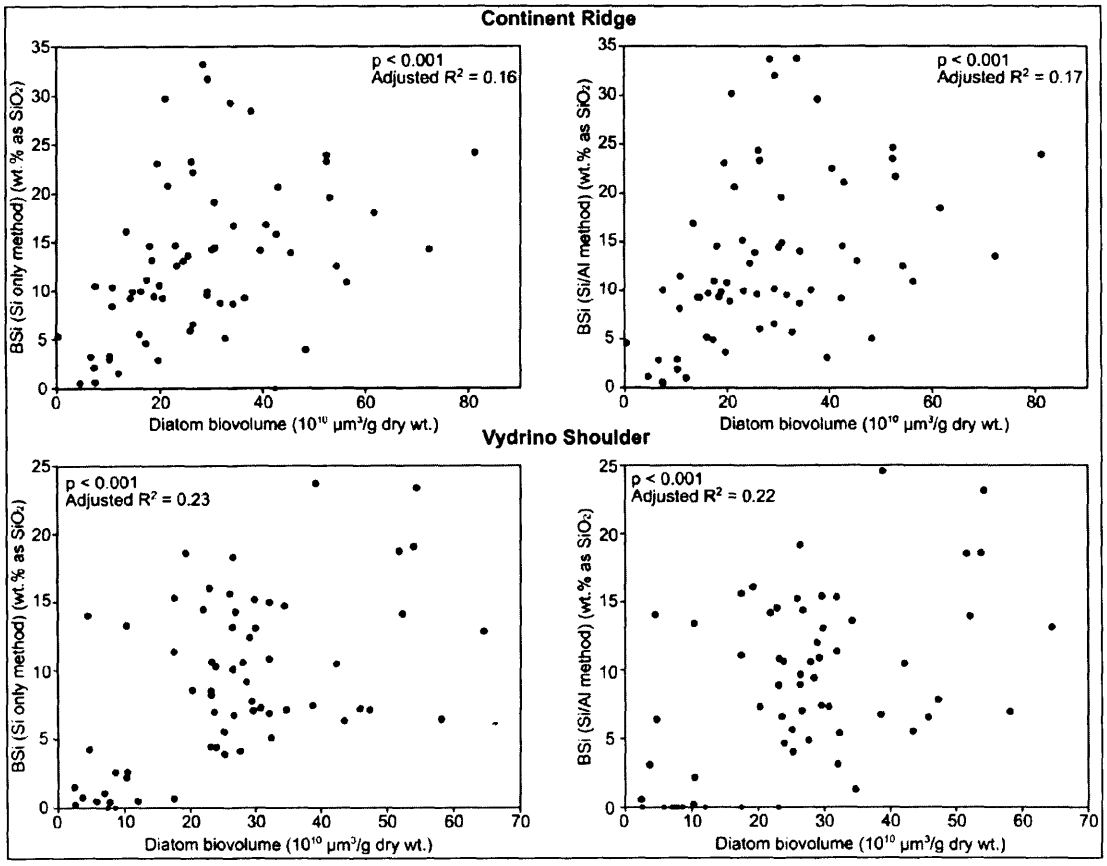

Figure 40: Comparison of diatom biovolumes to the Si/time and sequential Si/Al BSi methods.

Residual errors based on a linear regression through the dataset, however, are high at both sites (Fig. 40). At Continent Ridge the mean BSi residual is +5 to +20 wt.% as SiO_2 from 0-5 kyr BP and -5 to -10 wt.% as SiO_2 from 8 kyr BP onwards for both methods. At Vydrino Shoulder, residuals are +5 to +10 wt.% as SiO_2 from 0-6 kyr BP and -5 to -10 wt.% as SiO_2 thereafter.

7.4. Discussion

Previous work on the same samples analysed here have led to detailed late glacial/Holocene palaeoclimatic and palaeoenvironmental reconstructions based on the diatom species assemblages (Morley, 2005; Rioual *et al.*, in prep). Holocene reconstructions at other sites in Lake Baikal have also been derived from BSi concentrations (e.g., Qui *et al.*, 1993; Carter and Colman, 1994; Karabanov *et al.*, 2004). As such, no attempt is made here to related the temporal change in BSi observed in Figure 38 to palaeoclimatic or palaeoenvironmental conditions. Instead, the discussion will focus on attempting to understand the possible advantages/disadvantages in using a sequential Si/Al method over a Si/time method and the link between microscope observation of diatom frustules and wet-alkaline measurements of BSi.

7.4.1. Si/time v Si/Al

Results in Chapter 6 revealed significant differences between the Si/time and sequential Si/Al BSi methods in samples EQ2 from the East Equatorial Pacific Ocean and samples LB1 and LB2 from glacial aged samples in Lake Baikal. The lower sequential Si/Al BSi values were suggested in Chapter 6 to more accurately represent the true amount of BSi within the sediment due to the methods direct accountability for non-BSi digestion during the alkaline extraction. Such conclusions, though, are not in line with the results presented within this chapter in which a strong 1:1 relationship exists at both Continent Ridge and Vydrino Shoulder between the two method (Fig. 39). The presence of such a strong relationship is not entirely surprising given that both the Si/time and the sequential Si/Al methods are dependent on the same initial Si values. Indeed for most samples, BSi concentrations from the sequential Si/Al method are marginally lower than the Si/time method. However, this difference is largely minimal (mean difference is 0.11 wt.% as SiO_2 at Continent Ridge and 0.33 wt.% as SiO_2 at Vydrino Shoulder) and within the combined Root Mean Squared Error (RMSE) analytical reproducibility for the two methods (0.99 wt.% as SiO_2) (Fig. 41).

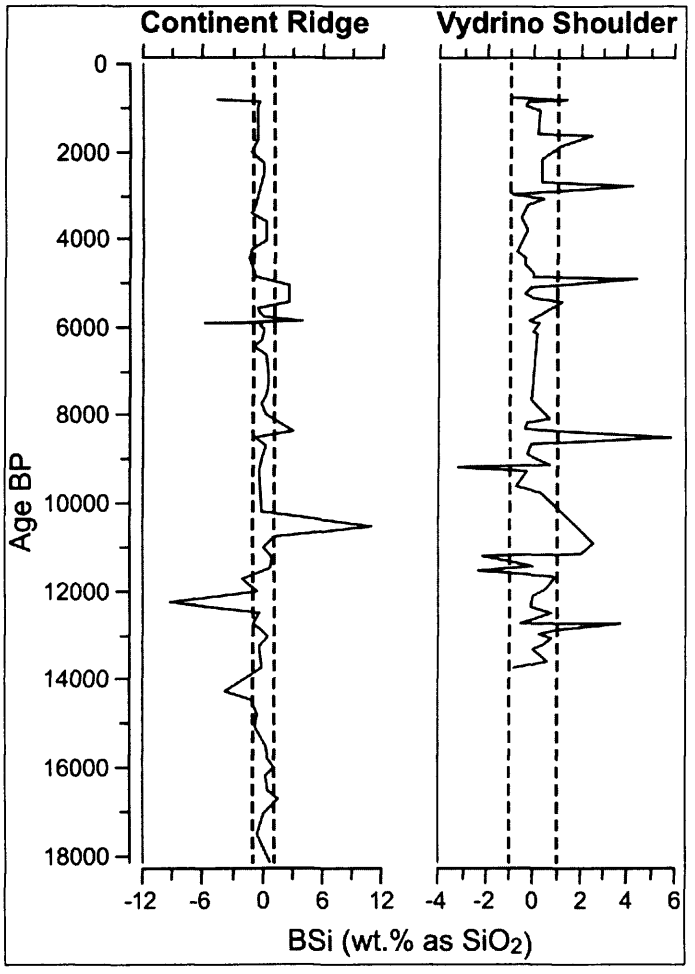

Figure 41: Difference in BSi concentration between the two methods at Continent Ridge and Vydrino Shoulder (Si/time method minus sequential Si/Al method). Dashed lines represent the RMSE of the two methods (0.99 wt.% as SiO_2).

The most likely explanation for the similar results between the two methods, given that both are dependent on the same Si concentration data, are changes in the amount of Al dissolved during the alkaline digestion. Mean Al concentrations of sample aliquots at Continent Ridge and Vydrino Shoulder are 0.17 wt.% and 0.25 wt.% respectively. These are significantly lower than the mean Al concentrations of 0.45 wt.% observed in Chapter 6 for sample EQ2, which produced significantly lower BSi values when using the sequential Si/Al method relative to conventional Si only methods. Mean Al concentrations of 0.17 wt.% and 0.25 wt.% at Continent Ridge and Vydrino Shoulder are, however, similar to concentrations of 0.30 wt.% for samples C1-C3 in Chapter 6, which showed no significant difference between the Si/Al and Si only BSi methods. As such, the lack of a difference here between the two BSi methods, and in samples C1-C3 in Chapter 6, may tentatively be attributed to reduced aluminosilicate and associated non-BSi release during the alkaline digestion in these samples.

Evidence to support this theory of reduced aluminosilicate digestion is found by comparing the Lake Baikal late-glacial/Holocene samples analysed here to the Lake Baikal glacial samples analysed in Chapter 6, which showed marked differences between the Si only and sequential Si/Al methodologies. As with sample EQ2, mean Al concentrations of 0.66 wt.% for sample LB1 (50.2 kyr BP) and 0.56 wt.% for sample LB2 (25.2 kyr BP) are significantly greater than mean late-glacial/Holocene concentrations here of 0.17 wt.% and 0.25 wt.% at Continent Ridge and Vydrino Shoulder respectively. This is despite the samples analysed here being digested in a significantly strongly alkaline solution (5% Na_2CO_3 compared to 1% Na_2CO_3 in Chapter 6). In order to confirm this observation, a further 12 samples, spread across the MIS 2-4 interval at Continent Ridge, were digested using the methodology outlined above in Section 7.2. All of these additional samples indicate high Al concentration similar to those in Chapter 6 (mean = 0.54 wt.%, 1σ = 0.11). Although a proportion of the lower Al concentrations in the late-glacial/Holocene samples will be due to the increased amounts of diatoms, relative to clays, in the sediment, this is not sufficient to explain all of the difference. For example, if a sediment BSi concentration of 33.7 wt.% as SiO_2 (the highest BSi value observed in this chapter) is used together with the mean digested Al value for this sample of 0.13 wt.%, using a simple mass balanced equation a digested Al concentration of c. 0.17 wt.% would be expected in a 100% pure clay sample when assuming a similar clay matrix, rate of aluminosilicate digestion and after consideration of diatom bound Al. Reduced aluminosilicate digestion within the late-glacial/Holocene samples, relative to glacial aged samples, is most likely connected to the relative reactivity and/or the quantity and different types of clays within the sediment. Sediments at both Vydrino Shoulder, Continent Ridge and elsewhere in Lake Baikal are dominated by illite and smectite over the late Quaternary (Fagel *et al.*, 2003; 2007). While records show different relative abundances of these two clay minerals between Vydrino Shoulder and Continent Ridge, no significant change in these proportions occurs over time (Fagel *et al.*, 2007). As such, the cause of increased aluminosilicate digestion in glacial aged samples from Lake Baikal remains unknown.

Whilst in this instance, with late-glacial/Holocene aged samples from Lake Baikal, no advantage exists in using a sequential Si/Al over a Si/time methodology, the results highlight the importance in considering aluminosilicate dissolution when analysing BSi. For example, when aluminosilicate digestion is high, such as with samples LB1, LB2 and EQ2 in Chapter 6, significant differences exist between the two techniques. Since the amount of aluminosilicate digestion during the alkaline extraction is rarely known in advance, the sequential Si/Al method should still remain preferential to either a Si/time or other Si only techniques. This is particularly true when analysing sample aliquots via ICP-AES, as virtually no additional work is required to measure Al and other elemental concentrations alongside dissolved Si.

7.4.2. BSi/diatom biovolumes relationship

A second aim of this work was to determine the link between wet-alkaline measurements of BSi and sedimentary diatom/siliceous concentrations. This is necessary in order to determine the accuracy of wet-alkaline BSi measurements in recording siliceous organisms and therefore changes in diatom productivity. Evidence here of a strong relationship ($p<0.001$) between BSi and diatom biovolumes (Fig. 40) is in apparent agreement with existing laboratory investigations and studies on sediment material from Lake Baikal which demonstrate strong links between diatom populations and wet-alkaline BSi concentrations (Qui *et al.*, 1993; Colman et al., 1995; 1997; Williams *et al.* 1997; Horiuchi *et al.*, 2000; Khursevich *et al.*, 2001; Ryves *et al.* 2001; Karabanov *et al.* 2004). As such, increase/decreases in diatom concentrations are marked by corresponding increases/decreases in BSi concentrations (Fig. 40). A significant difference between this work and previous studies, however, is the use here of diatom biovolume data, which provide a more accurate indicator of the actual amount of BSi within a sample than the diatom concentrations used in previous studies.

At both sites, however, the BSi/diatom biovolume relationship for both BSi methods is marked by large residual errors from a linear regression line of between 5 to 20 wt.% as SiO_2 (Fig. 40). This may suggest that wet-alkaline measurements of BSi are not suitable for making detailed quantitative interpretations as to changes in sedimentary siliceous microfossil concentrations and consequently levels of diatom palaeoproductivity. Such a comparison, though, between measurements of BSi and diatom biovolumes may be affected by the accuracy of the original diatom biovolume data used within this study. Diatom biovolumes at Continent Ridge (Rioual *et al.*, in prep) and Vydrino Shoulder (Morley, 2005) were calculated for all dominant taxa, including frustule fragments, within the sediment record. In most samples, however, a proportion of rarer taxa are present for which no biovolume measurements exist and which, consequently, do not contribute towards the sample biovolume measurements. In most cases this is not a significant issue as these taxa are both rare and generally have a smaller biovolume than other, more dominant taxa, within the sediment record. In some samples, however, the relative proportion of these rarer taxa increases, particularly in colder periods such as the late glacial when the number of rarer planktonic and benthic taxa increases (Morley, 2005; Rioual *et al.*, in prep), introducing a degree of uncertainty to the sample biovolume measurements. In order to eliminate this effect, all biovolume measurements which are based on less than 80% of the diatom frustules within the sediment assemblage are removed from the dataset. While at Continent Ridge this results in a clearer BSi/diatom biovolume relationship, r^2 remains low with BSi residuals ranging from -5 to +5 wt.% as SiO_2 (Fig. 42) At Vydrino Shoulder, though, the BSi/diatom biovolume relationship remains relatively weak with residuals of +10 to -5 wt.% as SiO_2 (Fig. 42).

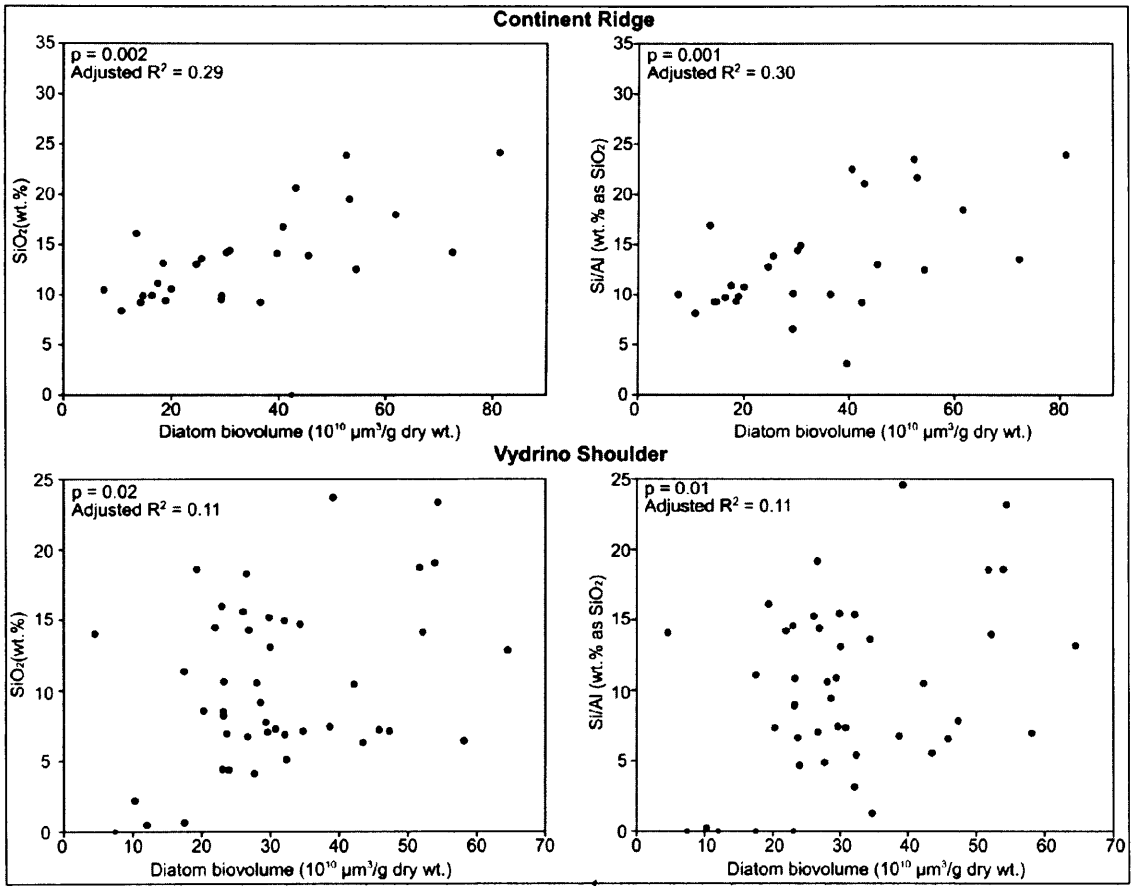

Figure 42: Comparison of diatom biovolumes to both BSi methods at Continent Ridge and Vydrino Shoulder for all samples in which diatom biovolumes include over 80% of the diatom frustules in the sediment assemblage.

The amount of silica/biovolume within a diatom frustule may also vary both within and between individual diatom species in response to changes in palaeoenvironmental conditions, such as change in temperature, ice cover, growth rate and nutrient availability (Rioual, unpublished data) (see reviews in Martin-Jézéquel *et al.* (2000) and Ragueneau *et al.* (2000, 2006)). All diatom biovolume measurements used within this study are based on taxa coefficients derived from light microscopy measurements across a selection of recent Holocene core samples at both sites (Morley, 2005; Rioual *et al.*, in prep). As such, the diatom biovolume coefficients should be broadly representative of the diatom frustules and possible variations in frustule dimensions across all the analysed samples. Whist diatom biovolume measurements do not account for pore spaces and other voids within the diatom frustule and while the biovolume coefficients will not be a perfect match for all frustules, such uncertainties should not lead to the poor relationship or large residual errors observed in Figures 40 and 42. It is possible, however, that the biovolume coefficients used here are not reflective of species biovolumes during periods of unusual/extreme climatic conditions, such as the cold and extended periods of ice cover which

may have prevailed during the Younger Dryas. However, almost all late glacial aged samples were removed from the dataset presented in Figure 42, due to the percentage of diatom frustules in the biovolume measurements being below the 80% threshold. It also seems unlikely that environmental conditions could have varied sufficiently, at least within the Holocene, to generate the large residual errors observed in the BSi/diatom relationship (Fig. 40, 42). This is reinforced by $\delta^{18}O_{diatom}$ measurements and high-resolution analyses of the diatom assemblages at Vydrino Shoulder, which indicate relatively stable conditions through the Holocene, including the absence of a 8.2 kyr events (Morley, 2005; Morley *et al*, 2005). Even if environmental conditions had been more varied, it would be expected that only an occasional sample from a period of extreme palaeoenvironmental conditions would result in a notable residual error. In practise errors of 5-10 wt.% as SiO_2 are present for most samples throughout the analysed sections, including the late Holocene and particularly for the samples from Vydrino Shoulder (Fig. 42).

A further factor which may be controlling the wet-alkaline BSi record is diatom dissolution, which can act to remove BSi from the sediment while leaving behind remains of the diatoms frustule for inclusion in diatom biovolume counts. Laboratory experiments, however, have shown that even after moderate dissolution a strong relationship should remain between wet-alkaline BSi measurements and diatom concentrations (Ryves *et al.*, 2001). While a variable BSi/diatom biovolume relationship, such as that observed in Figures 40 and 42, might be expected if diatom dissolution varied over time, results from Morley (2005) show dissolution to be low/moderate over the analysed interval at Vydrino Shoulder with no significant change in dissolution after 2.2 kyr BP. Dissolution is also relatively constant at Continent Ridge (*pers. comm.* Rioual, 2006). In Chapter 8, which examines the glacial BSi record from Lake Baikal and where diatom preservation is extremely poor, it is shown that the BSi/diatom biovolume relationship can break down in instances of extremely high diatom dissolution. However in the samples analysed here, which are marked by only low to moderate diatom dissolution, dissolution can tentatively be ruled out as a dominant control on the BSi/diatom biovolume relationship.

Based on the above, large deviations in the BSi/diatom biovolume relationship may be attributable to the relative inaccuracies of wet-alkaline BSi techniques to obtain both accurate and precise records of the true amount of BSi within an aquatic sediment sample. Whist some of the residual errors in the BSi/diatom biovolume relationship can be attributed to rarer taxa not being included in the diatom biovolume calculations, the possible extent to which this may have distorted the BSi/diatom biovolume relationship is likely minimal. A key assumption of wet-alkaline BSi measurements is that concentrations inherently accounts for variations in the size and biovolume of diatoms and other forms of BSi within the sediment. Evidence here that large

residual errors exist in the BSi/diatom biovolume relationship, however, indicates that this may not be true, at least in the late-glacial/Holocene aged material analysed here from Lake Baikal. This is unfortunate as wet-alkaline based BSi measurements require significantly less analytical time than diatom biovolume analysis. On the one hand, the magnitude of the residual BSi errors observed here of up to 10 wt.% as SiO_2 are not significantly greater than the between laboratory reproducibility achieved in the inter-laboratory comparison study of Conley (1998) for samples containing >30 wt.% as SiO_2. However, such errors are significant given that the majority of BSi concentrations analysed here over the late glacial and Holocene interval only contain 10-20 wt.% as SiO_2. As such, residual errors of up to 10 wt.% as SiO_2 are highly relevant when attempting to use wet-alkaline measurements of BSi to reconstruct and distinguish marked changes in diatom productivity and so palaeoenvironmental and palaeoclimatic events. For example, over glacial-interglacial cycles BSi concentration vary by 20-30 wt.% as SiO_2. (Granina *et al.* 1993; Colman *et al.* 1995, 1999; Williams *et al.* 1997). Errors of 10 wt.% as SiO_2 therefore approximate to between a third and a half of the total BSi interglacial-glacial variability in Lake Baikal. Even at the lower end of the observed residual errors, an uncertainty of c. 5 wt.% as SiO_2 still represents a significant proportion of the BSi glacial-interglacial variability in Lake Baikal, as well as a significant proportion of the variability within individual glacial and interglacial periods. Whilst results here indicate the unsuitability of using wet-alkaline measurements of BSi for quantitative palaeoenvironmental reconstructions in Lake Baikal, further tests are required at other marine and lacustrine sites and over other time intervals in order to fully assess the validity of these findings. As a first step towards this, the nature of wet-alkaline derived BSi records is examined further in Chapter 8 on glacial aged sediments from Lake Baikal.

7.5. Conclusions

Within Chapter 6, it was demonstrated that a sequential Si/Al methodological may result in more accurate wet-alkaline BSi measurements by directly accounting for digested levels of non-BSi. Here in Lake Baikal, no significant difference is detected between the sequential Si/Al and Si/time methodologies. This is attributed to the low concentrations of Al which are digested from the late-glacial/Holocene samples analysed here during the alkaline extraction. In contrast, material during full glacial conditions, from MIS 2 to MIS 4, indicates significantly higher levels of aluminosilicate digestion. Although results here do not advocate one wet-alkaline BSi method over another, given the potential for significant aluminosilicate digestion to occur and given that the amount of aluminosilicate digestion is not known in advance, the sequential Si/Al method should remain preferable to use when attempting to minimise any errors for wet-alkaline based measurements of BSi.

Despite these considerations, however, and whilst previous studies from Lake Baikal have

demonstrated strong links between diatom populations and wet-alkaline derived BSi concentrations (Qui *et al.*, 1993; Colman *et al.* 1995, 1999; Williams *et al.* 1997), results here suggest that wet-alkaline measurement of BSi are not capable of accurately documenting changes in diatom/siliceous fossil populations within sediment samples. While wet-alkaline measurements of BSi possess many advantages, including the ease and rapidity with which samples can be analysed, it is suggested that they may only be suitable for obtaining quick qualitative indications of major stratigraphical changes in BSi/palaeoproductivity. Instead it is proposed that more time consuming, but ultimately more accurate, diatom taxonomic counts and biovolume calculations are better suited for generating quantitative estimates of BSi concentrations and estimates of palaeoproductivity in Lake Baikal over both long, glacial-interglacial, and shorter, millennial, timescales (e.g., Rioual *et al.*, 2005; Morley, 2005). Whist errors do exist in the use of diatom biovolumes, including the possibility for individual species biovolumes to change over time (Rioual, unpublished data), these issues are most likely minimal and should not significantly alter the BSi/diatom biovolume relationship or lead to the large residual errors observed in Figure 40.

Chapter 8: Impact of diatom dissolution on BSi concentrations in Lake Baikal

8.1. Introduction

As outlined in Chapter 7, wet-alkaline based measurements of Biogenic Silica (BSi) have been one of the most important proxies for determining the palaeoclimate history of Lake Baikal over glacial-interglacial cycles. Such measurements, are regarded to be a more practical measurement of the amount of palaeoproductivity in the sediment than diatom species/biovolumes due to the methods simplicity, significantly reduced analytical time and the presumption that BSi measurements account for variations in diatom frustule size and biovolume. While results in Chapter 7 highlighted a link between wet-alkaline BSi concentrations and diatom biovolume measurements over the late glacial/Holocene interval, significant residual errors existed in the BSi/diatom biovolume relationship (Fig. 40). As such, this suggests that wet-alkaline measurements of BSi may only be suitable for making qualitative, not quantitative, reconstructions of diatom productivity/palaeoenvironmental change within the lake. To further investigate this issue and to complement the research on the late glacial/Holocene interval in Chapter 6, here the validity of wet-alkaline BSi measurements is assessed on glacial aged sediments from Lake Baikal.

An increasingly recognised feature of glacial lacustrine and marine sediment sequences around the globe are the presence of abrupt climate events, such as Heinrich and/or smaller amplitude Dansgaard/Oeschger (D/O) events (Heinrich 1988; Dansgaard *et al.*, 1993). While well studied in marine cores, uncertainty remains over the climatic response of these events in continental regions, particularly at sites far from oceanic influences. Obtaining reliable information from such sites, such as Lake Baikal (Fig. 37), is important since their reduced oceanic control permits associations to be made to hemispheric climatic processes and their global teleconnections. Additionally, these sites provide information concerning the rates of environmental change during these events in addition to their impact and regional leads and lags.

As research in Lake Baikal increasingly shifts towards the detection of abrupt glacial climatic events, it becomes crucial to understand the validity of wet-alkaline BSi measurements analysed in these glacial aged sediments, particularly in relation to the prevailing hydrological and sedimentary environments. Studies at the Buguldeika Saddle (Fig. 37), a hemipelagic site of moderate sedimentation in the south basin dominated by input from the Selenga River, have shown an apparently strong relationship between wet-alkaline measured BSi and diatom concentrations in MIS 3 leading to the detection of Heinrich events 5-2 (Colman *et al.*, 1999; Prokopenko *et al.*, 2001 a,b). Recent studies on diatom valve dissolution (e.g., Ryves *et al.*, 2003; Battarbee *et al.*, 2005; Straškrábová *et al.*, 2005) warrant for further consideration, though, that increased diatom dissolution may have impacted the sedimentary and

palaeoclimatic record in Lake Baikal during glacials periods, distorting the sedimentary siliceous microfossil record. Here an investigation is undertaken into the glacial relationship between wet-alkaline derived BSi measurements and diatom biovolumes at Continent Ridge, a site of low sedimentation within Lake Baikal (Fig. 37). While Heinrich events have previously been detected at this site during MIS 3 using diatom concentrations (Swann *et al.*, 2005), no assessment has yet been made on the reliability of BSi measurements in detecting abrupt glacial climatic events at these slow accumulating sites where the influence of turbidites is minimal (Charlet *et al.*, 2005), but rates of diatom dissolution extremely high.

8.2. Methodology

Samples from MIS 3/early MIS 2 were taken from a 3.9 m Kasten core (CON01-603-5) collected from Continent Ridge in the north basin of Lake Baikal (see Fig. 37). Age models for core CON01-603-5 are based on palaeomagnetism and radiocarbon dating (see Swann *et al.*, 2005). Core integrity has been confirmed by reflection seismic survey and side scan sonar data (Charlet *et al.*, 2005). BSi concentrations were measured on one hundred samples following the wet-alkaline digestion technique detailed in Chapter 7. Due to the lower amounts of BSi within these glacial aged sediments, samples were digested using a 1% Na_2CO_3, rather than a 5% Na_2CO_3 solution as used in Chapter 7. This should also act to reduce the magnitude of any aluminosilicate digestion during the alkaline extraction, which as shown in Chapter 7 is significantly greater in full glacial-aged samples relative to late glacial/Holocene aged samples in Lake Baikal. Samples were periodically shaken during the alkaline extraction with aliquots analysed for dissolved Si and Al using a Perkin Elmer Optima 3300RL ICP-AES at Royal Holloway, University of London.

All samples selected for BSi analysis have previously been analysed for diatom concentrations (Swann *et al.*, 2005). All frustules included within the diatom calculations were also assigned into one of three dissolution stages in order calculate a Diatom Dissolution Index (DDI) following Flower and Likhoshway (1993) (Swann et al., 2005). As in Chapter 7, comparing the diatom concentrations of Swann *et al.* (2005) to wet-alkaline BSi measurements is problematic since diatom concentrations fail to consider variations in the size and mass of different taxa (Conley, 1988). Within Lake Baikal, the range of diatom taxa sizes are considerable. For example, the two common MIS 3 taxa of *Cyclotella* sp. cf. *gracilis* (Nikiteeva and Likhoshway) and *Cyclotella baicalensis* (Meyer) Skv. have approximate cell biovolumes of 340 μm^3 (calculated here) and 81500 μm^3 (Morley, 2005) respectively. Diatom biovolumes, providing a more accurate indicator of expected changes in BSi, were therefore calculated here for the dominant planktonic and other large taxa based on the diatom concentration data in Swann *et al.* (2005). Individual diatom species biovolume coefficients were primarily taken from existing values from the Kazantsevo interglacial (approximately corresponding to MIS 5e) and the late

glacial/Holocene sequences in Lake Baikal (Morley 2005; Rioual and Mackay 2005). Where required, biovolume coefficients for other taxa were calculated from the MIS 3-2 samples analysed here following Hillebrand *et al.* (1999). Ideally, all species biovolume coefficients would have been calculated from the analysed MIS 3-2 sediments. However, this was avoided as far as possible due to the high extent of diatom dissolution with these samples, which could have led to considerable errors in calculating both species and sample biovolumes. Only when diatom coefficients could not be calculated from other better preserved sediments, due to a species absence from the sediment record, were coefficients derived from the MIS 3-2 samples.

8.3. Results

Ideally, BSi measurements within this chapter would have been calculated using both the Si/time and the Si/Al method outlined in Chapters 6 and 7. However, Al concentrations in almost all sample aliquots here were below ICP-AES detection limits. This is attributable to the mistake of diluting samples with a 0.021 N HCl solution to prevent sample digestion, as suggested by Conley and Schelske (2001). For this reason, this stage was eliminated in the preceding Chapters 6 and 7. Due to the lack of Al data, all wet-alkaline BSi concentrations reported below refer to values calculated using the Si/time methodology (De Master 1979, 1981) as outlined in Chapter 6. The absence of Al data does not, however, detract from the interpretation and discussion of results within this chapter as Si/Al measurements result in either similar or lower estimates of BSi than the Si/time method (see Chapters 6 and 7). Below, this chapter highlights the presence of large increases in diatom biovolumes for which no corresponding large increase occurs in Si/time measurements of BSi. Consequently, the same features, i.e. the absence of large changes in wet-alkaline measured BSi, would be apparent even if Si/Al BSi concentrations had been successfully calculated. As such, the data interpretation and discussion is not affected by the absence of Al data for these samples.

Low BSi concentrations were observed in all samples from Continent Ridge (range: 0.0-2.2 wt.% as SiO_2) with fluctuations of 1.0-1.5 wt.% as SiO_2 throughout the MIS 3/2 interval (Fig. 43). Sample reproducibility based on sample replicates of the analysed material is 0.41 wt.% as SiO_2. Similar to the BSi record, diatom concentrations are also low throughout the sequence (< 1×10^7 valves/g dry wt) except from 53.3-51.5 kyr BP when concentrations increase from 0.056 $\times 10^7$ valves/g dry wt. to 3.026 $\times 10^7$ valves/g dry wt. (Fig. 43), reflecting a warm interval terminated by Heinrich event 5 (Swann *et al.*, 2005). Diatom biovolumes exhibit similar trends to those in the diatom concentration record with values from 53.3-51.5 kyr BP significantly higher at 110×10^9 μm^3/g dry wt. (Fig. 43). The DDI, however, indicates that over 99% of all diatom valves preserved in the sediment are affected by dissolution (Fig. 43, 44).

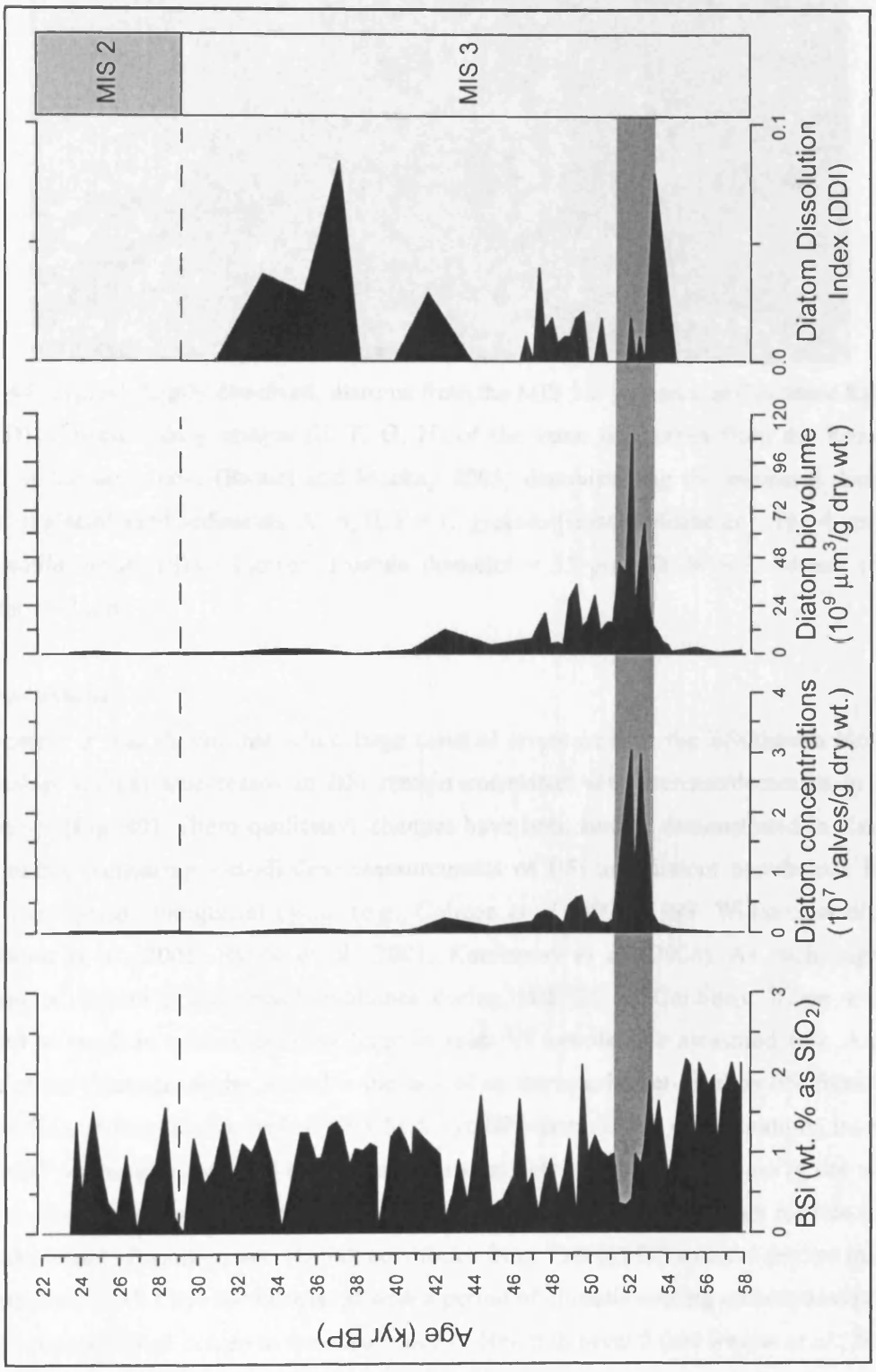

Figure 43: BSi measurements, diatom concentrations (Swann *et al.*, 2005), diatom biovolumes and Diatom Dissolution Index (DDI) at Continent Ridge, Lake Baikal during MIS 3/2. No relationship exists between BSi and diatom concentrations/biovolumes from 53.3-51.5 kyr BP (shaded) suggesting that measurements of BSi are not recording the glacial millennial-scale changes reflected in the diatom record.

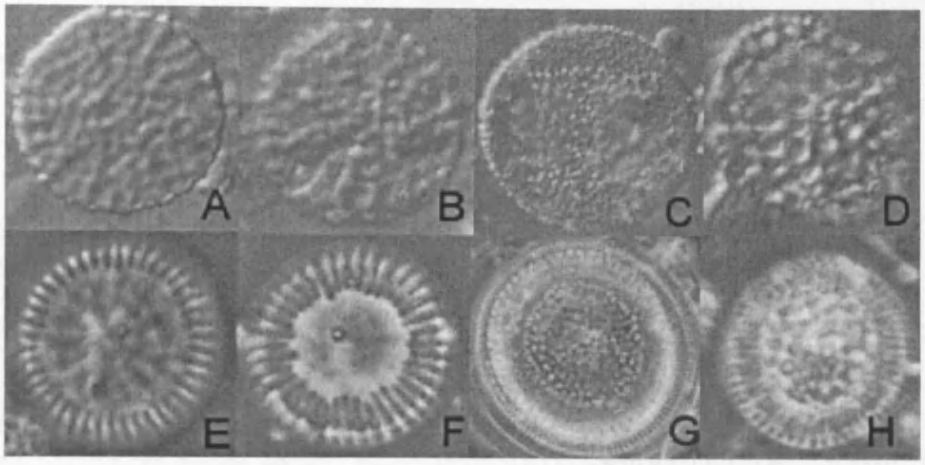

Figure 44: Typical, highly dissolved, diatoms from the MIS 3/2 sequence at Continent Ridge (A, B, C, D). Corresponding images (E, F, G, H) of the same taxa taken from the Kazantsevo section of the same core (Rioual and Mackay 2005) demonstrating the increased dissolution present in glacial aged sediments. A, B, E, F = *C. gracilis* (frustule diameter = 10-14 μm); C, G = *Cyclotella ornata* (Skv.) Flower (frustule diameter = 35 μm); D, H = *C. minuta* (frustule diameter = 12 μm).

8.4. Discussion

In Chapter 7 it was shown that while large residual errors exist in the BSi/diatom biovolume relationship, increases/decreases in BSi remain correlated with increase/decreases in diatom biovolumes (Fig. 40). These qualitative changes have been further demonstrated in a range of other studies comparing wet-alkaline measurements of BSi and diatom populations in Lake Baikal over glacial-interglacial cycles (e.g., Colman *et al.*, 1995; 1999; Williams *et al.*, 1997; Khursevich *et al.*, 2001; Ryves *et al.*, 2001; Karabanov *et al.*, 2004). As such, significant increases in diatom populations/biovolumes during MIS 3/2 at Continent Ridge would be expected to result in a corresponding large increase in wet-alkaline measured BSi. A notable feature of the Continent Ridge record is the lack of an increase in wet-alkaline BSi from 0.9-1.5 wt.% as SiO_2 during the interval at 53.3-51.5 kyr BP when diatom concentrations increase to 3.026 x 10^7 valves/g dry wt. and biovolume measurements rise to 110 x 10^9 μm^3/g dry wt. (Fig. 43). The absence of a wet-alkaline BSi increase is significant since the diatom records suggests the sudden onset of warmer, interstadial, conditions from 53.3 kyr BP with the decline in diatom concentrations at 51.5 kyr BP associated with a period of climatic cooling and expansion of ice-cover/thickness, linked in turn to the occurrence of Heinrich event 5 (see Swann *et al.*, 2005). In contrast, the wet-alkaline BSi record does not display or indicate the presence of any of these millennial-scale changes.

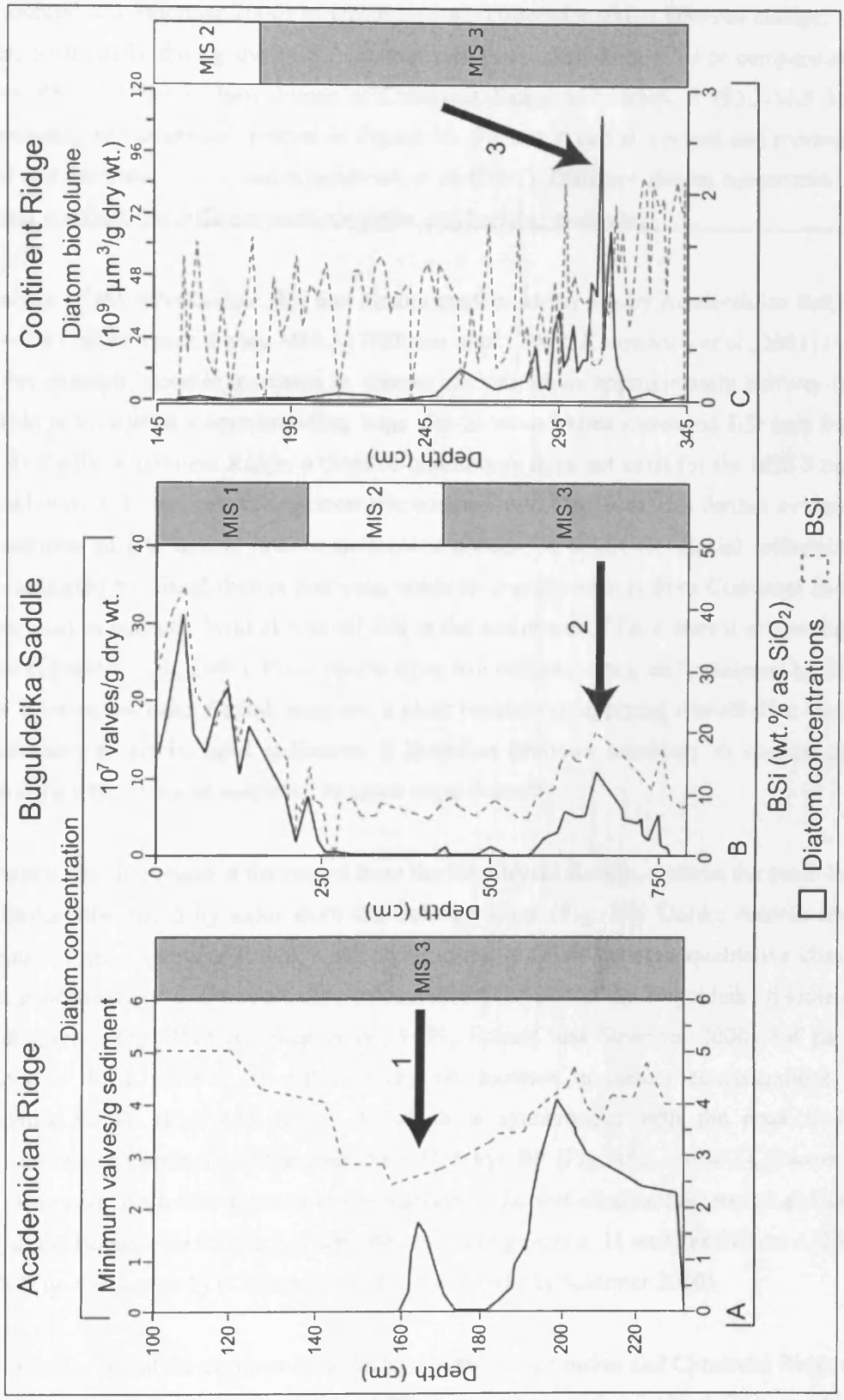

Figure 45: A) Wet-alkaline BSi and diatom concentrations from the Academician Ridge during MIS 3 (Williams *et al.*, 1997; Khursevich *et al.*, 2001). As at Continent Ridge, BSi does not increase when diatom concentrations increase significantly (arrow 1). B) Wet-alkaline [Cont...]

BSi and diatom concentrations from the Buguldeika Saddle during MIS 3-1 (Colman *et al.*, 1999; Edlund and Stoermer 2000) in which a strong correlation exists between changes in both proxies, particularly during the MIS 3 diatom rich phase (arrow 2). C) For comparison, wet-alkaline BSi and diatom biovolumes at Continent Ridge with arrow 3 (53.3-51.5 kyr BP) corresponding to the shaded interval in Figure 43. Figures A and B, revised and redrawn from Edlund and Stoermer (2000) and Khursevich *et al.* (2001). Different diatom concentration units for A and B reflect the different methodologies employed at each site.

Re-analysis of the wet-alkaline BSi and diatom profiles at the nearby Academician Ridge (Fig. 37) reveals similar trends during MIS 3 (Williams *et al.*, 1997; Khursevich *et al.*, 2001) (see Fig. 45a). For example, notable increases in diatom concentrations approximately halfway through MIS 3 do not result in a corresponding large rise in wet-alkaline measured BSi (see Fig. 45a: arrow 1). Unlike Continent Ridge, a detailed chronology does not exist for the MIS 3 record at the Academician Ridge, preventing inter-site comparisons. However, this further evidence that measurements of BSi appear unable, in some instances, to detect the glacial millennial-scale events indicated by visual diatom analyses, confirms that the results from Continent Ridge are not restricted to one site. With almost all BSi in the sediments of Lake Baikal originating from diatoms (Granina *et al.*, 1992), these results from two different sites, each analysed by different groups working on Lake Baikal, suggests a clear problem in applying wet-alkaline based BSi measurements to glacial aged sediments. It therefore becomes necessary to suggest possible mechanisms which may be operating to cause these features.

Important to the discussion is the record from the Buguldeika Saddle, a site in the south basin of Lake Baikal dominated by input from the Selenga River (Fig. 37). Unlike records from the Academician and Continent Ridge, a strong relationship exists between qualitative changes in diatom concentrations and wet-alkaline measurements of BSi at the Buguldeika Saddle during the last glacial (Fig. 45b) (Colman *et al.*, 1999; Edlund and Stoermer 2000). Of particular relevance is the c. 10.0 x 10^7 valves/g dry wt. increase in diatom concentrations at the Buguldeika Saddle (Fig. 45b, arrow 2) which is synchronous with the peak in diatom concentrations at Continent Ridge from 53.3-51.5 kyr BP (Fig. 45c, arrow 3) (Swann *et al.*, 2005). However, while this interval is not marked in the wet-alkaline BSi record at Continent Ridge, at the Buguldeika Saddle it is with BSi increasing from c. 11 wt.% as SiO_2 to c. 20 wt.% as SiO_2 (Fig. 45b, arrow 2) (Colman *et al.*, 1999; Edlund and Stoermer 2000).

One possibility is that the dominant diatom taxa at the Academician and Continent Ridge during the periods of high diatom production in MIS 3 are only weakly silicified. This would act to significantly reduce the amount of BSi within individual diatom frustules. At Continent Ridge samples from 53.3-51.5 kyr BP are dominated by *C.* sp. c.f. *gracilis* (63% abundance), an

extinct endemic species about whose ecology little is known. However, the simultaneous rise in diatom and wet-alkaline BSi concentrations at the Buguldeika Saddle, where a good BSi/diatom relationship exists (Fig. 45b, arrow 2), is also almost entirely related to increases in *C. gracilis*, which is almost certainly the same as the *C.* sp. c.f. *gracilis* observed at Continent Ridge (Swann *et al.*, 2005), with no other notable changes in individual diatom taxa concentrations (Edlund and Stoermer 2000). Consequently, *C. gracilis* is not likely to be weakly silicified. Similarly, the diatom sequence at the Academician Ridge during MIS 3 is dominated by *Aulacoseira baicalensis* (Meyer) Simonsen and *C. baicalensis*, both of which are also known not to be weakly silicified (Battarbee *et al.*, 2005).

The Academician Ridge, Continent Ridge and Buguldeika Saddle are all situated at similar water depths, 321-375 m, suggesting that sinking times to the sediment-water interface at each sites are approximately constant. Sedimentation rates, though, are markedly higher during MIS 3 at the Buguldeika Saddle (12.5 cm/kyr) compared to the Academician (c. 4.0 cm/kyr) and Continent Ridge (5.7 cm/kyr) (Prokopenko *et al.*, 2001a,b,c; Swann *et al.*, 2005). Differences in sedimentation rate alone, however, can not explain the differences in the BSi/diatom records since sedimentation rates are relatively constant at individual sites over glacial-interglacial cycles and highly correlated BSi/diatom population relationships have been documented at the Academician Ridge and the Buguldeika Saddle during interglacials (Williams *et al.*, 1997; Colman *et al* 1999; Edlund and Stoermer 2000; Khursevich *et al.*, 2001).

A more likely explanation for the discordant BSi/diatom trends at the Academician Ridge and Continent Ridge during MIS 3 may lie in the high degree of diatom dissolution in Lake Baikal. Dissolution is a predominant feature in Lake Baikal with only c. 1% of all living diatoms incorporated into the sedimentary record (Ryves *et al.*, 2003). In interglacials, diatom dissolution is moderate. For example, over the last 1000 years 40-60% of sedimentary valves in Lake Baikal are affected by some form of dissolution (Mackay *et al.*, 1998) while at Continent Ridge 60-90% of valves are affected by dissolution in the Kazantsevo interglacial (DDI = 0.1-0.4) (Rioual and Mackay 2005). Conversely the MIS 3/2 Continent Ridge DDI record, which to date is the only quantitative dissolution record available for glacial sediment within the lake, suggests that dissolution is significantly higher with c. 99% of frustules subjected to some form of dissolution (DDI = 0-0.1) and over 90% of all valves "heavily dissolved" (see Fig. 43, 44, and Swann *et al.*, 2005).

Diatom dissolution today in Lake Baikal predominantly occurs at the sediment-water interface for most species (Ryves *et al.*, 2003). It is therefore likely that during glacials, dissolution also mainly occurred here. It also follows that at slower sedimentation sites the potential for diatom dissolution and/or grazing by benthic organisms is greater due to the increased duration spent by

diatoms at the interface before burial. As such, during glacials it is possible the increased duration spent by diatoms at the sediment-water interface may have become a critical factor at slow sedimentation sites such as Continent Ridge and the Academician Ridge. This would have been marked by a relative increase in the amount of diatom dissolution, compared to interglacials, which would have increased the removal of diatom bound silica from the sedimentary record. Consequently, while microscopy based diatom counts are able to accurately document changes in sedimentary diatom concentrations, the removal of silica from diatom frustules would at the same time prevent or severely inhibit such changes being detected by wet-alkaline BSi measurements. Such a process would explain why the wet-alkaline BSi record is muted at both Continent Ridge, from 53.3-51.5 kyr BP (Fig. 43), and at the Academician Ridge (Fig. 45a: arrow 1). In contrast, the higher sedimentation rates at the Buguldeika Saddle during MIS 3 suggests that burial rates there were sufficiently high during the last glacial to prevent excessive diatom dissolution/BSi removal, resulting in the observed strong BSi/diatom relationship (Fig 4b). While issues of dissolution have previously been ruled out as having a significant impact on the wet-alkaline BSi record when dissolution is low to moderate (Ryves *et al.*, 2001), it is suggested that this does not hold for samples, such as those analysed here at Continent Ridge, were diatom dissolution is extremely high (Fig. 43, 44).

Several mechanisms might lead to higher relative diatom dissolution at slower accumulating sites such as Continent Ridge during glacials, relative to interglacials. Temperature is unlikely to play a major role as glacial bottom water temperatures are unlikely to alter significantly over glacial-interglacial cycles. Instead the role of biological processes on diatom dissolution is emphasised. Recent work has highlighted the role of bacterial action in aiding diatom dissolution by removing the protective layer of organic coating surrounding the frustules and thereby preparing the valve for chemical dissolution (Bidle and Azam 1999; Bidle *et al.*, 2002; 2003). Similarly other grazers, including zooplankton, also selectively remove diatom organic coatings leading to higher diatom dissolution (e.g., Cowie and Hedges 1996). Within Lake Baikal, microbial activity has also been observed (Kuznetsov 1951; Kozhova and Kazantseva 1961), including the presence of saprophytic bacteria in the deepest waters (Straškrábová *et al.*, 2005). The fully oxygenated water column of Lake Baikal also permits many benthic faunal communities such as amphipods to survive at the sediment-water interface feeding on organic matter. Studies have also shown that modern faunal communities in Lake Baikal have prevailed through at least the Quaternary (Sherbakov 1999). Therefore, although populations may have been lower during glacial periods, rates of biological attack may have continued but perhaps at a higher relative intensity due to the lower numbers of diatoms in the water column. It is therefore suggested that during glacials, diatoms reaching the sediment-water interface are more intensively acted upon by biological communities, relative to interglacials, leading to the highly dissolved diatom frustules which characterise glacial sequences, such as at Continent Ridge

(Fig. 44). In contrast at high accumulation sites as the Buguldeika Saddle, while a relative increase in biological action on diatoms may also have taken places, the faster accumulating sediments at these sites would have limited the time spent by diatoms at the sediment-water interface, resulting in better preservation and hence a stronger BSi/diatom relationship (Fig. 45b, arrow 2). In agreement with Carter and Colman (1994) therefore, "diatom barren" glacial sequences in Lake Baikal may reflect lower production, combined with sustained and more intensive diatom dissolution, rather than an extinction or retreat of diatoms to shallow-water refugia as suggested by Karabanov *et al.* (2004).

8.5. Conclusions

Wet alkaline measurements of BSi have been a fundamental proxy in establishing Lake Baikal's palaeoenvironmental history over glacial-interglacial cycles. Results and re-analysis of existing data, though, indicates no relationship between wet-alkaline BSi measurements and diatom concentrations over glacial millennial-scale events at two slow sedimentation sites (Fig. 45a, c). This is most likely due to a relative increase in diatom dissolution at slower sedimentation sites in glacials, removing diatom bound BSi from the sedimentary record (Fig. 44). This contrasts with results from the Buguldeika Saddle where sedimentation rates are significantly higher (Fig. 45b), suggesting that site selection and characteristics are important factors in determining whether wet-alkaline derived BSi measurements will display glacial millennial-scale events. Despite the increased analytical time involved, such changes in Lake Baikal may instead be best identified using diatom biovolume measurements rather than wet-alkaline measurements of BSi. This is important given the need for further work in Lake Baikal to address and understand glacial palaeoclimatic conditions and the teleconnections which appear to have prevailed between Europe and central Asia during these periods (see Prokopenko *et al.*, 2001a,b; Swann *et al.*, 2005). The use of diatom biovolume measurements in Lake Baikal is further reiterated in light of results in Chapter 7, which highlights large residual errors between wet-alkaline measurement of BSi and diatom biovolume concentration even when diatom dissolution is not significant.

Chapter 9: Conclusions and further research

9.1. Summary of findings

The aim of the research carried out in this thesis was twofold. The first was to assess the potential of using records of $\delta^{18}O_{diatom}$ in palaeoceanographic reconstructions as a means of increasing the number of biologically derived $\delta^{18}O$ records from high latitude regions. This was assessed at ODP Site 882 in the North West Pacific Ocean, a site at which both carbonates and diatoms are preserved within the sediment record. Particular aims within the thesis included developing methodologies for extracting pure, mono-specific diatoms from marine sediment samples, investigating the extent to which vital effects may be present in $\delta^{18}O_{diatom}$ and assessing the potential of $\delta^{18}O_{diatom}$ in palaeoceanographic reconstructions. The second part of the PhD was aimed at assessing the accuracy of wet-alkaline derived BSi measurements and the extent to which such measurements can be used in marine and lacustrine sequences to obtain information on the global silicon cycle. The sub-sections below summarise the extent to which these objective where achieved and the contribution of this research to the academic community. Finally, in Section 9.2 an assessment is made as to the current state of $\delta^{18}O_{diatom}$ and BSi research as well as the future research directions that are required within these areas.

9.1.1. Diatom extraction/preparation

Chapter 2 presented a method for extracting pure, near species specific, diatom frustules for isotope analysis from marine sediment samples that are both relatively rich and depleted in diatom microfossils. While heavily based upon existing methodologies (e.g., Morley *et al.*, 2004), the method demonstrated the importance of analysing the size range of individual taxa under a microscope in order to identify size fractions which would minimise species diversity within the extracted samples. This approach contrasts with previous studies which have focused on only extracting and analysing bulk diatom species samples for isotope analysis. In addition, the method also emphasises the importance of calculating the relative diatom species biovolumes in the final extracted sample as a means of identifying the relative contribution of individual taxa to a $\delta^{18}O_{diatom}$ measurement.

9.1.2. Diatom isotope vital/species effects

Chapters 2 and 3 demonstrated the presence of large $\delta^{18}O_{diatom}$ offsets between different size fractions of diatom over two time intervals at ODP Site 882 in the North West Pacific Ocean: 2.86-2.56 Ma and the last 200 kyr. In almost all instances, the offsets were significantly greater than the combined RMSE (Root Mean Squared Error) of the two size fractions. However, due to the multiple factors and different processes which may be contributing towards the offsets, and given that the mechanisms behind the fractionation of oxygen into diatoms remain relatively poorly understood, it is not currently possible to ascertain the precise mechanisms controlling the offsets. While these offsets are referred to as a species effect, due to isotopic equilibrium not

being known, these offsets may reflect an isotope vital effect in $\delta^{18}O_{diatom}$. In Chapter 2, 2.84-2.57 Ma, with the smaller 75-150 μm fraction having a higher $\delta^{18}O_{diatom}$ value than the >150 μm fraction at almost all levels (Fig. 11), the offset is concluded to reflect a possible size-related effect in $\delta^{18}O_{diatom}$. While Schmidt *et al.* (2001) suggested that differences in diatom growth rates may lead to differences in diatom oxygen isotope fractionation, no evidence of such a process could be distinguished here. The highly variable nature of the $\delta^{18}O_{diatom}$ offsets (mean = 1.23‰, max = 3.51‰), may also indicate that other processes, such as an inter-species effect, are also contributing to the offsets. In contrast to the size-related effect identified in Chapter 2, $\delta^{18}O_{diatom}$ offsets within Chapter 3 are highly variable with frequent changes in the direction of the isotope offsets (Fig. 16). Again the precise mechanisms causing these offsets is not known. However, evidence indicates that the offsets are not related to a seasonality or habit effect. The frequent changes in the direction of the offsets also makes it clear that the offsets are not dominated by a size effect similar to that present in Chapter 2. This raises the possibility that the offset documented in both Chapters 2 and 3 may be caused by a series of processes, the relative importance of which can vary over time. Possible factors which fall into this category include the effects of nutrient availability, growth rate, silica maturation and inter/intra-species and size-related vital/species effects.

Given the difficulties within this PhD in identifying the mechanisms/processes behind these offsets, an inherent problem when working with palaeoenvironmental data, there is a clear need for further laboratory culture, core top and water column experiments to better understand inter- and intra-species variations in the fractionation of oxygen into diatoms. In addition, since the role of silica maturation associated secondary isotope exchange remains a possible factor in contributing to the offsets, further research is also required into inter- and intra-species variations in the magnitude of secondary isotope exchange in diatoms. In the interim, the detection of large isotope offsets between different size fractions and possibly different diatom taxa has significant future implications for research involving $\delta^{18}O_{diatom}$. In contrast to existing $\delta^{18}O_{diatom}$ studies, which are often associated with analysing bulk diatom samples comprised of multiple taxa, here it is shown that there is a clear need for future studies to consider in detail the diatom species composition of samples analysed for $\delta^{18}O_{diatom}$. As such, future palaeoenvironmental studies using $\delta^{18}O_{diatom}$ need to focus on extracting and only analysing single species samples over a finite size range. In addition, the extracted taxa need to be focused towards blooming over a single season or period of time, within which photic zone environmental conditions are relatively constant, in order to eliminate any seasonality effect. While seasonality effects are shown in Chapter 2 and 3 to not be a significant issue within the $\delta^{18}O_{diatom}$ samples analysed here, it remains wise to minimise their impact as far as possible in all future studies. Such work, while difficult, may well be essential in further progressing $\delta^{18}O_{diatom}$ research and minimising both the analytical and interpretational errors often associated with

$\delta^{18}O_{diatom}$ based measurements

9.1.3. Diatom isotopes in palaeoceanographic reconstructions

The potential of using $\delta^{18}O_{diatom}$ in palaeoceanographic reconstructions is assessed in Chapters 4 and 5 at ODP Site 882. These chapters, for the first time, highlight the clear potential in using records of $\delta^{18}O_{diatom}$ in the North Pacific Ocean, provided that the issue of vital/species effects demonstrated in Chapters 2 and 3 can be avoided. Furthermore, they highlight the ability for $\delta^{18}O_{diatom}$ to both complement and extend the multitude of existing biological $\delta^{18}O$ records, predominantly foraminifera $\delta^{18}O$ records from mid and low latitude regions, into high latitude regions. Chapter 4 analysed $\delta^{18}O_{diatom}$ over the onset of major NHG. In conjunction with other proxy data including benthic and planktonic records of $\delta^{18}O_{foram}$, magnetic susceptibility, opal/diatom accumulation rates and U^{K}_{37}, it was shown that a significant freshening and warming of the surface waters occurred at 2.73 Ma, resulting in the development of a halocline driven stratified water system (Fig. 21:). In conjunction with model work in Haug *et al.* (2005), these changes caused the region to act as a major moisture source for Northern America. With *C. radiatus* and *C. marginatus* both primarily blooming during the autumn/early winter months, the results further suggest the warm pool of surface water in the region, and hence the moisture supply to the North American continent, would have continued into the winter months at the time most favourable for glacial growth.

Chapter 5 analysed the palaeoceanographic changes at ODP Site 882 over the last 200 kyr, covering the last two glacial cycles. In contrast to almost all previous studies, which argue for a constantly stratified system in the region from at least the last glacial onwards (Keigwin *et al.*, 1992; Sancetta, 1983; Jaccard *et al.*, 2005; Brunelle *et al.*, 2007), evidence was found to suggest that at least four intervals of unstratified conditions existed in the past (Fig. 27). Furthermore, these changes appear concomitant with changes in atmospheric CO_2 concentrations, as recorded in the Vostok ice core (Fig. 30) (Anklin *et al.*, 1997; Petit et al., 1999). As detailed below, further work is required to fully evaluate the spatial representativeness of this signal across the North Pacific Ocean. In addition, work is also required to improve the temporal resolution of this record and to establish a direct record of changes in surface water pCO_2. Without this, both the forcing mechanisms for these stratification changes and the contribution of the region towards changes in global concentrations of atmospheric CO_2 will remain unknown. However, based on the available evidence, it appears that the North Pacific Ocean may act as an important region for further understanding past changes in atmospheric CO_2 over both glacial-interglacial and millennial timescales.

Based on this demonstration with regards to the potential in using records of $\delta^{18}O_{diatom}$, it is reasonable to assume that the number of studies using $\delta^{18}O_{diatom}$ in palaeoceanographic studies

will increase over the next decade, particularly at sites where single species diatom samples can be easily extracted. This is likely to be furthered by the development of analytical procedures which require smaller numbers of diatom frustules for $\delta^{18}O$ analysis. An interesting finding of this thesis is the contrast between records of $\delta^{18}O_{diatom}$, which displays changes of up to 14‰, and the more muted records of planktonic $\delta^{18}O_{foram}$ over the same intervals (e.g., Figure 21: in Chapter 3 and Figure 24 in Chapter 4). On the basis of modern day water column studies, this is most likely attributable to the planktonic foraminifera living below the stratification boundary and away from the uppermost sections of the water column. As such records of $\delta^{18}O_{diatom}$ should be viewed, at least in the North Pacific Ocean, not only as a substitute to records of planktonic $\delta^{18}O_{foram}$, but also as a possible improvement due to the ability for $\delta^{18}O_{diatom}$ to provide more direct insights into actual surface water conditions and palaeoceanographic changes.

9.1.4. Biogenic Silica

It was expected that research within this thesis would further verify the validity of using BSi measurements in palaeoenvironmental research whilst also establishing the advantages of a Si/Al sequential extraction approach over a Si only methodology for measuring BSi. This is important as wet-alkaline measurements of BSi may provide valuable insights into the global silicon cycle, and so complement records of $\delta^{30}Si_{diatom}$. In Chapter 6 it was shown that clear potential exists in using a Si/Al approach over a Si only methodology. For samples in which relatively large amounts of Al were digested during the alkaline extraction, significant differences were observed between the Si/Al and Si only methodologies (Table 13). Given that the Si/Al methodology is able to more directly account for levels of non-BSi, i.e., clay/aluminosilicate digestion, it is proposed that the lower BSi values achieved with the Si/Al method represent an improved and more accurate estimate of the true amount of BSi within a sediment sample.

Evidence within Chapters 7 and 8, however, casts significant uncertainty over the future use of wet-alkaline BSi measurements in palaeoenvironmental research, regardless of the methods employed. In Chapter 7, comparisons between measurements of BSi (both Si/Al and Si/time) and records of diatom biovolume concentrations in Lake Baikal, which can be regarded to represent a more accurate indicator of the true amount of BSi within an analysed sample, indicate a poor relationship between the two variables with large residual errors (Fig. 40). As such, significant problems exist not only in the accuracy and reliability of wet-alkaline BSi measurements, but also in their suitability for documenting quantitative changes in diatom populations and associated shifts in the local silicon cycle.

Chapter 8 further highlighted the problem of wet-alkaline BSi concentrations in samples which are affected by extremely high levels of diatom dissolution. In the case of glacial aged samples

in Lake Baikal, it was found that significant diatom dissolution results in the scourging of silica from diatom frustules (Fig. 44). This in turn leaves behind only the highly dissolved remains of the diatom frustule in the sediment record, which can only be "measured" and accounted for through microscope based diatom biovolume observations, not by geochemical methods. As such, while diatom biovolume measurements document a series of large millennial scale climatic and environmental events during MIS 3, the wet-alkaline BSi records does not show any of these changes (Fig. 43). Based on this, and despite the increased analytical time involved, it is concluded that palaeoclimatic and palaeoenvironmental investigations into the silicon cycle and changes in diatom/BSi palaeoproductivity are best carried out using diatom biovolume concentrations rather than wet-alkaline measurements of BSi.

9.2. Further work

Based on the summaries of the PhD research highlighted above, several lines of future work can be identified:

1) A clear need exists for culture, sediment core top and water column studies to assess the extent to which vital/species effects exist within $\delta^{18}O_{diatom}$ in both marine and lacustrine systems. While Chapter 2 and 3 demonstrated significant isotope offsets between different size fractions of diatoms, it was not possible to determine the controlling mechanisms. This needs to be complemented by experiments to assess the extent to which inter- and intra-species variations exist in diatom hydroxyl layer thickness. Since diatom biovolume measurements on the unreacted purified sample provides important information on the contribution of individual taxa to a $\delta^{18}O$ measurement, it is crucial to ascertain whether corrections are required to account for variations in hydroxyl layer thickness. Without this, it may prove difficult to account for possible inter- and intra-species isotope effects in mixed taxa samples.

2) The greatest remaining uncertainty over the use of $\delta^{18}O_{diatom}$ in palaeoenvironmental reconstructions concerns the presence of silica maturation and secondary isotope exchange within diatoms. In particular, it precise operation and impact remains unknown with very little/no understanding as to inter- and intra-species variation in its magnitude and the processes which may cause changes in its magnitude. Further work to investigate this issue needs to determine the fractionation factor for secondary isotope exchange so that, if required, attempts can be made to correct for the possible effects of silica maturation on records of $\delta^{18}O_{diatom}$.This work is likely to be particularly critical in marine systems where large differences in $\delta^{18}O_{water}$ can exist between the surface and sub-surface waters. Whilst evidence in Chapters 2-5 points towards issues of secondary isotope exchanges as not being a significant factor at ODP Site 882,

further work on this issue is likely to ultimately control whether future records of $\delta^{18}O_{diatom}$ at other sites can be used to derive robust quantitative, as opposed to qualitative, palaeoenvironmental reconstructions.

3) Palaeoceanographic reconstructions in Chapters 4 and 5 were affected by the uncertainty over the true $\delta^{18}O_{diatom}$-temperature coefficient in marine systems. Whilst strong evidence exists that a coefficient of −0.2‰/°C applies to lacustrine systems (Brandriss et al., 1998; Moschen et al., 2005), in marine systems values range from c. −0.3‰/°C to −0.5‰/°C (Juillet-Leclerc and Labeyrie, 1987; Shemesh *et al.*, 1992). Within this thesis, separate calculations using coefficients of −0.2‰/°C and −0.5‰/°C were performed for each separate reconstruction. In order to reduce the errors associated with using $\delta^{18}O_{diatom}$ in future palaeoceanographic studies, it is necessary to resolve this issue. Water and modern diatom samples are being collected in a cruise across the North Pacific Ocean in collaboration with Jonaotaro Onodera (Kochi University, Japan) in late summer/autumn 2007. It is hoped that analysis of these samples will provide a solution to this issue.

4) Within the context of Chapter 4 covering the onset of major NHG at ODP Site 882, further work is required to improve the temporal resolution of the $\delta^{18}O_{diatom}$ record after 2.67 Ma in order to assess the stability and changes in the halocline stratification during the glacial-interglacial cycles that follow the onset of major NHG. At present, large changes in $\delta^{18}O_{diatom}$ are observed after 2.67 Ma (Fig. 21:) but their significance can not be fully evaluated in the absence of additional data. Attempts to resolve this during the PhD failed, due to the difficulties in extracting sufficiently clean diatom material for isotope analysis over this interval.

   It is also important to obtain a spring based $\delta^{18}O_{diatom}$ record from ODP Site 882. This would significantly complement the autumn/early winter record presented in Chapter 4 and further aid interpretation of the spring planktonic $\delta^{18}O_{foram}$ record. At present, measurements of planktonic $\delta^{18}O_{foram}$ over the onset of major NHG at ODP Site 882 indicate a significant decrease in SST (Maslin *et al.*, 1995; 1996). However, since it remains possible that the analysed foraminifera may have been living below the halocline boundary, a spring $\delta^{18}O_{diatom}$ record is required to fully evaluate changes in the region during the spring months. Attempts to do this during the PhD by analysing $\delta^{18}O_{diatom}$ in the smaller, primarily spring blooming, <75 μm size fractions were compromised by the presence of multiple taxa and large fragments of broken >75 μm autumn blooming taxa (*C. radiatus* and *C. marginatus*). Future attempts to obtain a spring $\delta^{18}O_{diatom}$ record will include the use of a micro-manipulator, which will allow the extraction of a single, spring blooming, taxa sample for isotope analysis.

5) Evidence in Chapter 5 provided evidence of several changes in the stratification state of the North Pacific Ocean over the last 200 kyr. However, at present it is not possible, due to the low resolution nature of the $\delta^{18}O_{diatom}$ record, to establish the precise timing of these changes, their controlling mechanisms, the extent to which similar changes occurred over millennial timescales and the extent to which the changes observed at ODP Site 882 are representative of transitions across the wider North Pacific Ocean. Furthermore, given the existing low resolution nature of the $\delta^{18}O_{diatom}$ record, it is possible that other stratification changes occurred in addition to those identified in Chapter 5 (Fig. 27). As such, there is a need for a significant increase in the number of $\delta^{18}O_{diatom}$ measurements over this interval, both at ODP Site 882 and elsewhere across the North Pacific Ocean. In order to fully evaluate the implications of these inferred shifts in stratification state, it is also essential to obtain a direct record of surface water pCO_2. Given these needs, attempts are currently underway to increase the temporal resolution of the $\delta^{18}O_{diatom}$ record at ODP Site 882. In addition, an investigation is being planned to analyse $\delta^{30}Si_{diatom}$ (to assess changes in nutrient utilisation and silica acid input to the photic zone) in addition to the $\delta^{13}C$ of the included organic matter within diatoms and compound specific biomarkers in alkenones, in order to obtain a record of changes in surface water pCO_2.

6) Part 2 of the PhD provided strong evidence against the use of wet-alkaline BSi measurements in future palaeoenvironmental studies. While the Si/Al technique may produce more accurate measurements of BSi, results in Chapters 7 and 8 highlighted significant problems with regards to the accuracy and meaningfulness of these measurements. Instead, it was suggested that significantly more accurate records of diatom palaeoproductivity and insights into the silicon cycle could be achieved through microscope measurements of diatom biovolumes. This could be complemented in future work by the increased usage and development of $\delta^{30}Si_{diatom}$ as a palaeoenvironmental proxy, in instances where sufficient pure diatom material can be extracted. However, given the widespread usage of wet-alkaline BSi measurements in palaeoenvironmental investigations over the past 20 years, it would be unwise to dismiss the proxy on the basis of this study alone. As such, further studies are required across a range of other marine and lacustrine sites in order to fully evaluate the relationship between wet-alkaline measurements of BSi and microscope based measurements of BSi/diatom biovolumes.

References

Adams, J.M., Faure, H., Faure-Denard, L., McGlade, J.M., and Woodward, F.I. (1990) Increases in terrestrial carbon storage from the Last Glacial Maximum to the present. *Nature*, 348, 711–714.

Adkins, J.F., and Schrag, D.P. (2001) Pore fluid constraints on deep ocean temperature and salinity during the last glacial maximum. *Geophysical Research Letters*, 28: 771–774.

Anklin, M., Schwander, J., Stauffer, B., Tschumi, J., Fuchs, A., Barnola, J.M., and Raynaud, D. (1997) CO_2 record between 40 and 8 kyr BP from the Greenland Ice Core Project ice core. *Journal of Geophysical Research.* 102: 26539-26545

Antonov, J. I., Locarnini, R.A., Boyer, T.P., Mishonov, A.V., and Garcia, H.E. (2006) World Ocean Atlas 2005, Volume 2: Salinity. S. Levitus, Ed. NOAA Atlas NESDIS 62, U.S. Government Printing Office, Washington, D.C., 182 pp.

Barker, P.A. (1992) Differential diatom dissolution in Late Quaternary sediments from Lake Manyara, Tanzania. *Journal of Paleolimnology*, 7: 235-251.

Barker, P.A., Street-Perrot, F.A., Leng, M.J., Greenwood, P.B., Swain, D.L., Perrot, R.A., Telford, R.J. and Ficken, K.J. (2001) A 14,000-Year oxygen isotope record from diatom silica in two alpine lakes on Mt. Kenya. *Science*, 292: 2307-2310.

Barker, P.A., Leng, M.J., Gasse, F. and Huang, Y. (2007) Century-to-millennial scale climatic variability in Lake Malawi revealed by isotope records. *Earth and Planetary Science Letters*, 261: 93-103.

Barrera, E. and Johnson, C. (eds). 1999. Evolution of the Cretaceous ocean-climate system. Geol. Soc. Am. Special Paper 332, pp. 1–445.

Bartoli, G., Sarnthein M., Weinelt M., Erlenkeuser H., Garbe-Schönberg D., and Lea D.W. (2005). Final closure of Panama and the onset of northern hemisphere glaciation. *Earth and Science Planetary Letters*, 237: 33-44.

Battarbee, R.W., Mackay, A.W., Jewson, D., Ryves, D.B., and Sturm, M. (2005) Differential dissolution of Lake Baikal diatoms: correction factors and implications for palaeoclimatic reconstruction. *Global and Planetary Change*, 46: 75-86.

Beck, L., Gehlen, M., Flank, A.-M., Van Bennekom, J.A. and Van Beusekom, J.E.E. (2002) The relationship between Al and Si in biogenic silica as determined by PIXE and XAS. *Nuclear Instruments and Methods in Physics Research B*, 189: 180–184.

Bemis, B.E., Spero, H., Bijma, J., and Lea, D.W. (1998) Reevaluation of the oxygen isotopic composition of planktonic foraminifera: experimental results and revised paleotemperature equations, *Paleoceanography*, 13: 150-160.

Berger, A., and Loutre, M.F. (1991), Insolation values for the climate of the last 10 million years, *Quaternary Sciences Review*, 10: 297-317.

Berger, W.H., Smetacek, V.S., and Wefer, G. (1989) Ocean productivity and paleoproductivity – an overview. In: Berger, W.H., Smetacek, V.S., Wefer, G. (Eds.), Productivity of the Ocean: Present and Past. J. Wiley and Sons, Chichester, pp. 429–455.

Bianchi, C. and Gersonde, R. (2004) Climatic evolution at the last deglaciation: the role of the Southern Ocean, *Earth and Planetary Science Letters*, 228: 407-424.

Bidle, K.D. and Azam, F. (1999) Accelerated dissolution of diatom silica by natural marine bacterial assemblages. *Nature*, 397: 508–512.

Bidle, K.D., Manganelli, M., and Azam, F. (2002) Regulation of oceanic silicon and carbon preservation by temperature control on bacteria. *Science*, 298: 1980-1984.

Bidle, K.D., Brzezinski, M.A., Long, R.A., Jones, J.L., and Azam, F. 2003. Diminished efficiency in the oceanic silica pump caused by bacteria-mediated silica dissolution. *Limnology and Oceanography*, 48: 1855-1868.

Binz P., (1987), Oxygen-isotope analysis on recent and fossil diatoms from Lake Walen and Lake Zurich (Switzerland) and its application on paleoclimatic studies, PhD Thesis, Swiss Federal Institute of Technology, Zurich, pp. 165.

Bird, M.I., Lloyd, J. and Farquhar, G.D. (1994) Terrestrial carbon storage at the LGM. *Nature*, 371: 566.

Birks, H.J.B. (1998) Numerical tools in palaeolimnology - progress, potentialities, and problems. *Journal of Paleolimnology*, 20: 307-332.

Bosilovich, M.G. (2002) On the vertical distribution of local and remote sources of water for precipitation. *Meteorology and atmospheric physics*. 80: 31-41.

Boyle, E. (1998) Pumping iron makes thinner diatoms. *Nature*, 393: 733-734.

Brandriss, M.E., O'Neil, J. R., Edlund, M.B., and Stoermer, E. F. (1998) Oxygen isotope fractionation between diatomaceous silica and water. *Geochimica et Cosmochimica Acta*, 62: 1119-1125.

Broecker, W.S. (1982a) Ocean chemistry during glacial time. *Geochimica et Cosmochimica Acta*. 46: 1689–1706.

Broecker, W.S. (1982b) Glacial to interglacial changes in ocean chemistry. *Progress in Oceanography*, 2: 151–197.

Bronk Ramsey C. (1995) Radiocarbon Calibration and Analysis of Stratigraphy: The OxCal Program. *Radiocarbon*, 37: 425-430.

Brzezinski, M.A., Pride, C.J., Franck, V.M., Sigman, D.M., Sarmiento, J.L., Matsumoto, K., Gruber, N., Rau, G.H. and Coale, K.H. (2002) A switch from $Si(OH)_4$ to NO_3^- depletion in the glacial Southern Ocean. *Geophysical Research Letters*, 29: 1564. doi: 10.1029/2001GL014349.

Brzezinski, M.A. Jones, J.L., Beucher, C.P., and Demarest, M.S. (2006) Automated determination of silicon isotope natural abundance by the acid decomposition of cesium hexafluosilicate . *Analytical Chemistry*, 78: 6109-6114.

Brunelle, B.G., Sigman, D.M., Cook, M.S., Keigwin, L.D., Haug, G.H., Plessen, B., Schettler, G., and Jaccard, S.L. (2007) Evidence from diatom-bound nitrogen isotopes for subarctic Pacific stratification during the last ice age and a link to North Pacific denitrification changes. *Paleoceanography*, 22, doi:10.1029/2005PA001205.

Burns, S. and Maslin, M.A. (1999) Composition and circulation of bottom water in the western Atlantic Ocean during the last glacial, based on pore-water analyses from the Amazon Fan. *Geology*, 27: 1011–1014.

Calvert, S.E. (1966) Accumulation of diatomaceous silica in the sediments of the Gulf of California. *Geological Society of America Bulletin*, 77: 569-596.

Carter, S.J. and Colman, S.M. (1994) Biogenic silica in Lake Baikal sediments: results from 1990-1992 American Cores. *Journal of Great Lakes Research*, 20: 751-760.

Charlet, F., Fagel, N., De Batist, M., Hauregard, F., Minnebo, B., Meischner, D., and SONIC Team. (2005) Sedimentary dynamics on isolated highs in Lake Baikal: evidence from detailed high-resolution geophysical data and sediment cores. *Global and Planetary Change*, 46: 125-144.

Chester, R., and Elderfield, H. (1968) The infrared determination of opal in siliceous deep-sea sediments. *Geochimica et Cosmochimica Acta*, 32: 1128-1140.

Chierici, M., Fransson, A. and Nojiri, Y. (2006) Biogeochemical processes as drivers of surface

fCO_2 in contrasting provinces in the subarctic North Pacific Ocean. *Global Biogeochemical Cycles*, 20: GB1009, doi: 10.1029/2004GB002356.

Chivas, A.R., De Deckker, P., Wang, S.X., and Cali, J.A. (2002) Oxygen-isotope systematics of the nektic ostracod Australocypris robusta, in The ostracoda: applications in Quaternary Research, AGU Geophysical Monograph 11, edited by Holmes J.A., and Chivas A.R. pp 301-313, American Geophysical Union, Washington DC,.

Chondrogianni, C., Ariztegui D., Rolph T., Juggins S., Shemesh A., Rietti-Shati M., Niessen F., Guilizzoni P., Lami A., McKenzie J.A., and Oldfield F. (2004) Millenial to interannual climate variability in the Mediterranean during the Last Glacial Maximum. *Quaternary International*, 122: 31-41.

Clayton, R.N. (1992) Silica-carbonate isotopic temperature calibration. *Science*, 258:1162-1163.

Clayton, R.N., and Mayeda, T.K. (1963), The use of bromine pentafluoride in the extraction of oxygen from oxide and silicates for isotope analysis. *Geochimica et Cosmochimica Acta*, 27: 43–52.

Clayton, R.N., Goldsmith, J.R., Karel, K.J., Mayeda, T.K., and Newton, R.C. (1975) Limits on the effect of pressure on isotopic fractionation. *Geochimica et Cosmochimica Acta*, 39: 1197-1201.

Colman, S.M., Peck, J.A., Karabanov, E.B., Carter, S.J., Bradbury, J.P., King, J.W., and Williams, D.F. (1995) Continental climate response to orbital forcing from biogenic silica records in Lake Baikal. *Nature*, 378: 769-771.

Colman, S.M., Peck, J.A., Hatton, J., Karabanov, E.B. and King J.W., (1999) Biogenic silica records from the BDP-93 site and adjacent areas of the Selenga Delta, Lake Baikal, Siberia. *Journal of Paleolimnology*, 21: 9-17.

Conley, D.J. (1998) An interlaboratory comparison for the measurements of biogenic silica in sediments. *Marine Chemistry*, 63: 39-48.

Conley, D.J., (2002) Terrestrial ecosystems and the global biogeochemical cycle. *Global Biogeochemical Cycles*, 16: 1121, doi:10.1029/2002GB001894.

Conley, D.J. and Schelske C.L. (2001) Biogenic Silica. In: Smol, J.P., Birks, H.J.B., and Last, W.M. (Eds.), Tracking environmental change using lake sediments: Volume 3. Kluwer Academic Publishers, Dordrecht, pp. 281-293.

Cook, M.S., Keigwin, L.D., and Sancetta, C.A. (2005) The deglacial history of surface and

intermediate water of the Bering Sea. *Deep-Sea Research II*, 52: 2163–2173

Cortese, G., Gersonde, R., Hillenbrand, C-D. and Kuhn, G. (2004) Opal sedimentation shifts in the World Ocean over the last 15 Myr. *Earth and Planetary Science Letters*, 224: 509-527.

Cowie G.L. and Hedges J.I. (1996) Digestion and alteration of the biochemical constituents of a diatom (Thalassiosira weissflogii) ingested by an herbivorous zooplankton (Calanus pacificus). *Limnology and Oceanography*, 41: 581-594.

Craig, H. (1957) Isotopic standards for carbon and oxygen and correction factors for mass spectrmatic analysis of carbon dioxide. *Geochimica et Cosmochimica Acta*, 12: 133-149.

Criss R.E. (1999) Principles of stable isotope distribution. Oxford University Press, New York, 254 pp.

Crosta, X., Sturm, A., Armand, L.,. and Pichon J.J. (2004) Late Quaternary sea ice history in the Indian sector of the Southern Ocean as recorded by diatom assemblages. *Marine Micropaleontology*, 50: 209-223.

Crosta, X., Shemesh, A., Etourneau, J., Yam, R., Billy, I., and Pichon, J.J. (2005) Nutrient cycling in the Indian sector of the Southern Ocean over the last 50,000 years. *Global and Biogeochemical Cycles*. 19, GB3007, doi:10.1029/2004GB002344.

Crowley, T.J. (1995) Ice-Age terrestrial carbon changes revisited. *Global Biogeochemical Cycles*, 9: 377–389.

Dansgaard, W. (1964) Stable isotopes in precipitation. *Tellus*, 16: 436-468.

Dansgaard, W., Johnsen, S.J., Clausen, H.B., Dahl-Jensen, N.S., Hammer, C.U., Hvidberg, C.S., Steffensen, J.P., Sveinbjörnsdottir, A.E., Jouzel, J., and Bond, G. (1993) Evidence for general instability of past climate from a 250-kyr ice-core record. *Nature*, 364: 218–220.

de Baar, H.J.W, Boyd, P.W., Coale, K.H., Landry, M.R., Tsuda, A., Assmy, P., Bakker, D.C.E., Bozec, Y., Barber, R.T., Brzezinski, M.A., Buesseler, K.O., Boye, M., Croot, P.L., Gervais, F., Gorbunov, M.Y., Harrison, P.J., Hiscock, W.T., Laan, P., Lancelot, C., Law, C.S., Levasseur, M., Marchetti, A., Millero, F.J., Nishioka, J., Nojiri, Y., van Oijen, T., Riebesell, U., Rijkenberg, M.J.A., Saito, H., Takeda, S., Timmermans, K.R., Veldhuis, M.J.W., Waite, A.M., and Wong, C-S. (2005) Synthesis of iron fertilisation experiments: from the Iron Age in the age of enlightenment. *Journal of Geophysical Research*, 110: C09S16, doi:10.1029/2004JC002601.

de Boer, A.M., Sigman, D.M., Toggweiler, J.R., and Russell, J.L. (2007) Effect of global ocean temperature change on deep ocean ventilation. *Paleoceanography*, 22; PA2210, doi:10.1029/2005PA001242.

De La Rocha, C.L., (2002) Measurement of silicon stable isotope natural abundances via multicollector inductively coupled plasma mass spectrometry (MC-ICP-MS), *Geochemistry, Geophysics, Geosystems*, 3: DOI:10.1029/2002GC000310.

De La Rocha, C.L. (2006) Opal-based isotopic proxies of paleoenvironmental conditions. *Global Biogeochemical Cycles*, GB4S09: doi:10.1029/2005GB002664.

De Master, D.J. (1979) The marine budget of silica and ^{32}Si. Ph.D. Thesis, Yale University, unpublished.

De Master D.J. (1981) The supply and accumulation of silica in the marine environment. *Geochimica et Cosmochimica Acta*, 45: 1715-1732.

Dezileau, L., Bareille, G., Reyss, J.L., and Lemoine, F. (2000) Evidence for strong sediment redistribution by bottom currents along the southeast Indian ridge. Deep-Sea Research Part I, 47: 1899–1936.

Dixit, S. and Van Cappellen, P.A. (2002) Surface chemistry and reactivity of biogenic silica. *Geochimica et Cosmochimica Acta*, 66: 2559-2568.

Dixit, S., Van Cappellen, P.A., and van Bennekom, J. (2001) Processes controlling solubility of biogenic silica and pore water build-up of silicic acid in marine sediments. *Marine Chemistry*, 73: 333-352.

Duce, R.A., and Tindale, N.W. (1991) Atmospheric transport of iron and its deposition in the ocean. *Limnology and Oceanography*, 36: 1715-1726.

Duggen, S., Croot, P., Schacht, U., and Hoffmann, L. (2007) Subduction zone volcanic ash can fertilize the surface ocean and stimulate phytoplankton growth: Evidence from biogeochemical experiments and satellite data. *Geophysical Research Letters*. 34: L01612, doi:10.1029/2006GL027522.

Dugdale, R.C. Lyle, M. Wilkerson, F.P. Chai, F. Barber, R.T., and Peng, T-H. (2004) Influence of equatorial diatom processes on Si deposition and atmospheric CO_2 cycles at glacial/interglacial timescales. *Paleoceanography*, 19: PA3011: doi:10.1029/2003PA000929.

Duplessy, J.C., Lalou, C., Vinot, A.C. (1970) Differential isotopic fractionation in benthic

foraminifera and paleotemperatures revised. *Science*, 213: 1247-1250.

Duplessy, J-C., Shackleton, N.J., Fairbanks, R.J., Labeyrie, L.D., Oppo, D., and Kallel, N. (1988) Deepwater source variation during the last climatic cycle and their impact on the global deepwater circulation. *Paleoceanography*, 3: 343–360.

Duplessy, J-C., Labeyrie, L., Juillet-Leclerc, A., Maitre, F., Duprat, J., and Sarnthein, M. (1991) Surface salinity reconstruction of the North Atlantic Ocean during the last glacial maximum. *Oceanologica Acta*, 14: 311–324.

Duplessy, J-C, Labeyrie, L., Arnold, M., Paterne, M., Duprat, J., and van Weering, T. (1992) Changes in surface water salinity of the North Atlantic Ocean during the last deglaciation. *Nature*, 358: 485–488.

Duplessy, J-C., Labeyrie, L., and Waelbroeck, C. (2002), Constraints on the oxygen isotopic enrichment between the Last Glacial Maximum and the Holocene: Paleoceanographic implications. *Quaternary Science Reviews*, 21: 315-330.

Edlund, M.B. and Stoermer, E.F. (2000) A 200,000-year, high-resolution record of diatom productivity and community makeup from lake Baikal shows high correspondence to the marine oxygen-isotope record of climate change. *Limnology and Oceanography*, 45: 948–962.

Eggimann, D.W., Manheim, F.T., and Betzer P.R. (1980) Dissolution and analysis of amorphous silica in marine sediments. *Journal of Sedimentary Petrology*, 51: 215–225

Eisma, D. and Van der Gaast, S.J. (1971) Determination of opal in marine sediments by X-ray diffraction. *Netherlands Journal of Sea Research*, 5: 382-389.

Eldrett, J.S., Harding, I.C., Wilson, P.A., Butler, E., and Roberts, A.P. (2007) Continental ice in Greenland during the Eocene and Oligocene. *Nature*, 446: 176-179.

Ellwood, M.J., and Hunter, K.A., (1999) Determination of the Zn/Si ratio in diatom opal: a method for the separation, cleaning and dissolution of diatoms. *Marine Chemistry*, 66: 149-160.

Ellwood, M.J., and Hunter, K.A. (2000) Variations in the Zn/Si record over the last interglacial glacial transition. *Paleoceanography*, 15: 506-514.

Emiliani, C. (1955) Pleistocene temperatures. *Journal of Geology*, 63: 538–578.

Emiliani, C. (1971) The amplitude of Pleistocene climatic cycles at low latitudes and the isotopic composition of glacial ice. In: Turehian K.K. (ed.), The late Cenozoic glacial

ages. Yale University, New Haven, Connecticut, pp. 183–197.1

Emile-Geay, J., Cane, M.A., Naik, N. Seager, R., Clement, A.C., and van Green, A. (2003) Warren revisited: atmospheric freshwater fluxes and "Why is no deep water formed in the North Pacific". *Journal of Geophysical Research*, 108, C6: 3178, doi:10.1029/2001JC001058.

Epstein, S., and Taylor, H.P. (1970a) The concentration and isotopic composition of hydrogen, carbon and silicon in Apollo 11 lunar rocks and minerals. *Proceedings of the Apollo 11 lunar science conference*, 2: 1085–1096.

Epstein, S. and Taylor, H.P. (1970b) Stable isotopes, rare gases, solar wind and spallation products. *Science*, 167: 533–535.

Epstein, S. and Taylor, H.P. (1971) O^{18}/O^{16}, Si^{30}/Si^{28}, D/H and C^{13}/C^{12} ratios in lunar samples. *Proceedings of the second lunar conference*, 2: 1421-1441.

Fagel, N. Boski, T., Likhoshway, L., and Oberhäensli, H. (2003) Late Quaternary clay mineral record in Central Lake Baikal (Academician Ridge, Siberia). *Palaeogeography, Palaeoclimatology, Palaeoecology*, 193: 159-179.

Fagel, N., Thamó-Bózsó, E., and Heim, B. (2007). Mineralogical signatures of Lake Baikal sediments: sources of sediment supplies through Late Quaternary. *Sedimentary Geology*, 194: 37-59.

Fietz, S. and Nicklisch, A. (2004). An HPLC analysis of the summer phytoplankton assemblages in Lake Baikal. *Freshwater Biology*, 49: 332-345.

Fietz, S., Nicklisch, A., and Oberhänsli, H. (2007) Phytoplankton response to climate changes in Lake Baikal during the Holocene and Kazantsevo Interglacials assessed from sedimentary pigments. *Journal of Paleolimnolgy*, 37:177-203

Flower, R.J. and Likhoshway, Y.V. (1993) Diatom preservation in Lake Baikal. In: Grachev M.A. (ed.), Diatom algae as indicators of the changes of climate and environment: Fifth Workshop on Diatom Algae. Botanical Society Publications, Irkutsk, pp. 77-78.

François, R.F., Altabet, M.A., Yu, E.-F., Sigman, D.M., Bacon, M.P., Frank, M., Bohrmann, G., Bareille, G., and Labeyrie, L.D. (1997) Water column stratification in the Southern Ocean contributed to the lowering of glacial atmospheric CO_2. *Nature*, 389: 929–935.

Fröhlich, F. (1989) Deep-sea biogenic silica: new structural and analytical data from infrared analysis - geological implications. *Terra Nova*, 1: 267-273.

Ganssen, G.M., and Kroon, D. (2000), The isotopic signature of planktonic foraminifera from NE Atlantic surface sediments: implications for the reconstruction of past oceanic conditions. *Journal of the Geological Society London*, 157: 693-699.

Gargett, A.E. (1991) Physical processes and the maintenance of nutrient-rich euphotic zones. *Limnology and Oceanography*, 36: 1527-1545.

Garlick, G.D. (1974) The stable isotopes of oxygen, carbon, hydrogen in the marine environment. In: Goldberg G.D. (ed.), The Sea. John Wiley & Sons, New York, pp. 393–425.

Gehlen, M. and van Raaphorst, W. (1993) Early diagenesis of silica in sandy North Sea sediments: quantification of the solid phase. *Marine Chemistry*, 42: 71-83.

Gehlen, M., Beck, L., Calas, G., Flank, A.M., van Bennekom, A.J., and van Beusekom, J.E.E. (2002) Unraveling the atomic structure of biogenic silica: Evidence of the structural association of Al and Si in diatom frustules. *Geochimica et Cosmochimica Acta*, 66: 1601-1609.

Geochemical Ocean sections Study (GEOSEC) (1987) *Atlantic Pacific and Indian Ocean expiditions: shorebased data and graphics*, vol 7, Craig H., H.G. Ostlund, W.S. Broecker, and D. Spencer. National Science Foundation, Washington D.C., USA.

Gersonde, R., Crosta, X., Abelmann, A., and Armand, L. (2005) Sea-surface temperature and sea ice distribution of the Southern Ocean at the EPILOG Last Glacial Maximum - a circum-Antarctic view based on siliceous microfossil records. *Quaternary Science Reviews*, 24: 869-896.

Goldberg, E.D. (1958) Determination of opal in marine sediments. *Journal of Marine Research*, 17: 71-83.

Gorbarenko, S.A. (1996) Stable isotope and lithologic evidence of late-Glacial and Holocene oceanography of the northwestern Pacific and its marginal seas. *Quaternary Research*, 46: 230–250.

Granina, L.Z., Karabanov, E.B., Shimaraeva, M.K., Williams, D.F., and Kuptsov, V.M. (1992) Biogenic silica of Baikal bottom sediments used for palaeo reconstruction. In: International project on palaeolimnology and lake Cenozoic climate newsletter. 6: 53-59. Universitätsverlag Wagner, Innsbruck.

Granina, L.Z., Grachev, M.A., Karabanov, E.B., Kuptsov, V.M., Shimaraeva, M.K. and Williams D.F. 1993. Accumulation of biogenic silica in bottom sediments of Baikal.

Russian Geology and Geophysics, 34: 126–135. (In Russian).

Grootes, P.M. (1993) Interpreting continental oxygen isotopes records. In: Swart P.K., Lohmann K.C., McKenzie J. and Savin S. (eds), Climate change in continental isotope records. AGU Geophysical Monograph. 78: 37–46.

Harada, N., Sato, M., Shiraishi, A., and Honda, M.C. (2006) Characteristics of alkenone distributions in suspended and sinking particles in the northwestern North Pacific. *Geochimica et Cosmochimica Acta*, 70: 2045-2062.

Harrison, P.J., Boyd, P.W., Varela, D.E., Takeda, S., Shiomoto, A., and Odate, T. (1999) Comparison of factors controlling phytoplankton productivity in the NE and NW subarctic Pacific gyres. *Progress in Oceanography*, 43: 205-234.

Haimson, M. and Knauth, L.P. (1983) Stepwise fluorination – a useful approach for the isotopic analysis of hydrous minerals. *Geochimica et Cosmochimica Acta*, 47: 1589–1595.

Harrison, K.G. (2000) Role of increased marine silica input on paleo-pCO_2 levels. *Paleoceanography*, 15: 292-298.

Haug, G.H. (1995) The evolution of Northwest Pacific Ocean over the last 6 Ma: ODP LEG 145, PhD thesis, pp 200., University of Kiel, Kiel, Germany.

Haug, G.H., and Tiedemann, R. (1998) Effect of the formation of the Isthmus of Panama on Atlantic Ocean thermohaline circulation. *Nature*, 393: 673-676.

Haug, G.H. (1995) The evolution of Northwest Pacific Ocean over the last 6 Ma: ODP LEG 145, PhD thesis, pp 200., University of Kiel, Kiel, Germany.

Haug, G.H., Sigman, D.M., Tiedemann, R., Pedersen, T.F., and Sarnthein, M. (1999) Onset of permanent stratification in the subarctic Pacific Ocean. *Nature*, 401: 779-782.

Haug, G.H., Tiedemann, R., Zahn, R., and Ravelo, A.C. (2001) Role of Panama uplift on oceanic freshwater balance. *Geology*, 29: 207-210.

Haug, G.H., Sigman, D.M., Tiedemann, R., Pedersen, T.F., and Sarnthein M. (2004) Onset of permanent stratification in the subarctic Pacific Ocean. *Nature*, 401: 779–782.

Haug, G.H., Ganopolski, A., Sigman, D. M., Rosell-Mele, A., Swann, G.E.A., Tiedemann, R., Jaccard, S, Bollmann, J., Maslin, M.A., Leng, M.J., and Eglinton, G. (2005) North Pacific seasonality and the glaciation of North America 2.7 million years ago. *Nature*, 433: 821-825.

Hays, P.D and Grossman, E.L. (1991) Oxygen isotopes in meteoric calcite cements as indicators of continental paleoclimate. *Geology*, 19: 441–444.

Heinrich H. (1988) Origin and consequences of cyclic ice rafting in the Northeast Atlantic ocean during the past 130,000 years. *Quaternary Research*, 29: 142–152.

Hemleben, C., Spindler, M., and Anderson, O.R. (1989), *Modern Planktonic Foraminifera*, pp. 363., Springer, New York.

Hillenbrand, C-D and Cortese, G. (2006) Polar stratification: a critical view from the Southern Ocean. *Palaeogeography, Palaeoclimatology, Palaeoecology*, 242: 240-252.

Hillebrand, H., Dürselen, C-D., Kirschtel, D., Pollingher, U., and Zohary, T. (1999) Biovolume calculation for pelagic and benthic microalgae. *Journal of Phycology*, 35: 403-424.

Hodell, D.A., Kanfoush, S.L., Shemesh, A., Crosta, X., Charles, C. D., and Guilderson, T.P. (2001) Abrupt cooling of Antarctic surface waters and sea ice expansion in the South Atlantic sector of the Southern Ocean at 5000 cal yr BP. *Quaternary Research*, 56: 191-198.

Hoefs J. (1997) Stable isotope geochemistry. Spinger-Verlag, Berlin, 213 pp.

Holmes, J.A., and Chivas A.R. (2002) Ostracod shell chemistry – overview, in The ostracoda: applications in Quaternary Research, AGU Geophysical Monograph 11, edited by Holmes J.A., and Chivas A.R., pp 185-204, American Geophysical Union, Washington DC,.

Honda, M.C., Imai, K., Nojiri, Y., Hoshi, F., Sugawarad, T., and Kusakabe, M. (2002) The biological pump in the northwestern North Pacific based on fluxes and major components of particulate matter obtained by sediment-trap experiments (1997–2000). Deep-Sea Research II, 49: 5595–5625.

Horiuchi, K. Minoura, K,, Hoshino, K., Oda, T., Nakamura, T., and Kawai, T. (2000) Palaeoenvironmental history of Lake Baikal during the last 23000 years. *Palaeogeography, Palaeoclimatology, Palaeoecology*, 157: 95-108.

Hovan, S.A., Rea, D.K., and Pisias, N.G. (1991) Late Pleistocene continental climate and oceanic variability recorded in Northwest Pacific sediments. *Paleoceanography*, 6: 349-370.

Hu, F.S. and Shemesh, A. (2003) A biogenic silica delta[18]O record of climatic change during the last glacial-interglacial transition in southwestern Alaska. *Quaternary Research*, 59:

379-385.

Hu, F.S., Kaufman, D., Yoneji, S., Nelson, D., Shemesh, A., Huang, Y., Tian, J., Bond, G., Clegg, B., and Brown T. (2003) Cyclic variations and solar forcing of Holocene climate in the Alaskan Subarctic. *Science*, 301: 1890-1893.

Hurd, D.C. (1972) Factors affecting solution rate of biogenic opal in seawater. *Earth and Planetary Science Letters*, 15: 411-417.

Hurd, D.C., Wenkam, C., Pankratz, H.S., and Fugate, J. (1979) Variabile porosity in siliceous skeletons: determination and importance. *Science*, 203: 1340-1342.

Hutchins, D.A. and Bruland, K.W. (1998) Iron-limited diatom growth and Si:N uptake ratios in a coastal upwelling zone. *Nature*, 393: 561–564.

Hutchinson, D.R., Golmshtok, A.J., Zonenshain, L.P., Moore, T.C., Scholz, C.A., and Klitford, K.D. (1992) Depositional and tectonic framework of the rift basins of Lake Baikal from multichannel seismic data. *Geology*, 21: 589-592.

Huybers, P., and Molnar P. (2007) Tropical cooling and the onset of America glaciation. *Climate of the Past*, 3: 549-557.

Jacobson, D.M., and Anderson, D.M. (1986) Thecate heterotrophic dinoflagellates: feeding behavior and mechanism. *Journal of Phycology*, 22: 249–258.

Jaccard, S.L., Haug, G.H, Sigman, D.M., Pedersen, T.F., Thierstein, H.R., and Röhl, U. (2005) Glacial/interglacial changes in subarctic North Pacific stratification. *Science*, 308: 1003-1006.

Jickells, T.D., An, Z.S., Andersen, K.K., Baker, A.R., Bergametti, G., Brooks, N., Cao, J.J., Boyd, P.W., Duce, R.A., Hunter, K.A., Kawahata, H., Kubilay, N., laRoche, J., Liss, P.S., Mahowald, N., Prospero, J.M., Ridgwell, A.J., Tegen, I., and Torres, R.. (2005) Global iron connections between desert dust, ocean biogeochemistry, and climate, *Science*, 308: 67-71.

Jones, V.J., Leng, M.J., Solovieva, N., Sloane, and H.J. Tarasov, P. (2004) Holocene climate of the Kola Peninsula; evidence from the oxygen isotope record of diatom silica. *Quaternary Science Reviews*, 23: 833-839.

Juillet-Leclerc, A. (1986) Cleaning process for diatomaceous samples, in *Proceedings of the 8th Diatom Symposium*, edited by Ricard M., pp. 733–736, Koeltz Scientific Books, Koenigstein.

Juillet, A. (1980a) Structure de la silice biogenique: nouvelles donnes apportees par l'analyse isotopique de l'oxygene. C.R.Academy of Science, Paris 290.D: 1237-1239.

Juillet, A. (1980b) Analyse isotopique de la silice des diatomees lacustres et marines: fractionnement des isotopes de l'oxygene en fonction de la temperature. Diss. Paris XI These de 3e cycle.

Juillet-Leclerc, A. (1986) Cleaning process for diatomaceous samples, in *Proceedings of the 8th Diatom Symposium*, edited by M. Ricard, pp. 733–736, Koeltz Scientific Books, Koenigstein.

Juillet-Leclerc, A., and Labeyrie, L., (1987) Temperature dependence of the oxygen isotopic fractionation between diatom silica and water. *Earth and Planetary Science Letters*, 84: 69-74.

Juillet-Leclerc, A. and Schrader, H. (1987) Variations of upwelling intensity recorded in varved sediment from the Gulf of California during the past 3,000 years. *Nature*, 329: 146-149.

Kalmychkov, G.V., Kuz'min, M.I., Pokrovskii, B.G., and Kostrovaa, S.S. (2005) Oxygen isotopic composition in diatom algae frustules from Lake Baikal sediments: annual mean temperature variations during the last 40 ka. *Doklady Earth Sciences*, 413: 206–209.

Kamatani, A (1974) Studies on the dissolution of diatomaceous silica as a function of heating. *Journal of Oceanographical Society of Japan*, 30: 157-162.

Kamatani, A. and Oku, O. (2000) Measuring biogenic silica in marine sediments. Marine Chemistry, 68: 219–229.

Karabanov, E.B., Prokopenko, A.A., Williams, D.F., and Colman, S.M. (1998) Evidence from Lake Baikal for Siberian Glaciation during Oxygen-Isotope Substage 5d. *Quaternary Research*, 50: 46-55.

Karabanov, E.B., Williams, D.F., Kuzmin, M.I., Sideleva, V., Khursevich, G.K., Prokopenko, A.A., Solotchina, E., Tkachenko, L., Fedenya, S., Kerber, E., Gvozdkov, A., Khlustov, O., Bezrukova, E., Letunova, P., and Krapivina, S. (2004) Ecological collapse of Lake Baikal and Lake Hovsgol ecosystems during the Last Glacial and consequences for aquatic species diversity. *Palaeogeography, Palaeoclimatology, Palaeoecology*, 209: 227-243.

Kastner, M. (1981) Authigenic silicates in deep-sea sediments: formation and diagenesis. In: Emiliani, C. (Ed.), The Oceanic Lithosphere. The Sea, vol. 7. Wiley, New York, pp.

915–980.

Kastner, M. and Stonecipher, S.A. (1979) Zeolites in pelagic sediments of the Atlantic, Pacific, and Indian Oceans. In: Sand, L.B. and Mumpton, F.A. (Eds.), Natural Zeolites: Occurrence, Properties, Use. Pergamon Press, New York, pp.199-220.

Katsuki, K., Takahashi K., and Okada M. (2003), Diatom assemblage and productivity changes during the last 340,000 years in the subarctic Pacific. *Journal of Oceanography*, 59: 695-707.

Katsuki, K., and Takahashi, K. (2005) Diatoms as paleoenvironmental proxies for seasonal productivity, sea-ice and surface circulation in the Bering Sea during the late Quaternary, *Deep-Sea Research Part II*, 52: 2110-2130.

Kawahata, H., Okamoto, T., Matsumoto, E., and Ujiie, H. (2000) Fluctuations of eolian flux and ocean productivity in the mid-latitude North Pacific during the last 200 kyr. *Quaternary Science Reviews*, 19: 1279-1292.

Keeling, R.F., and Stephens, B.B. (2001) Antarctic sea ice and the control of Pleistocene climate instability. *Paleoceanography*, 16: 112-131.

Keeling, R.F., and Visbeck, M. (2001) Paleoceanography: Antarctic stratification and glacial CO_2. *Nature*, 412: 605-606.

Keifer, L.D., Jones, G.A., and Froelich, P.N. (2001) A 15,000 year paleoenvironmental records from Meiji Seamount, far northwestern Pacific. *Earth and Planetary Science Letters*, 111: 425-440.

Keigwin, L.D. (1998) Glacial-age hydrology of the far northwest Pacific Ocean. *Paleoceanography*, 13: 323-339.

Kennett, J. P., and Shackleton, N.J. (1976) Oxygen isotopic evidence for the development of the psychrosphere 38 Myr ago. *Nature*, 260, 513–515

Kemp, A.E.S. and Dugdale R.C. (2006) Introduction to special section: the role of diatom production and Si flux and burial in the regulation of global cycle. *Global Biogeochemical Cycles*, 20, GB4S01, doi:10.1029/2006GB002894.

Kemp, A.E.S., Pike, J., Pearce, R. B., and Lange, C.B. (2000) The "Fall dump" - A new perspective on the role of a "shade flora" in the annual cycle of diatom production and export flux. *Deep Sea Research Part II*, 47: 2129-2154.

Khursevich, G.K., Karabanov, E.B., Prokopenko, A.A., Williams, D.F., Kuzmin, M.I., Fedenya,

S.A., and Gvozdkov, A.A. (2001) Insolation regime in Siberia as a major factor controlling diatom production in Lake Baikal during the past 800,000 years. *Quaternary International*, 80-81: 47-58.

Kienast, S.S., Hendy, I.L., Crusius, J., Pedersen, T.F., and Calvert S.E. (2004) Export production in the Subarctic North Pacific over the last 800 kyr: no evidence for iron fertilisation. *Journal of Oceanography*, 60: 189-203.

Kienast, S.S., Kienast, M., Jaccard, S., Calvert, S. E., and Francois, R. (2006) Testing the silica leakage hypothesis with sedimentary opal records from the eastern equatorial Pacific over the last 150 kyrs. *Geophysical Research Letters*, 33: L15607, doi:10.1029/2006GL026651.

Kim, S.T., and O'Neil, J.R. (1997) Equilibrium and nonequilibrium oxygen isotope effects in synthetic carbonates. *Geochimica et Cosmochimica Acta*, 61: 3461-3475.

Kleiven, H.F., Jansen, E., Fronval, T., and Smith, T.M. (2002) Intensification of Northern Hemisphere glaciations in the circum Atlantic region (3.5-2.4 Ma) - ice-rafted detritus evidence. *Palaeogeography, Palaeoclimatology, Palaeoecology*, 184: 213-223.

Knauth, L.P. (1973) *Oxygen and hydrogen isotope ratios in cherts and related rocks*. PhD thesis. California Institute of Technology.

Kohfeld, K.E., and Harrison, S.P. (2001) DIRTMAP: the geological record of dust, *Earth Science Reviews*, 54: 81-114.

Kohfeld, K.E., Fairbanks, R.G., Smith, S.L., and Walsh, I.D. (1996), *Neogloboquadrina pachyderma* (sinistral coiling) as paleoceanographic tracers in polar oceans: Evidence from Northeast Water Polynya plankton tows, sediment traps, and surface sediments. *Paleoceanography*, 11: 679-699.

Kohfeld, K.E., Le Quere, C., Harrison, S.P., and Anderson, R.F. (2005) Role of marine biology in glacial–interglacial CO_2 cycles. *Science*, 308: 74–78.

Komuro, C., Narita, H., Imai, K., Nojiri, Y., and Jordan, R.W. (2005) Microplankton assemblages at Station KNOT in the subarctic western Pacific 1999-2000. *Deep-Sea Research II*, 52: 2206-2217.

Koning, E. Epping, E., and van Raaphorst, W. (2002) Determining Biogenic Silica in marine samples by tracking silicate and aluminium concentrations in alkaline leaching solutions. *Aquatic Geochemistry*, 8: 37–67.

Koning, E., Gehlen M., Flank, A. M., Calas, G., and Epping, E. (2007) Rapid post-mortem incorporation of aluminum in diatom frustules: evidence from chemical and structural analyses. *Marine Chemistry*, 103: 97–111.

Koster, R., Jouzel, J., Suozzo, R., Russell, G., Broecker, W., Rind, D., and Eagleson, P. (1986) Global sources of local precipitation as determined by the NASA/GISS GCM. *Geophysical Research Letters*, 13: 121-1241.

Kotilainen, A.T. and Shackleton, N.J. (1995) Rapid climate variability in the North Pacific Ocean during the past 95,000 years. *Nature*, 377: 323-326.

Kozhova, O.M., and Kazantseva, E.A. (1961) O sezonnykh izmeneniyakh chislennostyi bakterioplanktona v vodakh ozera Baikal. *Mikrobiologiya*, 3: 113-117. (In Russian).

Krissek, L. (1995) Late Cenozoic ice-rafting records from Leg 145 sites in the North Pacific: Late Miocene onset, Late Pliocene intensification, and Pliocene-Pleistocene events. In Proc. ODP, Scientific Results, 145, edited by D. K. Rea, I. A. Basov, D. W. Scholl, and J. F. Allan, pp. 3-19, College Station, Texas.

Kroon, D., and Ganssen, G. (1989) Northern Indian ocean upwelling cells and the stable isotope composition of living foraminifera. *Deep-sea Research*, 36: 1219–1236.

Kuroyanagi, A., and Kawahata, H. (2004) Vertical distribution of living planktonic foraminifera in the seas around Japan. *Marine Micropaleontology*, 53, 173-196.

Kuroyanagi, A., Kawahata, H., Nishi, H., and Honda, M.C. (2002) Seasonal changes in planktonic foraminifera in the northwestern North Pacific Ocean: sediment trap experiments from subarctic and subtropical gyres. *Deep-Sea Research II*, 49: 5627-5645.

Kuznetsov, S.I. (1951) Sravnitel'naya kharakteristika biomassy bakterii i fitoplanktona v poverkhnostnom sloe vody Sredniego Baikala. *Trudy Baikalskoy Limnologicheskoy stancii*, 13: 217-224. (In Russian).

Lal., D., Charles, C., Vacher, L., Goswami, J.N., Jull, A.J.T., McHargue, L., and Finkel R.C., (2006) Paleo-ocean chemistry records in marine opal: implications for fluxes of trace elements, cosmogenic nuclides (^{10}Be and ^{26}Al), and biological productivity. *Geochimica et Cosmochimica Acta*, 70: 3275-3289.

Labeyrie, L.D. (1974) New approach to surface seawater paleotemperatures using (18)O/(16)O ratios in silica of diatom frustules. *Nature*, 248: 40–42.

Labeyrie, L.D. (1979) La composition isotopique de l'oxygene de la silice des valves de

diatomees. Mise au point d'une nouvelle methode de palaeo-climatologie. Diss. Universitie de Paris XI. [In French]

Labeyrie L.D., and Juillet, A. (1980) Isotopic exchange of the biogenic silica oxygen. *Comptes Rendus Hebdomadaires des Seances de L'Academie des Sciences Serie D*, 290: 1185-1188.

Labeyrie, L.D., and Juillet, A. (1982) Oxygen isotopic exchangeability of diatom valve silica; interpretation and consequences for palaeoclimatic studies. *Geochimica et Cosmochimica Acta*, 46: 967–975.

Labeyrie, L.D., Pichon, J.J., Labracherie, M., Ippolito, P., Duprat, J., and Duplessy, J.C. (1986) Melting history of Antarctica during the past 60,000 years. *Nature*, 322: 701-706.

Lamb, A.L., Leng, M.J., Sloane, H.J, and Telford, R.J. (2005) A comparison of the palaeoclimatic signals from diatom oxygen isotope ratios and carbonate oxygen isotope ratios from a low latitude crater lake. *Palaeogeography, Palaeoclimatology, Palaeoecology*, 223: 290-302.

Lamb, A.L., Brewer, T.S., Leng, M.J., Sloane, H.J., and Lamb, H.F. (2007) A geochemical method for removing the effect of tephra on lake diatom oxygen isotope records. *Journal of Paleolimnology*, 37: 499-516.

Lawson, D.S., Hurd, D.C., and Pankratz, H.S. (1978) Silica dissolution rates of decomposing phytoplankton assemblages at various temperatures. *American Journal of Science*, 278: 1373– 1393.

Lear, C.H., Elderfield, H., and Wilson, P.A. (2000) Cenozoic deep-sea temperatures and global ice volumes from Mg/Ca in benthic foraminiferal calcite. *Science*, 287: 269–272.

Lear, C.H., Rosenthal, Y., and Wright, J.D. (2003) The closing of a seaway: ocean water masses and global climate change. *Earth and Planetary Science Letters*, 210: 425-436.

Leinen, M. (1977) a normative calculation technique for determination if biogenic opal in sediments and particulate matter. *Geochimica et Cosmochimica Acta*, 40: 671-676.

Leinen. M. (1985) Techniques for determining opal in deep-sea sediments: a comparison of radiolarian counts and X-ray diffraction data. *Marine Micropaleontology*, 9: 375-383.

Leng, M.J., and Marshall J.D. (2004) Palaeoclimate interpretation of stable isotope data from lake sediment archives. *Quaternary Science Reviews*, 23: 811-831.

Leng, M. J., and Barker, P.A. (2006) A review of the oxygen isotope composition of lacustrine

diatom silica for palaeoclimate reconstruction. *Earth Science Reviews*. 75: 5-27.

Leng, M.J., Greenwood, P.B., and Sloane, H.J. (1998) Oxygen isotopes in diatomite from Lake Pinarbasi, Turkey, *NIGL Report no. 131*.

Leng, M.J., and Barker, P.A., Greenwood, P., Roberts N., and Reed J. (2001) Oxygen isotope analysis of diatom silica and authigenic calcite from Lake Pinarbasi, Turkey. *Journal of Paleolimnology*. 25: 343–349.

Leng, M.J., Lamb, A.L., Heaton, T.H.E., Marshall, J.D., Wolfe, B.B., Jones, M.D., Holmes, J.A., and Arrowsmith C. (2005a) Isotopes in lake sediments. In: Leng, M.J. (ed.), Isotopes in Palaeoenvironmental Research, Springer, Dordrecht, The Netherlands, 148-184.

Leng, M.J., Metcalfe, S.E., and Davies, S.J. (2005b) Investigating late Holocene climate variability in central Mexico using carbon isotope ratios in organic matter and oxygen isotope ratios from diatom silica within lacustrine sediments. *Journal of Paleolimnology*, 34: 413-431.

Lewin. J.C. (1961) The dissolution of silica from diatom walls. *Geochimica et Cosmochimica Acta*, 21: 182-198.

Li, X.S., Berger, A., Loutre, M. F., Maslin, M. A., Haug, G. H., and Tiedemann, R. (1998), Simulating late Pliocene northern hemisphere climate with the LLN two dimensional Model. *Geophysical Research Letters*, 25: 915-918.

Lin, H-L. and Chen, C-J., (2002) A late Pliocene diatom Ge/Si record from the Southeast Atlantic. *Marine Chemistry*, 180: 151-161.

Lisiecki, L.E., and Raymo, M.E. (2005) A Pliocene-Plesitocene stack of 57 globally distributed benthic $\delta^{18}O$ records. *Paleoceanography*, 20, PA1003: doi:10.1029/2004PA001071.

Locarnini, R.A., Mishonov, A.V., Antonov, J.I., Boyer, T.P., and Garcia, H.E. (2006) World Ocean Atlas 2005, Volume 1: Temperature. Levitus, S. Ed. NOAA Atlas NESDIS 61, U.S. Government Printing Office, Washington, D.C., 182 pp.

Loutre, M.F., and Berger, A. (2003) Marine isotope stage 11 as an analogue for the present interglacial. *Global and Planetary Change*, 36: 209-217.

Lücke, A., Moschen, R., and Schleser, G.H. (2005) High temperature carbon reduction of silica: A novel approach for oxygen isotope analysis of biogenic opal. *Geochimica et Cosmochimica Acta*, 69: 1423-1433.

Lyle, A.O., and Lyle, M. (2002) Determination of biogenic opal in pelagic marine sediments: a

simple method revisited. In: Lyle, M., Wilson, P.A. and Janecek, T.R. (Eds.), Proceedings of the Ocean Drilling Program, Initial Reports, Vol. 199: Chapter 6.

McCrea, J.M. (1950) On the isotopic chemistry of carbonates and palaeo-temperature scale. *Journal of Chemical Physics*, 18: 849-857.

McDonald, D., Pedersen, T.F., and Crusius, J. (1999) Mulitple late Quaternary episodes of exceptional diatom production in the Gulf of Alaska. *Deep Sea Research Part II*, 46: 2993-3017.

Mackay, A.W., Flower, R.J., Kuzmina, A.E., Granina, L.Z., Rose, N.L., Appleby, P.G., Boyle, J.F., and Battarbee, R.W. (1998) Diatom succession trends in recent sediments from Lake Baikal and their relation to atmospheric pollution and to climate change. *Philosophical Transactions of The Royal Society of London. B*, 353: 1011-1055.

Mackay, *et al.*, (In prep) Diatom oxygen isotope in Lake Baikal during the Eemian.

Marchitto, T.M., Lehman, S.J., Ortiz, J.D., Flückiger, J, van Geen, A. (2007) Marine Radiocarbon Evidence for the Mechanism of Deglacial Atmospheric CO_2 Rise. *Science*, 316: 1456-1459.

Martin, J.H. (1990) Glacial-Interglacial CO_2 change: the iron hypothesis. *Paleoceanography*. 5: 1-13.

Martin, J.H. and Knauer, G.A. (1973) The elemental composition of plankton. *Geochimica et Cosmochimica Acta*, 37: 1639-1653.

Martin-Jézéquel, V., Hildebrand, M., and Brzezinski, M.A. (2000) Silicon metabolism in diatoms: implications for growth. *Journal of Phycology*, 36: 821-840.

Maslin, M.A., and Swann, G.E.A. (2005) Isotopes in lake sediments. In: Leng, M.J. (ed.), Isotopes in Palaeoenvironmental Research, Springer, Dordrecht, The Netherlands, pp 227-290.

Maslin, M.A., Shackleton, N.J., and Pflaumann U. (1995a) Temperature, salinity and density changes in the Northeast Atlantic during the last 45,000 years: Heinrich events, deep water formation and climatic rebounds. *Paleoceanography*, 10: 527–544.

Maslin, M.A., Haug, G.H., Sarnthein, M., Tiedemann, R., Erlenkeuser, H., and Stax, R. (1995b) Northwest Pacific Site 882: The initiation of major Northern Hemisphere Glaciation. In Proc. ODP, Scientific Results, 145, edited by Rea D.K., Basov I.A., Scholl D.W., and Allan J.F., pp. 315-329, College Station, Texas.

Maslin, M.A., Haug, G.H., Sarnthein, M., and Tiedemann, R. (1996) The progressive intensification of northern hemisphere glaciation as seen from the North Pacific. *Geologische Rundschau*, 85, 452-465.

Maslin, M.A., Li, X-S., Loutre, M-F., and Berger, A. (1998) The contribution of orbital forcing to the progressive intensification of Northern Hemisphere glaciation., *Quaternary Science Reviews*, 17: 411-426.

Matheney, R.K., and Knauth, L.P. (1989) Oxygen-isotope fractionation between marine biogenic silica and seawater. *Geochimica et Cosmochimica Acta*, 53: 3207–3214.

Matsumoto, K., Sarmiento, J.L., and Brzezinski, M.A. (2002) Silicic acid leakage from the Southern Ocean: A possible explanation for glacial atmospheric pCO_2. *Global Biogeochemical Cycles*, 16: 1031. doi: 10.1029/2001GB001442.

Mikkelsen N., Labeyrie L., and Berger W.H. (1978) Silica oxygen isotopes in diatoms: A 20,000 yr record in deep-sea sediments. *Nature*, 271: 536–538.

Miller, C.B., Nelson, D.M., Weiss, C., and Soeldner, A.H. (1990) Morphogenesis of opal teeth in calanoid copepods. *Marine Biology*, 106: 91–101.

Miller, K.G., Wright, J.D. and Fairbanks, R.G. (1991) Unlocking the ice house: Oligocene-Miocene oxygen isotopes, eustasy, and margin erosion. *Journal of Geophysical Research*, 96 (B4): 6829–6849.

Mix, A. and Ruddiman, W.F. (1984) Oxygen isotope analyses and Pleistocene Ice Volumes. *Quaternary Research*, 21: 1-20.

Mochizuki, M., Shiga, N., Saito, M., Imai, K., and Nojiri, Y. (2002) Seasonal changes in nutrients, chlorophyll *a* and the phytoplankton assemblages of the western subarctic gyre in the Pacific Ocean. *Deep-Sea Research II*, 49: 5421-5439.

Mohiuddin, M.M., Nishimura, A., Tanaka, Y., and Shimamoto, A. (2002) Regional and interannual productivity of biogenic components and planktonic foraminiferal fluxes in the northwestern Pacific Basin. *Marine Micropaleontology*, 45: 57-82.

Mohiuddin, M.M., Nishimura, A., and Tanaka, Y. (2005) Seasonal succession, vertical distribution, and the dissolution of planktonic foraminifera along the Subarctic Front: implications for paleoceanographic reconstruction in the northwestern Pacific. *Marine Micropaleontology*, 55: 129-156.

Moore, J.K., Abbott, M.R., Richman, J.G., and Nelson, D.M. (2000) The Southern Ocean at the

last glacial maximum: a strong sink for atmospheric carbon dioxide. *Global Biogeochemical Cycles*, 14: 455-475.

Mopper K., and Garlick G.D. (1971) Oxygen isotope fractionation between biogenic silica and ocean water. *Geochimica et Cosmochimica Acta*, 35: 1185-1187.

Morales Maqueda, M.A., and Rahmstorf, S. (2002) Did Antarctic sea-ice expansion cause glacial CO2 decline? *Geophysical Research Letters*, 29: doi:10.1029/2001GL013240.

Morley, D.W. (2005) Reconstructing past climatic change in continental Eurasia. Ph.D Thesis University College London, London, 388 pp.

Morley, D.W., Leng, M.J., Mackay, A.W., Sloane, H.J., Rioual, P., and Battarbee, R.W. (2004), Cleaning of lake sediment samples for diatom oxygen isotope analysis. *Journal of Paleolimnology*, 31: 391–401.

Morley, D. W., Leng, M.J., Mackay, A.W., and Sloane, H.J. (2005) Late Glacial and Holocene environmental change in the Lake Baikal region documented by oxygen isotopes from diatom silica. *Global and Planetary Change*, 46: 221-233.

Mortlock, R.A., and Fröhlich, P.N. (1989) A simple and reliable method for the rapid determination of biogenic opal in pelagic sediments. *Deep-Sea Research*, 36: 1415-1426.

Moschen, R., Lücke, A., and Schleser, G. (2005) Sensitivity of biogenic silica oxygen isotopes to changes in surface water temperature and palaeoclimatology. *Geophysical Research Letters*, 32: L07708, doi:10.1029/2004GL022167.

Moschen, R., Lücke, A. , Parplies, J., Radtke, U., and Schleser, G.H. (2006) Transfer and early diagenesis of biogenic silica oxygen isotope signals during settling and sedimentation of diatoms in a temperate freshwater lake (Lake Holzmaar, Germany). *Geochimica et Cosmochimica Acta*, 70: 4367–4379.

Motoi, T., Chan, W-L, Minobe, S., and Sumata, H. (2005) North Pacific halocline and cold climate induced by Panamanian Gateway closure in a coupled ocean-atmosphere GCM. *Geophysical Research Letters*, 32: L10618, doi:10.1029/2005GL022844.

Mulitza, S., Durkoop, A., Hale, W., Wefer, G. and Niebler, H.S. (1997) Planktonic foraminifera as recorders of past surface water stratification. *Geology*, 25: 335–338.

Müller, P.J. and Schneider, R. (1993) An automated leaching method for the determination of opal in sediments and particulate matter. Deep-Sea Research I, 40: 425-444.

Nagashima, K., Tada, R., Matsui, H., Irino, T., Tani, A., Toyoda, S.. (2007) Orbital- and millennial-scale variations in Asian dust transport path to the Japan Sea. *Palaeogeography, Palaeoclimatology, Palaeoecology*, 247: 144-161.

Nakatsuka, T., Watanabe, K., Handa, N., Matsumoto, E., and Wada, E. (1995) Glacial to interglacial surface nutrient variations of Bering deep basins recorded by $\delta^{13}C$ and $\delta^{15}N$. *Paleoceanography*, 10: 1047-1061.

Narita, H., Sato, M., Tsunogai, S., Murayama, M., Nakatsuka, T., Wakatsuchi, M., Harada, N. and Ujiie, Y. (2002) Biogenic opal indicating less productive northwestern North Pacific during the glacial ages. *Geophysical Research Letters*, 29: 1732. doi: 10.1029/2001GL014320.

Nelson, D.M., Tréguer, P., Brzezinski, M.A., Leynaert, A., and Quéguiner, B. (1995) Production and dissolution of biogenic silica in the ocean: revised global estimates, comparison with regional data and relationship to biogenic sedimentation. *Global Biogeochemical Cycles*, 9: 359-372.

Niebler, H-S., Hubberten, H-W. and Gersonde, R. (1999) Oxygen isotope values of planktonic foraminifera: a tool for the reconstruction of surface water stratification. In: Fischer, G. and Wefer, G. (eds), Use of proxies in Paleoceanography. Springer, Berlin, pp. 165–189.

Nürnberg, D. and Tiedemann, R. (2004) Environmental change in the Sea of Okhotsk during the last 1.1 million years. *Paleoceanography*, 19: PA4011, doi:10.1029/2004PA001023.

O'Neil, J., Clayton, R. and Mayeda, T. (1969) Oxygen isotope fractionation in divalent metal carbonates. *Journal Chemical Physics*, 51: 5547–5558.

O'Neil, J. (1986) Theoretical and experimental aspects of isotopic fractionation. In: Stable isotopes in high temperature geological processes. (eds. Valley J.W., Taylor Jr. H.P., and O'Neil, J.R.) Rev Mineral, 16: 1-40.

Ohkouchi, N., Kawamura, K., Kawahata, H., and Okada, H. (1999) Depth ranges of alkenone production in the central Pacific Ocean. *Global Biogeochemical Cycles*, 13: 695-704

Onodera, J., and Takahashi, K. (2005) Silicoflagellates fluxes and environmental variations in the northwestern North Pacific during December 1997-May 2000. *Deep-Sea Research I*, 52: 371-388.

Onodera, J., Takahashi, K., and Honda, M.C. (2005), Pelagic and coastal diatom fluxes and the environmental changes in the northwestern North Pacific during 1997-2000. *Deep Sea Research II*, 52: 2218-2239.

Open University (1999) Ocean chemistry and deep-sea sediments. Open University and Pergamon, Milton Keynes, pp. 134.

Pagani, M., Freeman, K.H., Ohkouchi, N., and Caldeira, K. (2002) Comparison of water column [CO_{2aq}] with sedimentary alkenone-based estimates: a test of the alkenone-CO_2 proxy, *Paleoceanography*, 17: doi: 10.1029/2002PA000756.

Pearson, P.N., and Palmer, M.R. (1999) Middle Eocene seawater pH and atmospheric carbon dioxide concentrations. *Science*, 284: 1824–1826.

Pearson, P.N., and Palmer, M.R. (2000) Atmospheric carbon dioxide concentrations over the past 60 million years. *Nature*, 406: 695–699.

Perry C.C. (1989) Chemical studies of biogenic silica. In Mann S., Webb J, Williams R.J.P (Eds.), Biomineralization: chemical and biological perspectives. VCH Verlagsgesellschaft, Weinheim, pp. 223-256.

Petit, J.R., Jouzel, J., Raynaud, D., Barkov, N.I., Barnola, J.-M., Basile, I., Bender, M., Chappellaz, J., Davis, M., Delaygue, G., Delmotte, M., Kotlyakov, V.M., Legrand, M., Lipenkov, V.Y., Lrius C., Pepin, L., Ritz, C., Saltzman, E., and Stievenard, M. (1999) Climate and atmospheric history of the past 420,000 years from the Vostok ice core, Antarctica. *Nature*, 399, 429–436.

Piotrowska, N., Bluszcz, A., Demske, D., Granoszewski, W., and Heumann, G. (2004) Extraction and AMS radiocarbon dating of pollen from Lake Baikal sediments. *Radiocarbon*, 46: 181–187.

Polissar, P.J., Abbott, M.B., Shemesh, A., Wolfe, A.P., and Bradley, R.S. (2006) Holocene hydrologic balance of tropical South America from oxygen isotopes of lake sediment opal, Venezuelan Andes. *Earth and Planetary Science Letters*, 242: 375-389.

Pondaven, P, Ragueneau, O., Tréguer, P., Hauvespre, A. Dezileau, L., and Reyss, J.L. (2000) Resolving the opal paradox in the Southern Ocean. *Nature*, 405: 168-172.

Popovskaya, G.I. (2000) Ecological monitoring of phytoplankton in Lake Baikal. *Aquatic Ecosystem Health and Management*, 3:215–225.

Popp, B.N., Takigiku, R., Hayes, J.M., Louda, J.W., and Baker, E.W. (1989) The post-paleozoic chronology and mechanism of ^{13}C depletion in primary marine organic matter. *American Journal of Science*, 289: 436-454.

Prokopenko, A.A., Williams, D.F., Karabanov, E.B., and Khursevich, G.K. (2001a) Continental

response to Heinrich events and bond cycles in sedimentary record of Lake Baikal, Siberia. *Global and Planetary Change*, 28: 217-226.

Prokopenko, A.A., Karabanov, E.B., Williams, D.F., Kuzmin, M.I., Khursevich, G.K., and Gvozdkov, A.N. (2001b) The detailed record of climatic events during the past 75,000 BP from the Lake Baikal drill core BDP-93-2. *Quaternary International*, 80-81: 59-68.

Prokopenko, A.A., Karabanov, E.B., Williams, D.F., Kuzmin, M.I., Shackleton, N.J., Crowhurst, S.J., Peck, J.A., Gvozdkov, A.N., and King,. J.W. (2001c) Biogenic Silica Record of the Lake Baikal Response to Climatic Forcing during the Brunhes. *Quaternary Research*, 55: 123-132.

Prokopenko, A.A. Hinnov, L.A., Williams, D.F., Kuzmin, M.I (2006) Orbital forcing of continental climate during the Pleistocene: a complete astronomically tuned climatic record from Lake Baikal, SE Siberia. *Quaternary Science Reviews*, 25: 3431-3457.

Prueher, L.M., and Rea, D.K. (2001) Volcanic triggering of late Pliocene glaciation: evidence from the flux of volcanic glass and ice-rafted debris to the North Pacific Ocean. *Palaeogeography, Palaeoclimatology, Palaeoecology*, 173: 215-230.

Pudsey, C.J. (1992) Calibration of a point-counting technique for estimation of biogenic silica in marine sediments. *Journal of Sedimentary Petrology*, 63: 760-762.

Qui, L., Williams, D.F., Gvorzdikov, A., Karabanov, E., Shimaraeva, M. (1993) Biogenic silica accumulation and paleoproductivity in the northern basin of Lake Baikal during the Holocene. *Geology*, 21: 25-28.

Raubitschek, S., Lücke, A., and Schleser, G.H. (1999) Sedimentation patterns of diatoms in Lake Holzmaar, Germany - (on the transfer of climate signals to biogenic silica oxygen isotope proxies). *Journal of Paleolimnology*, 21: 437-448.

Ragueneau, O., Tréguer, P., Leynaert, A., Anderson, R. F., Brzezinski, M. A., DeMaster, D. J., Dugdale, R. C., Dymond, J., Fischer, G., Francois, R., Heinze, C., Maier-Reimer, E., Martin-Jézéquel, V., Nelson, D. M., and Quéguiner, B. (2000) A review of the Si cycle in the modern ocean: recent progress and missing gaps in the application of biogenic opal as a paleoproductivity proxy. *Global and Planetary Change*, 26: 317-365.

Ragueneau, O., Savoye, N., Del Amo, Y., Cotton, J., Tardiveau, B., and Leynaert, A. (2005) A new method for the measurement of biogenic silica in suspended matter of coastal waters: using Si:Al ratios to correct for the mineral interference. *Continental Shelf Research*, 25: 697-710.

Ragueneau, O., Schultes, S., Bidle, K., Claquin, P., and Moriceau, B. (2006) Si and C interactions in the world ocean: importance of ecological processes and implications for the role of diatoms in the biological pump. *Global Biogeochemical Cycles*, 20: GB4S02 doi:10.1029/2006GB002688.

Raubitschek, S., Lücke, A., and Schleser, G.H. (1999) Sedimentation patterns of diatoms in Lake Holzmaar, Germany - (on the transfer of climate signals to biogenic silica oxygen isotope proxies). *Journal of Paleolimnology*, 21, 437-448.

Ravelo, A., and Andreasen, D. (1999) Using planktonic foraminifera as monitors of tropical surface ocean. In: Abrantes, F., and Mix, A. (eds), Reconstructing Ocean History: A window into the future. Kluwer Academic, New York, pp. 217–243.

Ravelo, A.C., Andreasen, D.H., Lyle, M., Lyle, A.O., and Wara, M.W. (2004) Regional climate shifts caused by gradual cooling in the Pliocene epoch. *Nature*, 429, 263-267.

Raymo, M.E. (1994) The Himalayas, organic-carbon burial, and climate in the Miocene. *Paleoceanography*, 9: 399-404.

Rea, D.K., and Schrader, H. (1985) Late Pliocene onset of glaciation: ice-rafting and diatom stratigraphy of North Pacific DSDP cores. *Palaeogeography, Palaeoclimatology, Palaeoecology*, 49: 313-325.

Rea, D.K., Basov, I.A., Scholl, D. W., and Allan, J. F. (Eds.) (1995), Proc. ODP, Sci. Results, 145: College Station, Texas.

Rickert, D., Schlüter, M., and Wallmann, K. (2002) Dissolution kinetics of biogenic silica from the water column to the sediments. *Geochimica et Cosmochimica Acta*, 66: 439-455.

Rietti-Shati, M., Shemesh, A., and Karlen, W.. (1998) A 300-year climate record from biogenic silica oxygen isotopes in an equatorial high-altitude lake. *Science*, 281: 980-982.

Rings, A., Lücke, A., and Schleser, G.H. (2004) A new method for the quantitative separation of diatom frustules from lake sediments. *Limnology and Oceanography Methods*, 2: 25-34.

Rioual, P. and Mackay, A.W. (2005) A diatom record of centennial resolution for the the Kazantsevo Interglacial stage in Lake Baikal (Siberia). *Global and Planetary Change*, 46: 199-219.

Rioual, P., Andrieu-Ponel, V., Rietti-Shati, M., Battarbee, R.W., De Beaulieu, J.L., Cheddadi, R., Reille, M., Svobodovas, H., and Shemesh, A.. (2001) High resolution record of climate stability in France during the last interglacial period. *Nature*, 413: 293-296.

Rioual *at al.*, (In prep) Lake Baikal diatom records during the Holocene.

Robinson, R.S., Brunelle, B.G., and Sigman, D.M. (2004) Revisiting nutrient utilisation in the glacial Antarctic: evidence from a new method for diatom-bound N isotopic analysis. *Paleoceanography*, 19: PA3001, doi: 10.1029/2003PA000996.

Rohling, E.J. (2000) Paleosalinity: confidence limits and future applications. *Marine Geology*, 163, 1-11.

Rohling, E.J, Sprovieri, M., Cane, T., Casford, J.S.L., Cooke, S., Bouloubassi, I., Emeis, K.C., Schiebel, R., Rogerson, M., Hayes, A., Jorissen, F.J., and Kroon, D. (2004) Reconstructing past planktic foraminiferal habitats using stable isotope data: a case history for Mediterranean sapropel S5. *Marine Micropaleontology*, 50: 89–123.

Romero, O., Mollenhauer, G., Schneider, R.R., Wefer, G. (2003) Oscillations of the siliceous imprint in the central Benguela Upwelling System from MIS 3 through to the early Holocene: the influence of the Southern Ocean. *Journal of Quaternary Science*, 18: 733–743.

Rosell-Melé, A., Bard, E., Emeis, K.C., Grimalt, J.O., Muller, P., Schneider, R., Bouloubassi, I, Epstein, B., Fahl, K., Fluegge, A., Freeman, K., Goni, M., Guntner, U., Hartz, D., Hellebust, S., Herbert, T., Ikehara, M., Ishiwatari, R., Kawamura, K., Kenig, F., de Leeuw, J., Lehman, S., Mejanelle, L., Ohkouchi, N., Pancost, R.D, Pelejero, C., Prahl, F., Quinn, J., Rontani, J.F., Rostek, F., Rullkotter, J., Sachs, J., Blanz, T., Sawada, K., Schutz-Bull, D., Sikes, E., Sonzogni, C., Ternois, Y., Versteegh, G., Volkman, J.K., and Wakeham, S. (2001) Precision of the current methods to measure the alkenone proxy $U_{37}^{K'}$ and absolute alkenone abundance in sediments: Results of an interlaboratory comparison study. *Geochemistry Geophysics Geosystems*, 2: doi:10.1029/2000GC000141.

Rosqvist, G.C., Rietti-Shati, M., and Shemesh, A. (1999) Late glacial to middle Holocene climate record of lacustrine biogenic silica oxygen isotopes from a Southern Ocean Island, *Geology*, 27: 967-970.

Rosqvist, G., Jonsson, C., Yam, R., Karlén, W., and Shemesh, A. (2004) Diatom oxygen isotopes in pro-glacial lake sediments from northern Sweden: a 5000 year record of atmospheric circulation. *Quaternary Science Reviews*, 23: 851-859.

Ruddiman, W.F., and Raymo, M.E. (1988) Northern Hemisphere climate regimes during the past 3 Ma: possible tectonic connections. *Philosophical Transactions of the Royal Society of London. Series B, Biological Sciences*, 318: 411-430.

Ryves, D.B., Juggins, S., Fritz, S.C., and Battarbee, R.W. (2001) Experimental diatom dissolution and the quantification of microfossil preservation in sediments. *Palaeogeography Palaeoclimatology Palaeoecology*, 172: 99-113.

Ryves, D.B., Jewson, D.H., Sturm, M., Battarbee, R.W., Flower, R.J., Mackay, A.W., and Granin N.G. (2003) Quantitative and qualitative relationships between planktonic diatom communities and diatom assemblages in sedimenting material and surface sediments in Lake Baikal, Siberia. *Limnology and Oceanography*, 48: 1643-1661.

Ryves, D.B., Battarbee, R.W., Juggins, S., Fritz, S.C., and Anderson N.J. (2006) Physical and chemical predictors of diatom dissolution in freshwater and saline lake sediments in North America and West Greenland. *Limnology and Oceanography*, 51: 1355-1368.

Saccone, L. Conley, D.J., Sauer, D., (2006) Methodologies for amorphous silica analysis. *Journal of Geochemical Exploration*, 88: 235-238.

Sancetta, C (1982) Distribution of diatom species in surface sediments of the Bering and Okhotsk seas. *Micropaleontology*, 28: 221-257.

Sancetta, C. (1983) Effect of Pleistocene glaciation upon oceanographic characteristics of the North Pacific Ocean and Bering Sea. *Deep Sea Research Part A. Oceanographic Research Papers*, 30: 851-869.

Sancetta, C., Heusser L., Labeyrie L., Sathy Naidu A., S. Robinson W. (1985) Wisconsin - Holocene paleoenvironment of the Bering Sea: evidence from diatoms, pollen, oxygen isotopes and clay minerals. *Marine Geology*, 62: 55-68.

Sapota, T., Aldahan ,A., Possnert, G., Peck, J., King, J., Prokopenko, A., Kuzmin, M (2004) A late Cenozoic Earth's crust and climate dynamics record from Lake Baikal. *Journal of Paleolimnology*, 32: 341–349.

Sarnthein, M., Gebhardt, H., Kiefer, T., Kucera, M., Cook, M., and Erlenkeuser, H. (2004) Mid Holocene origin of the sea-surface salinity low in the subarctic North Pacific. *Quaternary Science Reviews*, 23: 2089-2099.

Sarnthein, M., Kiefer, T., Grootes, P. M., Elderfield, H., and Erlenkeuser, H. (2006) Warmings in the far northwestern Pacific promoted pre-Clovis immigration to America during Heinrich event 1. *Geology*, 34: 141-144.

Sauer, D., Saccone, L., Conley, D.J., Herrmann, L.. and Sommer, M. (2006) Review of methodologies for extracting plant-available and amorphous Si from soils and aquatic sediments. *Biogeochemistry*, 80: 89-108.

Sautter, L.R., and Thunell, R.G. (1991) Seasonal variability in the $\delta^{18}O$ and $\delta^{13}C$ of planktonic foraminifera from an upwelling environment. *Paleoceanography*, 3: 307–334.

Schmidt, G.A., Bigg, G.R., and Rohling, E.J. (1999) Global seawater oxygen-18 database. http://data.giss.nasa.gov/o18data/

Schmidt, M., Botz, R., Stoffers, P., Anders, T., and Bohrmann, G. (1997) Oxygen isotopes in marine diatoms: A comparative study of analytical techniques and new results on the isotopic composition of recent marine diatoms. *Geochimica et Cosmochimica Acta*, 61: 2275-2280.

Schmidt, M., Botz, R., Rickert, D., Bohrmann, G., Hall, S.R., and Mann, S. (2001) Oxygen isotope of marine diatoms and relations to opal-A maturation. *Geochimica et Cosmochimica Acta*, 65: 201-211.

Schneider, B., and Schmittner, A. (2006) Simulating the impact of the Panamanian seaway closure on ocean circulation, marine productivity and nutrient cycling. *Earth and Science Planetary Letters*, 246: 367-380.

Schlüter, M. and Rickert, D. (1998) Effect of pH on the measurement of biogenic silica. *Marine Chemistry*, 63: 81-92.

Schrag, D.P., Hampt, G., and Murray, D.W. (1996) Pore fluid constraints on the temperature and oxygen isotope composition of the glacial ocean. *Science*, 272: 1930–1932.

Schrag, D.P., Adkins, J.F., McIntyre, K., Alexander, J.L., Hodell, D.A., Charles, C.D. and McManus, J.F. (2002) The oxygen isotope composition of seawater during the Last Glacial Maximum. *Quaternary Science Reviews*, 21: 331–342.

Seki, O., Ikehara, M., Kawamura, K., Nakatsuka, T., Ohnishi, K., Wakatsuchi, M., Narita, H., and Sakamoto, T. (2004) Reconstruction of paleoproductivity in the Sea of Okhotsk over the last 30 kyr. *Paleoceanography*, 19: PA1016, doi:10.1029/2002PA000808.

Seki, O. Nakatsuka, T., Kawamura, K., Saitoh, S-I., and Wakatsuchi, M. (2007) Time-series sediment trap record of alkenones from the western Sea of Okhotsk. *Marine Chemistry*, 104: 253-265.

Shackleton, N.J. (1967) Oxygen isotope analyses and Pleistocene temperatures re-assessed. *Nature*, 215: 15-17.

Shackleton, N.J. (1974) Attainment of isotopic equilibrium between ocean water and the benthic foraminifera Genus Uvigerina: isotope changes in the ocean during the last glacial. In:

Les méthodes quantitatives d'étude des variations due climat au cours du Pleistocene, 219. Colloques Internationaux de Central National de la Recherce Scientifique CNRS, Paris, pp. 203-209.

Shackleton, N.J. (2000) The 100,000 year ice age cycle identified and found to lag temperature, carbon dioxide and orbital eccentricity. *Science*, 289: 1897–1902.

Shackleton, N.J., Hall, M.A., and Pate, D. (1995) Pliocene stable isotope stratigraphy of Site 846, in *Proc. ODP, Scientific Results*, 138, edited by Pisias, N.G., Mayer, L.A., Janecek, T.R., Palmer-Julson, A., and van Andel, T. H., pp 337-357, College Station, Texas.

Shackleton, N.J., Sánchez-Goñi, M.F., Pailler, D., and Lancelot, Y. (2003) Marine isotope substage 5e and the Eemian interglacial. *Global and Planetary Change*, 36:151–155.

Shemesh, A. (1992) Silica-Carbonate Isotopic Temperature Calibration. *Science*, 258: 1163.

Shemesh, A. and Peteet, D. (1998) Oxygen isotopes in fresh water biogenic opal-Northeastern US Allerod-Younger Dryas temperature shift. *Geophysical Research Letters*, 25: 1935-1938.

Shemesh, A., Mortlock, R.A., Smith, R.J., and Fröhlich, F. (1988) Determination of Ge/Si in marine siliceous microfossils: separation, cleaning and dissolution of diatoms and radiolaria. *Marine Chemistry*, 25: 305-323.

Shemesh, A., Charles, C.D., and Fairbanks R.G. (1992) Oxygen isotopes in biogenic silica: global changes in ocean temperature and isotopic composition. *Science*, 256, 1434-1436.

Shemesh, A., Burckle, L.H., and Hays, J.D. (1994) Meltwater input to the Southern Ocean during the Last Glacial Maximum. *Science*, 266: 1542–1544.

Shemesh, A., Burckle, L.H., and Hays, J.D. (1995) Late Pleistocene oxygen isotope records of biogenic silica from the Atlantic sector of the Southern Ocean. *Paleoceanography*, 10: 179-196.

Shemesh, A., Rosqvist, G., Rietti-Shati, M., Rubensdotter, L., Bigler, C., Yam, R., Karlén, W. (2001a) Holocene climatic change in Swedish Lapland inferred from an oxygen-isotope record of lacustrine biogenic silica. *The Holocene*, 11: 447-454.

Shemesh, A., Rietti-Shati, M., Rioual, P., Battarbee, R., de Beaulieu, J-L., Reille, M., Andrieu, V., and Svobodova, H. (2001b) An oxygen isotope record of lacustrine opal from a European Maar indicates climatic stability during the last interglacial. *Geophysical*

Research Letters, 28: 2305-2308.

Shemesh, A., Hodell, D., Crosta, C., Kanfoush, S., Charles, C., and Guilderson, T. (2002) Sequence of events during the last deglaciation in Southern Ocean sediments and Antarctic ice cores. *Paleoceanography*, 17: 1056. doi: 10.1029/2000PA000599.

Sherbakov, D.Y. (1999) Molecular phylogenetic studies on the origin of biodiversity in Lake Baikal. *Trends in Ecology and Evolution*, 14: 92-95.

Siddall, M., Rohling, E.J., Almogi-Labin, A., Hemleben, C., Meischner, D., Schmelzer, I., and Smeed, D.A. (2003) Sea-level fluctuations during the last glacial cycle. *Nature*, 423: 853–858.

Sigman, D.M., and Boyle, E.A. (2000) Glacial/interglacial variations in atmospheric carbon dioxide. *Nature*, 407: 859-869.

Sigman, D.M., and Boyle, E.A. (2001) Paleoceanography: Antarctic stratification and glacial CO_2. *Nature*, 412: 606.

Sigman, D.M. and Haug, G.H. (2003) The biological pump of the past. In Treatise on Geochemistry Vol 6, edited by Elderfield, H, pp 491-528, Elsevier, Amsterdam.

Sigman, D.M. Altabet, M.A., Francois, R., McCorkle, D.C., and Gaillard, J-F.. (1999) The isotopic composition of diatom-bound nitrogen in Southern Ocean sediments. *Paleoceanography*, 14: 118-134.

Sigman, D.M., Jaccard, S.L., and Haug, G.H. (2004) Polar ocean stratification in a cold climate. *Nature*, 428: 59-63.

Simstich, J., Sarnthein, M., and Erlenkeuser, H. (2003) Paired $\delta^{18}O$ signals of *Neogloboquadrina pachyderma* (s) and *Turborotalita quinqueloba* show thermal stratification structure in Nordic Seas. *Marine Micropaleontology*, 48: 107–125.

Skinner, L.C., Shackleton, N.J., and Elderfield, H. (2003), Millennial scale variability of deep-water temperature and $\delta^{18}O_{dw}$ indicating deep-water source variations in the Northeast Atlantic, 0-34 cal. ka BP. *Geochemistry Geophysics Geosystems*, 4: 1098, doi:10.1029/2003GC000585.

Spero, H.J., and Lea, D.W. (1993) Intraspecific stable isotope variability in the planktonic foraminifera Globigerinoides sacculifer: results from laboratory experiments. *Marine Micropaleontolgy*, 22: 221-234.

Spero, H.J. and Lea, D.W. (1996) Experimental determination of stable isotope variability in

Globigerina bulloides: implications for paleoceanographic reconstructions. *Marine Micropaleontology*, 28: 231-246.

Spero, H. J., Bijma, J., Lea, D.W., and Bemis, B. (1997) Effect of seawater carbonate chemistry on planktonic foraminiferal carbon and oxygen isotope values. *Nature*, 390: 497-500.

St. John, K.E.K and Krissek, L.A. (1999) Regional patterns of Pleistocene ice-rafted debris flux in the North Pacific. *Paleoceanography*, 14: 653-662.

Steph, S., Tiedemann, R., Prange ,M., Groeneveld, J., Nümberg, D., Reuning, L., Schulz, M., and Haug G.H.. (2006) Changes in Caribbean surface hydrography during the Pliocene shoaling of the Central American Seaway. *Paleoceanography*, 21: PA4221, doi:10.1029/2004PA001092.

Stephens, B.B. and Keeling, R.F. (2000) The influence of Antarctic sea ice on glacial–interglacial CO_2 variations. *Nature*, 404: 171–174.

Straškrábová, V., Izmest'eva, L.R., Maksimova, E.A., Fietz, S., Nedomal, J., Borovec, J., Kobanova, G.I., Shchetinina, E.V., and Pislegina, E.V. (2005) Primary production and microbial activity in the euphotic zone of Lake Baikal (Southern Basin) during late winter. *Global and Planetary Change*, 46: 57-73.

Street-Perrott, F.A., Ficken, K.J., Huang, Y., Eglinton, G. (2004) Late Quaternary changes in carbon cycling on Mt. Kenya, East Africa: an overview of the $\delta^{13}C$ record in lacustrine organic matter. *Quaternary Science Reviews*, 23: 861–879.

Sullivan, B.K., Miller, C.B., Peterson, W.T., and Soeldner, A.H. (1975) A scanning electron microscope study of the mandibular morphology of boreal copepods. *Marine Biology*, 30: 175–182.

Sun, Y., and An, Z. (2005) Late Pliocene-Pleistocene changes in mass accumulation rates of eolian deposits on the central Chinese Loess Plateau. *Journal of Geophysical Research*, Vol. 110, D23101, doi:10.1029/2005JD006064.

Swann, G.E.A., Mackay, A.W., Leng, M.J., and Demory, F. (2005) Climatic changes in Central Asia during MIS 3/2: a case study using biological responses from Lake Baikal. *Global and Planetary Change*, 46: 235-253.

Swann, G.E.A., Maslin, M.A., Leng, M.J., Sloane, H.J., and Haug, G.H. (2006) Diatom δ18O evidence for the development of the modern halocline system in the subarctic northwest Pacific at the onset of major Northern Hemisphere glaciation. *Paleoceanography*, 21, PA1009, doi: 10.1029/2005PA001147.

Swann, G.E.A., Leng, M.J., Sloane, H.J., Maslin, M.A., and Onodera, J. (2007) Diatom oxygen isotopes: evidence of a species effect in the sediment record. *Geochemistry, Geophysics, Geosystems*, 8, Q06012, doi:10.1029/2006GC001535.

Tabata, S. (1975) The general circulation of the Pacific Ocean and a brief account of the oceanographic structure of the North Pacific Ocean. Part I, Circulation and volume transports. *Atmosphere*, 13: 134-168.

Takahashi K. (1986) Seasonal fluxes of pelagic diatoms in the subarctic Pacific, 1982–1983. *Deep Sea Research Part A*, 33: 1225–1251.

Takahashi, K., Hisamichi, K., Yanada, M., and Maita, Y. (1996) Seasonal changes of marine phytoplankton productivity: a sediment trap study. *Kaiyo Monthly*, 10: 109–115. [In Japanese]

Takeda, S. (1998) Influence of iron availability on nutrient consumption ratio of diatoms in oceanic waters. *Nature*, 393: 774-777.

Taylor, H.P., and Epstein, S. (1962) Relationships between $^{18}O/^{16}O$ ratios in coexisting minerals of igneous and metamorphic rocks, part I, Principles and experimental results. *Bulletin of the Geological Society of America*, 73: 461–480.

Telford, R.J., and Birks, H.J.B. (2005) The secret assumption of transfer functions: problems with spatial autocorrelation in evaluating model performance. *Quaternary Science Reviews*, 24: 2173-2179.

Telford R.J., Andersson, C., Birks, H.J.B., Juggins, S. (2004) Biases in the estimation of transfer function prediction errors. *Paleoceanography*, 19: PA4014, doi:10.1029/2004PA001072.

Tiedemann, R., and Haug, G.H. (1995) Astronomical calibration of cycle stratigraphy for Site 882 in the northwest Pacific, in Proc. ODP, Scientific Results, 145, edited by Rea D.K., Basov, I.A., Scholl, D.W., and Allan, J.F., pp. 283-292, College Station, Texas.

Thorliefson,, J.T., and Knauth, L.P. (1984) An improved stepwise fluorination procedure for the oxygen isotopic analysis of hydrous silica. *Geological Society of America Abstracts Progress*, 16: 675.

Tréguer, P., Nelson, D.M., Van Bennekom, A.J., DeMaster, D.J., Leynaert, A., and Queguiner, B. (1995) The silica balance in the world ocean – a re-estimate. *Science*, 268: 375–379.

Tsuda, A., Takeda, S., Saito, H., Nishioka, J., Nojiri, Y., Kudo, I., Kiyosawa, H., Shiomoto, A., Imai, K., Ono, T., Shimamoto, A., Tsumune, D., Yoshimura, T., Aono, T., Hinuma, A.,

Kinugasa, M., Suzuki, K., Sohrin, Y., Noiri, Y., Tani, H., Deguchi, Y., Tsurushima, N., Ogawa, H., Fukami, K., Kuma, K., and Saino, T. (2003) A Mesoscale Iron Enrichment in the Western Subarctic Pacific Induces a Large Centric Diatom Bloom. *Science*, 300: 958-961.

Tyler, J.J., Leng, M.J., and Sloane, H.J. (2007) The effects of organic removal treatment on the integrity of $\delta^{18}O$ measurements from biogenic silica. *Journal of Paleolimnology*, 37: 491-497.

Ueno, H., and Yasuda, I. (2000) Distribution and formation of the mesothermal structure (temperature inversion) in the North Pacific subarctic region. *Journal of Geophysical Research*, 105: 16,885–16,897.

Unesco (1983) Algorithms for computation of fundamental properties of seawater. *Unesco Technical Papers in Marine Science*, No. 44, 53 pp.

Urey, H.C. (1947) The thermodynamic properties of isotopic substances. Journal *of the Chemical Society*, 152: 190–219.

Urey, H.C. (1948) Oxygen isotopes in nature and in the laboratory. *Science*, 108: 489–496.

Urey, H.C., Lowenstam, H.A., Epstein, S., and McKinney, C.R. (1951) Measurement of palaeotemperatures and temperatures of the upper Cretaceous of England, Denmark and south-eastern United States. *Geological Society of America Bulletin*, 62: 399-416.

van Bennekom, A.J., Berger, G.W., van der Gaast, S.J., and de Vries, R.T.P. (1988) Primary productivity and the silica cycle in the Southern Ocean (Atlantic sector). *Palaeogeography, Palaeoclimatology, Palaeoecology*, 67: 19-30.

van Bennekom, A.J., Jansen, J.H.F., van der Gaast, S.J., van Iperen J.M., and Pieters J. (1989) Aluminum-rich opal: an intermediate in the preservation of biogenic silica in the Zaire (Congo) deep-sea fan. *Deep-Sea Research*, 36: 173–190.

van Bennekom, A.J., Buma, A.G.J., and Nolting, R.F. (1991) Dissolved aluminum in the Weddell-Scotia confluence and effect of Al on the dissolution kinetics of biogenic silica. *Marine Chemistry*, 35: 423-434.

van Cappellen, P., Dixit, S., and van Bennekom, J. (2002) Biogenic silica dissolution in the ocean: reconciling experimental and field-based dissolution rates. *Global and Planetary Change*, 16: 1075 doi:10.1029/2001GB001431.

von Grafenstein, U., Erlenrkeuser, H., and Trimborn, P. (1999) Oxygen and carbon isotopes in

modern freshwater ostracod valves: assessing vital offsets and autecological effects of interest for palaeoclimate studies, *Palaeogeography, Palaeoclimatology, Palaeoecology*, 148: 133–152.

Waelbroeck, C., Labeyrie, L., Michel, E., Duplessy, J.C., McManus, J.F., Lambeck, K., Balbon, E., and Labracherie, M. (2002) Sea level and deep water temperature changes derived from benthic foraminifera isotope records. *Quaternary Science Reviews*, 21: 295–305.

Wang, C-H., and Yeh, H-W. (1985) Oxygen isotope compositions of DSDP Site 480 diatoms: Implications and applications. *Geochimica et Cosmochimica Acta*, 49: 1469-1478.

Warren, B.A. (1983) Why is no deep water formed in the North Pacific? *Journal of Marine Research*, 41: 327-347.

Wefer, G., and Berger, W.H. (1991) Isotope paleontology: growth and composition of extant calcareous species. *Marine Geology*, 100: 207-248.

Werner, M., Tegen, I., Harrison, S.P., Kohfeld, K.E., Prentice, I.C., Balkanski, Y., Rodhe, H., and Roelandt, C. (2002) Seasonal and interannual variability of the mineral dust cycle under present and glacial climate conditions. *Journal of Geophysical Research*, 107 (D24): 4744, doi:10.1029/2002JD002365.

Williams, D.F., Peck, J.. Karabanov, E.B.. Prokopenko, A.A.. Kravchinsky, V.. King, J., and Kuzmin, M.I. (1997) Lake Baikal record of continental climate response to orbital insolation during the past 5 million years. *Science*, 278: 1114-1117.

Williams, D.F., Kuzmin, M.I., Prokopenko, A.A., Karabanov, E.B., Khursevich, G.K., and Bezrukova, E.V. (2001) The Lake Baikal drilling project in the context of a global lake drilling initiative. *Quaternary International*, 80-81: 3-15.

Xia, J., Ito, E., and Engstrom, D.R. (1997) Geochemistry of ostracode calcite: 1. an experimental determination of oxygen isotope fractionation. *Geochimica et Cosmochimica Acta*, 61: 377–382.

Yamamoto, M., Tanaka, N., and Tsunogai, S. (2001) Okhotsk Sea intermediate water formation deduced from oxygen isotope systematics. *Journal of Geophysical Research*, 106 (C12) 31,075-31,084.

Yuan, W., and Zhang, J. (2006) High correlations between Asian dust events and biological productivity in the western North Pacific. *Geophyiscal Research Letters*, 33: L07603, doi:10.1029/2005GL025174.

Zachos, J.C., Quinn, T.M., and Salamy, K.A. (1996) High-resolution (104 years) deep-sea foraminiferal stable isotope records of the Eocene-Oligocene climate transition. *Palaeoceanography*, 11: 251–266.

Zachos, J.C., Pagani, M., Sloan, L., Thomas, E., and Billups, K. (2001) Trends, rhythms and aberrations in Global Climate 65 Ma to present. *Science*, 686-693.

Zahn, R., Pedersen, T.F., Bornhold, B.D., and Mix, A.C. (1991) Water mass conversion in the glacial Subarctic Pacific (54°N, 148°W): physical constraints and the benthic-planktonic stable isotope record. *Paleoceanography*, 6: 543-560.

Appendix (on CD)

Thesis data

All data collected during the PhD and presented within this thesis is included within the enclosed CD.

Published papers from PhD research

Chapter 2:

Swann, G.E.A., Leng, M.J., Sloane, H.J., Maslin, M.A. and Onodera, J. (2007) Diatom oxygen isotopes: evidence of a species effect in the sediment record. *Geochemistry, Geophysics, Geosystems*. 8, Q06012, doi:10.1029/2006GC001535.

Chapter 3

Swann, G.E.A., Leng, M.J., Sloane, H.J., Maslin, M.A. (Submitted) Isotope offsets in marine diatom $\delta^{18}O$. *Journal of Quaternary Science*.

Chapter 4

Haug, G.H., Ganopolski, A., Sigman, D.M., Rosell-Mele, A., Swann, G.E.A., Tiedemann, R., Jaccard, S., Bollmann, J., Maslin, M.A., Leng, M.J. and Eglinton, G. (2005) North Pacific seasonality and the glaciation of North America 2.7 million years ago, *Nature*. 433: 821-825.

Swann, G.E.A., Maslin, M.A., Leng, M.J., Sloane, H.J. and Haug, G.H. (2006) Diatom $\delta^{18}O$ evidence for the development of the modern halocline system in the subarctic northwest Pacific at the onset of major Northern Hemisphere glaciation. *Paleoceanography*. 21, PA1009, doi: 10.1029/2005PA001147

Chapter 8

Swann, G.E.A. and Mackay, A.W. (2006) Potential limitation of biogenic silica as an indicator of abrupt climate change in Lake Baikal, Russia. *Journal of Paleolimnology*. 36: 81-89.